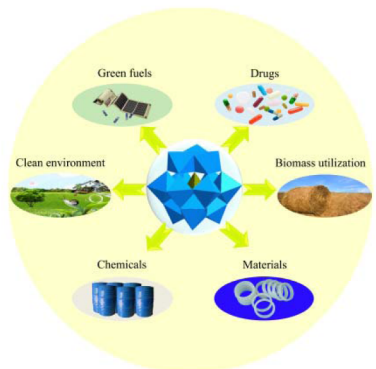


Recent Advances in Polyoxometalate-Catalyzed Reactions

Sa-Sa Wang[†] and Guo-Yu Yang*,^{†,‡}

[†]State Key Laboratory of Structural Chemistry, Fujian Institute of Research on the Structure of Matter, Chinese Academy of Sciences, Fuzhou, Fujian 350002, China

[‡]MOE Key Laboratory of Cluster Science, School of Chemistry, Beijing Institute of Technology, Beijing 100081, China



CONTENTS

| | | | |
|---|------|--|--|
| 1. Introduction | | | |
| 1.1. General Information | 4893 | | |
| 1.2. Catalytic Properties | 4893 | | |
| 1.2.1. Active Sites | 4894 | | |
| 1.2.2. Stability | 4894 | | |
| 1.2.3. Photocatalysis | 4895 | | |
| 1.2.4. Electrocatalysis | 4895 | | |
| 1.2.5. Homogeneous and Heterogeneous Catalysis with POMs/HPAs | 4896 | | |
| 1.2.6. Overview of POM/HPA-Catalyzed Reactions | 4897 | | |
| 2. Oxidation | | | |
| 2.1. Oxidation of Alkenes | 4897 | | |
| 2.1.1. To Epoxides | 4897 | | |
| 2.1.2. To Carbonyl Compounds | 4905 | | |
| 2.2. Oxidation of Alkanes | 4906 | | |
| 2.2.1. To Oxygenates | 4906 | | |
| 2.2.2. To Alkenes | 4909 | | |
| 2.3. Oxidation of Arenes and Derivatives | 4909 | | |
| 2.4. Oxidation of Organosilanes | 4911 | | |
| 2.5. Oxidation of Alcohols and Phenols | 4912 | | |
| 2.6. Cleavage of Single C–C Bonds | 4915 | | |
| 2.7. Cleavage of M–C Bonds | 4915 | | |
| 2.8. Oxidation of Carbonyl Compounds | 4916 | | |
| 2.9. Oxidation of Sulfur-Containing Compounds | 4916 | | |
| 2.10. Oxidation of Nitrogen-Containing Compounds | 4921 | | |
| 2.11. Oxidative Halogenation of Unsaturated Compounds | 4921 | | |
| 2.12. Oxidative Coupling Reactions | 4922 | | |
| 3. Reduction | | | |
| 3.1. Reduction of Organic Compounds | 4925 | | |
| 3.2. Photoreduction of CO ₂ | 4926 | | |
| 3.3. Photoreduction of Metal Cations | 4927 | | |
| 4. Alkene Polymerization | 4928 | | |
| 5. Acid Catalysis | 4929 | | |
| 5.1. Reactions Involving C–C Bond Formation | 4929 | | |
| 5.2. Reactions Involving C–X Bond Formation (X = N, S) | 4934 | | |
| 5.3. Esterification, Hydration, and Related Reactions | 4935 | | |
| 5.3.1. Esterification, Transesterification, and Reversible Hydrolysis | 4935 | | |
| 5.3.2. Hydrolysis of Phosphoester | 4937 | | |
| 5.3.3. Hydrolysis of Peptides | 4938 | | |
| 5.3.4. Other Hydrolysis and Reversible Dehydration Reactions | 4939 | | |
| 6. Base Catalysis | 4939 | | |
| 7. Other Reactions | 4940 | | |
| 7.1. Cycloaddition of Organic Azides | 4941 | | |
| 7.2. Cyclopropanation of Alkenes | 4941 | | |
| 7.3. Cycloaddition of CO ₂ to Epoxides | 4942 | | |
| 7.4. Coupling Reactions | 4942 | | |
| 8. POM-Based Bifunctional Catalysts | 4942 | | |
| 9. Oxygen Evolution | 4943 | | |
| 10. Hydrogen Evolution | 4949 | | |
| 11. Conclusion and Perspectives | 4952 | | |
| Author Information | 4952 | | |
| Corresponding Author | 4952 | | |
| Notes | 4952 | | |
| Biographies | 4952 | | |
| Acknowledgments | 4953 | | |
| References | 4953 | | |

1. INTRODUCTION

1.1. General Information

Polyoxometalates (POMs) are composed of cations and polyanion clusters¹ with structural diversity, in which the oxometal polyhedra of MO_x ($x = 5, 6$) are the basic construction units. Here, M generally represents early transition metals (TMs) in their high oxidation state, e.g., W, Mo, V, Nb, Ta, and so on, which can be partly substituted by other metals, including Al, Ti, Cr, Mn, Fe, Co, Ni, Cu, Zn, Zr, Ru, Pd, Ag, Hf, Ln, etc. To date, many good examples of TM-substituted POMs have been reported.^{2–4} Some polyanions are centered by heteroatoms that significantly affect their properties. These heteroatoms are usually main-group elements, including Si, P, S, Ge, As, Se, B, Al, and Ga, but are not limited to these. Some late TMs such as Co and Fe are also found as heteroatoms. Polyanions are bulky and have a highly negative charge. On the

Received: July 20, 2014

Published: May 12, 2015

surface of polyanions are abundant oxygen atoms that can donate electrons to electron acceptors. Thus, polyanions can be regarded as soft bases. Unambiguously, the metal ions on the skeleton of polyanions possess unoccupied orbitals that can accept electrons. In this way, polyanions can also act as Lewis acids. Therefore, polyanions may play the roles of Lewis acid and Lewis base under different conditions. In addition, polyanions are often recognized as electron reservoirs because they have a strong capacity to bear electrons and release electrons, indicating their available redox nature.⁵ More importantly, these polyanions are designable. To obtain special properties, their structure and constituent elements can be tuned artificially, in which the substitution of polyhedra, the variation of the heteroatom, and the arrangement patterns of the basic construction units are the most common pathways.

However, it should be made clear that the above assumptions about POM anions are true only in general contexts, because they are impacted by many parameters, such as solvents, POM–cation interactions, and covalently bonded organic addenda of POM anions. These parameters mainly function via interaction with POM anions. The electronic properties of POM anions can be changed by these interactions. In addition, the chirality of cations and organic addenda can transfer to POM anions. Thus, the acidic, basic, oxidative, and chiral properties of POM anions are impacted by these parameters. For example, the basicity of POM anions will be shielded when they are put into protonic solvents, the achiral POM anion may become chiral when it is paired with chiral cations or covalently attached to chiral organic addenda, and the Lewis acidity and capacity to bear/release electrons may vary owing to the electron transfer between POM anions and cations or covalently bonded organic addenda. It is notable that solvents also change the electronic properties of POM anions via acting on the ion pairing. Thus, the properties of POM anions can also be designed by changing the counterions, covalently attaching organic addenda, and choosing appropriate solvents.

As mentioned before, the nature of cations in POMs also greatly impacts the properties of the POM compounds, including electronic and crystallographic properties and solubilities.^{6,7} As is known, the parent acids of POMs only contain protons as their cations. Those centered by heteroatoms are called heteropolyacids (HPAs). However, a POM may contain one or more kinds of cations. The most common cations are inorganic cations, including H⁺, Na⁺, K⁺, Cs⁺, NH₄⁺, Ag⁺, etc. However, the number of inorganic cations is limited, and these inorganic cations are impossible to modify, although they can be replaced by other cations through ion exchange. In this context, organic cations are attractive because they are designable and can be modified flexibly. Many functional groups and metals can be embodied into organic cations when needed. Thus, the number of organic cations is unlimited, and their functions can be multiple. Quaternary ammonium ions are the most common organic cations in POMs.

On the theoretical level, the aforementioned anions and cations can be associated at random. Owing to the designability of both anions and cations, the properties of POMs can be controlled at the atomic and molecular levels.

1.2. Catalytic Properties

POMs/HPAs have occupied researchers' interests for about two centuries owing to their unique properties. They have been applied to broad fields,⁸ such as catalysis,^{9–13} materials,^{14–16}

and medicine.¹⁷ The application of POMs to catalysis is stimulated by their fascinating properties, including tunable acidity and redox properties, inherent resistance to oxidative decomposition, high thermal stability, and impressive sensitivity to light and electricity. These remarkable properties have a close relationship with their structures and compositions. The well-defined atomic connectivity of POMs provides the compositional diversity required by a rigorous assessment of the consequences of composition on catalytic reactivity.¹⁸ Keggin-type POMs are the most well studied structures in catalysis due to their unique stability. With tempting prospects in industry, these robust catalysts have been studied for decades. To date, several processes with POMs/HPAs as the catalysts have been industrialized, including hydration of propene,¹⁹ isobutene,²⁰ and 2-butene to the corresponding alcohols,²¹ oxidation of isobutyraldehyde with O₂ to isobutyric acid,²⁰ polymerization of tetrahydrofuran,^{22,23} amination of ketones to imines,²⁴ oxidation of ethylene with O₂ to acetic acid,²⁵ and esterification of acetic acid with ethylene to ethyl acetate.²⁶

1.2.1. Active Sites. POMs/HPAs can be viewed as versatile catalysts because of their multiple active sites, including protons, oxygen atoms, and metals. Apparently, protons can act as Brønsted acids to promote acid-catalyzed reactions. Some oxygen atoms on the surface of POM anions, in particular those on the lacunary sites of lacunary POM anions with a high negative charge, are basic enough to react with protons, even to abstract active protons from organic substrates. That is to say, these surface oxygens of POM catalysts can be the active sites in base-catalyzed reactions.

However, most attention should be focused on the metals of POM/HPA catalysts because they are active sites in all oxidative reactions, part acid-catalyzed reactions, and most other reactions. To date, numerous POM/HPA catalysts have been used in oxidative reactions. Nearly all of them are W/Mo-based compounds. For di/tetrานuclear and unsubstituted multinuclear oxo-W/Mo clusters, W/Mo atoms are the active sites and the genuine active species are peroxy-W/Mo groups. For substituted oxo-W/Mo clusters, the case is complicated, depending on the substituting metals. For example, V is the active site in the epoxidation of alkenes with TBA₄[γ -V₂(μ -OH)₂SiW₁₀O₃₈] (TBA₄(γ -V₂SiW₁₀); TBA = (n-C₄H₉)₄N⁺),²⁷ Fe is the active site in the oxidation of alkanes with TBA₄[Fe(H₂O)PW₁₁O₃₉] (TBA₄(FePW₁₁)),²⁸ and Mo is the active site in the oxidation of alcohols with [(C₈H₁₇)₃NCH₃]₄⁻[M^{II}(DMSO)₃Mo₇O₂₄] (M = Ru, Os).²⁹ In Lewis acid-catalyzed reactions, the used POM catalysts are generally those substituted by metals with strong Lewis acidity (e.g., Al, Zr, Hf, Ln, etc.).^{30–32} Thus, the substituting TMs serve as active sites preferentially. In addition, the activities of POM catalysts for Suzuki–Miyaura cross-coupling,³³ 1,3-dipolar cycloaddition of organic azides to alkynes,³⁴ cyclopropanation of alkenes,³⁵ etc. also depend on the type of substituting metal. In a word, several components of POM/HPA catalysts can work as active sites. For a given reaction, the active site depends on the reaction type.

All scientists would like to have catalysts with constant activity. On one hand, measures should be taken to protect the catalyst from the loss of active sites. For example, protons in POM/HPA catalysts are easily lost under high temperature, TMs in POM/HPA catalysts may be poisoned by strong ligands, and, particularly, active sites may leach into solution for heterogeneous POM/HPA catalysts. On the other hand, the

structural stabilities of POM/HPA catalysts should be of concern. This is important for the constant activities in general, but not necessary for every case. Some POMs/HPAs work as catalyst precursors. They may decompose to small active species during the reactions. This point is demonstrated by Ishii's work.⁹

1.2.2. Stability. Also, catalyst stability is a major concern, in part because it impacts catalyst activity and recyclability. The stabilities referring to POM/HPA catalysts usually include thermal stability, hydrolytic stability, and oxidative stability. Those stabilities greatly change depending on the type of POM/HPA catalyst.

Generally, POM/HPA catalysts possess appealing thermal stabilities. Some Keggin-type HPA catalysts are so thermally stable that they are applicable to gas-phase reactions conducted at high temperatures. In the family of saturated Keggin-type HPAs, the thermal stability sequence is $H_3PW_{12}O_{40}$ (H_3PW_{12}) > $H_4SiW_{12}O_{40}$ (H_4SiW_{12}) > $H_3PMo_{12}O_{40}$ (H_3PMo_{12}) > $H_4SiMo_{12}O_{40}$ (H_4SiMo_{12}).³⁶ Keggin-type H_3PW_{12} is much more stable than Dawson-type $H_6P_2W_{18}O_{62}$ ($H_6P_2W_{18}$).¹⁰ However, the high thermal stabilities of POMs/HPAs are relative. For example, H_3PW_{12} loses its protons at 723–743 K to form $\{PW_{12}O_{38.5}\}$, and the structure is completely destroyed at about 873 K.³⁶ Hence, appropriate reaction temperatures are crucial for the systems using the Brønsted acid sites of POM/HPA catalysts, especially for the gas-phase systems conducted at high temperatures, because high temperature will cause the loss of active protons. Additionally, the thermal stabilities are also important for the catalyst regeneration processes. High temperature often leads to coking on the POM/HPA catalyst during the reaction, resulting in the deactivation of the catalyst. Thus, the regeneration of the catalyst involves decoking, which usually needs a high temperature. The appropriate decoking temperature should be lower than the temperature at which the active protons are lost.

Apart from heteroatoms, substituting metals and the counterions significantly affect the thermal stabilities of POMs/HPAs. In general, substituted POM anions are more labile than their unsubstituted parents. For example, V atoms release from the skeleton of $H_{3+n}V_nPMo_{12-n}O_{40}$ ($H_{3+n}V_nPMo_{12-n}$) at elevated temperature, forming monomeric vanadium species and PMo_{12} .^{37,38} The detachment of substituting metals also happens for $[FePMo_{11}O_{39}]^{4-}$ ($FePMo_{11}$).³⁹ However, the detaching temperature is closely related to its counterion. When NH_4^+ is used as the counterion, the release of Fe from the Keggin anion happens at 470 K by the reaction of Fe^{3+} with NH_4^+ , while, when Cs^+ is used as the counterion, release of Fe occurs at 570 K.

POMs/HPAs usually have remarkable hydrolytic stabilities and oxidative stabilities due to the absence of organic ligands. Although the polyhedral subunits of their anions may detach from the skeletons in the presence of water, they are stable in a certain pH range. Many reactions with POM/HPA catalysts can even be conducted in pure water.^{40–48} Moreover, POM anions have strong persistence against oxidants. Thus, this type of catalyst can be used in water- and oxygen-rich systems without the protection of inert gases that is necessary for many organometallic catalysts. The strongest evidence is the oxidations of organic substrates by dilute H_2O_2 ⁴⁹ and the recently booming water oxidation with POM/HPA catalysts.⁴⁸

In a word, the three types of catalyst stability (thermal, hydrolytic, and oxidative stability) are all important, and their

relative importance depends on the type of catalysis and transformation.

1.2.3. Photocatalysis. POM/HPA anions in their ground states can be excited by UV or near-visible light. The essence of excitation is the charge transfer from an oxygen atom to the d^0 TM in the presence of light with abundant energy. For example, the excitation of PW_{12} refers to the charge transfer from O^{2-} to W^{6+} , leading to the formation of a hole center (O^-) and trapped electron center (W^{5+}) pair.⁵⁰ The excited POM/HPA anions usually show better performance than their ground states, as both electron donors and electron acceptors.⁵¹ Thus, some POMs/HPAs, which are catalytically inactive under dark conditions, even when a high reaction temperature is employed, may become powerful reagents capable of oxidizing or reducing a variety of substrates under the irradiation of UV or near-visible light. In addition, the well-defined HOMO–LUMO band gaps of POM/HPA anions inhibit the recombination of electrons and holes generated by the irradiation of light energy higher than or equal to their band gap energy.⁵⁰ Thus, the photogenerated electrons and holes are capable of initiating the chemical reaction due to the strong photooxidative ability of the holes and photoreductive ability of the electrons. Under mild conditions, many photocatalytic reactions proceed readily in the presence of POMs/HPAs, including the oxidation of alcohols,^{52–54} benzene,⁵⁵ and phenol,⁵⁶ the oxidative bromination of arenes and alkenes,⁵⁷ the reduction of CO_2 ,^{58,59} etc. More importantly, the photooxidation properties are very useful for the degradation of various aqueous organic pollutants,^{60–70} and the photoreduction properties can be used to remove inorganic TM ions from water.⁷¹ In addition, Marci et al. found some HPA catalysts are also active for photoassisted propene hydration.^{72,73}

In 2012, Streb et al. reviewed new trends in POM photoredox chemistry.⁷⁴ As shown by the review, homogeneous POM/HPA photocatalysts have several advantages besides the facile photoexcitation using UV or near-visible light, including strong light absorption with high molecular absorption coefficients ($\epsilon > 1 \times 10^4 M^{-1} L^{-1}$), high redox activity, high structural stability, a multielectron redox property, and easy reoxidation of reduced species. However, an important issue is that the light absorption by POM/HPA anions generally only occurs in the region of 200–500 nm. Thus, photosensitization might be employed as one strategy to allow the use of visible light. Some photosensitizers, such as fullerene, can be covalently attached to POM/HPA anions; some cationic photosensitizers can be associated with POM/HPA anions via electrostatic interaction.

With the purpose of application, emphasis in the field of photocatalysis by POMs/HPAs is given to heterogeneous POM/HPA photocatalysts. Parent POMs/HPAs are usually supported on other materials to form composite heterogeneous photocatalysts. The most used supports are TiO_2 ,^{75–79} SiO_2 ,^{63,80–84} ZrO_2 ,^{85,86} etc. Besides the solidification of POMs/HPAs, the combination of POMs/HPAs with supports provides POMs/HPAs with much larger specific surface areas, which may increase their catalytic activities by providing large contact areas between the catalysts and substrates for the surface-mediated electron-transfer reactions.⁹ In addition, with semiconductor metal oxides as the supports, the combination can create improved photoactivities due to the synergistic effect between the two parts.^{85,87,88} Another series of heterogeneous POM photocatalysts are acidic Cs salts $Cs_xH_{3-x}PW_{12}$ ($x \leq 3$),

which have porous structures, relatively high surface areas, and strong acid sites. $\text{Cs}_3\text{PW}_{12}$ is the first heterogeneous POM photocatalyst used for photooxidation of propan-2-ol to acetone in an aqueous solution.⁸⁹ Guo's group has contributed many publications to the field of POM/HPA-based heterogeneous photocatalysts. Detailed content can be seen in their review paper and the cited references.⁹⁰ Recently, Marci's group⁹⁰ and Yoon's group⁹¹ also reviewed POM/HPA-based heterogeneous photocatalysts. Thus, this review will not introduce related content in detail.

1.2.4. Electrocatalysis. Owing to the high oxidation states of M in peripheral metal–oxygen polyhedra of MO_x , POM/HPA anions undergo several rapid one- and two-electron reversible reductions, and further irreversible multielectron reductions with concomitant decomposition.¹¹ If all M atoms are identical, the electrons are delocalized on all MO_x at room temperature by rapid intramolecular electron transfer. The reduction increases the negative charge density at the POM/HPA anions and thus their basicity. As a consequence, the reduction can be accompanied by protonation depending on the pK_a of the produced anions. Thus, the potentials of the reversible redox pairs of POM/HPA anions are affected significantly by the pH. In such a neutral aqueous or organic solution where no protonation can occur, both Keggin- and Dawson-type POM/HPA anions may undergo several one-electron reductions.¹⁰ Thus, several Keggin- and Dawson-type POMs/HPAs have been applied as reductive and oxidative electrocatalysts. Notice that each POM/HPA exhibits featured electrochemical behavior because of its specific redox potential, pK_a , and stability. As for Keggin-type heteropolytungstates and heteropolymolybdates, the reducibility increases in the sequence α -, β -, and γ -isomers; the reduction potential of the one-electron waves becomes more negative when the valence of the heteroatom decreases.

In 1998, Steckhan et al. elegantly introduced the electrochemical properties of POMs/HPAs as electrocatalysts.¹¹ Since then, great developments in POM/HPA-based electrocatalysis have been made by chemists. Nadjo et al. reviewed POM/HPA-based homogeneous catalysis of electrode reactions.⁹² Thus, the present review will not provide an exhaustive coverage of POM/HPA-based electrocatalysts. However, some important examples will be introduced in the following sections.

1.2.5. Homogeneous and Heterogeneous Catalysis with POMs/HPAs. POMs/HPAs can be used as both homogeneous and heterogeneous catalysts. Pure HPAs are often used as homogeneous catalysts owing to their good solubilities in water or organic solvents. In comparison with HPAs, most POMs, especially those with large inorganic counterions, have lower solubilities. To obtain good solubilities in organic solvents, organic cations with suitable alkyls are often introduced as the counterions of the POM/HPA anions. In general, homogeneous systems are characterized by high efficiency owing to the plenary exposure of the active sites of the catalysts to the substrates and thus frequent collision between the active sites and the substrates. In homogeneous catalysis with HPAs/POMs, the research focuses on the molecular design of new catalysts to govern their inherent properties by introducing specific components into the polyanions or by changing the arrangement patterns of the polyanions.

The research method of heterogeneous POM/HPA catalysts is quite different from that of homogeneous ones. In heterogeneous catalysis with HPAs/POMs, emphasis is given

to the solidification of POM/HPA catalysts, to achieve good recovery and recyclability besides high activity. Several methods have been used to solidify active soluble POMs/HPAs, including the introduction of large inorganic cations and dendritic organic cations, encapsulation by MOFs (metal organic frameworks), and combination with supporting materials, such as various C/Si-based materials, metal oxides, polymers, etc. Another important difference between the homogeneous and the heterogeneous systems with POM/HPA catalysts is their reaction fields. The homogeneous reactions happen in the solution because POM/HPA catalysts uniformly distribute in the solution. However, the case for heterogeneous reactions is quite complicated. There are three completely different catalysis modes for heterogeneous POM/HPA catalysts, that is, surface-type catalysis, pseudoliquid bulk-type catalysis, and bulk-type catalysis in the presence of electrons or protons (Figure 1).⁹³ Surface-type catalysis takes

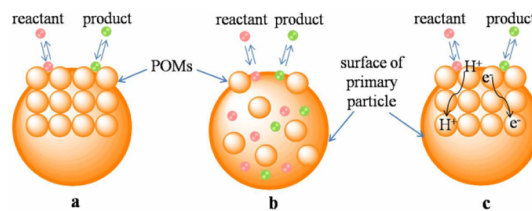


Figure 1. Three catalysis models for solid POM catalysts: (a) surface type; (b) pseudoliquid bulk type; (c) bulk type.

place on the outer surface of heterogeneous POM/HPA catalysts (Figure 1a). POM/HPA catalysts provide the reactions with a two-dimensional reaction field.⁹³ For pseudoliquid bulk-type catalysis and bulk-type catalysis, the reaction fields are three-dimensional (Figure 1b,c). In a three-dimensional field, the reactions proceed as in solution. Thus, POM/HPA catalysts often exhibit high catalytic activities and unique selectivities in heterogeneous catalysis. When the diffusion of reactant molecules in the lattice of the solid is faster than the reaction, the solid bulk forms a pseudoliquid phase where catalysis happens (Figure 1b). In this model, POM/HPA catalysts appear as solids but behave like liquids (solvent). As the active sites in the solid bulk, e.g., protons, participate in catalysis, very high catalytic activities can be achieved in the bulk phase (Figure 1c). For some heterogeneous POM/HPA catalysts with a flexible nature, polar or basic reactant molecules are readily absorbed into the solid lattice and react therein.

POMs have also been modified into surfactant-type catalysts by several research groups. Some of these surfactant-type catalysts feature automatic behavior. They are sensitive to temperature, chemicals, or light. Temperature-controlled catalysts are homogeneous during the reaction with elevated temperature and precipitate from the reaction solution when the temperature drops. For chemical-controlled catalysts, when some chemical exists in the reaction mixture, the catalysts are soluble; once the specific chemical is used up, the catalysts precipitate from the solution. The automatic behaviors endow these catalysts with the advantages of homogeneous catalysts and heterogeneous catalysts. Besides, some surfactant-type catalysts exhibit interesting self-assembly behavior and create emulsive systems, especially in H_2O_2 -based oxidation reactions. These catalysts are very useful for deep oxidative desulfurization of oil.

1.2.6. Overview of POM/HPA-Catalyzed Reactions. In recent years, the dominative reports on POM/HPA catalysts have been those related to chemical oxidation, photochemical oxidation, electrochemical oxidation, and acid catalysis, but the reports are not limited to these. Reduction reactions, base-catalyzed reactions, and other new reactions are also boosted by versatile POM/HPA catalysts. As for oxidation reactions of organic compounds, the oxygenation of alkenes and alkanes receives the most attention. In the case of acid catalysis, many classical reactions such as condensation reaction, Fried–Crafts reaction, isomerization reaction, amination reaction, cracking reaction, etc. are improved by POM/HPA catalysts. In the above reactions, POM/HPA catalysts often lead to interesting results, including unique chemoselectivity, regioselectivity, and stereoselectivity. Most recently, publications on water splitting to oxygen and/or hydrogen with POM catalysts have sprung up with the increasing demand of clean energy. The remarkable redox properties of POM catalysts guarantee their activities. In addition, POMs have good persistence against oxidants and are hydrolytically stable in a certain pH range. Thus, they can survive in oxygen- and water-rich environments.

Although the application of POM/HPA catalysts in organic reactions is a relatively mature field, it continues to be attractive. The reasons are as follows: (1) POMs/HPAs are highly efficient; (2) POMs/HPAs are resistant to oxidative degradation and hydrolysis; (3) POMs/HPAs can stabilize metal ions that are unstable in air; (4) POMs/HPAs are environmentally benign.

In 1998, Kozhevnikov et al. reviewed POM/HPA-catalyzed liquid-phase reactions,⁹ Misono et al. reviewed POM/HPA-based heterogeneous catalysts,¹⁰ and Steckhan et al. reviewed POM/HPA-based electrocatalysts.¹¹ After that, several reviews on the subject of POM/HPA catalysis were also published. Besides the aforementioned reviews on this subject, Lubánska et al. reviewed the application of POM/HPA catalysts in the synthesis of tertiary ethers MTBE (methyl *tert*-butyl ether) and ETBE (ethyl *tert*-butyl ether),⁹⁴ Mizuno et al. reviewed catalytic oxidation of hydrocarbons with H₂O₂ as the oxidant and vanadium-based POMs as the catalysts,⁴⁹ Hill et al. reviewed POM-catalyzed water oxidation,^{48,95} Sun et al. reviewed POM/HPA-based catalytic oxidation of light alkanes,⁹⁶ and Kozhevnikov et al. reviewed Friedel–Crafts acylation and related reactions catalyzed by HPAs.⁹⁷ In addition, recent reviews concerning the syntheses, the properties, and the applications of POMs are also available.^{98–105} However, most of the reviews concerning HPA/POM catalysis focus on the traditional oxidative reactions or acid-catalyzed reactions. The newly developed reactions with POM/HPA catalysts draw negligible attention of reviewers. In this review, we summarize the development of POM/HPA catalysts in the past 15 years in a more comprehensive manner, with reaction types as a clue.

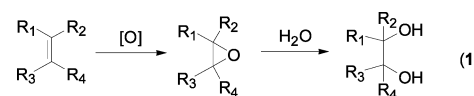
2. OXIDATION

Oxidation is one of the most important chemical processes. It not only affords various useful organic blocks bearing versatile functional groups, such as hydroxyl, carbonyl, and carboxyl, but also provides a feasible route to a clean environment. Traditional oxidative processes usually employ strong oxidants such as peroxy acids, HNO₃, and HIO₄, which produce large amounts of wastes. With increasing demands for a clean environment, green oxidants H₂O₂ and O₂ are used as the terminal oxygen source in current oxidative processes, producing H₂O as the sole byproduct. However, such oxidative

processes often need catalysts. Metal catalysts are the most attractive choice. Organometallic catalysts are popular in organic reaction, but they are disadvantaged by their oxidative and hydrolytic instability in H₂O₂- and O₂-based systems. In contrast, POMs are preponderant catalysts due to their notable redox properties, strong persistence against oxidants, and environmental compatibility. The combinations of POM catalysts and green oxidants can not only oxygenate the C sites in alkenes, aromatic rings, and even inert aliphatic alkanes, but also oxygenate the S sites and N sites in organic compounds.

2.1. Oxidation of Alkenes

2.1.1. To Epoxides. Initial oxidation of alkenes usually provides epoxides that pellucidly undergo hydrolysis to diols in the presence of water (eq 1). Although both epoxides and diols



are of great importance, high selectivity for one of them in a reaction is expected, especially for epoxides. However, the objective is impeded by the existence of water. Venturello–Ishii systems are famous for the epoxidation of alkenes with POM catalysts and H₂O₂ oxidant.^{106–108} At first, Venturello et al. carried out alkene epoxidation in biphasic systems with tungstate and phosphate ions as the catalyst precursors and H₂O₂ as the oxygen donor. To increase the accessibility of lipophilic alkenes to the aqueous soluble catalyst precursors, the salts of quaternary ammonium modified by long-chain alkyl groups (C₆–C₁₈) were introduced into the systems as phase-transfer agents. Under the reaction conditions, tungstate reacts with phosphate to form a peroxy intermediate, {PO₄[WO(O₂)₂]₄}³⁻, which has been isolated and characterized crystallographically. The isolated peroxy complex is active for the epoxidation of alkenes under analogous conditions, and is thus postulated to be the active oxygen-transfer species. Ishii et al. also put much effort into Venturello–Ishii systems.⁹ They initially used H₃PW₁₂ or H₃PMo₁₂ as the catalyst precursor and H₂O₂ as the oxidant. Again, ammonium salts with long-chain alkyls were combined as phase-transfer agents. In these protocols, the selectivities for epoxides are deteriorated in spades due to the presence of highly active protons in the catalysts, which accelerate the hydrolysis of epoxides. In this context, quaternary ammonium cations with long-chain alkyls are introduced into the catalyst precursors to replace the protons. As a result, the catalyst precursors contain a catalytically active moiety and a phase-transfer moiety. Thus, the organic–inorganic hybrids simultaneously act as the catalyst and phase-transfer agent. Taking [π-C₅H₅N(CH₂)₁₅CH₃]₃PW₁₂ as an example, it can be easily prepared by reacting inorganic H₃PW₁₂ with organic [π-C₅H₅N(CH₂)₁₅CH₃]Cl, and effectively accelerates the oxidation of alkenes in biphasic systems using CHCl₃ as the solvent and H₂O₂ as the oxidant. In the presence of H₂O₂, polyanions [PM₁₂O₄₀]³⁻ (M = W, Mo) decompose into a variety of peroxy complexes, including {PO₄[MO(O₂)₂]₄}³⁻. These peroxy species are preferentially formed in the aqueous phase and transfer oxygen atoms to alkenes in the organic phase with the aid of long-tailed quaternary ammonium cations. In Venturello–Ishii systems, tungsten-based catalysts are usually superior to molybdenum-based ones. The result may be caused by the reactivity

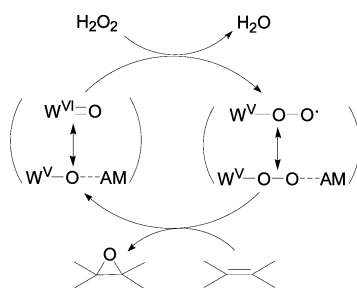
difference between $\{\text{PO}_4[\text{WO}(\text{O}_2)_2]_4\}^{3-}$ and $\{\text{PO}_4[\text{MoO}(\text{O}_2)_2]_4\}^{3-}$.

In the early years, epoxidation systems with POMs as the catalysts and O_2 as the oxygen donor were also published.⁹ In these systems, aldehydes are usually needed as sacrificial agents because of the relatively low reactivity of O_2 . They initially react with O_2 to form peroxy acids and evolve to carboxylic acids at the end of the reactions. Although such systems are effective for alkene oxidation, they have been ignored somewhat in recent years because of the following disadvantages: (1) aldehydes are used as sacrificial agents, negating the superiority of using O_2 , an environmentally and economically benign oxidant; (2) the reactions undergo a free radical mechanism, tending to yield complicated byproducts and thus entangle operators in tedious product separation problems.

To exploit the applicable value of the effective anion PW_{12} and derived peroxy complex $\{\text{PO}_4[\text{WO}(\text{O}_2)_2]_4\}^{3-}$, many operations have been carried out in recent years. In 2003, the aqueous soluble peroxy species $\{\text{PO}_4[\text{WO}(\text{O}_2)_2]_4\}^{3-}$ was used to construct an efficient water-in-oil microemulsion system for alkene epoxidation.¹⁰⁹ Coupled with ultrafiltration, it shows potential application in continuous production of epoxides. The assembly of $\{\text{PO}_4[\text{WO}(\text{O}_2)_2]_4\}^{3-}$ with dendritic quaternary ammonium cations by ionic bonding yields supramolecular catalytic materials that work as recoverable and reusable heterogeneous catalysts.^{110–112} The use of $[\text{Bmim}]_3\text{PW}_{12}$ ($\text{Bmim} = 1\text{-butyl-3-methylimidazolium}$) in ionic liquid (IL) reveals that IL can enhance the turnover frequency (TOF) and the selectivity of the reaction.¹¹³ It is pointed out that the Venturello complex, $\{\text{PO}_4[\text{WO}(\text{O}_2)_2]_4\}^{3-}$, is still the active species in IL.

Wang's group made an efficient heterogeneous catalyst by protonating and anion-exchanging amino-attached cations with H_3PW_{12} .¹¹⁴ The resulting ionic hybrid nanospheres have advantages of convenient recovery, steady reuse, simple preparation, and flexible composition. The strong interaction between amino on the cation and oxygen on the surface of the anion has a great impact on the catalytic nature of PW_{12} , and consequently opens up a unique reaction pathway (Scheme 1)

Scheme 1. Proposed Epoxidation Mechanism with the Amino-Functionalized Hybrid Nanospheres¹¹⁴



that is different from the Venturello complex pattern. Initially, $\text{W}=\text{O}$ reacts with H_2O_2 to form a tungsten peroxy radical ($\text{W}-\text{O}-\text{O}\cdot$) that may be nonselective for epoxidation. The amino stabilizes the peroxy radical by bonding the single electron of $\text{W}-\text{O}-\text{O}\cdot$ with the delocalized electron from amino to form a unique amino-stabilized terminal tungsten-peroxy transition structure ($\text{W}-\text{O}-\text{O}\cdots\text{AM}$), which should account for the excellent catalytic performance of the hybrid nanospheres. In the process, the bonding of amino with oxygen is reversible.

To obtain more heterogeneous POM catalysts, the polyanion PW_{12} is chemically immobilized on supports. Modified silica with a diverse silica-surface morphology and surface-modification agents are the most used supports. The performance of this kind of POM catalyst can be improved by finely tuning the silica-surface morphology and the surface-modification agents. The catalyst PW_{12} immobilized on modified hydrophobic mesoporous silica gel gives >97% yields of epoxides for several alkenes, including nonactivated aliphatic terminal alkenes, using 15% H_2O_2 under neat conditions.¹¹⁵ Although the reactions are conducted with diluted H_2O_2 at relatively high temperatures ranging from 343 to 363 K, no significant hydrolysis of epoxides or cleavage of $\text{C}=\text{C}$ bonds occurs.

A remarkable achievement in alkene epoxidation with a multinuclear tungstate catalyst was documented by Xi's group in 2001.¹¹⁶ The insoluble salt $[\pi\text{-C}_5\text{H}_5\text{NC}_{16}\text{H}_{33}]_3[\text{PO}_4(\text{WO}_3)_4]$ exhibits an exciting reaction-controlled phase-transfer nature in H_2O_2 -mediated systems. It converts into a soluble peroxy complex, $[\pi\text{-C}_5\text{H}_5\text{NC}_{16}\text{H}_{33}]_3[\text{PO}_4[\text{WO}_2(\text{O}_2)]_4]$, the assumed active species, in the presence of H_2O_2 in organic solvents. Once H_2O_2 is used up, the active peroxy species returns to its initial insoluble form for easy recycling. The IR spectral analysis indicates that the insolubility of fresh $[\pi\text{-C}_5\text{H}_5\text{NC}_{16}\text{H}_{33}]_3[\text{PO}_4(\text{WO}_3)_4]$ and recovered catalyst is caused by the intermolecular interaction of W atoms with the O atoms on another molecule. Therefore, the fresh catalyst and the recovered catalyst exist in the form of complicated polymeric states. This behavior may be led by the lack of O atoms in a single molecule of $[\pi\text{-C}_5\text{H}_5\text{NC}_{16}\text{H}_{33}]_3[\text{PO}_4(\text{WO}_3)_4]$. In the presence of H_2O_2 , W atoms are coordinated to the O atoms of H_2O_2 , resulting in the depolymerization of the polymeric structures and the formation of a soluble intermediate, $[\pi\text{-C}_5\text{H}_5\text{NC}_{16}\text{H}_{33}]_3[\text{PO}_4[\text{WO}_2(\text{O}_2)]_4]$. The system takes advantage of both homogeneous and heterogeneous catalysts through reaction-control properties of the catalyst; namely, it is efficient, recoverable, and recyclable. The ratiocination is manifested by the selective epoxidation of propylene and other alkenes, including linear terminal alkenes, internal alkenes, cyclic alkenes, styrene, and allyl chloride. Notably, when coupled with the 2-ethyl-anthraquinone/2-ethylanthrahydroquinone redox process for H_2O_2 production in situ, O_2 can be used for the epoxidation of propylene without any byproducts. Li's group understood the catalyst behaviors in detail through FT-IR, Raman, and ^{31}P NMR spectroscopy.¹¹⁷ FT-IR spectra indicate that the interaction between the anion and the cation is changed in the reaction process. The ^{31}P NMR monitor did not trap the assumed active species $\{\text{PO}_4[\text{WO}_2(\text{O}_2)]_4\}^{3-}$, probably due to its high reactivity. However, it reveals that $\{\text{PO}_4[\text{WO}_2(\text{O}_2)]_4\}^{3-}$ is not the single species derived from $[\text{PO}_4(\text{WO}_3)_4]$; other peroxy species such as $\{\text{PO}_4[\text{WO}(\text{O}_2)_2]_4\}^{3-}$, $\{\text{PO}_4[\text{WO}(\text{O}_2)_2]_2[\text{WO}(\text{O}_2)_2(\text{H}_2\text{O})]\}^{3-}$, and $\{[\text{PO}_3(\text{OH})][\text{WO}(\text{O}_2)_2]\}^{2-}$ are also formed during the reaction. These peroxy species result from the depolymerization and degradation of the fresh catalyst in the presence of H_2O_2 . When H_2O_2 is used up, the catalyst precipitates spontaneously due to the polymerization of these smaller anions to larger ones.

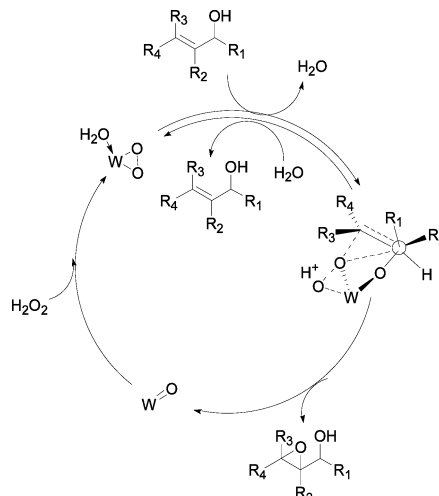
The dinuclear peroxtungstate $\text{K}_2\{[\text{WO}(\text{O}_2)_2(\text{H}_2\text{O})]_2(\mu\text{-O})\}\cdot 2\text{H}_2\text{O}$, which is intrinsically stable in the pH range of 2.5–7 is robust in the selective epoxidation of allylic alcohols with H_2O_2 in water at 305 K (Table 1).⁴⁰ The reactions with $\text{K}_2\{[\text{WO}(\text{O}_2)_2(\text{H}_2\text{O})]_2(\mu\text{-O})\}\cdot 2\text{H}_2\text{O}$ exhibit remarkable chemoselectivity, stereoselectivity, and regioselectivity. The hydroxyl group on the substrate is impregnated. When 2-

Table 1. Selective Epoxidation of Allylic Alcohols with $K_2\{[WO(O_2)_2(H_2O)]_2(\mu-O)\} \cdot 2H_2O$

| Allylic alcohol | Product | Yield (%) | Ref. |
|-----------------|-------------------------|-----------|------|
| | | 95 | 40 |
| | | 96 | 40 |
| | | 97 | 40 |
| | | 90 | 40 |
| | | 98 | 40 |
| | | 85 | 40 |
| | erythro:threo=6:94 | 85 | 40 |
| | erythro:threo=76:24 | 83 | 40 |
| | erythro:threo=62:38 | 83 | 119 |
| | erythro:threo=66:34 | 77 | 119 |

propen-1-ol is selected as a model substrate, 96% conversion, 99% selectivity for 2,3-epoxy-1-propanol, and 97% efficiency of H_2O_2 utilization are achieved. For the epoxidation of *cis*- and *trans*-allylic alcohols, the configurations around the C=C moieties are retained in the corresponding epoxy alcohols. Regioselective epoxidation of 3,7-dimethyl-2,6-octadien-1-ol happens at the electron-deficient allylic 2,3-double bond to afford only 2,3-epoxy alcohol in high yield. Additionally, ring opening of epoxides to diols is invisible in all cases, although water is used as the reaction medium. Notably, the catalyst can be easily recycled by extraction while maintaining its catalytic performance, and water is the most effective solvent. Thus, the present system provides an environmentally benign methodology to epoxide production. The immobilization of $\{[WO(O_2)_2(H_2O)]_2(\mu-O)\}^{2-}$ on IL covalently modified silica via electrostatic interactions creates an inherently heterogeneous catalyst, whose reactivity is comparable to that of the corresponding homogeneous analogue $[n-C_{12}H_{25}N(CH_3)_3]_2\{[WO(O_2)_2(H_2O)]_2(\mu-O)\}$.¹¹⁸ The heterogeneous catalyst can be easily recovered by filtration and reused at least three times without loss of the catalytic activity and selectivity. The mechanism insight reveals that the water ligands in the catalyst play a pivotal role in the epoxidation processes of allylic alcohols (Scheme 2).¹¹⁹ They initially exchange with the substrate to form tungsten–alcoholate species. Then oxygen is inserted into the C=C bond, followed by the regeneration of the catalyst by H_2O_2 . The oxygen transfer from the dinuclear peroxotungstate to the double bond is considered as the rate-limiting step for a terminal allylic alcohol such as 2-propen-1-ol. The hydroxyl on the substrate is helpful for the process but not essential. The substrates without hydroxyl are also converted into the corresponding epoxides in the presence of $\{[WO(O_2)_2(H_2O)]_2(\mu-O)\}^2$.¹¹⁸

Scheme 2. Proposed Mechanism of Allylic Alcohol Epoxidation with $K_2\{[WO(O_2)_2(H_2O)]_2(\mu-O)\}$ ¹¹⁹



The congener dinuclear peroxotungstate without a water ligand, $\{(n-C_3H_7)_4N\}_2\{[WO(O_2)_2]_2(\mu-O)\}$, is almost inactive for alkene epoxidation with 30% H_2O_2 at 305 K.¹²⁰ However, the reaction rates increase linearly with the addition of H^+ ions into the system and do not change much upon addition of 0.5 equiv or more of H^+ ions. The catalyst activity is enhanced by around 60-fold finally. The enhancement of activity presages the formation of a new peroxotungstate intermediate in the presence of H^+ ions, which is servable for alkene epoxidation. The intermediate has been isolated from the mixture of $\{(n-C_3H_7)_4N\}_2\{[WO(O_2)_2]_2(\mu-O)\}$ and HNO_3 , and characterized structurally by X-ray analysis (Figure 2a). The anionic part of

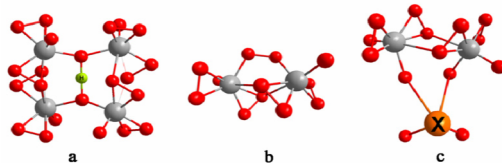


Figure 2. Structures of (a) $\{H[W_2O_2(O_2)_4(\mu-O)]_2\}^{3-}$, (b) $\{[WO(O_2)_2]_2(\mu-O_2)\}^{2-}$, and (c) $\{XO_4[WO(O_2)_2]_2\}^{2-}$

the new structure consists of two $\{[WO(O_2)_2]_2(\mu-O)\}$ units. The signal at 15.8 ppm in the 1H NMR spectrum is indicative of the existence of a proton with strong intramolecular hydrogen bonds ($O-H\cdots O$) in the structure. Thus, the tetranuclear oxotungsten cluster is formulated as $\{H-[W_2O_2(O_2)_4(\mu-O)]_2\}^{3-}$. In the presence of the tetranuclear oxotungsten cluster, various alkenes without any functional group are selectively oxidized to the corresponding epoxides at low temperature (Table 2).¹²⁰ It engenders a higher TOF than the di- and tetranuclear peroxotungstates with XO_4^{n-} ligands ($X = Se, S, As, P, Si$). It has been reported that, in the d^0 TM-catalyzed epoxidation, the metal centers function as Lewis acids by withdrawing electrons from the peroxy bond ($O-O$), and their oxidation states are not changed during the catalysis.^{121–123} Apparently, active catalysts are those containing metal centers with strong Lewis acidity. Thus, the improved activity of $\{H[W_2O_2(O_2)_4(\mu-O)]_2\}^{3-}$ can be ascribed to the increased Lewis acidity of the tungsten sites rising from the presence of the proton. Strong Lewis acidity makes the electrophilic oxygen transfer from peroxotungstate to substrate

Table 2. Selective Alkene Epoxidation with $[(n\text{-C}_3\text{H}_7)_4\text{N}]_3\{\text{H}[\text{W}_2\text{O}_2(\text{O}_2)_4(\mu\text{-O})]_2\}$ ¹²⁰

| Alkene | Product | Yield (%) |
|--------|---------|-----------|
| | | 81 |
| | | 77 |
| | | 92 |
| | | 94 |
| | | 71 |
| | | 77 |
| | | 74 |
| | | 93 |
| | | 72 |

easier. A similar reactivity improvement also happens for $[\text{HDIm}]_2\{[\text{WO}(\text{O}_2)_2]_2(\mu\text{-O})\}$ (HDIm = protic *N*-dodecylimidazolium).¹²⁴ The protic catalyst readily catalyzes alkene epoxidation with a reaction-controlled phase-separation nature, while the absence of an active proton in the cations makes the catalyst more inert.

The catalytic performance of $\{[\text{WO}(\text{O}_2)_2]_2(\mu\text{-O})\}^{2-}$ is also improved by concentrated H_2O_2 , although it is inert in the presence of 30% H_2O_2 at low temperature.¹²⁵ In the system without an active proton, $\{[\text{WO}(\text{O}_2)_2]_2(\mu\text{-O})\}^{2-}$ can be oxidized to an energetic $\mu\text{-}\eta^1\text{:}\eta^1$ -peroxo-bridging dinuclear tungsten species, $\{[\text{WO}(\text{O}_2)_2]_2(\mu\text{-O}_2)\}^{2-}$ (Figure 2b), by 97% H_2O_2 under nonaqueous conditions. The low XSO (XSO = (nucleophilic oxidation)/(total oxidation)) value of $\{[\text{WO}(\text{O}_2)_2]_2(\mu\text{-O}_2)\}^{2-}$ in comparison with that of $\{[\text{WO}(\text{O}_2)_2]_2(\mu\text{-O})\}^{2-}$ for the stoichiometric oxidation of thianthrene 5-oxide reveals that $\{[\text{WO}(\text{O}_2)_2]_2(\mu\text{-O}_2)\}^{2-}$ is more electrophilic than $\{[\text{WO}(\text{O}_2)_2]_2(\mu\text{-O})\}^{2-}$. It energetically oxidizes several alkenes to the corresponding epoxides. However, the selectivity for allylic alcohol epoxidation is lower than that with $\text{K}_2\{[\text{WO}(\text{O}_2)_2(\text{H}_2\text{O})]_2(\mu\text{-O})\}\cdot 2\text{H}_2\text{O}$.

The magnetic separation of a water-lacking anion, $\{[\text{WO}(\text{O}_2)_2]_2(\mu\text{-O})\}^{2-}$, is realized by covering a magnetic Fe_3O_4 core with IL-modified silica, and immobilizing the anion on the outer shell of the silica shell via electrostatic interaction.¹²⁶ The modification of silica with IL is achieved via hydrogen bonding or a covalent Si–O linkage. The resulting catalysts exhibit essentially constant high activity at 333 K, even after 10 consecutive cycles. The improvement enables the catalyst to be separated conveniently with the aid of an external magnetic field. The method of attaching an IL to silica by hydrogen bonds allows a much easier tuning of the necessary IL amount, and certainly opens a new way toward a facile and rational strategy in creating excellent heterogeneous catalysts.

With the purpose of tuning the reactivity of dinuclear peroxotungstate, XO_4^{n-} groups are usually introduced into the

structure. The nature of the heteroatoms X in the ligands is crucial in increasing the Lewis acidity of the active tungsten sites. The electrophilic oxygen transfer reactivity of $\mu_2\text{-}\eta^2\text{:}\eta^1$ -type peroxy complexes $\{\text{XO}_4[\text{WO}(\text{O}_2)_2]_2\}^{2-}$ (Figure 2c) has been researched extensively. According to the paper by Brégeault, the sulfate species $\{\text{SO}_4[\text{WO}(\text{O}_2)_2]_2\}^{2-}$ is the most active one among three $\{\text{XO}_4[\text{WO}(\text{O}_2)_2]_2\}^{2-}$ catalysts ($\text{X} = \text{HAs, HP, S}$).¹²⁷ Latterly, the research on $\{\text{XO}_4[\text{WO}(\text{O}_2)_2]_2\}^{n-}$ ($\text{X} = \text{As, P, S, Se, Si}; n = 2, 3, 4$) highlighted that SeO_4^{2-} significantly activates the dimeric peroxotungstate unit $[\text{WO}(\text{O}_2)_2]_2$ in $\text{TBA}_2\{\text{SeO}_4[\text{WO}(\text{O}_2)_2]_2\}$ because of its weak coordination to tungsten.^{128,129} The catalytic activity of $\{\text{XO}_4[\text{WO}(\text{O}_2)_2]_2\}^{2-}$ decreases in the sequence $\text{Se} > \text{S} > \text{As} > \text{P} > \text{Si}$, in line with that of the pK_a values of H_nXO_4 . This sequence suggests that the strongest Lewis acidity of W atoms in $\{\text{SeO}_4[\text{WO}(\text{O}_2)_2]_2\}^{2-}$ results in the highest activity for alkene epoxidation. With $\text{TBA}_2\{\text{SeO}_4[\text{WO}(\text{O}_2)_2]_2\}$, diverse homoallylic and allylic alcohols transfer into the corresponding epoxides. The TOF reaches up to 150 h^{-1} in the case of a 10 mmol scale epoxidation of *cis*-3-hexen-1-ol, which is one of the highest values among those reported for TM-catalyzed epoxidation of homoallylic alcohols with H_2O_2 . Unlike that with $\text{K}_2\{[\text{WO}(\text{O}_2)_2(\text{H}_2\text{O})]_2(\mu\text{-O})\}\cdot 2\text{H}_2\text{O}$,¹¹⁹ the reaction proceeds without the formation of tungsten–alcoholate species. The transition state is stabilized by the hydrogen bond between $\text{TBA}_2\{\text{SeO}_4[\text{WO}(\text{O}_2)_2]_2\}$ and hydroxyl groups on the substrates. However, the substrates without hydroxyls are also reactive in such systems,¹²⁹ suggesting that the double bond can interact with catalyst without the assistance of a hydrogen bond or hydroxyl groups.

In the past 15 years, the divacant Keggin-type polyanion $[\gamma\text{-SiW}_{10}\text{O}_{36}]^{8-}$ ($\gamma\text{-SiW}_{10}$) has received much attention in the field of catalysis. Generally, it is used as a catalyst precursor or a “structural motif”. The catalyst $\gamma\text{-H}_4\text{SiW}_{10}$, prepared by protonating $\gamma\text{-SiW}_{10}$ at pH 2, exhibits fascinating catalytic performance for the epoxidation of various alkenes with H_2O_2 at 305 K.¹³⁰ The advantages of this catalyst are evidenced by $\geq 99\%$ selectivity for epoxide, $\geq 99\%$ H_2O_2 utilization efficiency, high stereospecificity, and easy recovery of the catalyst from the homogeneous reaction mixture. Notably, in the case of the epoxidation of nonactivated aliphatic terminal $\text{C}_3\text{–C}_8$ alkenes, such as propylene, 1-butene, 1-hexene, and 1-octene, the corresponding epoxides are formed readily with about 90% yield and $\geq 99\%$ selectivity. No isomerization and cleavage of the double bond and hydration of the corresponding epoxides occur in the epoxidation process. For the epoxidation of *cis*- and *trans*-2-octenes, the configurations around the $\text{C}=\text{C}$ moieties are retained in the corresponding epoxides, and *cis*-2-octene is epoxidized much faster than the *trans*-isomer. In the competitive epoxidation of *cis*- and *trans*-2-octenes, the ratio of the formation rate of *cis*-2,3-epoxyoctane to that of the *trans*-isomer ($R_{\text{cis}}/R_{\text{trans}}$) is 11.5. The high stereospecific reactivity is contributed by a structurally rigid, nonradical oxidant generated on the divacant lacunary site of $\gamma\text{-H}_4\text{SiW}_{10}$. For nonconjugated dienes, $\gamma\text{-H}_4\text{SiW}_{10}$ shows a specific regioselectivity owing to the electronic and steric natures of the generated active oxidant, different from those with peroxotungstates $\{\text{PO}_4[\text{WO}(\text{O}_2)_2]_4\}^{3-}$ and $[\text{W}_2\text{O}_3(\text{O}_2)_4(\text{H}_2\text{O})]^{2-}$.^{131,132} Exemplarily, in the epoxidation of 7-methyl-1,6-octadiene and 4-vinyl-1-cyclohexene with $\gamma\text{-H}_4\text{SiW}_{10}$, the $\text{C}=\text{C}$ moieties with higher electron density are epoxidized regioselectively to give the corresponding monoepoxide without the successive epoxidation of the other $\text{C}=\text{C}$ fragment, while, in the epoxidation of 1-

methyl-1,4-cyclohexadiene, the more accessible but less nucleophilic double bond is much more selectively epoxidized, and the ratio of 4,5-epoxide to total epoxides is 0.89. The generated active oxidant from the reaction between $\gamma\text{-H}_4\text{SiW}_{10}$ and H_2O_2 is identified as a strongly electrophilic intermediate, and the generation process should be responsible for the observed induction period of the epoxidation process.¹³¹ However, the isolated diperxo species [$\gamma\text{-SiW}_{10}\text{O}_{32}(\text{O}_2)_2$]⁴⁻, which forms immediately when H_2O_2 is added to the fresh catalyst $\gamma\text{-H}_4\text{SiW}_{10}$, is inactive for the epoxidation reaction. Thus, the active oxidant may evolve from [$\gamma\text{-SiW}_{10}\text{O}_{32}(\text{O}_2)_2$]⁴⁻. Regrettably, the active oxidant has not been isolated. The in situ IR, NMR, and UV-vis spectra and the kinetic study provide sufficient evidence for the fact that the structural integrity of the catalyst is maintained well under turnover conditions.^{130,132}

The single-crystal X-ray structural analysis of $\gamma\text{-H}_4\text{SiW}_{10}$ shows that ten tungstens are connected with a central SiO_4 unit and two W–O bonds (W2–O3 and W4–O7) are notably longer than the others (Figure 3).¹³⁰ Mizuno et al. think that

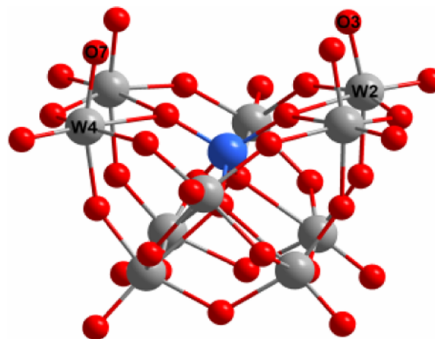


Figure 3. Structure of $\gamma\text{-H}_4\text{SiW}_{10}$.

two oxygen atoms at the vacant sites were diprotonated, resulting in two water ligands (Figure 4a). The addition of 2

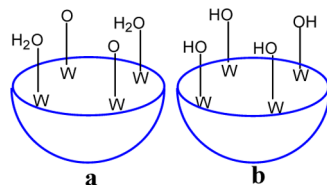
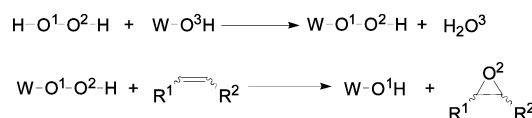


Figure 4. Two distribution patterns of four protons in $\gamma\text{-H}_4\text{SiW}_{10}$.

equiv of imidazole or pyridine with respect to $\gamma\text{-H}_4\text{SiW}_{10}$ strongly inhibits the epoxidation reaction due to the neutralization of two active protons by basic imidazole or pyridine.¹³¹ The findings reveal the great importance of active protons in enhancing the activity of $\gamma\text{-H}_4\text{SiW}_{10}$. The diprotonated pattern was also supported by Bonchio's group.¹³³ They found that the active catalyst $\gamma\text{-H}_4\text{SiW}_{10}$ could be isolated within only a narrow pH range, and the sample precipitating at pH 2 exhibited the highest activity. Additionally, only two protons in $\gamma\text{-H}_4\text{SiW}_{10}$ are acidic enough to react with (TBA) OH . From these experimental results, we can deduce that only two of the four acidic protons in $\gamma\text{-H}_4\text{SiW}_{10}$ contribute to the promotion of oxygen transfer. Although the diprotonated pattern is supported by the experimental results obtained by Mizuno's group and Bonchio's group,^{130,133,134} it is challenged by Musaev and co-workers. They proposed a

tetrahydroxy isomer (Figure 4b) according to computational and Brønsted acidity studies.^{135,136} In the isomer, four oxygens at lacunary sites are monoprotonated to form four terminal hydroxo ligands. The observed and calculated asymmetry of the terminal W–O bond distances is explained by the existence of a hydrogen bond between hydroxyls.¹³⁵ On the basis of the tetrahydroxy model, a two-step mechanism is proposed (Scheme 3). In the first step, one O–H bond of H–O–O–

Scheme 3. Two-Step Mechanism Based on the Tetrahydroxy Model of $\gamma\text{-H}_4\text{SiW}_{10}$ ¹³⁶



H (H_2O_2) is broken, and the hydroperoxide (W–OOH) species and a water molecule are produced in a concerted manner. In the second step, the O–H bond and O–O bond of the W–OOH species are cleaved, and one oxygen atom is transferred to the substrate to form an epoxide. The second step is appointed as the rate-limiting step of the whole catalytic cycle.¹³⁶ However, the calculated geometry of the tetrahydroxy model does not conclusively describe the experimental structure; thus, further attention is required.

The sample of $\text{TBA}_4(\gamma\text{-H}_4\text{SiW}_{10})$, prepared through a bottom-up approach, shows a promising size-selective property as a flexible nonporous heterogeneous catalyst in ethyl acetate,¹³⁷ which is absent in acetonitrile-mediated homogeneous systems.¹³¹ Smaller substrates are oxidized preferentially in the heterogeneous system. In the reaction, ethyl acetate molecules are adsorbed by the nonporous $\text{TBA}_4(\gamma\text{-H}_4\text{SiW}_{10})$. These molecules are highly mobile in the solid bulk of the catalyst and probably contribute to the easy cosorption of the substrates and H_2O_2 , which leads to high activity of the catalyst. Furthermore, the high mobility of TBA^+ cations and the highly flexible crystal structure of $\text{TBA}_4(\gamma\text{-H}_4\text{SiW}_{10})$ lead to a uniform distribution of the reactant and oxidant molecules throughout the solid bulk of the catalyst, facilitating the activity promotion of the catalyst.¹³⁸ $[(\text{CH}_3)_4\text{N}]^+$, $[(n\text{-C}_3\text{H}_7)_4\text{N}]^+$, and $[(n\text{-C}_5\text{H}_{11})_4\text{N}]^+$ are less useful than TBA^+ . A similar effect of cations on the activities of POM catalysts is also observed for $[\text{TiPW}_{11}\text{O}_{40}]^{5-}$ (TiPW_{11})-based catalysts.¹³⁹ However, $\text{TBA}_5(\text{TiPW}_{11})$ shows poor activity in ethyl acetate in comparison with $\text{CTA}_5(\text{TiPW}_{11})$ and $(\text{C}_{12}\text{mim})_5(\text{TiPW}_{11})$ (CTA = cetyltrimethylammonium; C_{12}mim = 1-dodecyl-3-methylimidazolium). $(\text{C}_{12}\text{mim})_5(\text{TiPW}_{11})$ shows the highest activity and $\text{CTA}_5(\text{TiPW}_{11})$ shows moderate activity. The results indicate that the length of the alkyl on the cation is crucial for the activity of the whole catalyst. Moreover, the imidazolyl on the cation may influence the electron nature of TiPW_{11} . Therefore, the atomic structure of the active sites as well as the structure and dynamics of the surroundings should be taken into consideration in the design and synthesis of highly active heterogeneous POM catalysts.

To impart a strong stability to the vacant structure and generate catalyst diversity, including the most desirable chiral upgrade, the lacunary oxygen atoms of $\gamma\text{-SiW}_{10}$ are covalently functionalized by organic moieties.^{140,141} The attached organic moieties tune the activity of the POM skeleton through influencing the electron density on proximal W atoms. With the hybrid POM [$\gamma\text{-SiW}_{10}\text{O}_{36}(\text{PhPO})_2$]⁴⁻ as the catalyst, fast

Table 3. Alkene Epoxidation with TBA Salts of γ -V₂XW₁₀ (X = P, Si)

| X | Alkene | Product | Yield (%) | Ref. | X | Alkene | Product | Yield (%) | Ref. |
|----|--------|---------|-----------|------|----|--------|---------|-----------|------|
| | | | | | | | | | |
| Si | | | 87 | 157 | Si | | | 90 | 27 |
| Si | | | 91 | 157 | Si | | | 76 | 27 |
| Si | | | 92 | 157 | P | | | 88 | 159 |
| Si | | | 93 | 157 | P | | | 86 | 159 |
| Si | | | 90 | 157 | P | | | 83 | 159 |
| Si | | | 88 | 157 | P | | | 89 | 159 |
| Si | | | 93 | 157 | P | | | 84 | 159 |
| Si | | | 88 | 157 | P | | | 94 | 159 |
| Si | | | 90 | 157 | P | | | 94 | 159 |
| Si | | | 91 | 157 | P | | | 86 | 159 |
| Si | | | 87 | 157 | P | | | 48 | 159 |
| Si | | | 90 | 27 | P | | | 56 | 159 |
| Si | | | 83 | 27 | P | | | 59 | 159 |

alkene epoxidation with H₂O₂ is conducted under microwave irradiation in acetonitrile and IL, respectively. The reaction in IL needs a shorter time because of the ready absorption of microwave by IL.

To improve the catalytic performances of POM catalysts, secondary TMs are often introduced into the skeleton of vacant POMs. Mono/disubstituted POMs are common in catalysis. Trisubstituted examples are rare.¹⁴² Mono-metal-substituted POM catalysts for alkene epoxidation are mainly those containing Co, Ti, or Zr. Among them, [M(L)PW₁₁O₃₉]ⁿ⁻ (M = Co, Ti, Zr) are the subject of the most studies. Their catalytic properties were explored in the early years.^{143–146} Recently, Kholdeeva et al. supported [Co(H₂O)PW₁₁O₃₉]⁵⁻ (CoPW₁₁) on NH₂-modified mesoporous silicate matrixes¹⁴⁷ and MIL-101¹⁴⁸ to realize the oxidation of α -pinene with O₂. However, the oxidation occurs at the allylic position. Verbenol and verbenone are the major products. However, when isobutyraldehyde is added into the reaction mixture, co-oxidation of α -pinene and isobutyraldehyde occurs, selectively producing α -pinene epoxide with 94% selectivity at 96% alkene conversion.

The research on mono-Ti-substituted POM catalysts was stimulated initially by the outstanding catalytic performance of titanium–silicalite molecular sieves for the oxidation reactions with H₂O₂ and the limitations caused by their small pore size. With the purpose of designing effective POM catalysts to overcome the limitations of titanium–silicalite molecular sieves,

recent studies focus on the mechanism insight and detailed catalyst behaviors. In H₂O₂-based systems, hydroperoxotitanium (Ti–OOH) is the most accepted active species. The epoxidation rate depends on the formation rate of Ti–OOH, which is strongly influenced by the structure around the Ti center.¹⁴⁹ Protonation of the oxygen atoms adjacent to the Ti center has a great impact on the product distribution of alkene oxidation.^{143,150,151} Taking H₂O₂-based cyclohexene oxidation with Na_{5-n}H_n(TiPW₁₁) as an example, allylic oxidation products 2-cyclohexene-1-ol and 2-cyclohexene-1-one are yielded when n = 1, along with comparable amounts of the corresponding epoxide and diol, strongly supporting a homolytic oxidation mechanism, while *trans*-cyclohexane-1,2-diol is the main product when n = 2–5, suggesting a heterolytic oxygen-transfer mechanism. To understand these processes at the molecular level, Poblet et al. further studied the role of protons in the reaction and their location within the POM skeleton.¹⁵² Apparently, the protonation reduces the overall negative charge of the POM anion and makes the oxygen on the anion more electrophilic, favoring the transfer of electrophilic oxygen to nucleophiles and leading to a unique pathway. Thus, the protonation of Ti-containing POM can significantly lower the energy barrier for the heterolytic oxygen transfer from the Ti–hydroperoxo intermediate (Ti–OOH) to alkenes, increasing the activity and selectivity of alkene epoxidation, whereas the homolytic mechanism is affected to a minor extent. However, the situation is different for mono-Zr-substituted

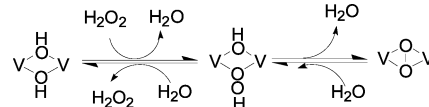
POM catalysts. The oxidations of alkenes with two dimers, $\text{TBA}_7\{\text{[Zr}(\mu\text{-OH})\text{PW}_{11}\text{O}_{39}]\}_2\}$ ($\text{TBA}_7\text{H}(\text{ZrPW}_{11})_2$) and $\text{TBA}_8(\text{ZrPW}_{11})_2$, containing two active protons and one active proton, respectively, follow a homolytic oxidation mechanism to give allylic oxidation products uniformly.¹⁵³ No reaction mechanism change occurs with increasing proton number. However, the proton number still affects the activity of Zr-POM catalysts. Although H_2O_2 decomposes seriously in the presence of $\text{TBA}_7\text{H}(\text{ZrPW}_{11})_2$ and $(\text{ZrPW}_{11})_2$, the catalytic activities of the two catalysts are obvious. On the contrary, $\text{TBA}_9\{\text{[ZrPW}_{11}\text{O}_{39}]\}_2(\mu\text{-OH})(\mu\text{-O})\}$ without acidic protons shows negligible activity.

Disubstituted Keggin-type POMs receive considerable attention in catalytic oxidation of organic compounds. The oxidation of alkenes and alkanes with the Fe-containing silicotungstate $\{\gamma\text{-SiW}_{10}[\text{Fe}(\text{OH})_2]_2\text{O}_{38}\}^{6-}$ ($\gamma\text{-Fe}_2\text{SiW}_{10}$) is evaluated extensively.^{42,154-156} Mizuno et al. reported that, in the epoxidation of alkenes, $\gamma\text{-Fe}_2\text{SiW}_{10}$ gives higher conversion and H_2O_2 utilization efficiency than its structurally analogous $[\gamma\text{-Mn}_2\text{SiW}_{10}\text{O}_{38}]^{6-}$ and $\{\gamma\text{-[Cu(OH)}_2\text{]SiW}_{10}\text{O}_{38}\}^{8-}$, mono-Fe-substituted $[\alpha\text{-Fe}(\text{OH})_2\text{SiW}_{11}\text{O}_{39}]^{5-}$ ($\alpha\text{-FeSiW}_{11}$), tri-Fe-substituted $\{\alpha\text{-[Fe(OH)}_3\text{]SiW}_9\text{O}_{37}\}^{7-}$, and nonsubstituted $\gamma\text{-SiW}_{12}$.¹⁵⁴ Mizuno's group also reported that when cyclooctene is oxidized by 1 atm of O_2 at 356 K in the presence of $\gamma\text{-Fe}_2\text{SiW}_{10}$, cyclooctene oxide is selectively produced together with small amounts of 2-cycloocten-1-ol and 2-cycloocten-1-one.¹⁵⁶ After 385 h, the conversion and selectivity for cyclooctene oxide reach up to 82% and 98%, respectively. In this case, a high turnover number (TON) of 10 000 is obtained, albeit with a modest TOF of 26 h^{-1} . They reported that the TON value is more than 100 times higher than those reported for the epoxidation of cyclooctene with 1 atm of O_2 alone. The reaction is proposed by Mizuno's group to principally proceed via a nonradical pathway, inconsistent with the results of Bonchio's group¹⁵⁵ and Hill's group,⁴² who believe that the catalytic epoxidation of alkenes by O_2 in the presence of $\gamma\text{-Fe}_2\text{SiW}_{10}$ undergoes a ubiquitous radical chain mechanism.¹⁵⁵ It is notable that Hill's group obtained rates, conversions, and TONs for cyclooctene oxidation similar to those reported by Mizuno under their nearly equivalent (but distinct) conditions.⁴² However, they found the control reactions without $\gamma\text{-Fe}_2\text{SiW}_{10}$ proceed with rates and epoxidation selectivities similar to those of the reactions that contain $\gamma\text{-Fe}_2\text{SiW}_{10}$. Thus, they propose that the epoxidation of alkenes by O_2 is minimally affected by the presence of their $\gamma\text{-Fe}_2\text{SiW}_{10}$. The different effects of $\gamma\text{-Fe}_2\text{SiW}_{10}$ reported by the two groups are probably caused by the small differences in $\gamma\text{-Fe}_2\text{SiW}_{10}$ preparation methods used by the two groups.

V-based oxidation with H_2O_2 often involves a radical mechanism, and the H_2O_2 utilization efficiency is intrinsically low due to the fast decomposition catalyzed by vanadium. The oxidation of alkenes mainly occurs at the allylic position. Embodying vanadium into the POM skeleton can greatly change the reaction pathway and improve the H_2O_2 utilization efficiency. The bis(μ -hydroxo)-bridged di-V-substituted POM $\text{TBA}_4(\gamma\text{-V}_2\text{SiW}_{10})$ is an exemplary compound.^{27,157} It exhibits high catalytic activity (Table 3) and gives approximately 90% H_2O_2 utilization efficiency in the epoxidation of various alkenes. Notably, the system with $\text{TBA}_4(\gamma\text{-V}_2\text{SiW}_{10})$ shows unique stereospecificity, diastereoselectivity, and regioselectivity that are quite different from those reported for the epoxidation systems with $\text{TBA}_4(\gamma\text{-H}_4\text{SiW}_{10})$. In the case of nonconjugated dienes, the more accessible, but less nucleophilic double bonds

are oxidized preferentially. Under optimized reaction conditions, the amounts of allylic oxidation products and glycols produced by hydrolysis are negligible for all cases. When $\gamma\text{-V}_2\text{SiW}_{10}$ is immobilized on IL-modified SiO_2 by ion exchange, the reaction rate of epoxidation is decreased, but the intrinsic catalytic nature of $\gamma\text{-V}_2\text{SiW}_{10}$ is retained.¹⁵⁸ Notice that immobilization makes the active anion easily recoverable and recyclable. A detailed study reveals that the bridged $\{\text{VO}-(\mu\text{-OH})_2\text{-VO}\}$ core was oxidized to $\{\text{VO}-(\mu\text{-OH})(\mu\text{-OOH})-\text{VO}\}$ by a small H_2O_2 molecule during the reaction, and the process was reversible (Scheme 4).²⁷ Bulky TBHP (*tert*-butyl

Scheme 4. Formation of the Active $\mu\text{-}\eta^2\text{:}\eta^2$ -Peroxo Group¹⁵⁹



hydroperoxide) is a loser in the process due to the steric repulsion from the POM skeleton. The following dehydration of $\{\text{VO}-(\mu\text{-OH})(\mu\text{-OOH})-\text{VO}\}$ affords a $\mu\text{-}\eta^2\text{:}\eta^2$ -peroxo group that is a strong electrophilic oxidant species with strong steric hindrance and is proposed to be the active oxygen-transfer agent.

An analogue with a different heteroatom, $[\gamma\text{-V}_2(\mu\text{-OH})_2\text{-PW}_{10}\text{O}_{38}]^{3-}$ ($\gamma\text{-V}_2\text{PW}_{10}$), is even more active than $\gamma\text{-V}_2\text{SiW}_{10}$.¹⁵⁹ It robustly catalyzes the epoxidation of electron-deficient alkenes with H_2O_2 , which is difficult to achieve because of the low electron density on the involved double bond and usually requires a strongly electrophilic oxidant. Alkenes bearing acetate, ether, carbonyl, and chloro groups at the allylic positions readily convert to the corresponding epoxides in the presence of $\gamma\text{-V}_2\text{PW}_{10}$ (Table 3). Even acrylonitrile and methacrylonitrile are also epoxidized without the formation of the corresponding amides. The evolution of the catalyst is identical to that of $\gamma\text{-V}_2\text{SiW}_{10}$ (Scheme 4). The intermediate $[\gamma\text{-V}_2(\mu\text{-}\eta^2\text{:}\eta^2\text{-O}_2)\text{PW}_{10}\text{O}_{38}]^{3-}$ is the genuine active species that shows a higher electrophilicity than $[\gamma\text{-V}_2(\mu\text{-}\eta^2\text{:}\eta^2\text{-O}_2)\text{SiW}_{10}\text{O}_{38}]^{2-}$. In addition, the observed activity difference between $\gamma\text{-V}_2\text{SiW}_{10}$ and $\gamma\text{-V}_2\text{PW}_{10}$ is partly attributed to the different acidities of the derived hydroperoxo species, which play an important role in the following dehydration activity. The faster dehydration rate of $[\gamma\text{-V}_2(\mu\text{-OH})(\mu\text{-OOH})\text{PW}_{10}\text{O}_{38}]^{3-}$ than that of $[\gamma\text{-V}_2(\mu\text{-OH})(\mu\text{-OOH})\text{SiW}_{10}\text{O}_{38}]^{4-}$ leads to a significant increase of the overall reaction rate.

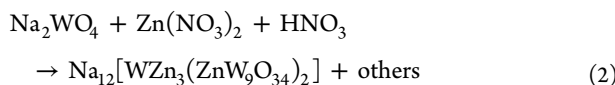
In contrast to the most common Keggin-type and Wells-Dawson-type structures, sandwich-type POMs have stronger resistance toward hydrolysis and oxidative degradation.¹⁶⁰ The robustness and persistence of this kind of catalyst in H_2O_2 -based systems were fully documented in the early years.¹⁶⁰⁻¹⁶⁷ At present, they are valued continuously in catalysis. The catalysts represented by $[\text{ZnWM}_2(\text{ZnW}_9\text{O}_{34})_2]^{q-}$ ($\text{M} = \text{Mn}^{\text{II}}$, Ru^{III} , Fe^{III} , Pd^{II} , Pt^{II} , Zn^{II} ; $q = 10\text{-}12$) show notable chemo-, diastereo-, and regioselectivity in the epoxidation of chiral allylic alcohols with H_2O_2 in biphasic systems (Table 4).^{168,169} In the reactions, allylic alcohols are coordinated to the catalyst through tungsten-alcoholate bonding. Both 1,2- and 1,3-allylic strains dominate in the stereocontrol of the oxygen transfer to chiral allylic alcohols. 1,3-Allylically strained substrates give *threo* diastereomers (entries 1–4), and 1,2-allylically strained substrates predominately give *erythro* diastereomers (entries 5

Table 4. Epoxidation of Chiral Allylic Alcohols by H₂O₂ in the Presence of [ZnWM₂(ZnW₉O₃₄)₂]^{q-}

| Entry | M | Alkene | Yield of 1 (%) (threo:erythro) | | 1:2 |
|-------|-------------------|--------|--------------------------------|-----------|-----|
| | | | threo-1 | erythro-1 | |
| 1 | Mn ^{II} | | 88 (92:8) | >95:5 | |
| 2 | Ru ^{III} | | 95 (92:8) | >95:5 | |
| 3 | Fe ^{III} | | 90 (95:5) | >95:5 | |
| 4 | Zn ^{II} | | 85 (95:5) | >95:5 | |
| 5 | Mn ^{II} | | 95 (8:92) | >95:5 | |
| 6 | Mn ^{II} | | 95 (45:55) | >95:5 | |
| 7 | Mn ^{II} | | 83 (55:45) | 95:5 | |
| 8 | Mn ^{II} | | >90 (93:7) (3,4-isomer) | >95:5 | |
| 9 | Zn ^{II} | | >90 (95:5) (3,4-isomer) | >95:5 | |

and 6). Tungsten–alcoholate bonding furnishes the reactions of unconjugated diene with high regioselectivity (entries 8 and 9). The chemoselectivities for acyclic allylic alcohols are much higher than those for the cyclic allylic alcohols due to the formation of significant amounts of enone in the epoxidation of cyclic allylic alcohols. A tungsten–peroxy complex is considered as the key intermediate in such systems, rather than a high-valent oxo-TM species. TMs in the central ring have no effect on the activity, chemoselectivity, and stereoselectivity when H₂O₂ is used as the oxidant. However, the nature of the TMs (OV^{IV}, Mn^{II}, Ru^{III}, Fe^{III}, Pd^{II}, Pt^{II}, Zn^{II}) significantly affects the activity, chemoselectivity, regioselectivity, and stereoselectivity when organic chiral hydroperoxides are used as the oxidants.¹⁷⁰ With the sterically demanding hydroperoxide TADOOH ([*(4R,5R)-5-[*(hydroperoxy-diphenyl)methyl]-2,2-dimethyl-1,3-dioxolan-4-yl]diphenylmethanol) as the regenerative chiral oxygen source, the OV^{IV}-substituted [ZnW(VO)₂(ZnW₉O₃₄)₂]¹²⁻ gives the highest chemo-, regio-, and stereoselectivities. The quite different functions of the TMs in the two systems can be explained by the different activation forms of the oxidants. The organic hydroperoxide is activated in the form of peroxy-type vanadium, whereas H₂O₂ is activated in the form of peroxotungsten.^{170,171}

Water-soluble Na₁₂[WZn₃(ZnW₉O₃₄)₂] (Na₁₂[WZn₃(ZnW₉)₂]) is an amazing catalyst for H₂O₂-based systems. It has several industrially valuable advantages.¹⁷² First, the reactions with Na₁₂[WZn₃(ZnW₉)₂] start without an induction period on the addition of H₂O₂, and consequently leave out the catalyst activation step that is troublesome on a large scale. Second, the catalyst can be expediently made by simple mixing of readily available, cheap inorganic components in water through self-assembly (eq 2). Third, such available “self-



assembled catalyst solutions” can be directly used to catalyze epoxidation without catalyst isolation, and the aqueous solution containing Na₁₂[WZn₃(ZnW₉)₂] can be recycled by simple phase separation from the organic phase.¹⁷³ After being treated by solvent-resistant nanofiltration using an α -alumina-supported mesoporous γ -alumina membrane, the resulting WZn₃(ZnW₉)₂-involving catalyst combines the high-performance characteristics of homogeneous catalysts with the ease of recycling of heterogeneous catalysts.¹⁷⁴

Keplerate-type spherical ball-like cluster $\{(\text{NH}_4)_{42-} [\text{Mo}^{\text{VI}}_{72}\text{Mo}^{\text{V}}_{60}\text{O}_{372}(\text{CH}_3\text{COO})_{30}(\text{H}_2\text{O})_{72}]\}$ {Mo₁₃₂} is a nanoscale POM catalyst (Figure 5). It serves as the most desirable

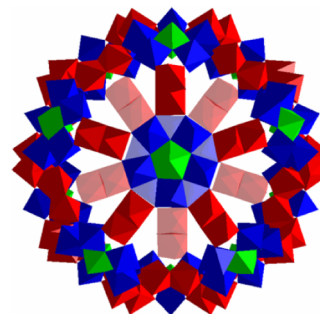


Figure 5. Structure of {Mo₁₃₂} (only Mo and O are represented).

oxidative system using water as the reaction medium and O₂ as the oxidant, and without any reducing agents or radical initiators. In the presence of the {Mo₁₃₂} cluster, the aerobic epoxidation of alkenes in water at ambient temperature and pressure provides good to high yields and desired selectivities (Table 5). Cyclooctene, cyclohexene, norbornene, styrene, α -methylstyrene, and indene are quantitatively converted within 2–4 h. No allylic oxidation occurs in these processes. Less reactive 1-octene gives a 90% yield of the corresponding epoxide as the sole product within 4 h. 1,1,2-Trisubstituted alkenes and (*E*)-alkenes are poorly reactive due to the steric hindrance. Electron-deficient 2-cyclohexen-1-one is oxidized to the corresponding epoxide in 40% yield. In addition, the {Mo₁₃₂}-mediated system possesses a novelty regarding chemoselectivity and stereoselectivity. The oxygen-sensitive hydroxyl group remains completely intact. Norbornene gives *exo*-epoxide exclusively. The configurations of *cis*- and *trans*-stilbenes are absolutely retained in their corresponding epoxides. The epoxidation of *cis*-stilbene is much faster than that of the *trans*-isomer. However, 1-octen-3-ol gives erythro- and *threo*-1,2-epoxy-3-octanol with a ratio of 55:43. Moreover, the catalyst is recyclable. It can be reused at least 10 times with a negligible decrease in catalyst performance. Thus, such a system not only significantly contributes to green chemistry, but is suitable for industrial goals.

In combination with chiral components, POM catalysts can promote the asymmetric oxidation of the alkenes. Duan et al. obtained two enantiomorphs, Ni-PYI1 and Ni-PYI2, by incorporating the oxidative component [BW₁₂O₄₀]⁵⁻ (BW₁₂) and the chiral group L/D-pyrrolidin-2-ylimidazole (PYI) into one framework via self-assembly.¹⁷⁵ The structure of Ni-PYI1 is depicted in Figure 6. BW₁₂ is embedded in the channels of the MOF. The remainder of the space in the channels with hydrophilic/hydrophobic properties allows the molecules of H₂O₂ and alkene ingress and egress. The coexistence of the chiral directors and the oxidants within a confined space

Table 5. Aerobic Alkene Epoxidation in Water Catalyzed by $\{\text{Mo}_{132}\}$ ⁴⁴

| Alkene | Product | Yield (%) | Time (h) |
|------------------------|------------------------------|-----------|----------|
| cyclohexene | cyclohexene oxide | 96 | 2 |
| cyclopentene | cyclopentene oxide | 92 | 3 |
| 1-methylcyclohexene | 1-methylcyclohexene oxide | 60 | 5 |
| 1-phenylcyclohexene | 1-phenylcyclohexene oxide | 33 | 5 |
| norbornene | norbornene oxide | 95 | 2 |
| styrene | styrene oxide | 93 | 3 |
| 1-phenylpropene | 1-phenylpropene oxide | 94 | 4 |
| 1-phenylprop-1-ene | 1-phenylprop-1-en-3-ol | 45 | 5 |
| indene | indene oxide | 89 | 4 |
| hex-1-ene | hex-1-en-3-ol | 90 | 4 |
| 3-hydroxybut-1-ene | 3-hydroxybut-1-en-3-ol | 96 | 5 |
| 4-hydroxybut-1-ene | 4-hydroxybut-1-en-3-ol | 55 | 5 |
| 5-hydroxybut-1-ene | 5-hydroxybut-1-en-3-ol | 43 | 5 |
| cyclohexanone | cyclohexanone oxide | 40 | 5 |
| 2-hydroxycyclohexanone | 2-hydroxycyclohexanone oxide | 80 | 5 |
| 1-phenyl-1-butene | 1-phenyl-1-butanol | 25 | 5 |
| 1,4-diphenylbenzene | 1,4-diphenyl-1-butanone | 97 | 5 |

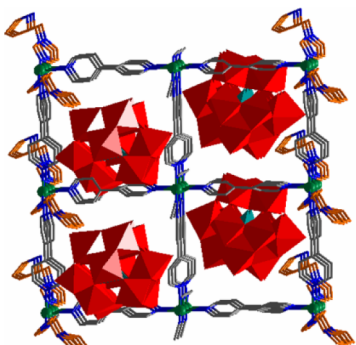
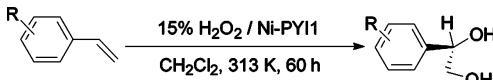


Figure 6. Crystal structure of Ni-PYI1.

provides a special environment for the formation of the reaction intermediates in a stereoselective manner with high selectivity. Therefore, Ni-PYI1 and Ni-PYI2 are used as amphiphatic catalysts to prompt the asymmetric dihydroxylation of alkenes. The reactions of styrene and derivatives using 15% H_2O_2 as the oxidant and 0.7 mol % Ni-PYI1 as the heterogeneous catalyst give 67–95% ee values of (*R*)-products (Scheme 5). The low conversion of 3,5-di-*tert*-butyl-4'-

Scheme 5. Asymmetric Dihydroxylation of Arylalkenes with Ni-PYI1¹⁷⁵



| | conversion (%) | ee (%) |
|---|----------------|--------|
| styrene | 75 | >95 |
| 2-chlorovinylbenzene | 76 | >67 |
| 3-chlorovinylbenzene | 79 | >95 |
| 4-chlorovinylbenzene | 75 | >95 |
| 3,5-di- <i>tert</i> -butyl-4'-vinylbiphenyl | <10 | nd |

vinylbiphenyl is attributed to negligible adsorption by Ni-PYI1 due to its large molecule size compared to the size of the channels of Ni-PYI1. This result reveals that the asymmetric dihydroxylation indeed occurs in the channels of the catalyst, not on the external surface. The homogeneous system with $\text{Ni}_2\text{HBW}_{12}$ and L-PYI gives 45% styrene conversion and a 15% ee value. These values are far lower than those with Ni-PYI1. The higher conversion with Ni-PYI1 is attributed to the suitable distribution of pairs of the chiral PYI moiety and BW_{12} oxidant that provides effective contacts with substrates at the same time. The control experiments prove that the chiral induction happens during the epoxidation process, not the ring-opening process. In the dihydroxylation process, the formation of hydrogen bonds between the protonated pyrrolidine ring and the terminal oxygen atoms of BW_{12} may play important roles. On one hand, it activates the related $\text{W}=\text{O}_t$ bonds to generate an active peroxytungstate intermediate by H_2O_2 . On the other hand, the hydrogen bonds shorten the proximity between the conventional electrophilic oxidant and the chiral directors to provide additional steric orientation, driving the catalysis to occur in a stereoselective manner.

2.1.2. To Carbonyl Compounds. Apart from epoxides and diols, the oxidation of alkenes with POM catalyst can also produce carbonyl compounds via the cleavage of the double $\text{C}=\text{C}$ bond under suitable conditions. The oxidation of styrene to benzaldehyde is the most studied process in this subfield because benzaldehyde is the second most important aromatic molecule in the cosmetics and flavor industries. $(\text{Bmim})_3\text{PMo}_{12}$ ¹⁷⁶ and several monosubstituted POMs^{177–179} are powerful for the process. With H_2O_2 as the oxidant, mono-Co-substituted POMs appear more effective than other metal-substituted analogues.¹⁸⁰ For monosubstituted phosphotungstates, $\text{Cs}_5(\text{CoPW}_{11})$ is more active than $\text{Cs}_5[\text{Mn}(\text{H}_2\text{O})\text{PW}_{11}\text{O}_{39}]$.¹⁷⁷ The study on phosphomolybdates $\text{Cs}_5[\text{M}(\text{H}_2\text{O})\text{PMo}_{11}\text{O}_{39}]$ ($\text{Cs}_5(\text{MPMo}_{11})$; $\text{M} = \text{Co}^{\text{II}}, \text{Mn}^{\text{II}}, \text{Ni}^{\text{II}}$) shows that the activities of phosphomolybdates follow the sequence $\text{CoPMo}_{11} > \text{NiPMo}_{11} > \text{MnPMo}_{11}$.¹⁷⁸ Among various silicotungstates $\text{TBA}_4\text{H}_x[\text{M}(\text{H}_2\text{O})\text{SiW}_{11}\text{O}_{39}]$ ($x = 1, 2$; $\text{M} = \text{Co}^{\text{II}}, \text{Fe}^{\text{III}}, \text{Mn}^{\text{III}}$), $\text{TBA}_4\text{H}_2[\text{Co}(\text{H}_2\text{O})\text{SiW}_{11}\text{O}_{39}]$ gives the

highest activity.¹⁷⁹ The Co-substituted sandwich-type supramolecular network $[\text{Co}(\text{H}_2\text{O})_6]_2[\{\text{Co}(\text{H}_2\text{O})_4\}_2[\text{Co}(\text{H}_2\text{O})_5\}_2\cdot\text{WZn}[\text{Co}(\text{H}_2\text{O})_2(\text{ZnW}_9\text{O}_{34})_2]\cdot10\text{H}_2\text{O}$ gives 99% selectivity to benzaldehyde at 96% styrene conversion.¹⁸¹ Co²⁺ linkers of the solid structure play a pivotal role in enhancing the catalytic performance. They function as pillars to brace the 3D supramolecular network and expose the active site to substrates.

In fact, POMs/HPAs act not only as the catalysts, but also as the stabilizers, electron-transfer agents, and supports in catalytic oxidation of alkenes. Their high negative charges can prevent particles from aggregation by electrostatic repulsion. Thus, they have been used to stabilize nanoparticles.^{182–184} For example, Pt, Ag, and Ru nanoparticles can be stabilized highly by H₅PV₂Mo₁₀O₄₀ (H₅V₂PMo₁₀).¹⁸⁵ The average size of the obtained nanoparticles ranges from 2.6 nm for Pt_n-POM to 5 nm for Ag_n-POM and Ru_n-POM. Moreover, POMs can be used to stabilize TM complexes by assembling them into hybrid materials via electrostatic interactions^{186,187} or coordination.¹⁸⁸ For example, the association of cationic metalloporphyrin and anionic PW₁₂ provides extra stabilization to metalloporphyrins against deactivation during catalytic cycles.¹⁸⁶ As electron reservoirs, HPAs can substitute for CuCl₂ in Wacker-type oxidation of alkenes to ketones, which is traditionally catalyzed by PdCl₂ and CuCl₂, to guarantee the regeneration of Pd^{II}, the genuine catalyst for Wacker-type reactions.^{189,190} The rudimentary reaction system was originally developed by Matveev and co-workers.^{191,192} More practically, Grate et al. also greatly contributed to this area.^{193–197} Detailed information can be found in their papers and patents.

2.2. Oxidation of Alkanes

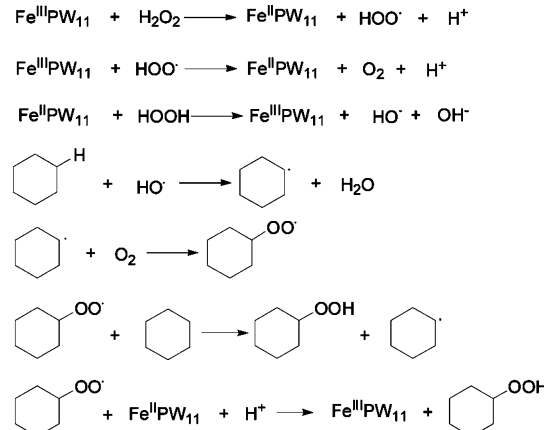
2.2.1. To Oxygenates. Selective oxidation of alkanes into organic oxygenates or alkenes affords an attractive route for the utilization of abundant light alkanes.¹⁹⁸ Although intensive efforts have been made in this field, the selective oxidation of C₁–C₄ alkanes still remains an unsolved challenge, except for the conversion of *n*-butane to maleic anhydride. The main reason is that the activation of alkanes generally requires severe conditions due to the inertia of the C–H bond in alkanes. However, severe conditions often cause consecutive oxidation of the reactive target products to undesirable CO and CO₂,^{199,200} and consequently lead to low selectivities for target products at reasonably high conversions. Therefore, developing catalysts that efficiently work under mild conditions is a project of interest. In view of the remarkable redox properties of POM catalysts, they are prospective alternatives. Up to now, numerous POM catalysts have been developed for alkane oxidation. Those containing Fe, Co, V, and Ru are used broadly.

The activity of peroxotungstates for alkane oxidation was first demonstrated by THA₂{[WO(O₂)₂]₂(μ-O)} (THA = tetrahexylammonium).²⁰¹ In the presence of excess H₂O₂, the oxidation of cyclooctane proceeds via a radical mechanism that is unusual for the catalysts with W atoms as the active sites because of the inertia of W in the decomposition of H₂O₂. Cyclooctyl hydroperoxide is the dominant product, along with cyclooctanol and cyclooctanone. Higher selectivity for cyclooctyl hydroperoxide is achieved in a shorter time, revealing that cyclooctyl hydroperoxide is the initial product, which decomposes to cyclooctanol and then converts into cyclooctanone.

In 1999, cyclohexane oxidation with monosubstituted TBA₄H(CuPW₁₁O₃₉) and TBA₄H_x[M(H₂O)PW₁₁O₃₉]

(TBA₄H_x(MPW₁₁); M = Co^{II}, Mn^{II}, Ni^{II}, Fe^{III}; n = 5, 4; x = 1, 0) was carried out by Cavaleiro's group.²⁰² With H₂O₂ as the oxidant, TBA₄H(CuPW₁₁O₃₉) and TBA₄H(MPW₁₁) (M = Co^{II}, Mn^{II}, Ni^{II}) only give cyclohexanol and cyclohexanone as the products with a low cyclohexane conversion (<20%). The situation is totally different from that for TBA₄(FePW₁₁), which shows a much higher activity, and gives cyclohexyl hydroperoxide as the main product. Excess H₂O₂ affords a higher selectivity for cyclohexyl hydroperoxide.²⁸ In the presence of TBA₄(FePW₁₁), 74% cyclooctane conversion and 80% selectivity for cyclooctyl hydroperoxide are achieved after 2 h, using an excess of H₂O₂. The reaction proceeds via a radical pathway (Scheme 6). Apart from the substituting metals and

Scheme 6. Proposed Pathway for the Formation of Cyclooctyl Hydroperoxide with TBA₄(FePW₁₁)²⁸



the dosage of H₂O₂, the selectivity for cyclooctyl hydroperoxide is also influenced by the heteroatoms of the used mono-substituted POM catalysts.

In the presence of 1 atm of O₂ as the sole oxidant, the mono-Ru-substituted TBA₄H[Ru^{III}(H₂O)SiW₁₁O₃₉] (TBA₄H(RuSiW₁₁) can activate tertiary, secondary, and benzylic C–H bonds of a wide range of alkanes, and the main products are ketones for secondary C–H bond oxidation.²⁰³ In contrast, the related compounds TBA₄H₄(SiW₁₁O₃₉) (TBA₄H₄(SiW₁₁)), RuCl₃, and Na₂WO₄, mixture of TBA₄H₄(SiW₁₁) and RuCl₃, and mixture of Na₂WO₄ and RuCl₃ are almost inactive under identical conditions, suggesting that the cooperation of Ru^{III} with TBA₄H₄(SiW₁₁) creates a synergistic effect between the two components. Ru^{III} is regarded as the active site. The activity of the mono-Ru-substituted catalyst is more than 10 times higher than those of the sandwich-type {[ZnWRu₂(OH)(H₂O)](ZnW₉O₃₄)₂}^{11−} (ZnWRu₂(ZnW₉)₂) and Ru-hydrotalcite.

Di-Fe-substituted TBA_{3.5}H_{2.5}(γ-Fe₂SiW₁₀) works well in the oxidation of cyclohexane, *n*-hexane, *n*-pentane, and adamantine at a temperature ranging from 305 to 356 K, using H₂O₂ as the oxygen donor.²⁰⁴ With TBA_{3.5}H_{2.5}(γ-Fe₂SiW₁₀), the H₂O₂ utilization efficiency reaches up to 100% for the oxygenation of cyclohexane under mild conditions, much higher than that with TS-1 (32%),²⁰⁵ [PW₉O₃₇{Fe_{3-x}Ni_x(OAc)₃}]^{(9+x)−} (x = predominantly 1) (14%),²⁰⁶ [Fe₂O(bipy)₄(OH₂)₂][ClO₄]₄ (8%),²⁰⁷ the FeCl₃/py/Ph₂S/picolinic acid system (79%), Fe₃O(OAc)₆(H₂O)₃ (4%), etc.²⁰⁹ The main products are cyclohexanone and cyclohexanol with a ratio of ca. 1. Only a trace of dicyclohexyl is formed by coupling of two cyclohexyl

radicals. The product distribution is quite different from that with monosubstituted TBA₄(FePW₁₁).^{28,202} The process is deemed as nonradical to a major degree. The structures of the Fe centers remarkably influence the catalytic activities. The nonsubstituted and mono-Fe- and tri-Fe-substituted silicotungstates are much less active than the di-Fe-substituted TBA_{3.5}H_{2.5}(γ -Fe₂SiW₁₀).^{204,210} However, the verdict depends on the reaction conditions. A disparate conclusion is drawn with 1 atm of O₂ as the oxygen donor.²¹¹ The mono-Fe-substituted silicotungstate α -FeSiW₁₁ is more active than di-Fe-substituted γ -Fe₂SiW₁₀ in the presence of O₂. The selectivity for the mixture of cyclohexanol and cyclohexanone reaches up to 95% with α -FeSiW₁₁. The reaction undergoes a radical chain oxidation propagated by Fe-catalyzed decomposition of cyclohexyl hydroperoxide that ultimately depends on the redox properties and structural arrangement of the iron moiety within the POM cage. Moreover, the activity of di-Fe-substituted γ -Fe₂SiW₁₀ is even lower than that of the analogous { γ -[Mn^{III}(OH₂)₂SiW₁₀O₃₈]}⁶⁻ when O₂ is used as the oxidant, but higher than that of { γ -[Mn^{II}(OH₂)₂SiW₁₀O₃₈]}⁸⁻ and { γ -[Cu^{II}(OH₂)₂SiW₁₀O₃₈]}⁸⁻.²¹²

V-substituted HPA catalysts H₄VPMo₁₁O₄₀ (H₄VPMo₁₁), H₅V₂PMo₁₀, and H₆V₃PMo₉O₄₀ (H₆V₃PMo₉) are robust in the oxidation of adamantane with 1 atm of O₂ as the sole oxidant without any additives such as reductants and radical initiators.³⁷ However, the incorporation of VO_n units into the primary Keggin structure of H_{3+n}V_nPMo_{12-n} by substitution for MoO_n groups leads to a decrease in the thermal stability of the Keggin units.³⁸ The surface structures of these catalysts are dynamic at elevated temperature. V atoms release from the skeleton in the form of monomeric vanadium species V^VO₂⁺ and V^{IV}O₂²⁺ during the reaction, and Keggin-type anion PMo₁₂ is formed.³⁷ The detachment of substituting metals is also observed for FePMo₁₁, and the situation can be restrained by choosing suitable counterions.³⁹ In the reaction with H_{3+n}V_nPMo_{12-n} the free vanadium species initially abstracts hydrogen from adamantane to form adamantyl radical and reduced vanadium species.³⁷ The formed adamantyl radical initiates the successive formation of the key intermediates, such as more adamantyl radical and hydroperoxide species. The formed PMo₁₂ anions subsidiarily promote the reaction.

In the liquid-phase oxygenation of methane with H₂O₂, H₄VPMo₁₁ accounts for the highest catalytic performance in the H_{3+n}PV_nMo_{12-n} ($n = 0, 1, 2, 3$) family.^{213,214} Only trace CO₂ is produced with H₄VPMo₁₁ at 353 K.²¹⁴ When a small portion of Pd is introduced into the catalyst, a H₂-O₂ gas mixture can be used to replace H₂O₂, which is unsuitable for gas-phase oxygenation of methane.²¹⁵ Exemplarily, in the reaction with Pd_{0.08}Cs_{2.5}H_{0.34}(VPMo₁₁), Pd facilitates the in situ production of active oxygen species, H₂O₂ or H₂O₂-derived species, with the aid of acidic sites of the catalyst. The sequent reaction of the active oxygen species with methane is mainly catalyzed by VPMo₁₁. Due to the synergy of Pd²⁺ and VPMo₁₁, the reaction rate reaches up to 1.2 × 10⁻⁴ mol h⁻¹ g⁻¹ at 573 K. This value is about 300 times higher than that with the FePO₄ catalyst. The authors also found that the addition of steam could promote the production of formic acid in the H₂-O₂ system, and the yield reaches a maximum value when the partial pressure of steam is 9.1 kPa.

In 2004, Neumann et al. constructed a more attractive bifunctional catalyst, [Pt(Mebipym)Cl₂](H₄V₂PMo₁₀), for the methane oxygenation by combining a cationic Pt^{II} complex with disubstituted [H₄V₂PMo₁₀]⁻ via electrostatic interaction

(Figure 7).²¹⁶ According to a previous report,²¹⁷ Pt^{II} complexes are active in electrophilic alkane activation and oxidation. The

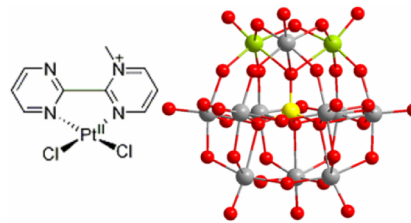
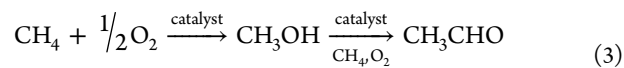


Figure 7. Structure of [Pt(Mebipym)Cl₂](H₄V₂PMo₁₀).

combination of [Pt(Mebipym)Cl₂]⁺ and [H₄V₂PMo₁₀]⁻ reinforces the activity of each individual component. The enhanced catalyst activity allows the utilization of O₂ to replace H₂O₂ or the mixed gas H₂-O₂. Thus, [Pt(Mebipym)Cl₂]-[H₄V₂PMo₁₀]⁻ will make the reaction safer, more effective, and thus more suitable for industrial production. In the presence of the hybrid catalyst, methane smoothly converts to methanol and then partially further to acetaldehyde at a temperature as low as 320–330 K and an O₂ pressure as low as 1–2 bar. Under the mild conditions, no significant formation of CO, CO₂, and acetic acid happens due to the stopped further oxidation of acetaldehyde. The most likely scenario for acetaldehyde formation is the oxidation of methane to formaldehyde via methanol, followed by its coupling with methane (eq 3). The



disubstituted anion [H₄V₂PMo₁₀]⁻ is the key in promoting mild aerobic oxidation of methane. It also possibly functions to facilitate both the oxidation of Pt^{II} to Pt^{IV} intermediates and the addition of methane (also methanol) to a Pt^{II} center by providing a conduit for improved oxidation of intermediate hydride species.

The bulky bis(μ -hydroxo) di-V-substituted phosphotungstate γ -V₂PW₁₀, with a strong oxidizing capacity, is also effective for the oxidation of alkanes.²¹⁸ In H₂O₂-based alkane oxidation, the derived strong electrophilic oxidant with high steric hindrance leads to high selectivities for alcohols (>96%), complete stereospecificity, and specific regioselectivity (Table 6). All the reactions are completed in a time of 1–4 h at a temperature of 333 or 342 K. The bulky framework of the catalyst makes the oxidation of the secondary C–H bond easier than that of the weaker tertiary C–H bonds. Thus, secondary alcohols are the main products. Moreover, the catalyst leaves out wasteful decomposition of H₂O₂, which is prone to result in the production of hydroxyl radicals and lead to nonselective oxidation and further oxidation of the desired products. These advantages of the catalyst allow the purposive production of more valuable organic compounds from abundant and inexpensive alkanes. Especially, the catalyst will contribute to the stereoselective and shape-selective hydroxylation of alkanes creatively.

As for sandwich-type POMs, the performance of ZnWRu₂(ZnW₉)₂ for alkane oxidation was studied in the early years.^{161,219,220} In 2007, the catalysts [B- α -M₄(H₂O)₂(PW₉O₃₄)₂]ⁿ⁻ (B- α -M₄(PW₉)₂; M = Co^{II}, Mn^{II}, Fe^{III}) were used for the oxidation of cyclohexane and cyclooctane with H₂O₂.²²¹ The Fe^{III}-sandwiched catalyst is more active than

Table 6. Hydroxylation of Alkanes with $TBA_3(\gamma\text{-V}_2\text{PW}_{10})^{218}$

| R-H | $H_2O_2 / TBA_3(\gamma\text{-V}_2\text{PW}_{10})$ | $\xrightarrow{\quad} R-\text{OH}$ |
|----------------------------|---|---|
| Substrate | Alcohol Yield (%) | Product /Selectivity (%) |
| cyclohexane | 92 | cyclohexanol (98) |
| cyclooctane | 84 | cyclooctanol (99) |
| cyclononane | 79 | cyclononanol (98) |
| cyclopentane | 98 | cyclopentanol (82), 1-methylcyclopentanol (15), 2-methylcyclopentanol (3) |
| isobutane | 80 | 2-methylpropanol (94), 2,2-dimethylpropanol (6) |
| n-hexadecane | 56 | 1-hexadecanol (2), 2-hexadecanol (66), 3-hexadecanol (26) |
| cyclohexene | 59 | 1-hydroxy-1-cyclohexene (10), 2-hydroxy-1-cyclohexene (4), 3-hydroxy-1-cyclohexene (86) |
| cyclohexane-1,2-diol | 51 | 1,2-dihydro-1,2-dihydrocyclohexane-1,2-diol (93) |
| cyclohexane-1,3-diol | 72 | 1,2-dihydro-1,3-dihydrocyclohexane-1,3-diol (22), 1,2-dihydro-1,3-dihydrocyclohexane-1,2-diol (36), 1,2-dihydro-1,3-dihydrocyclohexane-3,4-diol (40) |
| cyclohexane-1,4-diol | 75 | 1,2-dihydro-1,4-dihydrocyclohexane-1,4-diol (16), 1,2-dihydro-1,4-dihydrocyclohexane-1,2-diol (9), 1,2-dihydro-1,4-dihydrocyclohexane-1,3-diol (44), 1,2-dihydro-1,4-dihydrocyclohexane-3,4-diol (24) |
| 2-methylcyclohexane | 64 | 2-hydroxy-2-methylcyclohexane (3), 2-hydroxy-2-methylcyclohexane (7), 2-hydroxy-2-methylcyclohexane (53), 2-hydroxy-2-methylcyclohexane (25), 2-hydroxy-2-methylcyclohexane (4) |
| 2,2,4-trimethylcyclohexane | 67 | 2-hydroxy-2,2,4-trimethylcyclohexane (63), 2-hydroxy-2,2,4-trimethylcyclohexane (24) |

those sandwiched by Mn^{II} or Co^{II} . With the Fe-sandwiched POM, alkyl hydroperoxides are the most abundant products. With $B\text{-}\alpha\text{-Co}_4(\text{PW}_9)_2$, cyclooctanone is obtained with a selectivity of 83% at 92% cyclooctane conversion. In the aerobic oxidation of *n*-hexadecane with air at 423 K under solvent-free conditions, SBA-15-supported $[Fe_4^{III}(\text{H}_2\text{O})_{10}(\alpha\text{-XW}_9\text{O}_{33})_2]^{n-}$ ($Fe_4(\alpha\text{-XW}_9)_2$; $n = 4, 6$; $X = Se^{IV}, Te^{IV}, As^{III}, Sb^{III}$) give ca. 50% selectivity for C_{16} ketones and ca. 28% selectivity for C_{16} alcohols.²²² The combustion of *n*-hexadecane simultaneously happens, yielding shorter carbon chain (mainly $C_6\text{-}C_{13}$) carboxylic acids (ca. 12%), and trace aldehydes, paraffins, and ketones with less than 10 carbon atoms. The activity comparison indicates that the catalysts with an X^{IV} center are slightly more robust than those with an X^{III} center.

Among these catalysts, $Fe_4(\alpha\text{-SeW}_9)_2/\text{SBA-15}$ gives the highest *n*-hexadecane conversion.

In 2009, Richards et al. synthesized four organo-Ru-grafted oxotungsten clusters, $[X_2\text{W}_{20}\text{O}_{70}(\text{RuC}_6\text{H}_6)_2]^{10-}$ (Figure 8a)

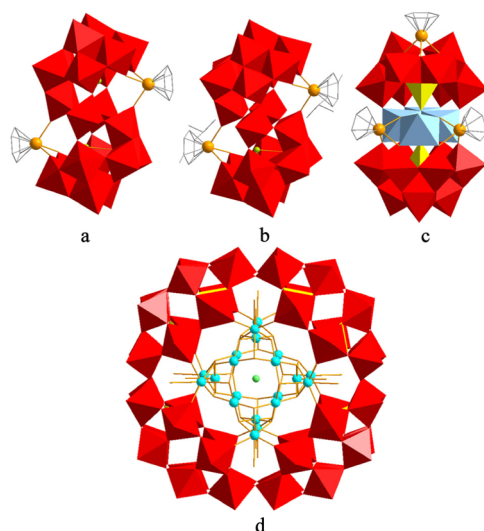
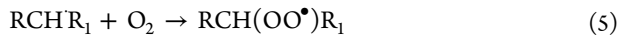


Figure 8. Structures of (a) $[X_2\text{W}_{20}\text{O}_{70}(\text{RuC}_6\text{H}_6)_2]^{10-}$ ($X = \text{Sb, Bi}$), (b) $[X_2\text{W}_{20}\text{O}_{70}(\text{RuC}_{10}\text{H}_{14})_2]^{10-}$ ($X = \text{Sb, Bi}$), (c) $\text{Ru}_3[\text{M}_4(\text{AsW}_8)(\text{AsW}_9)]$ ($\text{M} = \text{Ni}^{II}, \text{Zn}^{II}, \text{Cu}^{II}, \text{Mn}^{II}, \text{Co}^{II}$), and (d) $\text{Cu}_{20}\text{P}_8\text{W}_{48}$.

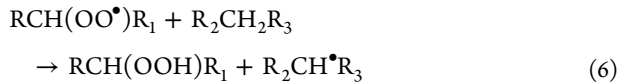
and $[X_2\text{W}_{20}\text{O}_{70}(\text{RuC}_10\text{H}_{14})_2]^{10-}$ (Figure 8b) ($X = \text{Sb, Bi}$), and used them for the oxidation of *n*-hexadecane and *p*-xylene.²²³ In the structures, Ru groups are covalently embedded in the lacunary structures. Experimental results disclose that the four catalysts are more active than their precursors, $\text{Na}_{12}[\text{Sb}_2\text{W}_{22}\text{O}_{74}(\text{OH})_2]\cdot44\text{H}_2\text{O}$ and $\text{Na}_{12}[\text{Bi}_2\text{W}_{22}\text{O}_{74}(\text{OH})_2]\cdot44\text{H}_2\text{O}$, indicating the positive effect of Ru on the catalyst activity. After that, another five organo-Ru-grafted sandwich-type POMs, $\{[\text{M}_4(\text{OH})_2(\text{H}_2\text{O})_2][(\text{RuC}_6\text{H}_6)_3][B\text{-}\alpha\text{-AsW}_9\text{O}_{33}\text{(OH)}][B\text{-}\beta\text{-AsW}_8\text{O}_{30}\text{(OH)}]\}^{6-}$ ($\text{Ru}_3[\text{M}_4(\text{AsW}_8)(\text{AsW}_9)]$; $\text{M} = \text{Ni}^{II}, \text{Zn}^{II}, \text{Cu}^{II}, \text{Mn}^{II}, \text{Co}^{II}$; Figure 8c) were explored by Wu's group.²²⁴ These structures consist of an $\{\text{AsW}_8\}$ Keggin fragment and an $\{\text{AsW}_9\}$ Keggin fragment. A rhomblike tetrameric cluster is sandwiched by the two lacunary Keggin fragments. One Ru group bonds to the top of the $\{\text{AsW}_8\}$ unit via three Ru–O bonds, and two Ru groups graft to the rhomblike tetrameric cluster via six Ru–O bonds. The activity study reveals that $\text{Ru}_3[\text{M}_4(\text{AsW}_8)(\text{AsW}_9)]$ show better performance than $[\text{M}_4(\text{H}_2\text{O})_2\text{As}_2\text{W}_{18}\text{O}_{68}]^{10-}$ ($\text{M}_4(\text{AsW}_9)_2$) in the oxidation of *n*-hexadecane with air as the oxidant and without any additives and solvents. The activity comparisons follow the sequences (1) $\text{Ru}_3[\text{M}_4(\text{AsW}_8)(\text{AsW}_9)] > \text{M}_4(\text{AsW}_9)_2$, (2) $\text{Co}_4(\text{AsW}_9)_2 > \text{Zn}_4(\text{AsW}_9)_2 > \text{Ni}_4(\text{AsW}_9)_2 > \text{Mn}_4(\text{AsW}_9)_2 > \text{Cu}_4(\text{AsW}_9)_2$, and (3) $\text{Ru}_3[\text{Co}_4(\text{AsW}_8)(\text{AsW}_9)] > \text{Ru}_3[\text{Zn}_4(\text{AsW}_8)(\text{AsW}_9)] > \text{Ru}_3[\text{Ni}_4(\text{AsW}_8)(\text{AsW}_9)] > \text{Ru}_3[\text{Mn}_4(\text{AsW}_8)(\text{AsW}_9)] > \text{Ru}_3[\text{Cu}_4(\text{AsW}_8)(\text{AsW}_9)]$. Moreover, $\text{M}_4(\text{AsW}_9)_2$ are more active than their precursor $[\text{AsW}_9\text{O}_{34}]^{9-}$, and $\text{Ru}_3[\text{M}_4(\text{AsW}_8)(\text{AsW}_9)]$ are more active than $[(\text{RuC}_6\text{H}_6)\text{AsW}_9\text{O}_{34}]^{7-}$. These sequences are indicative of the positive synergistic effect of Ru and M. To some extent, AsWRuM can be considered as bimetallic catalysts. Thus, this work opens a new avenue for the design of bimetallic catalysts.

Cu compounds are common in O_2 -based catalytic reactions, but there are few good examples of Cu-POMs for alkane oxidation. Richards et al. applied a wheel-shaped Cu_{20}

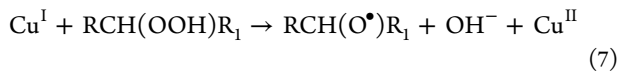
polyoxotungstate, $[\text{Cu}^{\text{II}}_{20}\text{Cl}(\text{OH})_{24}(\text{H}_2\text{O})_{12}(\text{P}_8\text{W}_{48}\text{O}_{184})]^{25-}$ ($\text{Cu}_{20}\text{P}_8\text{W}_{48}$; Figure 8d) anchored on (3-aminopropyl)-triethoxysilane-modified SBA-15, to the solvent-free oxidation of *n*-hexadecane with 1 atm of air.²²⁵ The catalyst is resistant to poisoning by CS_2 and exhibits an exceptionally high TOF of 20 000 h^{-1} at 423 K. The activity of $\text{Cu}_{20}\text{P}_8\text{W}_{48}$ is much higher than that of $\text{Fe}_4(\alpha\text{-XW}_9)_2$ ($n = 4, 6$; X = Se^{IV} , Te^{IV} , As^{III} , Sb^{III}). The product pattern is similar to that with $\text{Fe}_4(\alpha\text{-XW}_9)_2$. C_{16} ketones and C_{16} alcohols are the main products. The sole SBA-15 shows negligible activity in the reaction, and the free $\text{Cu}_{20}\text{P}_8\text{W}_{48}$ shows very low activity. However, SBA-15-supported $\text{Cu}_{20}\text{P}_8\text{W}_{48}$ exhibits a much higher activity than free $\text{Cu}_{20}\text{P}_8\text{W}_{48}$ and SBA-15, which can be understood by a strong ligand interaction between the copper species and the amino moieties in the SBA-15 material. In the catalyst, Cu^{II} is the active site. During the reaction, one-electron transfer from *n*-hexadecane to Cu^{II} initially happens, giving Cu^{I} and *n*-hexadecanyl radical species $\text{RCH}^{\bullet}\text{R}_1$ (eq 4). The radical



$\text{RCH}^{\bullet}\text{R}_1$ reacts with O_2 to form $\text{RCH}(\text{OO}^{\bullet})\text{R}_1$ (eq 5), which in turn reacts with *n*-hexadecane to form another *n*-hexadecanyl radical and *n*-hexadecanyl peroxide (eq 6). The reduced Cu^{I}



species then reacts with *n*-hexadecanyl peroxide to regenerate Cu^{II} and products (eq 7). The interaction between $\text{Cu}_{20}\text{P}_8\text{W}_{48}$



and SBA-15 may facilitate the intrinsic $\text{Cu}^{\text{II}}/\text{Cu}^{\text{I}}$ redox processes, and finally cause the promotion of catalyst activity. In addition, the heterogeneous catalyst is recyclable. The good performance, poison tolerance, and easy recyclability of the catalyst raise the prospect of the catalyst for practical applications.

It is worth mentioning that polymers arouse a great interest in POM-mediated catalysis because they can confer to the catalytic materials some unique physical-chemical properties. In 2006, Bonchio et al. reported hybrid fluoropolymeric membranes with 25% loading of the fluorous-tagged $(\text{R}_f\text{N})_4\text{W}_{10}\text{O}_{32}$ ($\text{R}_f\text{N} = [\text{CF}_3(\text{CF}_2)_7(\text{CH}_2)_3]_3\text{CH}_3\text{N}^+$), which effects the solvent-free photooxygenation of benzylic C–H bonds with TONs of up to 6100 in 4 h.²²⁶ On one hand, the solvent-free system allows the use of O_2 . On the other hand, the application of fluoropolymeric membrane technology provides POM-mediated catalysis with the combination of advanced molecular separation and selective transport properties, with reactivity on a heterogeneous support. Thus, the protocol represents an encouraging step forward in sustainable catalysis.

2.2.2. To Alkenes. The oxidative dehydrogenation of alkanes to alkenes is another aspect of alkane oxidation. In the

presence of $\text{H}_3\text{PMo}_{12}$, the oxidative dehydrogenation of alkanes using TBHP proceeds readily at 353 K.²²⁷ For a series of cyclic alkanes, the formation of the dehydrogenated product dominates typically with $90 \pm 5\%$ selectivity for alkenes. For those with cyclohexyl moieties, there is some tendency for aromatization. For acyclic alkanes, the relative percentage of dehydrogenation depends on the linearity of the alkanes. As the branches of the alkanes increase, the selectivities toward dehydrogenation increase from 60% for *n*-octane to 100% for 2,2,4-trimethylpentane. Double bonds are preferentially formed at the less substituted carbon centers. The oxidative dehydrogenation mechanism involves a combination of *tert*-butoxy radical formation and electron-transfer oxidation of an intermediate alkyl radical. The effectiveness of $\text{Cs}_{2.5}\text{Cu}_{0.08}\text{H}_{3.34-}(\text{V}_3\text{PMo}_9)$ for the selective oxidative dehydrogenation of propane with O_2 is evidenced at 653 K.²²⁸ The selectivity of 25% for propene is achieved at a propane conversion of 40%. In oxidative dehydrogenation reactions, acidic sites on the catalysts significantly influence the selectivities for alkenes.^{229–231} Generally, low acidity facilitates the formation of alkenes. Contrarily, high acidity will enhance the selectivity for CO_x and oxygenated products.

It has been reported that NiO serves dehydrogenation reactions.^{232–234} However, single NiO is hard to employ as a stable catalyst with high catalytic performance because it is easily reduced to Ni^0 . The nanocomposites of NiO and $\text{Cs}_{2.5}\text{H}_{0.5}\text{PMo}_{12}$ with particle size in the range of 5–10 nm exhibit excellent catalytic performance in the oxidative dehydrogenation of propane and isobutane.²³⁵ The oxidative dehydrogenation of propane at 723 K yields 20% propene stably, in contrast to the previously reported highest 12% over the composites with relatively higher stability toward reduction, such as $\text{Ni}-\text{Ce}-\text{O}$, $\text{Ni}-\text{Nb}-\text{O}$, and $\text{Ni}-\text{Ti}-\text{O}$. For isobutane, the selectivity for isobutene and methacrolein reaches up to 90% at an isobutane conversion of 15%.

2.3. Oxidation of Arenes and Derivatives

The oxidation of arenes and their derivatives provides a practical way to acquire phenols, quinones, and derivatives. POMs are qualified for these reactions. It has been previously documented that $\text{H}_5\text{V}_2\text{PMo}_{10}$ can activate arenes with relatively low oxidation potentials such as anthracene and 4-methoxytoluene by initially extracting an electron from the hydrocarbon through the formation of a radical cation intermediate, followed by oxygen transfer, from the HPA anions to substrates, to form oxygenates.^{236–238} In the presence of $\text{H}_5\text{V}_2\text{PMo}_{10}$ and 1 atm of O_2 , the selective oxidation (>99%) of anthracene to anthraquinone is achieved at 333 K after 18 h.²³⁶ To acquire phenols, Fe- and V-substituted POM/HPA catalysts are extensively investigated for the oxidative hydroxylation of benzene.^{239–245} These catalysts show remarkable activity. However, the selective hydroxylation of substituted arenes is still challenging. Because the regioselectivities of aromatic substitution reactions are often beyond control and arene substrates are less reactive than the initial phenol products, the selective hydroxylation of substituted arenes is often accompanied by the formation of regioisomers, polyhydroxylated arenes, quinones, and tars.²⁴⁶ Especially difficult is the selective hydroxylation of a deactivated arene with electron-withdrawing moieties, such as nitrobenzene, which has a significantly high oxidation potential. The first example of the aerobic regioselective hydroxylation of nitrobenzene is set by $\text{H}_5\text{V}_2\text{PMo}_{10}\cdot 34\text{H}_2\text{O}$.²⁴⁷ A selectivity of 99% for 2-nitrophenol

at a ~5% maximum yield is achieved by heating a 0.01 M solution of $\text{H}_5\text{V}_2\text{PMo}_{10}\cdot34\text{H}_2\text{O}$ in neat nitrobenzene at 413 K under 2 bar of O_2 . Since the C–H bond strengths are similar at all positions, the regioselective hydroxylation should be the result of an intramolecular preference with the resulting thermokinetic advantage for the reaction at the *ortho* position. The reaction stops after about 30–40 h, although the catalyst appears to remain intact. The reasonable explanation is that no protons are generated in the present reaction. The addition of 4 Å molecular sieves to the reaction mixture inhibits the reaction due to the complete removal of water. According to these results, a hydrogen-bond-containing intermediate is assumed (Figure 9). Unexpectedly, the addition of water is not helpful

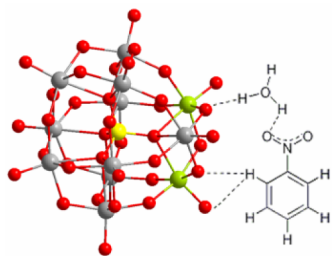


Figure 9. A representative model for the interaction of nitrobenzene with the acidic catalyst $\text{H}_5\text{V}_2\text{PMo}_{10}$.

for the reaction. The inactivities of isostructural H_3PW_{12} , $\text{H}_3\text{PMo}_{12}$, and $\text{TBA}_5(\text{V}_2\text{PMo}_{10})$ indicate that the incorporation of vanadium into the anionic framework and the presence of protons are indispensable for the catalytic transformation. Apart from di-*V*-substituted molybdophosphoric acid, the mono- and trisubstituted analogues are also effective for the reaction. The relative reaction rates for 0.01 M $\text{H}_{3+n}\text{V}_n\text{PMo}_{12-n}$ in nitrobenzene are 1.0, 3.0, and 5.1 for n from 1 to 3, respectively, relative to $\text{H}_4\text{VPMo}_{11}$. Ni-substituted oxovanadium cluster $\text{K}_7\text{NiV}_{13}\text{O}_{38}\cdot16\text{H}_2\text{O}$ is also active for the hydroxylation of aromatics bearing an electron-withdrawing group using 30% H_2O_2 as the oxygen donor.²⁴⁸ However, HOAc is needed as an acidic additive. For methyl benzoate, the yield of hydroxylated products reaches up to 73%. The ratio of *o*-, *m*-, and *p*-OH isomers is 70:20:10. For nitrobenzene, 87% selectivity for 2-nitrophenol at 9% yield is obtained.

Usually, the oxidation of alkylarenes takes place preferentially at the side chain sp^3 C–H bonds rather than the aromatic ring sp^2 C–H bonds because the bond dissociation energies of the $\text{ArCR}_2\text{—H}$ bonds are much lower than those of the Ar—H bonds.^{249–251} Therefore, it is difficult to obtain alkylphenols selectively by direct oxidation of alkylarenes. However, chemo- and regioselective direct hydroxylation of structurally diverse arenes, including alkylarenes with reactive secondary and tertiary side chain sp^3 C–H bonds, is achieved by the versatile di-*V*-substituted phosphotungstate $\gamma\text{-V}_2\text{PW}_{10}$ using H_2O_2 as the oxidant (Table 7).²⁵² The system shows a unique preference for the formation of *p*-phenols for monosubstituted benzenes without significant formation of side chain oxygenated products. As for anisole, the oxidative demethylation is suppressed successfully. The *para*-hydroxylation of anisole preferentially proceeds and gives a yield of 85%. The *ortho*-, *meta*-, and *para*-isomer ratio is 5:<1:95, compared with 100:0:0 with $\text{K}_7\text{NiV}_{13}\text{O}_{38}\cdot16\text{H}_2\text{O}$.²⁴⁸ As for toluene, 86% selectivity for hydroxylated products with the ratio of *o*-, *m*-, and *p*-OH isomers equivalent to 7:16:77 is determined.

Table 7. Chemo- and Regioselective Hydroxylation of Arenes with $\text{TBA}_3(\gamma\text{-V}_2\text{PW}_{10})^{252}$

| Substrate | Product | Yield (%) | Selectivity (%) |
|-----------|-------------------------|-----------|-----------------|
| | | 85 | >99 |
| | | 78 | >99 |
| | | 93 | >99 |
| | | 56 | 99 |
| | | 86 | 85 |
| | | 63 | >99 |
| | | 60 | 86 |
| | | 66 | 77 |
| | | 55 | 88 |
| | | 47 | 97 |
| | | 43 | 87 |
| | | 61 | 98 |
| | 2,3:3,4=5:95 | 71 | 96 |
| | 2,4,3,5,2,6=90:9:<1 | 98 | 45 |

According to Nomiya's investigation, the product distribution pattern of toluene hydroxylation is related to both the cation and anion structures of the used POM catalysts.²⁵³ For example, the reactions with $\text{TBA}_4(\text{V}_2\text{PW}_{10}\text{O}_{40})$ prefer side chain oxidation, the reactions with $\text{K}_5(\text{V}_2\text{PW}_{10}\text{O}_{40})$ and $\text{K}_7(\text{Mo}_2\text{VP}_2\text{W}_{15}\text{O}_{62})$ show preferential ring oxidation, in particular, favoring the selective production of *o*-cresol, the reactions with $\text{K}_4(\text{VPMo}_{11})$ and $\text{Na}_4(\text{VPMo}_{11})$ show comparable side chain oxidation and ring oxidation, and the reactions with $\text{TBA}_4(\text{VPMo}_{11})$ show low selectivity for side

chain oxidation, although the ring oxidation is very similar to those with $K_4(VPMo_{11})$ and $Na_4(VPMo_{11})$.

2.4. Oxidation of Organosilanes

Oxidation of organosilanes results in silanols, the building blocks for silicon-based polymer materials and organic donors in metal-catalyzed cross-coupling reactions.^{254,255} Traditional methods to produce silanols with a strong acid or base as the catalyst often need strictly controlled reaction conditions. The selectivity for silanols, especially for the sterically exposed silanols that easily undergo condensation to form disiloxanes, is challenging. Some POM catalysts can address the problem of selectivity. With the tetranuclear oxotungsten cluster $TPA_3\{H-[W_2O_2(O_2)_4(\mu-O)]_2\}$ ($TPA = (n-C_3H_7)_4N^+$), triethylsilane is oxidized to triethylsilanol by H_2O_2 with 76% yield and 87% selectivity without addition of any additives.¹²⁰ With the divacant Keggin-type catalyst $TBA_4(\gamma-H_4SiW_{10})$, a series of silanols, including sterically exposed ones, are produced with high yields and selectivities via the oxidation of organosilanes using only 1 equiv of diluted aqueous H_2O_2 with respect to the substrates under common conditions.²⁵⁶ The results are listed in Table 8. These reactions readily proceed without any acidic or basic additives. Notice that $TBA_4(\gamma-H_4SiW_{10})$ set an example of catalytic oxidation of alkoxysilanes to the corresponding silanols, which is difficult in traditional base-catalyzed systems. For optically active silane, the configuration is highly retained after reaction. Furthermore, the present system is applicable for a 20 mmol scale oxidation of some substrates with a high TOF of ca. 700 h^{-1} . The value for triethylsilane is 680 h^{-1} , much higher than those of hydrolytic oxidation systems such as $\{[RuCl_2(p\text{-cymene})]\}_2$ (285 h^{-1}), $\{[IrCl(C_8H_{12})]\}_2$ (80 h^{-1}), Ru–hydroxyapatite (HAP; 3 h^{-1}), Au–HAP (60 h^{-1}), Ag–HAP ($<1\text{ h}^{-1}$), and Pt nanoclusters (125 h^{-1}), and those of H_2O_2 -based oxidation systems such as methyltrioxorhenium/zeolite NaY (2 h^{-1}) and Ti- β ($<1\text{ h}^{-1}$). The value for dimethylphenylsilane (MTO) is 690 h^{-1} , much higher than those of $\{[IrCl(C_8H_{12})]\}_2$ (85 h^{-1}), Ru–HAP (78 h^{-1}), Au–HAP (40 h^{-1}), Ag–HAP (178 h^{-1}), Pt nanoclusters (200 h^{-1}), MTO/zeolite NaY (2 h^{-1}), and Ti- β ($<1\text{ h}^{-1}$), while the value is lower than that of $\{[RuCl_2(p\text{-cymene})]\}_2$ (5460 h^{-1}). However, the cost of $TBA_4(\gamma-H_4SiW_{10})$ may be lower than that of the noble-metal-containing $\{[RuCl_2(p\text{-cymene})]\}_2$.

Lacunary POMs can be considered as inorganic, multidentate ligands.² When $\gamma-H_2SiW_{10}$ is used as the multidentate oxygen-donor ligand, it can stabilize catalytically active metal cations. Tetrasilver cluster $TBA_8[Ag_4(DMSO)_2(\gamma-H_2SiW_{10}O_{36})_2]$ ($TBA_8[Ag_4(\gamma-H_2SiW_{10})_2]$; Figure 10a)²⁵⁷ and hexasilver cluster $TBA_8[Ag_6(\gamma-H_2SiW_{10}O_{36})_2]$ ($TBA_8[Ag_6(\gamma-H_2SiW_{10})_2]$; Figure 10b),²⁵⁸ encapsulated by two $\gamma-H_2SiW_{10}$ polyanions are effective for hydrolytic oxidation of silanes using abundant H_2O as a safe oxidant (Table 8). These reactions produce clean H_2 as the sole byproduct. With $TBA_8[Ag_4(\gamma-H_2SiW_{10})_2]$, various silanes convert to the corresponding silanols selectively and quickly with high yields of 72–96%. The hydrolytic oxidation of dimethylphenylsilane conducted with 0.004 mol % $TBA_8[Ag_4(\gamma-H_2SiW_{10})_2]$ at 343 K gives dimethylphenylsilanol in a yield of 72% over 10 min. In this case, the TOF based on silver is $27\,000\text{ h}^{-1}$, in contrast to 178 h^{-1} at 353 K with Ag–HAP and 690 h^{-1} at 333 K with $TBA_4(\gamma-H_4SiW_{10})$. When the silver salt $Ag(OAc)$ is used in place of $TBA_8[Ag_4(\gamma-H_2SiW_{10})_2]$, glossy precipitates (metal silver) are formed during the process, resulting in low yields of the silanols. However, the phenomenon is invisible for $TBA_8[Ag_4(\gamma-H_2SiW_{10})_2]$, indicat-

Table 8. Oxidation of Various Silanes to Silanols with TBA Salts of $\gamma-H_4SiW_{10}$, $Ag_4(\gamma-H_2SiW_{10})_2$, or $Ag_6(\gamma-H_2SiW_{10})_2$

| Catalyst | Time (min) | a | Yield of b (%) | Ref. | R_1 | R_2 | R_3 |
|------------------------------|------------|---|----------------|------|-------|-------|-------|
| | | | | | R_1 | R_2 | R_3 |
| a | b | | | | | | |
| $\gamma-H_4SiW_{10}$ | 240 | | 83 | 256 | | | |
| $Ag_4(\gamma-H_2SiW_{10})_2$ | 4 | | 96 | 257 | | | |
| $Ag_6(\gamma-H_2SiW_{10})_2$ | 1 | | 98 | 258 | | | |
| $\gamma-H_4SiW_{10}$ | 240 | | 77 | 256 | | | |
| $\gamma-H_4SiW_{10}$ | 180 | | 83 | 256 | | | |
| $Ag_4(\gamma-H_2SiW_{10})_2$ | 2 | | 83 | 257 | | | |
| $Ag_6(\gamma-H_2SiW_{10})_2$ | 1 | | 93 | 258 | | | |
| $\gamma-H_4SiW_{10}$ | 240 | | 78 | 256 | | | |
| $Ag_4(\gamma-H_2SiW_{10})_2$ | 180 | | 92 | 257 | | | |
| $Ag_4(\gamma-H_2SiW_{10})_2$ | 7 | | 96 | 257 | | | |
| $Ag_6(\gamma-H_2SiW_{10})_2$ | 1 | | 95 | 258 | | | |
| $\gamma-H_4SiW_{10}$ | 300 | | 78 | 256 | | | |
| $Ag_4(\gamma-H_2SiW_{10})_2$ | 5 | | 91 | 257 | | | |
| $Ag_6(\gamma-H_2SiW_{10})_2$ | 1 | | 99 | 258 | | | |
| $\gamma-H_4SiW_{10}$ | 180 | | 88 | 257 | | | |
| $Ag_4(\gamma-H_2SiW_{10})_2$ | 10 | | 95 | 258 | | | |
| $Ag_4(\gamma-H_2SiW_{10})_2$ | 180 | | 94 | 257 | | | |
| $Ag_6(\gamma-H_2SiW_{10})_2$ | 60 | | 96 | 258 | | | |
| $Ag_4(\gamma-H_2SiW_{10})_2$ | 10 h | | 78 | 257 | | | |
| $\gamma-H_4SiW_{10}$ | 240 | | 90 | 256 | | | |
| $Ag_4(\gamma-H_2SiW_{10})_2$ | 8 h | | 78 | 257 | | | |
| $Ag_6(\gamma-H_2SiW_{10})_2$ | 270 | | 93 | 258 | | | |
| $\gamma-H_4SiW_{10}$ | 240 | | 90 | 256 | | | |
| $\gamma-H_4SiW_{10}$ | 240 | | 78 | 256 | | | |
| $\gamma-H_4SiW_{10}$ | 180 | | 78 | 256 | | | |
| $\gamma-H_4SiW_{10}$ | 240 | | 82 | 256 | | | |
| $Ag_4(\gamma-H_2SiW_{10})_2$ | 24 h | | 72 | 257 | | | |
| $Ag_6(\gamma-H_2SiW_{10})_2$ | 24 h | | 92 | 257 | | | |
| $\gamma-H_4SiW_{10}$ | 300 | | 77 | 256 | | | |
| $\gamma-H_4SiW_{10}$ | 240 | | 49 | 256 | | | |
| $\gamma-H_4SiW_{10}$ | 30 | | 40 | 256 | | | |
| $\gamma-H_4SiW_{10}$ | 90 | | 72 | 256 | | | |
| $\gamma-H_4SiW_{10}$ | 150 | | 62 | 256 | | | |

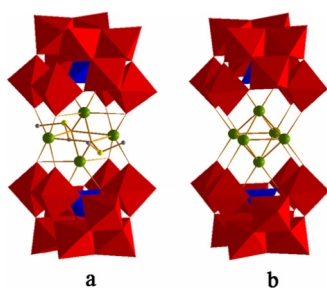


Figure 10. Structures of (a) $\text{Ag}_4(\gamma\text{-H}_2\text{SiW}_{10})_2$ and (b) $\text{Ag}_6(\gamma\text{-H}_2\text{SiW}_{10})_2$.

ing that the all-inorganic ligand γ -H₂SiW₁₀ protects Ag⁺ from reducing to Ag.

2.5. Oxidation of Alcohols and Phenols

The selective oxidation of hydroxyl groups to carbonyl compounds is a key transformation in organic synthesis for both fundamental research and industrial manufacturing because of the usefulness of carbonyl compounds for pharmaceuticals, agricultural chemicals, and fragrances.²⁵⁹ The early Venturello–Ishii systems have disclosed the remarkable performance of PW₁₂ for the oxidation of alcohols with H₂O₂. Since then, much work focusing on immobilization of the proven active polyanion has been carried out. Ikegami et al. supported it on PNIPAAm polymer with a Disperse Red moiety (Figure 11a),²⁶⁰ Uozumi et al. supported it on a poly(ethylene oxide–pyridinium) matrix (Figure 11b),²⁶¹ Xia et al. supported it on IL-modified polystyrene resin beads (Figure 11c),²⁶² etc.

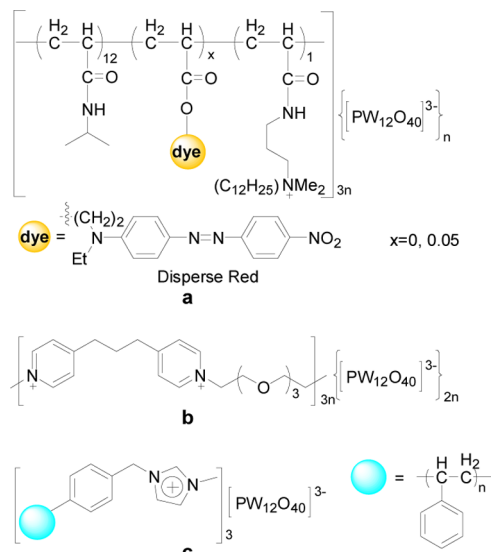


Figure 11. Three supported PW₁₂-based catalysts.

In 2003, Neumann's group reported two heptamolybdates, $[(C_8H_{17})_3NCH_3]_4[M^{II}(DMSO)_3Mo_7O_{24}]$ ($M = Ru, Os$) for the aerobic oxidation of alcohols to ketones/aldehydes.²⁹ In the presence of the catalysts, all the tested benzyl alcohols are quantitatively oxidized to the corresponding aldehydes (Table 9). Secondary allylic alcohols are oxidized to the corresponding ketones with high yields. However, the conversions and selectivities for primary aliphatic alcohols are relatively low. It has been reported that the reactions with more reduced forms

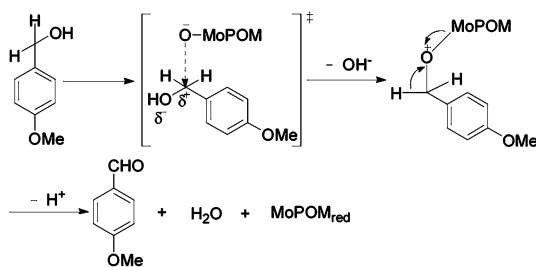
Table 9. Aerobic Oxidation of Alcohols Catalyzed by $[(C_8H_{17})_3NCH_3]_4[M^{II}(DMSO)_3Mo_7O_{24}]$ ($M = Ru, Os$)²⁹

of TMs, such as Pd^{II} and Ru^{II}, typically proceed via a hydrometal-type mechanism, and base is usually needed to facilitate the alkoxide formation and then coordination to the metal center.^{263,264} However, the present system needs no additives. It supports a variation of an oxometal-type mechanism (Scheme 7), in which Mo rather than Ru/Os is the catalytically active site. It is notable that the oxometal mechanism is differentiated delicately for substrates with electron-donating substituents and those with electron-withdrawing substituents. For the substrates with electron-donating substituents, an oxygen atom of the POM catalyst nucleophilically attacks the benzylic carbon, leading to the formation of a new C–O bond with hydroxyl as the leaving group. Subsequently, a proton and the reduced POM are released with the formation of benzylic aldehyde. For the substrates with electron-withdrawing substituents, the significantly higher acidity of the benzylic hydrogen leads to a partial negative charge at the benzylic carbon. The POM catalyst initially abstracts a proton from the benzylic carbon. Then the protonated POM catalyst recombines with a carbanionic species, leading to the formation of a new C–O bond. In the following step, a proton, a hydroxyl, and the reduced POM catalyst leave in a synergic manner and benzylic aldehyde is formed.

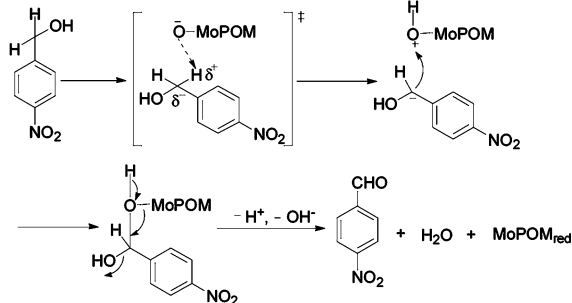
V-substituted POMs are more extensively utilized to promote the oxidation of alcohols than other TM-substituted POMs.²⁶⁵ In the oxidation of benzyl alcohol using H₂O₂, the surfactant-type salt [C₁₈H₃₇NH(CH₃)₂]₄(VPMo₁₁) gives benzaldehyde with a selectivity of 99% at 60.6% benzyl alcohol conversion under organic solvent-free conditions.²⁶⁶ The result-

Scheme 7. Proposed Oxometal Mechanisms for 4-Methoxybenzyl Alcohol and 4-Nitrobenzyl Alcohol²⁹

For substrates with electron donating substituent:



For substrates with electron withdrawing substituent:



benefits from the amphiphilic nature of the catalyst. The hydrophobic alkyl chains encapsulate the relatively less polar benzyl alcohol and promote the release of the more polar benzaldehyde. The hydrophilic POM anions easily access H_2O_2 to form active peroxy species. However, the length of the alkyl chain on the cations should be moderate. Chains that are too long will inhibit the interaction of anions with H_2O_2 , though the encapsulation of benzyl alcohol is enhanced. Chains that are too short make the formation of active species easy, but deteriorate the accessibility of alcohols to hydrophilic active species.

Neumann et al. have conducted alcohol oxidation with $\text{H}_5\text{V}_2\text{PMo}_{10}$ in DMSO under an O_2 atmosphere.²⁶⁷ Interestingly, DMSO was found as an oxygen donor. The performance of $\text{H}_5\text{V}_2\text{PMo}_{10}$ has also been evaluated in PEG-200²⁶⁸ and supercritical carbon dioxide (scCO_2),²⁶⁹ using O_2 as the oxidant. As green solvents, both PEG-200 and scCO_2 afford recyclable methods for $\text{H}_5\text{V}_2\text{PMo}_{10}$. However, the reactions in scCO_2 present much higher TON and average TOF values than those in PEG-200 under comparable conditions. Silica provides solidification for $\text{V}_2\text{PMo}_{10}$. In the presence of air, $\text{V}_2\text{PMo}_{10}$ supported on mesoporous SBA-15 can be reused five times with retention of catalytic activity.²⁷⁰ The stable nitroxyl radical 2,2,6,6-tetramethylpiperidine-1-oxyl (TEMPO) and the derivatives are energetic additives in alcohol oxidation with O_2 . The combination of $\text{V}_2\text{PMo}_{10}$ and TEMPO shows enhanced performance. In the reaction, $\text{V}_2\text{PMo}_{10}$ oxidizes TEMPO to nitrosium cation, the active alcohol-oxidizing species.²⁷¹ In fact, the cocatalysis effect of $\text{V}_2\text{PMo}_{10}$ in alcohol oxidation is also observed with active carbon supports and quinones.²⁷² The magnetic silica $\text{Fe}_3\text{O}_4/\text{SiO}_2$ supported hybrid IL combining TEMPO and $\text{V}_2\text{PMo}_{10}$ (Figure 12) opens a good method of recycling $\text{V}_2\text{PMo}_{10}$ and expensive TEMPO.²⁷³

Most recently, Hu et al. combined a Pd complex with $\text{V}_2\text{PMo}_{10}$, resulting in the catalyst $[\text{Pd}(\text{dpa})(\text{DMSO})_2]_2 \cdot [\text{HV}_2\text{PMo}_{10}] \cdot 4\text{DMSO}$ ($\text{dpa} = 2,2'$ -dipyridylamine), which is

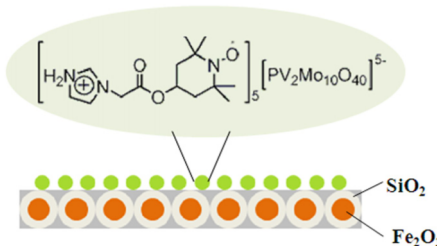


Figure 12. Magnetic silica supported hybrid IL combining TEMPO and $\text{V}_2\text{PMo}_{10}$.

effective for the aerobic oxidation of alcohols at ambient pressure.²⁷⁴ Valuably, a ternary intermediate, $\{\text{Pd}(\text{dpa})_2[\text{VO}(\text{DMSO})_5]_2\}[\text{PMo}_{12}]_2 \cdot 4\text{DMSO}$, is isolated and characterized crystallographically. It proves to be the true active species. Notice that the anion of the active species differs from that of the catalyst precursor, revealing that, during the catalytic reaction, VO^{2+} is removed from the parent anion $\text{HV}_2\text{PMo}_{10}$ and the cationic species $[\text{VO}(\text{DMSO})_5]^{2+}$ is formed, and at the same time the remaining fragment reassembles into PMo_{12} . The similar detachment of mononuclear vanadium species, which usually happens under acidic conditions, is also reported by Streb et al.²⁷⁵ and Neumann et al.²⁷⁶ With the isolated active species, several aromatic alcohols are converted into the corresponding aldehydes/ketones with 98.1–99.8% conversions and 91.5–99.1% selectivities. The Pd complex, the mononuclear vanadium cluster, and the Keggin-type POM of the active species synergically contribute to the catalysis. The isolation of the active species not only enriches the structural database of POMs, but also helps to gain insight into catalytic process of POMs.

Trisubstituted POM catalysts for alcohol oxidation are less explored. Tri-Co-substituted anions $\{\alpha\text{-}[\text{Co}(\text{H}_2\text{O})]_3\text{-SiW}_9\text{O}_{37}\}^{10-}$ have been intercalated between the layers of MgAl-hydrotalcite and used for the liquid-phase selective oxidation of cyclohexanol using 1 atm of O_2 .²⁷⁷ After intercalation, the activity of the trisubstituted catalyst toward cyclohexanol is retained well. In terms of the oxidation of benzyl alcohol, the intercalated catalyst even shows higher activity and selectivity than the unintercalated sample. In addition, the Co_3 -POM pillared hydrotalcite sample shows much higher activity than those pillared by other $\{\alpha\text{-}[\text{M}(\text{H}_2\text{O})]_3\text{SiW}_9\text{O}_{37}\}^{n-}$ ($\text{M} = \text{Cu}^{\text{II}}, \text{Ni}^{\text{II}}, \text{Fe}^{\text{III}}, \text{Cr}^{\text{III}}; n = 10, 7$) anions.

Zn/Al-sandwiched POM catalysts are very useful for the oxidation of alcohols. The isomers of $\alpha/\beta\text{-}[\text{Zn}_2\text{Sb}^{\text{III}}_2(\text{ZnW}_9\text{O}_{34})_2]^{14-}$ with variable valence of antimony catalyze the reaction via their respective high-valent derivatives $\alpha/\beta\text{-}[\text{Zn}_2\text{Sb}^{\text{V}}_2(\text{OH})_2(\text{ZnW}_9\text{O}_{34})_2]^{12-}$.²⁷⁸ The water-soluble POM $\text{Na}_{12}[\text{ZnWZn}_2(\text{H}_2\text{O})_2(\text{ZnW}_9\text{O}_{34})_2]$ ($\text{Na}_{12}[\text{ZnWZn}_2(\text{ZnW}_9)_2]'$) triggers a biphasic system with H_2O_2 and without organic solvent, which serves a wide range of alcohols.¹⁷³ Liquid secondary alcohols including 2-propanol, 2-pentanol, 2-octanol, 1-phenylethanol, cyclohexanol, and cyclooctanol are selectively oxidized to the corresponding ketones in high yields (>90%). The substrates with strongly electron-withdrawing substituents adjacent to the carbinol center such as 1-cyclohexyl-3,3,3-trifluoro-2-propanol are not oxidized. Primary alcohols are primarily oxidized to the corresponding carboxylic acids. The formation of carboxylic acid is partially inhibited by the addition of catalytic amounts of TEMPO, and the oxidation stops at the aldehyde stage. A 1,3-diol, 2-ethyl-1,3-hexanediol, is

almost exclusively oxidized at the secondary position to yield the appropriate 3-keto alcohol with some C–C bond cleavages. 2-Butyl-4-chloro-5-(hydroxymethyl)imidazole, an intermediate for angiotensin II inhibitors, also reacts to yield the corresponding carboxylic acid, and the nitrogen-based moiety is not susceptible. However, the N sites in some compounds can be oxidized under appropriate conditions with $\text{Na}_{12}^-[ZnWZn_2(\text{ZnW}_9)_2]'$.⁴¹ Pyridine derivatives are oxidized to the respective N-oxides, primary amines are oxidized to oximes, and aniline derivatives are oxidized to the corresponding azoxy or nitro products, depending on the substitution pattern of the aromatic ring. The case for primary alcohols is significantly changed by attaching Pd to $[ZnWZn_2(\text{ZnW}_9)_2]'$.²⁷⁹ The resulting catalyst ($\text{PdCl}_2\text{O}_{0.5}\text{Q}_{12}^-[ZnWZn_2(\text{ZnW}_9)_2]'$ ($\text{Q} = \text{C}_{16}\text{H}_{33}(\text{CH}_3)_3\text{N}$) shows high selectivities for aldehydes in the fast aerobic oxidation of primary aliphatic alcohols using 2 bar of O_2 . No additive is required to prevent the formation of carboxylic acids or to activate the alcohols. Autoxidation is successfully inhibited, although O_2 is used as the oxidant. Uniquely, the catalyst shows a significant preference for the oxidation of primary versus secondary aliphatic alcohols.

In 2006, a cross-linked poly(ethylenimine)-POM catalyst assembly was prepared by embodying active $[ZnWZn_2(\text{ZnW}_9)_2]'$ in the pore of inactive cross-linked polyethylenimine (Figure 13) to achieve a distinctive lip-

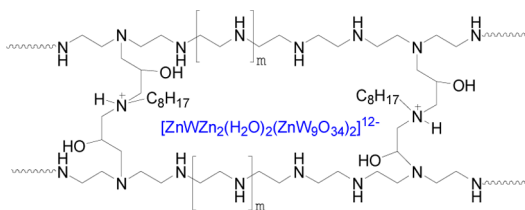


Figure 13. Cross-linked poly(ethylenimine)-POM catalyst.

ophiloselectivity in aqueous media.⁴³ In such a system, more lipophilic 2-alkanols are preferentially oxidized by H_2O_2 . Apparently, this is a meaningful strategy for the reaction involving a lipophilic reagent in water, the most desirable reaction medium in terms of the environmental and economical aspects.

Sandwiched metals in sandwich-type POM catalysts may create a definite reactivity “umpolung” with respect to plenary POMs or different metal-sandwiched POMs.¹⁶⁵ Tetra-Al^{III}-sandwiched POMs $\text{TBA}_4[\text{Al}^{III}_4(\text{H}_2\text{O})_{10}(\beta\text{-XW}_9\text{O}_{33}\text{H})_2]$ ($\text{TBA}_4[\text{Al}_4(\beta\text{-HXW}_9)_2]$; X = As, Sb) preferentially catalyze the oxidation of hydroxyl when double bonds exist, leaving the double bonds unaffected.²⁸⁰ However, the In^{III} derivative $\text{TBA}_6[\text{In}^{III}_4(\text{H}_2\text{O})_{10}(\beta\text{-AsW}_9\text{O}_{33})_2]$ ($\text{TBA}_6[\text{In}_4(\beta\text{-AsW}_9)_2]$) is less effective for alcohol oxidation. It shows an intermediate behavior. In the presence of $\text{TBA}_6[\text{In}_4(\beta\text{-AsW}_9)_2]$, 2-cyclohexen-1-ol is converted into the corresponding enone and epoxide with lower chemoselectivity. The unique chemoselectivity of $\text{TBA}_4[\text{Al}_4(\beta\text{-HXW}_9)_2]$ to hydroxyl oxidation results from the easy formation of aluminum-alcoholate due to the strong Lewis acidity of Al^{III}. The tetra-Zn-sandwiched $\text{TBA}_8\{[\text{Zn}(\text{OH}_2)(\mu_3\text{-OH})]_2[\text{Zn}(\text{OH}_2)_2]_2[\gamma\text{-HSiW}_{10}\text{O}_{36}]_2\}$ ($\text{TBA}_8[\text{Zn}_4(\gamma\text{-HSiW}_{10})_2]$) shares similar reactivity “umpolung”.²⁸¹ $\text{TBA}_4(\gamma\text{-HSiW}_{10})$ has been confirmed as a good catalyst for alkene epoxidation, but it is much less active for the oxidation of hydroxyl groups.¹³¹ However, $\text{TBA}_8[\text{Zn}_4(\gamma\text{-HSiW}_{10})_2]$ performs in a totally inverse way. For example,

the oxidation of 2-cyclohexen-1-ol with $\text{TBA}_4(\gamma\text{-HSiW}_{10})$ gives the corresponding epoxy alcohol, while the reaction with $\text{TBA}_8[\text{Zn}_4(\gamma\text{-HSiW}_{10})_2]$ exclusively gives the corresponding enone. Thus, a pathway involving zinc-alcoholate is logical. Apart from $\text{TBA}_8[\text{Zn}_4(\gamma\text{-HSiW}_{10})_2]$, the stable isomers of $\text{TBA}_8\{[\text{Zn}_2\text{W}(\text{O})_3]_2\text{H}_4[\alpha/\beta\text{-SiW}_9\text{O}_{33}]_2\}$, derived from the metastable $\text{TBA}_8[\text{Zn}_4(\gamma\text{-HSiW}_{10})_2]$, are also active for the oxidation of structurally diverse alcohols, including aliphatic, benzylic, allylic, and propargylic alcohols, to afford the corresponding carbonyl compounds.²⁸² These findings suggest that some metals (e.g., Al, Zn) with strong Lewis acidity trend to form alcoholates with hydroxyl groups. In catalysis, these metals likely facilitate the oxidation of hydroxyl groups; in inorganic synthesis, they may be helpful for the construction of novel functional polymers using multihydroxyl ligands.

Dawson-type POMs $\text{K}_6\text{Mo}_x\text{P}_2\text{W}_{18-x}\text{O}_{62}$ ($\text{K}_6\text{Mo}_x\text{P}_2\text{W}_{18-x}$, $x = 0, 5, 6$) and $\text{K}_7(\alpha_1/\alpha_2\text{-Mo}_5\text{VP}_2\text{W}_{12}\text{O}_{62})$ ($\text{K}_7(\alpha_1/\alpha_2\text{-Mo}_5\text{VP}_2\text{W}_{12})$) have been investigated for methanol oxidation at 533 K in the presence of O_2 .²⁸³ The compositions and the relative positions of the W, Mo, and V atoms in the anionic framework lead to different acidic and redox properties that control the selectivity orientation between the intermolecular dehydration and the oxidation reaction. In other words, the product distribution (formaldehyde, methyl formate, dimethyl ether, dimethoxymethane) depends on the composition and the symmetry of the anionic framework. As shown in Table 10,

Table 10. Product Distribution of Methanol Oxidation with Dawson-Type POMs and O_2 ²⁸³

| catalyst | conversion (%) | selectivity (%) | | | | |
|--|----------------|-----------------|------|------|------|------|
| | | 1 | 2 | 3 | 4 | 5 |
| $\text{K}_6(\alpha\text{-P}_2\text{W}_{18})$ | 27.3 | 0.0 | 1.3 | 98.4 | 0.0 | 0.0 |
| $\text{K}_6(\alpha_2\text{-Mo}_5\text{P}_2\text{W}_{13})$ | 27.7 | 0.4 | 26.6 | 19.2 | 28.4 | 25.3 |
| $\text{K}_6(\alpha\text{-Mo}_6\text{P}_2\text{W}_{12})$ | 11.8 | 4.7 | 18.4 | 23.4 | 53.4 | 0.0 |
| $\text{K}_7(\alpha_1\text{-Mo}_5\text{VP}_2\text{W}_{12})$ | 18.7 | 1.4 | 18.2 | 18.2 | 48.8 | 13.3 |
| $\text{K}_7(\alpha_2\text{-Mo}_5\text{VP}_2\text{W}_{12})$ | 17.3 | 2.9 | 40.8 | 26.4 | 18.9 | 11.0 |

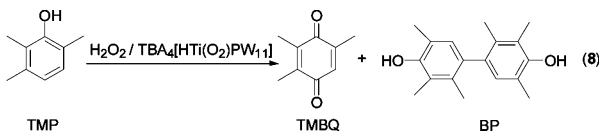
$\text{K}_6(\alpha\text{-P}_2\text{W}_{18})$ is very selective for dimethyl ether, reflecting its high acidic character, $\text{K}_6(\alpha\text{-Mo}_6\text{P}_2\text{W}_{12})$ and $\text{K}_7(\alpha_1\text{-Mo}_5\text{VP}_2\text{W}_{12})$ are selective for methyl formate, reflecting their bifunctional acid-oxidative character, and $\text{K}_7(\alpha_2\text{-Mo}_5\text{VP}_2\text{W}_{12})$ is selective for formaldehyde, reflecting its high oxidative character. The results appear as a good example of directing the reaction of methanol toward desired products by the choice of elements and the arrangement of atoms constructing the polyanions of POM catalysts.

As seen in previous content, most POM/HPA catalysts are oxotungsten and oxomolybdenum clusters and their substituted derivatives. Other types of oxometal clusters for catalysis are rather rare, probably due to their challenging syntheses. However, their catalytic performance is non-negligible. In 2008, Kortz et al. revealed that the nanosized molecular oxo-Pd cluster $[\text{Pd}_{13}\text{As}_8\text{O}_{34}(\text{OH})_6]^{8-}$ is active for the aerobic oxidation of benzyl alcohols in water.²⁸⁴ In 2013, Wang et al. found the imidazole-functionalized hexanuclear oxovanadium clusters $\text{V}^{\text{V}}\text{O}_{15}(\text{Mim})_8$ and $\text{V}^{\text{IV}}_2\text{V}^{\text{V}}_4\text{O}_{14}(\text{Eim})_8$ ($\text{Mim} = 1\text{-methylimidazole}$; $\text{Eim} = 1\text{-ethylimidazole}$) also work for the aerobic oxidation of benzyl alcohols.²⁸⁵ The two catalysts even show

higher activities and selectivities than H_4VPMo_{11} and $H_5V_2PMo_{10}$ under the same conditions.

The oxidation of phenolic substrates is a conventional route to produce quinone and its derivatives. POMs are qualified catalysts for the reaction. Monosubstituted $[\alpha\text{-V}^{\text{V}}\text{SiW}_{11}\text{O}_{40}]^{5-}$ ($\alpha\text{-VSiW}_{11}$) and $[\alpha\text{-Mn}^{\text{III}}\text{SiW}_{11}(\text{H}_2\text{O})\text{O}_{39}]^{5-}$ ($\alpha\text{-MnSiW}_{11}$) have redox potentials very comparable to those of phenoloxidase enzymes.²⁸⁶ They have been used as biomimetic models of the active phenoloxidase enzymes. The redox potentials of the two compounds are 0.67 and 0.76 V/NHE, respectively, and those of the phenolic substrates are in the range of 0.4–0.9 V/NHE in water. Thus, the resulting oxidation reactions are exoergonic or slightly endoergonic. The stronger oxidant $\alpha\text{-MnSiW}_{11}$ is more reactive than $\alpha\text{-VSiW}_{11}$ by ca. 2 orders of magnitude.

The isolated protonated titanium peroxy complex $TBA_4[\text{HTi}(\text{O}_2)\text{PW}_{11}\text{O}_{39}]$ ($TBA_4[\text{HTi}(\text{O}_2)\text{PW}_{11}]$) stoichiometrically reacts with 2,3,6-trimethylphenol (TMP) in MeCN, giving 2,2',3,3',5,5'-hexamethyl-4,4'-biphenol (BP) and 2,3,5-trimethyl-p-benzoquinone (TMBQ), an important intermediate for vitamin E (eq 8).²⁸⁷ The proportion of BP and TMBQ is



determined by the ratio of TMP to $TBA_4[\text{HTi}(\text{O}_2)\text{PW}_{11}]$. The reaction with a 2-fold excess of TMP dominantly gives BP (90%), while the reaction with a 2-fold excess of $TBA_4[\text{HTi}(\text{O}_2)\text{PW}_{11}]$ gives TMBQ as the main product (95%). The reaction proceeds via a homolytic oxidation mechanism involving the formation of phenoxy radicals ArO^\bullet . In contrast, the deprotonated $TBA_5[\text{Ti}(\text{O}_2)\text{PW}_{11}\text{O}_{39}]$ ($TBA_5[\text{Ti}(\text{O}_2)\text{-PW}_{11}]$) is inactive for the reaction,²⁸⁷ indicating the crucial role of the proton in the active $\text{HTi}(\text{O}_2)\text{PW}_{11}$. Several Ti-containing POMs, including the μ -oxo dimer $TBA_8-[(\text{TiPW}_{11}\text{O}_{39})_2\text{O}]$ ($TBA_8-[(\text{TiPW}_{11})_2\text{O}]$), the μ -hydroxo dimer $TBA_7-[(\text{TiPW}_{11}\text{O}_{39})_2\text{OH}]$ ($TBA_7-[(\text{TiPW}_{11})_2\text{OH}]$), and the two monomers $TBA_4[\text{Ti}(\text{L})\text{PW}_{11}\text{O}_{39}]$ ($\text{L} = \text{OH}, \text{OMe}$) are also active for the same reaction, because they evolve into the same protonated titanium peroxy complex $TBA_4[\text{HTi}(\text{O}_2)\text{-PW}_{11}]$ upon the interaction with aqueous H_2O_2 in MeCN.²⁸⁸ The catalytic activities of these POMs depend on the formation rates of $TBA_4[\text{HTi}(\text{O}_2)\text{PW}_{11}]$. The authors believe that the active proton in the isolated complex is most likely localized at the $\text{Ti}-\text{O}-\text{W}$ bridging oxygen rather than at the peroxy group because $\text{Ti}-\text{O}-\text{W}$ is the intrinsically most basic site. However, the TiOOH form is strongly stabilized by the interaction of the proton with solvent. Thus, $\text{Ti}-\text{OH}-\text{W}$ and TiOOH may coexist in solution.

2.6. Cleavage of Single C–C Bonds

The functionalized C–C bonds of cyclic vicinal diols and α -hydroxy ketones can be cleaved by oxidation reaction, providing various industrially valuable dicarbonyl compounds, including adipic acid. Keggin-type HPAs of $H_{3+n}V_nPMo_{12-n}$ are robust for these reactions using O_2 as the oxidant. For example, the homolytic C–C bond cleavage of 2-hydroxycyclohexanone happens in the presence of $H_6V_3PMo_9$ at 338 K in methanol, giving a total maximum 90% yield of adipic acid and its dimethyl ester.²⁸⁹ The oxidative cleavage of 1,2-cyclohexanediol at 348 K in ethanol in the presence of $H_{3+n}V_nPMo_{12-n}$ gives

adipic acid ethyl ester with 90% selectivity at 62% conversion.²⁹⁰ The reaction is suggested to proceed via an intermediate ternary complex involving the catalyst, O_2 , and the diol, which leads to simultaneous C–C and O–O bond cleavage. However, Neumann et al. proposed an electron–oxygen-transfer mechanism for the C–C bond cleavage of primary alcohols and vicinal diols with $H_5V_2PMo_{10}$.²⁹¹ The comparison between $H_4VPMo_{11}/H_5V_2PMo_{10}$ and $\text{Ru}(\text{OH})_3$ reveals that these HPAs are more selective for adipic acid than a basic catalyst of $\text{Ru}(\text{OH})_3$ in the oxidation of 1,2-cyclohexanediol.²⁹² The side reactions occurring under basic conditions are invisible in the acidic system involving $H_{3+n}V_nPMo_{12-n}$.

In fact, the oxidative cleavage of single C–C bonds also happens in the oxidation of acyclic alcohols/ketones^{291,293} and cyclic monohydroxyl or monocarbonyl compounds^{290,293} in the presence of $H_{3+n}V_nPMo_{12-n}$. The cleavage of single C–C bonds in cyclic monohydroxyl or monocarbonyl compounds also yields dicarbonyl compounds. Using O_2 as the oxidant, 2-methylcyclohexanone is cleaved at room temperature in the presence of $H_5V_2PMo_{10}$ to form 6-oxoheptanoic acid with 90% selectivity at 96% conversion.²⁹⁰

Apart from providing valuable chemicals, the C–C bond cleavage with $H_{3+n}V_nPMo_{12-n}$ also plays an active role in the utilization of biomass. Glucose, cellulose, and other biogenic feedstocks can be selectively converted into formic acid in the presence of $H_8V_5PMo_7$ or $H_5V_2PMo_{10}$.^{294,295} However, high O_2 pressures are required, and CO_2 is largely formed as the coproduct. Notably, Neumann et al. reported a two-step, one-pot production of synthesis gas (carbon monoxide and hydrogen) from cellulose and hemicellulose with $H_5V_2PMo_{10}$ as an electron-transfer–oxygen-transfer catalyst.²⁹⁶ High selectivity for synthesis gas is achieved under mild conditions. It is shown that carbon monoxide is formed by cleavage of all the C–C bonds through dehydration of initially formed formic acid. In this oxidation–reduction reaction, the hydrogen atoms are stored on the POM as protons and electrons, and can be electrochemically released from the POM as hydrogen. This research is the foundation for a new technology for the formation of synthesis gas from biomass. Additionally, in a hydrogen economy scenario, the catalytic system can also be used to convert carbon monoxide to hydrogen.

2.7. Cleavage of M–C Bonds

Most recently, Neumann et al. reported the cleavage of the M–C bond in the presence of $H_{3+n}V_nPMo_{12-n}$.²⁹⁷ The report pointed out that an oxygen atom from $H_5V_2PMo_{10}$ could insert into the Sn–C bond of $n\text{-Bu}_4\text{Sn}$ through its activation by electron transfer to yield 1-butanol and $(n\text{-Bu}_3\text{Sn})_2\text{O}$ in the presence of O_2 . In the initial step of the reaction, one electron transfers from $n\text{-Bu}_4\text{Sn}$ to $H_5V_2PMo_{10}$ to yield the ion pair $n\text{-Bu}_4\text{Sn}^\bullet+ - H_5V_2PMo_{10}^-$, which is relatively unstable and prone to form more stable Bu^+ and Bu_3Sn^+ cations coordinated to the catalyst. At higher temperature (393 K and above), Bu^+ and Bu_3Sn^+ are released in the forms of 1-butanol and $(n\text{-Bu}_3\text{Sn})_2\text{O}$, respectively. Under anaerobic conditions, the oxygen atoms in both 1-butanol and $(n\text{-Bu}_3\text{Sn})_2\text{O}$ come from the HPA anions. In the presence of O_2 , the reaction is catalytic. The oxygen atom in 1-butanol mostly comes from O_2 , whereas the oxygen atom in $(n\text{-Bu}_3\text{Sn})_2\text{O}$ is mostly from the HPA anions. The activity of H_4VPMo_{11} is equal to that of $H_5V_2PMo_{10}$. H_3PMo_{12} shows less activity, but the activity is increased by ~55% in the presence of $\text{VO}(\text{O}-i\text{-Pr})_3$. Analogous

tungstates, a monomeric vanadate, and a decavanadate are all unreactive. Me_4Sn shows much lower reactivity than $n\text{-Bu}_4\text{Sn}$ owing to its higher ionization potential. In a more general context, the insertion of an oxygen atom from O_2 into a M–C bond is an important step in the development of catalytic alkane oxidation to alcohol through a combination of C–H bond activation and oxygen atom insertion.

2.8. Oxidation of Carbonyl Compounds

Oxidation of aldehydes and ketones with POM catalysts is applicable to pollutant removal and organic synthesis. As is known, formaldehyde is a carcinogen that is fairly ubiquitous in indoor air and a cause of “sick building syndrome”. One of the most desirable approaches to remove formaldehyde is oxidizing it in aqueous solution under ambient conditions (1 atm of air and room temperature). However, the oxidation of formaldehyde is far harder than that of nearly all other aldehydes and ketones due to its hydration in aqueous solution. In 2004, Kholdeeva and Hill and their co-workers reported that supported Keggin-type Co-containing POMs $\text{TBA}_4\text{H}\text{-}(\text{CoPW}_{11}\text{O}_{39})$ and $\text{TBA}_5\text{(CoPW}_{11}\text{O}_{39})$ were effective for the aerobic oxidation of aldehydes (including formaldehyde) under ambient conditions.²⁹⁸ In 2005, they further investigated the catalytic activity of the Keggin-type Ce-containing POM $\text{NaH}_3\text{(CeSiW}_{11}\text{O}_{39})$ for the aerobic oxidation of formaldehyde.²⁹⁹ The Ce-containing POM is shown to be a selective and effective catalyst for the production of formic acid with a formaldehyde conversion of ~20% under mild conditions. In 2014, Hill’s group reported three Keggin-type V-containing POMs, $\text{TBA}_6\text{(V}_3\text{PW}_9\text{O}_{40})$ ($\text{TBA}_6\text{(V}_3\text{PW}_9)$), $\text{TBA}_5\text{H}_2\text{(V}_4\text{PW}_8\text{O}_{40})$, and $\text{TBA}_4\text{H}_5\text{(V}_6\text{PW}_6\text{O}_{40})$, for the aerobic oxidation of formaldehyde.³⁰⁰ These catalysts exhibit the best activities, comparable to those of $\text{TBA}_5\text{(CoPW}_{11}\text{O}_{39})$ and $\text{TBA}_4\text{(CeSiW}_{11}\text{O}_{39})$ in a DMA/ H_2O [20:1 (v/v)] solvent system. Notice that the number of V redox sites and the number of counterions are significant factors for catalytic activity. Among them, $\text{TBA}_4\text{H}_5\text{(V}_6\text{PW}_6\text{O}_{40})$ shows the highest activity. Under optimized conditions, a TON of ~57 is obtained with $\text{TBA}_4\text{H}_5\text{(V}_6\text{PW}_6\text{O}_{40})$. More practically, formaldehyde removal reactions with these V-containing POMs are less inhibited by water than the same oxidations catalyzed by supported noble metals. In pure water, the three V-containing POMs show much higher activities than Au/TiO_2 and reduced Pt/TiO_2 . Summarily, oxidative removal of formaldehyde with these POMs can be expediently conducted under ambient, high-humidity conditions. The achievements are valuable because they pave a way for the removal of formaldehyde in air.

Baeyer–Villiger oxidation of cyclic ketones provides various lactones. Traditionally, carboxylic acid or aldehyde is used as an additive to generate organic peracids when H_2O_2 or O_2 is used as the oxidant.³⁰¹ However, the S-shaped polyanion $\{[\gamma\text{-SiW}_{10}\text{O}_{32}(\text{H}_2\text{O})_2]_2(\mu\text{-O})_2\}^{4-}$ ($(\gamma\text{-H}_4\text{SiW}_{10})_2(\mu\text{-O})_2$; Figure 14), formed by the dimerization of $\gamma\text{-H}_4\text{SiW}_{10}$ via dehydrative condensation, can efficiently catalyze the Baeyer–Villiger oxidation of cycloalkanones with H_2O_2 as the sole oxidant.³⁰² No additives are needed. Lactones are given with selectivities higher than 90%. In the case of 12.5 mmol scale reactions, the yields and selectivities for cyclobutanone, cyclopentanone, and 2-adamantanone are higher than 95% and 99%, respectively, whereas the monomeric precursor $\gamma\text{-H}_4\text{SiW}_{10}$ and the closed dimer $[(\gamma\text{-SiW}_{10}\text{O}_{32})_2(\mu\text{-O})_4]^{8-}$ ($(\gamma\text{-SiW}_{10})_2(\mu\text{-O})_4$; Figure 14) are almost inactive for the reaction, although they share the common $[\gamma\text{-SiW}_{10}\text{O}_{32}]$ fragment. Compared with those in the

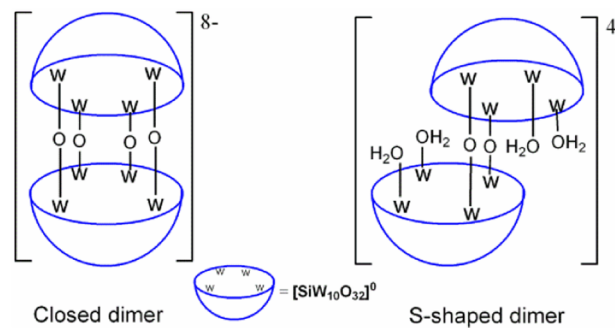
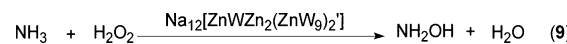


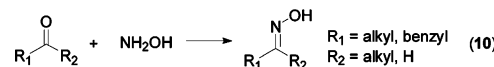
Figure 14. Closed dimer and S-shaped dimer derived from $\gamma\text{-H}_4\text{SiW}_{10}$.

closed dimer, the W atoms in the S-shaped dimer have stronger Lewis acidity due to the altitudinal protonation of adjacent O atoms. This may explain the transcendent activity of the S-shaped dimer.

The sandwich-type POM catalyst $\text{Na}_{12}[\text{ZnWZn}_2(\text{ZnW}_9)_2]'$ is effective for the oxidative oxidation of ketones and aldehydes with aqueous ammonia and H_2O_2 in aqueous biphasic systems, resulting in the formation of the valuable intermediates, oximes, which can be dehydrated to nitriles or undergo an acid-catalyzed Beckmann rearrangement to amides.³⁰³ In the first step, in situ oxidation of ammonia to hydroxylamine happens in the presence of $\text{Na}_{12}[\text{ZnWZn}_2(\text{ZnW}_9)_2]'$ (eq 9). Then the



resulting hydroxylamine further reacts with ketones or aromatic aldehydes to provide the corresponding oximes (eq 10). The



Integration of the two steps in oxime production leaves out the dangers caused by the direct use of a large amount of hydroxylamine. The reactivity sequence of diverse substrates is cyclic aliphatic ketones > acyclic aliphatic ketones > aromatic ketones. The reactions of ketones give oximes as the sole products, without further Beckmann rearrangement to amides. The reactions of some aromatic aldehydes tend to be less selective due to the formation of nitriles and amides because of the inherent acidity of the catalyst. The situation can be dramatically improved by intercalating the POM anions $[\text{ZnWZn}_2(\text{ZnW}_9)_2]'$ into layered double hydroxides, a kind of layered anionic clay that is expressed by the general formula $[\text{M}^{II}_{1-x}\text{M}^{III}_x(\text{OH})_2](\text{A}^{n-})_{x/n}\text{mH}_2\text{O}$.^{304,305} The basic hydroxyl groups on the layers of the layered double hydroxides can suppress the acid-catalyzed side reactions. The same function is also found in the epoxidation of alkenes.^{306,307}

2.9. Oxidation of Sulfur-Containing Compounds

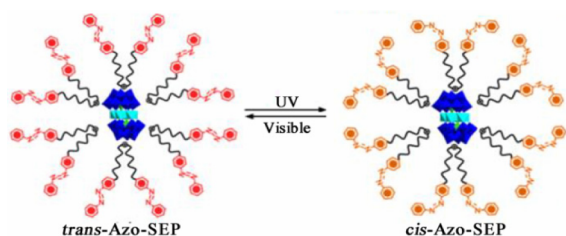
Oxidation of organosulfur compounds affords structurally diverse sulfoxides and sulfones, which are important intermediates in the synthesis of natural products and biologically significant molecules,^{308,309} ligands in asymmetric catalysis,³¹⁰ and oxo-transfer reagents.³¹¹ The transformation also affords a sustainable way to green globe via desulfurization of oil and aerobic decontamination of the toxic or pungent chemicals such as H_2S , 2-chloroethyl ethyl sulfide (CEES), and thiols.³¹² The highlighted POMs for alkene epoxidation, $\text{TPA}_3\{[\text{HW}_2\text{O}_2(\text{O}_2)_4(\mu\text{-O})_2]_2\}$,¹²⁰ $\text{TBA}_4(\gamma\text{-H}_4\text{SiW}_{10})$,¹³¹ $\text{TBA}_3\text{H}[\gamma\text{-SiW}_{10}\text{O}_{36}(\text{PhPO})_2]$,¹⁴⁰ $\gamma\text{-V}_2\text{SiW}_{10}/\text{SiO}_2$,¹⁵⁸ $\text{DA}_{11}[\text{La}$

$(PW_{11}O_{39})_2$] ($DA = C_{10}H_{21}N(CH_3)_3$)³¹³ and $TBA_3(\gamma-V_2PW_{10})$ ³¹⁴ are indubitably energetic for the oxidation of sulfides. Notably, the less explored Dawson-type polyanion $[V_3P_2W_{15}O_{62}]^{9-}$ ($V_3P_2W_{15}$) has received much attention in this area. Hill et al. evaluated the activities of a hydrolytically stable organic triester capped POM, $[RC(CH_2O)_3V_3P_2W_{15}O_{59}]^{6-}$ ($R = CH_3, NO_2, CH_2OH$), using the oxidation of tetrahydrothiophene (THT) as the probe reaction.³¹⁵ As a continuative work, the group prepared a dendrimer containing four $V_3P_2W_{15}$ units and investigated its catalytic activity.³¹⁶ Similarly, a linear-type polymeric material containing $V_3P_2W_{15}$ was also created for the oxidation of THT.³¹⁷ Thorimbert et al. inserted the carbonyl of amide into the $V_3P_2W_{15}$ sphere. It is found that the insertion of carbonyl leads to improved chemoselectivity in the oxidation of sulfides, without the activity loss of the vanadium core of the POMs.³¹⁸ The introduction of a Pd center with Lewis acidity into the catalyst results in a dual-site catalyst.³¹⁹ The oxidative property of the vanadium site is retained after the introduction of the Pd center.

For confirmed active HPA/POM catalysts, such as H_3PW_{12} and $H_{3+n}V_nPMo_{12-n}$ and their organic salts,^{320–322} recent investigations concern the factors affecting their effectiveness, especially their cations. The organic cations significantly influence the performance of POM catalysts via two main pathways.³²³ On one hand, the structures of these cations influence the mass transfer of the reaction. Different cation structures create different phase-transfer effects and catalyst solubilities. On the other hand, some cations contribute to the mutative activity of POM anions by essentially varying the electronic structure of the POM anions. The latter is conventionally realized through electron transfer. Of course, strong interactions between POM cations and anions, such as hydrogen bonding, also change the electronic structure of the anions. The changes are bound to affect the redox properties of POM catalysts, and finally the catalytic performances. The investigation on $(Bmim)_3PMo_{12}$, $(Bmim)_2HMo_{12}$, and $(Bmim)H_2PMo_{12}$ in a liquid–solid heterogeneous system with methanol as the solvent reveals that the introduction of organic cations makes the catalyst more efficient via the intramolecular charge transfer from the organic cations to POM anions.³²⁴ The insolubility of $(Bmim)_3PMo_{12}$ in methanol should be associated with the good crystallinities of the butylimidazolium salts and the hydrogen-bonding networks between the C–H bonds of the butyl groups and the oxygen atoms of the POM anions.

To construct a system combining the high activity of a homogeneous system and the easy catalyst separation of a heterogeneous system, Wu's group encapsulated anionic $[ZnWZn_2(ZnW_9)_2]'$ with cationic azobenzene (Azo)-ended surfactants, yielding a novel catalyst, Azo-SEP (Scheme 8),

Scheme 8. Reversible Transform between *trans*- and *cis*-Azo-SEP upon UV and Visible Light Irradiations³²⁵



where the structures of the polyanions were retained well.³²⁵ The Azo group is photosensitive and undergoes a reversible *trans/cis*-isomerization upon light irradiation. Under the UV light irradiation, the Azo groups isomerize into the *cis*-form; subsequent visible light irradiation makes the *cis*-form turn back to the *trans*-form (Scheme 8). In the *trans*-state, the Azo group is linear and has a small polarity, while, in the *cis*-state, the bent structure endows it with a large polarity. Thus, *trans*-Azo-SEP dissolves well in weakly polar toluene, while it is poorly soluble in a strongly polar mixture of H_2O and DMF. The case for *cis*-Azo-SEP is the reverse. When Azo-SEP is added into a two-phase liquid where the upper phase is toluene and the lower phase is the H_2O/DMF mixture, and irradiated by UV light and visible light alternately, the catalyst Azo-SEP transfers between the two phases reversibly. Thus, light-controlled automatic separation of the Azo-SEP catalyst can be easily realized. That is, the catalytic reactions can homogeneously proceed in one phase. After reaction, the catalyst transfers into another phase upon the irradiation of UV or visible light, while the products and the residual raw material are left in the reaction phase. Next, the catalyst can be separated by liquid–liquid separation. The methodology of creating such catalysts featuring light-controlled separation is universal. The samples prepared from Keplerate-type $(NH_4)_{72}[(Mo)Mo_5O_{21}(H_2O)_6]_{12}[Mo_2O_4(SO_4)]_{30}$ and disklike $K_{12.5}Na_{1.5}[NaP_5W_{30}O_{110}]$ also have the reversible light-controlled automatic separation properties. Compared with temperature-, magnetic-field-, nanofiltration-, and reaction-controlled separation, the light-driven catalyst separation is preferable because (1) no filtration procedure is needed, (2) the light is from nature and is noninvasive, (3) the wavelength, intensity, illuminated area, and duration can be mediated remotely, and (4) especially, such systems are of great value for microfluidic systems and trace utilizations because of the leaving out of the filtration procedure that is extensively used for catalyst recovery.

In addition to activity and recyclability, chirality is another aspect of concern of POM catalysts because the asymmetric oxidation of sulfides is an important branch. There are several methods to prepare chiral POM catalysts. Bonchio's group coupled chiral centers to a POM fragment by modifying the divalent Keggin-type polyanions $[\gamma-XW_{10}O_{36}]^{8-}$ ($X = Si, Ge$) with chiral organophosphonate via covalent interaction, resulting in hybrid catalysts $[(R^*PO)_2(\gamma-XW_{10}O_{36})]^{4-}$ ($R = N$ -protected aminoalkyl groups or O-protected amino acid derivatives).³²⁶ However, the most convenient way is to introduce chiral organic cations into POM catalysts. As an extensional work on dendritic cation modified POM catalysts,^{327,328} Nlate et al. made three chiral POM catalysts (Figure 15) by associating enantiopure dendritic quaternary ammonium cations with achiral trianionic Venturello anions, $\{PO_4[MO(O_2)_2]_4\}^{3-}$, through electrostatic interaction.^{329,330} All three dendritic compounds display chiroptical effects, highlighting the chirality transfer from the enantiopure dendritic wedge to the catalytically active POM units. The use of monopodal 1 in the asymmetric oxidation of thioanisole with aqueous H_2O_2 provides the corresponding optically active sulfoxide with a 14% ee value as a result of a chirality transfer, higher than that of their nondendritic counterparts (4% ee). Tripodal dendritic compound 3 shows an ee value of 13%, comparable to that of monopodal 1. Despite the fact that the enantioselectivity is not very exciting, the results confirm the chiroptical transfer properties from organic moieties to a reactive POM unit.

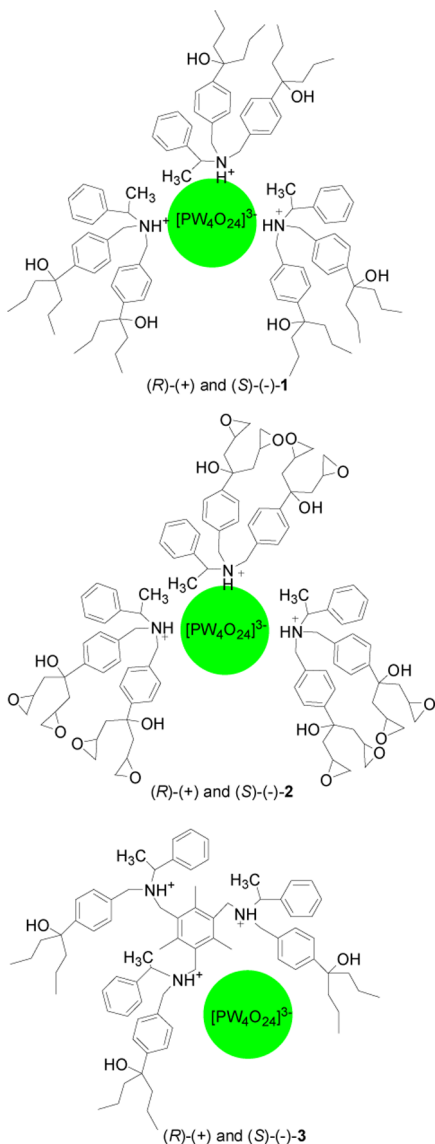
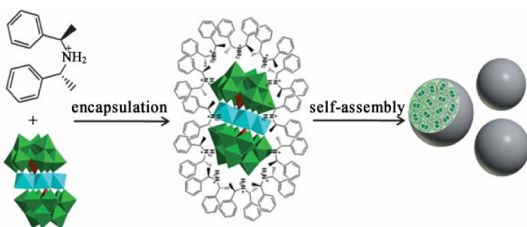


Figure 15. Three dendritic chiral POM catalysts based on Venturello anions.

The encapsulation of catalytically active POM anions $[\text{ZnWZn}_2(\text{ZnW}_9)_2]'$ by chiral amphiphilic cation bis(1-phenylethyl)ammonium (BPEA) through electrostatic interaction makes another chiral POM catalyst (Scheme 9).³³¹ The catalysts self-aggregate into spherical supramolecular assemblies with a diameter of ca. 100 nm in the reaction solution. After self-aggregation, the chirality of BPEA is retained well. No chirality transfer occurs, inconsistent with the understanding of

**Scheme 9. Preparation Procedure of BPEA-
[ZnWZn₂(ZnW₉)₂]’ Assemblies³³¹**

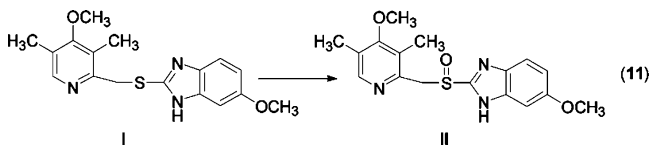


chiral heteropoly blues, BPEA- VPMo_{11} , where the chirality transfer from cations to polyanions is observed.³³² These assemblies serve as microreactors and exhibit a high asymmetric catalytic activity for the oxidation of sulfides. An ee value of 72% is achieved for methyl phenyl sulfide. The POM anions and the chiral organic cations display an evident synergistic effect in the catalytic process. The POM anions contribute to the catalysis of sulfoxidation, and the chiral organic part provides a chiral microenvironment. The coverage density of the chiral component on the POM surface has a significant influence on the enantioselectivity. With a decrease of the coverage density of the stereocenter, the enantioselectivity of methyl phenyl sulfide asymmetric oxidation dramatically decreases. An increase of the stereocenter coverage density causes more chiral groups to surround the POM anions, leading to a higher efficiency of chiral inducement. The self-assemblies increase the number of chiral cations surrounding the POMs, providing an efficient microenvironment for chiral inducement through a combined procedure of a less effective asymmetric sulfoxidation and an effective kinetic resolution of the yielded sulfoxide. The investigation offers a strategically universal protocol for the direct and efficient construction of supramolecular asymmetric POM-based catalysts, which is important for asymmetric synthesis.

In sulfoxidation reaction, the importance of protons for Ti-containing POM catalysts is confirmed again.³³³ The active μ -hydroxo dimeric POM $(\text{TiPW}_{11})_2\text{OH}$ forms readily in MeCN from the Keggin-type monomer TiPW_{11} upon the addition of 1.5 equiv of H^+ , via the protonated species $[\text{Ti(OH)}\text{PW}_{11}\text{O}_{39}]^{4-}$ ($\text{Ti(OH)}\text{PW}_{11}$). Both dimeric μ -hydroxo ($\text{TiPW}_{11}\text{O}_{39}$) and monomeric $\text{Ti(OH)}\text{PW}_{11}$ show higher catalytic activity than TiPW_{11} for thioether oxidation by H_2O_2 . Upon the addition of H_2O_2 , $(\text{TiPW}_{11})_2\text{OH}$ and $\text{Ti(OH)}\text{PW}_{11}$ convert into a hydroperoxo complex, $[\text{Ti(OOH)}\text{PW}_{11}\text{O}_{39}]^{4-}$ ($\text{Ti(OOH)}\text{PW}_{11}$), which is supported as the active peroxy species and directly reacts with thioethers under both stoichiometric and catalytic conditions. The formation rate of $\text{Ti(OOH)}\text{PW}_{11}$ from $\text{Ti(OH)}\text{PW}_{11}$ is higher than that from $(\text{TiPW}_{11})_2\text{OH}$ due to the additional hydrolysis step of $(\text{TiPW}_{11})_2\text{OH}$. When $(\text{TiPW}_{11})_2\text{OH}$ is used as a catalyst precursor, the rates of thioether oxidation and peroxy complex formation increase with increasing H_2O concentration, which favors the cleavage of $(\text{TiPW}_{11})_2\text{OH}$ to $\text{Ti(OH)}\text{PW}_{11}$, while TiPW_{11} converts into the peroxy-Ti complex $\text{Ti(O}_2\text{)}\text{PW}_{11}$ upon the addition of H_2O_2 . The two peroxy complexes differ in their protonation state and can interconvert rapidly. $\text{Ti(O}_2\text{)}\text{PW}_{11}$ completely converts into $\text{Ti(OOH)}\text{PW}_{11}$ when 1 equiv of H^+ is added. On the contrary, $\text{Ti(OOH)}\text{PW}_{11}$ completely converts into $\text{Ti(O}_2\text{)}\text{PW}_{11}$ when 1 equiv of OH^- is added.

Recently, the activities of other POM catalysts have also been explored. It is found that the octamolybdate of $\text{TBA}_4(\alpha\text{-Mo}_8\text{O}_{26})$ can efficiently catalyze the oxidation of various sulfides with a high ratio of substrate to catalyst (up to 10000:1).³³⁴ Excellent selectivities of 95–100% for sulfoxides are given. Functional groups, including the hydroxyl group and $\text{C}=\text{C}$ bonds, which are sensitive to oxidant, are tolerated in the reaction. Practically, the catalyst can promote the oxidation of the sulfide I to well-known antiulcer drug omeprazole (II) in 86.6% yield and 99.7% purity (eq 11).

The artificial Se-containing dinuclear peroxotungstate catalyst $\text{TBA}_2\{\text{SeO}_4[\text{WO}(\text{O}_2)_2]_2\}$ shows a catalytic activity comparable to that of a natural enzyme in the oxidation of various aromatic and aliphatic sulfides using 1 or 2 equiv of



H_2O_2 at 293 K (Scheme 10).^{335,336} The loadings of the catalyst are only 0.02–0.1 mol % with respect to the tested sulfides.

Scheme 10. Oxidation of Sulfides with $\text{TBA}_2\{\text{SeO}_4[\text{WO}(\text{O}_2)_2]_2\}$ ^{335,336}

| $\text{R}_1-\text{S}-\text{R}_2$ | $\text{H}_2\text{O}_2/\text{TBA}_2\{\text{SeO}_4[\text{WO}(\text{O}_2)_2]_2\}$ | CH_3CN | $\text{R}_1-\overset{\text{O}}{\underset{\text{S}}{\text{---}}} \text{R}_2 + \text{R}_1-\overset{\text{O}}{\underset{\text{S}}{\text{---}}} \text{R}_2$ |
|----------------------------------|--|------------------------|---|
| | | | |
| 99% yield | | | |
| | | | |
| 95% yield | | | |
| | | | |
| >99% yield | | | |
| | | | |
| >99% yield | | | |
| | | | |
| >99% yield | | | |
| | | | |
| 98% yield | | | |
| | | | |
| >99% yield | | | |
| | | | |
| 99% yield | | | |
| | | | |
| 99% yield | | | |
| | | | |
| 99% yield | | | |
| | | | |
| >99% yield | | | |
| | | | |
| >99% yield | | | |
| | | | |
| 96% yield | | | |
| | | | |
| >99% yield | | | |
| | | | |
| 97% yield | | | |
| | | | |
| >99% yield | | | |
| | | | |
| 98% yield | | | |
| | | | |
| 95% yield | | | |
| | | | |
| 96% yield | | | |

Cyclic disulfides are selectively oxidized to the corresponding monosulfoxides. Dibenzothiophenes are oxidized to the corresponding sulfone in 98% yield based on H_2O_2 . The introduction of the SeO_4^{2-} ligand increases the Lewis acidity of tungsten atoms, resulting in 8-fold higher activity of $\text{TBA}_2\{\text{SeO}_4[\text{WO}(\text{O}_2)_2]_2\}$ than that of the simple dinuclear peroxotungstate $\text{TBA}_2\{[\text{WO}(\text{O}_2)_2]_2(\mu\text{-O})\}$. The negative Hammett ρ value (-0.62) for the competitive oxidation of *para*-substituted thioanisoles and the low XSO value (0.14) for the oxidation of thianthrene 5-oxide shows that $\text{TBA}_2\{\text{SeO}_4[\text{WO}(\text{O}_2)_2]_2\}$ is a strong electrophilic oxidant. In the case of a 100 mmol scale oxidation of thioanisole, the TOF and the TON reach up to $70\,800\text{ h}^{-1}$ and $19\,500$, respectively. These values are among the highest values for the artificial catalytic systems.

The butterfly dimeric peroxy-POMs $[\text{M}_2(\text{O}_2)_2(\alpha\text{-XW}_{11}\text{O}_{39})_2]^{12-}$ ($\text{M} = \text{Zr}^{\text{IV}}$, $\text{X} = \text{Si, Ge}$; $\text{M} = \text{Hf}^{\text{IV}}$, $\text{X} = \text{Si}$) (Figure 16a) are capable of oxygen transfer to sulfides and sulfoxides in water.^{45,46} The reduced POMs are reversibly peroxidized by H_2O_2 . The activities of these butterfly dimers

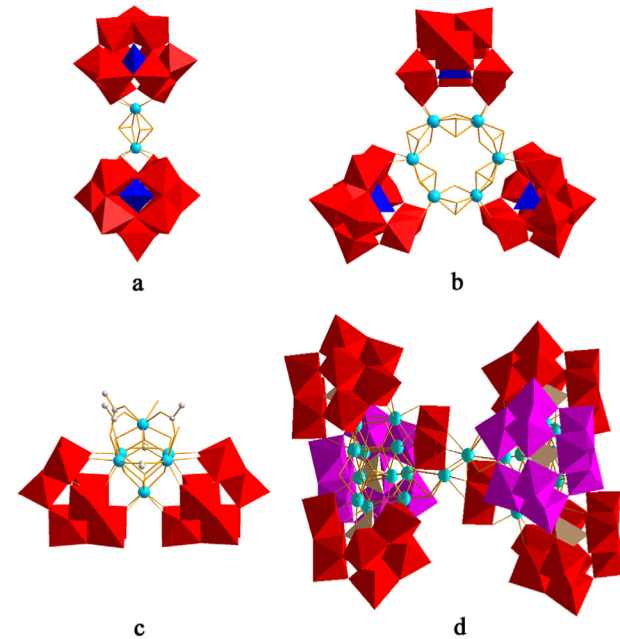


Figure 16. Structures of (a) $[\text{M}_2(\text{O}_2)_2(\alpha\text{-XW}_{11}\text{O}_{39})_2]^{12-}$ ($\text{M} = \text{Zr}^{\text{IV}}$, $\text{X} = \text{Si, Ge}$; $\text{M} = \text{Hf}^{\text{IV}}$, $\text{X} = \text{Si}$), (b) $[\text{M}_6(\text{O}_2)_6(\text{OH})_6(\gamma\text{-SiW}_{10}\text{O}_{36})_3]^{18-}$ ($\text{M} = \text{Zr}^{\text{IV}}$, Hf^{IV}), (c) $[\text{M}_6\text{O}_4(\text{OH})_4(\text{H}_2\text{O})_2(\text{CH}_3\text{COO})_5\text{-(AsW}_9\text{O}_{33})_2]^{11-}$ ($\text{M} = \text{Zr, Hf}$), and (d) $[\text{Zr}_{24}\text{O}_{22}(\text{OH})_{10}(\text{H}_2\text{O})_2\text{-(W}_2\text{O}_{10}\text{H})_2\text{(GeW}_9\text{O}_{34})_4\text{-(GeW}_8\text{O}_{31})_2]^{32-}$.

outperform that of the trimeric derivatives $[\text{M}_6(\text{O}_2)_6(\text{OH})_6(\gamma\text{-SiW}_{10}\text{O}_{36})_3]^{18-}$ ($\text{M} = \text{Zr}^{\text{IV}}, \text{Hf}^{\text{IV}}$) (Figure 16b) by 2 orders of magnitude, despite the fact that there are more peroxometals in the trimers. The nature of the Zr/Hf centers and the vacant POM ligands contribute the activity difference to a minor degree. The coordination mode and structural environment of the zirconium/hafnium peroxides primarily account for the different activities. In the butterfly dimers, each M is tightly connected to an $\{\alpha\text{-XW}_{11}\text{O}_{39}\}$ ligand by four M–O–W bonds. Therefore, the peroxometals are strongly electrophilic and easily transfer oxygen to the acceptors. However, the peroxometals in the trimers have a looser coordination mode. Each M is connected to a $\gamma\text{-SiW}_{10}$ ligand only by two M–O–W bonds. Therefore, the electrophilicity of the peroxometals in the trimers is weaker than that in the butterfly dimers. Another likely reason for the activity difference is that the peroxometals in the trimers are embraced by three bulky $\gamma\text{-SiW}_{10}$ blocks, so that the active peroxometals are less accessible to substrates. Although the trimers have lower activity, they still quantitatively oxidize several sulfides within a relatively longer time. Besides, the related M₆-containing tungstoarsenates $[\text{M}_6\text{O}_4(\text{OH})_4(\text{H}_2\text{O})_2(\text{CH}_3\text{COO})_5\text{-(AsW}_9\text{O}_{33})_2]^{11-}$ ($\text{M} = \text{Zr, Hf}$) (Figure 16c)³³⁷ and the gigantic Zr₂₄-containing germanotungstate $[\text{Zr}_{24}\text{O}_{22}(\text{OH})_{10}(\text{H}_2\text{O})_2\text{-(W}_2\text{O}_{10}\text{H})_2\text{(GeW}_9\text{O}_{34})_4\text{-(GeW}_8\text{O}_{31})_2]^{32-}$ (Figure 16d)³³⁸ also show remarkable activities for the oxidation of sulfides.

In aerobic decontamination, the ultimate goal is to oxidize sulfur-containing pollutants to far less toxic compounds under an ambient environment (room temperature and 1.0 atm of air). The trimer $\{[\text{Fe}_2(\text{OH})_3(\text{H}_2\text{O})_2]_3(\gamma\text{-SiW}_{10}\text{O}_{36})_3\}^{15-}$, which is derived from $\gamma\text{-Fe}_2\text{SiW}_{10}$, is competent for the aerobic oxidation of smelly mercaptoethanol to the corresponding disulfide in water by O_2 at ambient pressure and temperature.⁴² The mono-Fe-substituted POM with a hydrogen dinitrate group, $\{\text{Fe}[\text{H}(\text{ONO}_2)_2]\text{PW}_{11}\text{O}_{39}\}^{5-}$, is effective for the

oxidation of CEES (a common simulant for mustard gas) to its corresponding, far less toxic sulfoxide (CEESO) under the ambient environment.³³⁹ As for solid POM catalysts, cationic silica nanoparticles (Si/AlO_2)ⁿ⁺,³⁴⁰ ionic-liquid-modified silica,³⁴¹ fluorapatite,³⁴² mesoporous anatase TiO_2 ,³⁴³ and many other materials have been used to support active POM catalysts. In addition, the low-surface-area powder of $\text{Ag}_5\text{V}_2\text{PMo}_{10}$, where two $\text{V}_2\text{PMo}_{10}$ units are bridged by two Ag^+ ions and each POM unit has two additional nonbridging Ag^+ ions, is a solid catalyst itself.³⁴⁴ When 1 mol of surface-accessible $\text{Ag}_5\text{V}_2\text{PMo}_{10}$ is used for the oxidation of CEES in 2,2,2-trifluoroethanol using the ambient environment, ~2300 mol of CEESO is produced. Similarly, the Cu^{II} -containing coordination network polymer $\{[(\text{Cu}^{II}(\text{OH}_2)_4)_3(\text{OH})]\text{-V}_2\text{PMo}_{10}\}_n$ works in the same reaction.³⁴⁵ Interestingly, the reaction does not occur under identical conditions when soluble $\text{Na}_5\text{V}_2\text{PMo}_{10}$ is used in place of $\text{Ag}_5\text{V}_2\text{PMo}_{10}$. The superiority of $\text{Ag}_5\text{V}_2\text{PMo}_{10}$ is explained by a synergistic effect between the Ag^+ cationic centers and the redox-active V^{V} centers inside a fairly labile $\text{Ag}_5\text{V}_2\text{PMo}_{10}$. However, the analogues $\text{Ag}_5\text{V}_2\text{PW}_{10}\text{O}_{40}$ and $\text{Ag}_9\text{V}_3\text{P}_2\text{W}_{15}\text{O}_{62}$ are inactive under ambient conditions. The results suggest that the three metals of $\text{Ag}_5\text{V}_2\text{PMo}_{10}$ are relevant to its activity.

Hill's group made an inherently heterogeneous POM catalyst, $[\text{Cu}_3(\text{C}_9\text{H}_3\text{O}_6)_2]_4\{[(\text{CH}_3)_4\text{N}]_4\text{CuPW}_{11}\text{O}_{39}\text{H}\}$, by using MOF-199 (HKUST-1) and $\text{K}_5[\text{CuPW}_{11}\text{O}_{39}]^{5-}$.³¹² The size and charge of $[\text{CuPW}_{11}\text{O}_{39}]^{5-}$ allow it to snugly reside in the pore of MOF-199. The POM-MOF catalyst is active for the oxidation of thiols and H_2S in the presence of air. Thiols are rapidly oxidized to disulfides with obvious chemoselectivities and shape selectivities. Toxic H_2S is removed rapidly and sustainably in the form of S_8 . A TON of 4000 is obtained in less than 20 h. However, the POM alone is catalytically slow, and the MOF alone is inactive. The interactions between the two moieties lead to a dramatic increase of the catalytic turnover rate of the POM unit. The activation of the POM unit by encapsulation in the MOF likely involves electrostatic interactions between the two parts, resulting in a higher reduction potential of the POM anion. The catalyst only requires the ambient environment for some oxidation processes, indicating its potential value as a robust catalytic decontaminant. Considering that POMs and MOFs are two large classes with rich compositions and structures, the selective combinations of POM with MOF will afford more catalytic materials for the aerobic decontamination.

The unit $\{\text{V}_6\text{O}_{13}[(\text{OCH}_2)_3\text{C}(\text{NHCH}_2\text{C}_6\text{H}_4\text{-CO}_2)]_2\}_4^{4-}$ is a logically composable block for the construction of oxidative catalysts because bis(triester)hexavanadate units have extensive reversible redox chemistry and the alkoxy groups of chelating (triester)trivanadate units are very stable to hydrolysis.³⁴⁶ Its reaction with Tb^{III} ions and the linking agent 4,4'-bis(pyridine N -oxide) yields an open-framework coordination network of $\text{Tb}\{\text{V}_6\text{O}_{13}[(\text{OCH}_2)_3\text{C}(\text{NH}_2\text{CH}_2\text{C}_6\text{H}_4\text{-CO}_2)]_2\}_4^{4-}(\text{OCH}_2)_3\text{C}(\text{NHCH}_2\text{C}_6\text{H}_4\text{-CO}_2)]_2\}$ (Tb-V_6).³⁴⁷ The pores in the network allow the catalyst to uptake some guest molecules, including potential targets for catalytic oxidative decontamination by O_2/air , although large pores in the structure are occupied by solvent molecules. When the aerobic oxidation of PrSH , a model for odorants and mild toxics ubiquitous in human environments, is selected as the probe reaction, the solid catalyst Tb-V_6 produces 18.5 turnovers on the basis of the molar equivalents of V_6 groups and the desired nonodorous disulfide in 41% yield at 318 K after 30 days using only ambient

air as the oxidant. More valuably, the catalyst can be easily recovered and reused without loss of catalytic activity, and the framework is maintained under turnover conditions. Thus, the catalyst deserves further attention, although the occupation of channels by solvent molecules may negatively affect its activity. Additionally, future work of seeking similar open-framework redox-active materials with unoccupied pores is also desirable.

Oxidative desulfurization of fuels reduces environmental pollutants from the source. Many W-based POM catalysts, e.g., PW_{12} ,^{348,349} $[\text{W}_{10}\text{O}_{32}]^{4-}$,³⁵⁰ $[\text{W}_6\text{O}_{19}]^{2-}$,³⁵¹ and $\text{Tb}\{(\text{PW}_{11}\text{O}_{39})_2\}$ ³⁵² work for these reactions. With $\text{Na}_7\text{H}_2\text{LnW}_{10}\text{O}_{36}\cdot 32\text{H}_2\text{O}$ ($\text{Na}_7\text{H}_2\text{LnW}_{10}$; $\text{Ln} = \text{Eu}, \text{La}$) as the catalyst, $(\text{Bmim})\text{BF}_4$ as the extractant, and H_2O_2 as the oxidant, the most refractory sulfur compounds, including dibenzothiophene, 1-benzothiophene, and 4,6-dimethylbenzothiophene, can be completely removed under mild conditions.³⁵³ Sulfur removal follows the sequence dibenzothiophene > 4,6-dimethylbenzothiophene > 1-benzothiophene at 303 K. In the presence of $\text{Na}_7\text{H}_2\text{LaW}_{10}$, dibenzothiophene is completely removed in 25 min, and the catalyst was recycled 10 times with only a slight decrease in activity. $\text{Na}_7\text{H}_2\text{LnW}_{10}$ ($\text{Ln} = \text{Eu}, \text{La}$) show better activities than other isostructural Ln-containing POMs, as well as $\text{K}_{10}[\text{Co}_4(\text{PW}_9)_2]$ and $\text{Na}_{12}[\text{ZnWZn}_2(\text{ZnW}_9)_2]'$ under the same conditions.

To increase the compatibility of oily fuels with the most used oxidant H_2O_2 , scientists have made much effort on surfactant-type POM catalysts. These surfactant-type POMs simultaneously act as catalysts and surfactants. They have improved catalytic performances stemming from the hydrophobicity of the surfactant's alkyl chains and the hydrophilicity of the POM anions. The long alkyl chains on the surface of the POM catalysts capture the weakly polar sulfide molecules by hydrophobic-hydrophobic interactions.^{354,355} After reaction, the resulting sulfones easily escape from the catalyst because of their relatively strong polarity. The length of the alkyl chain and the number of long alkyl chains are important for the activities of surfactant-type POM catalysts. Although those surfactants bearing double or multiple long alkyl chains enhance the interaction probability of sulfide molecules with the catalysts, they limit the catalytic efficiency by hindering the interaction of H_2O_2 with POMs to form active peroxy-POM species. Sometimes, POM catalysts containing a single long alkyl chain, e.g., $[\text{C}_{18}\text{H}_{33}\text{N}(\text{CH}_3)_3]_3\text{PW}_{12}$,³⁵⁶ and $[\text{C}_{16}\text{H}_{33}\text{N}(\text{CH}_3)_3]_3\text{PW}_{12}$,³⁵⁷ may provide higher catalytic activity. On one hand, the amphiphilic catalyst may adsorb sulfide molecules on alkyl chains. On the other hand, it may provide enough channels to H_2O_2 for the formation of active peroxy-POM species.

It is notable that some surfactant-type POM catalysts show interesting self-assembly behavior.³⁵⁸ Some of them self-assemble into uniform nanowires and nanotubes at room temperature.³⁵⁷ The morphologies of these assemblies greatly depend on the length of the chains on the cationic surfactant. Those with nanospaces are expected to act as nanocontainers for guest materials. Wang's group have successfully constructed nanocone nanoreactors using $[(\text{C}_{18}\text{H}_{37})_2\text{N}(\text{CH}_3)_2]_3\text{PW}_{12}$ for the oxidation of sulfides.³⁵⁹ Besides, several emulsion systems have been created for oxidative desulfurization of fuels. Song's group made an IL emulsion system with $[(\text{C}_{18}\text{H}_{37})_2\text{N}(\text{CH}_3)_2]_9\text{-LnW}_{10}\text{O}_{36}$.³⁶⁰ Li's group contributed several microemulsion systems.³⁶¹⁻³⁶⁴ When surfactant-type $[(\text{C}_{18}\text{H}_{37})_2\text{N}(\text{CH}_3)_2]_3\text{-PW}_{12}$ ^{361,362} or $[\text{C}_{18}\text{H}_{37}\text{N}(\text{CH}_3)_3]_4\text{H}_2\text{NaPW}_{10}\text{O}_{36}$ ³⁶⁴ is mixed with H_2O_2 in diesel, metastable emulsion droplets (water in oil) are formed. These assembled microemulsion systems lower the

sulfur level in diesel from about 500 to 0.1 ppm under mild conditions, without changing the properties of diesel. After each cycle, the catalyst can be separated and recycled by reversible demulsification and reemulsification. Furthermore, the emulsion system composed of $[C_{18}H_{37}N(CH_3)_3]_5V_2PMo_{10}$ is even effective with O_2 as the oxidant and aldehyde as the sacrificial agent.³⁶³

Although emulsion systems containing cationic surfactants and POM anions are highly effective, they are sensitive to low pH and high ionic strength due to the relatively weak electrostatic interaction between anionic POMs and cationic surfactants. Wei's group have tried to covalently graft a long alkyl chain to POM anions to solve the problem.³⁶⁵ They created a disparate emulsion system by bonding a long alkyl chain to hexavanadate via esterification reaction. Monoesterification and diesterification of the hybrid hexavanadate $\{V_6O_{13}[(OCH_2)_3CCH_2OH]\}_2^{2-}$ with stearic anhydride give long-alkyl-tailed catalysts $\{V_6O_{13}[(OCH_2)_3CCH_2OH]_2[(OCH_2)_3CCH_2OOC(CH_2)_{16}CH_3]\}^{2-}$ ($V_6\text{-}1$) and $\{V_6O_{13}[(OCH_2)_3CCH_2OOC(CH_2)_{16}CH_3]_2\}^{2-}$ ($V_6\text{-}2$), respectively. In the presence of $V_6\text{-}1$ or $V_6\text{-}2$, thiophene, the most inert sulfide against an oxidizing agent among all its derivatives, is smoothly oxidized to water-soluble sulfur-containing species to leave from the oil phase and go into the aqueous phase. However, the pH value of the reaction media still influences the activities of the catalysts, because protons significantly decrease the surface charge of POM polar headgroups by associating with hexavanadate clusters, consequently changing the self-assembly of POM-based hybrid surfactants, and thus their amphiphilic properties. Static charge repulsion is expected to stabilize particles by preventing them from collapse. At low pH, the weaker static charge repulsion between the hexavanadates on the emulsion surface leads to larger emulsion sizes, that is, a smaller total interfacial area when a fixed amount of surfactants is put into the solution. In brief, $V_6\text{-}1$ - and $V_6\text{-}2$ -constructed emulsions are still not stable at very low pH since the hexavanadate clusters are weakly charged or neutral. Thus, the conversion of thiophene becomes lower when the pH of the solution drops.

Although low pH is unfavorable for surfactant-type POM involving emulsion systems, the case is quite different for common systems with POMs containing short-chain-tailed organic cations. The performances of a series of catalysts containing an N-methylimidazolyl moiety (Figure 17) are

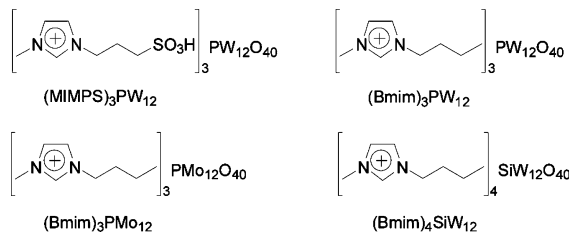


Figure 17. Structures of $(\text{MIMPS})_3\text{PW}_{12}$, $(\text{Bmim})_3\text{PW}_{12}$, $(\text{Bmim})_3\text{PMo}_{12}$, and $(\text{Bmim})_4\text{SiW}_{12}$.

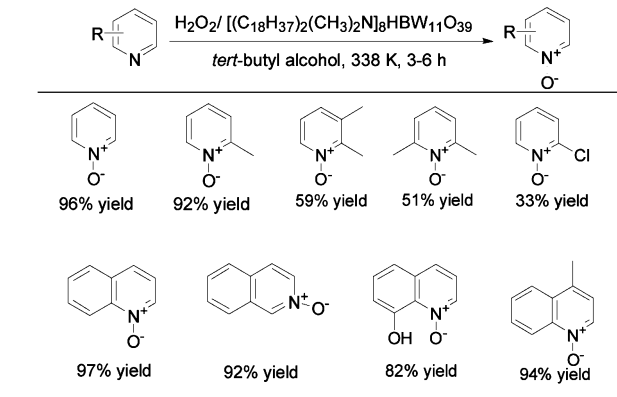
indicative of the importance of protons in enhancing the activities of POM catalysts.³⁶⁶ The acidic catalyst $(\text{MIMPS})_3\text{PW}_{12}$ is more active than the structurally analogous catalysts $(\text{Bmim})_3\text{PW}_{12}$, $(\text{Bmim})_3\text{PMo}_{12}$, and $(\text{Bmim})_4\text{SiW}_{12}$. The activity sequence is $(\text{MIMPS})_3\text{PW}_{12} > (\text{Bmim})_3\text{PW}_{12} > (\text{Bmim})_3\text{PMo}_{12} > (\text{Bmim})_4\text{SiW}_{12}$. The sequence also discloses

that the metals and heteroatoms in the catalysts are relevant to their catalytic activities. Generally, W-based POM catalysts are more active than the structurally identical Mo-based POM catalysts for oxidative desulfurization.

2.10. Oxidation of Nitrogen-Containing Compounds

Pyridine N-oxide derivatives can be used as oxidants, protecting groups, auxiliary agents, catalysts, surrogates for heterocyclic boronic acids, and ligands in metal complexes. More valuably, they represent a new class of anti-HIV compounds. These compounds are usually synthesized by the oxidation of pyridine and its derivatives. Water-soluble catalysts $\text{Na}_{12}[\text{ZnWZn}_2(\text{ZnW}_9)_2]$ ⁴¹ and $\text{K}_6(\text{V}_3\text{PW}_9)$ ⁴⁷ are qualified for the reaction in water. In the presence of $\text{K}_6(\text{V}_3\text{PW}_9)$, N-oxides are readily formed at room temperature. The catalyst shows much higher activity than $\text{NaVO}_3 \cdot 2\text{H}_2\text{O}$, $\text{Na}_2\text{HPO}_4 \cdot 12\text{H}_2\text{O}$, and $\text{Na}_2\text{WO}_4 \cdot 2\text{H}_2\text{O}$ and their mixture. When organic solvents are used in place of water, the yields of N-oxides are much lower. This is explained by the lower solubility of $\text{K}_6(\text{V}_3\text{PW}_9)$ in organic solvents. The combination of POM catalysts and water makes the reaction system clean and powerful. Preyssler's compound $\text{H}_{14}(\text{NaP}_5\text{W}_{30}\text{O}_{110})$ and mixed addenda of $\text{H}_{14}(\text{NaP}_5\text{W}_{29}\text{MoO}_{110})$ are effective for the oxidation of pyridinecarboxylic acids, such as nicotinic acid, picolinic acid, and quinolinic acid, to the corresponding N-oxides.³⁶⁷ N-Oxides are given in high yields along with decarboxylation occurring at the 2-position. The temperature-controlled POM catalysts $[(\text{C}_{18}\text{H}_{37})_2(\text{CH}_3)_2\text{N}]_7\text{PW}_{11}\text{O}_{39}$ ³⁶⁸ and $[(\text{C}_{18}\text{H}_{37})_2(\text{CH}_3)_2\text{N}]_8\text{HBW}_{11}\text{O}_{39}$ ³⁶⁹ are energetic for the oxidation of a series of pyridine and its derivatives. The results with $[(\text{C}_{18}\text{H}_{37})_2(\text{CH}_3)_2\text{N}]_8\text{HBW}_{11}\text{O}_{39}$ are depicted in Scheme 11.

Scheme 11. Oxidation of Pyridine and Its Derivatives Catalyzed by $[(\text{C}_{18}\text{H}_{37})_2(\text{CH}_3)_2\text{N}]_8\text{HBW}_{11}\text{O}_{39}$ ³⁶⁹



For pyridine and 2-picoline, yields of 96% and 92% are obtained after 3 h, respectively. Disubstituted pyridine derivatives are more difficult to oxidize. For 2,3-lutidine and 2,6-lutidine, 59% and 51% yields are given after 6 h. However, high to excellent yields (82–97%) of N-oxides are obtained for quinoline and its derivatives after 5 h. The two surfactant-type catalysts are temperature-responsive. Upon heating, they are soluble in the reaction mixture, and the catalysts precipitate from the liquid phase when the temperature is reduced to room temperature after reaction. Thus, they take advantage of automatic separation.

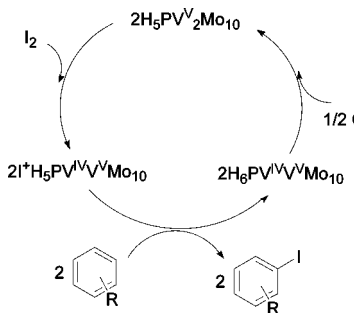
2.11. Oxidative Halogenation of Unsaturated Compounds

Halogenated organic compounds have been extensively utilized for pharmaceuticals, agrochemicals, dyes, and flame retardants.

The traditional methods to prepare halogenated organic compounds often use hazardous, toxic, and corrosive molecular halogens as the halogen sources. With a growing ecological awareness among chemists, recent investigations mainly focus on the green oxidative halogenations with H_2O_2 or O_2 as the oxidant and less poisonous halide ions as the halogen sources. Correlative work on green oxidative halogenations has been carefully reviewed by Iskra.³⁷⁰ In this field, POM/HPA catalysts receive considerable attention due to their unique stabilities to H_2O_2 and O_2 . Thereamong, V-substituted POMs/HPAs are of most interest because vanadium complexes can be viewed as functional mimics of halogenating enzymes.

In 2003, Neumann's group developed an inherently waste-free system for iodination of arenes using O_2 as the oxidant and $\text{H}_5\text{V}_2\text{PMo}_{10}$ as the catalyst.³⁷¹ In this work, molecular iodine is used as the halogenating reagent. Although molecular iodine is more toxic than I^- , its toxicity is significantly lower than that of other molecular halogens. Additionally, molecular iodine is nearly quantitatively consumed in the present system. The activated arenes are smoothly iodinated with high conversions (80–100%), high regioselectivities, and good to excellent selectivities for monoiodination products. As for the non-activated arenes, the reactions are more sluggish. However, higher temperature and prolonged time can retrieve the results. When HI is used in place of I_2 , no significant iodination occurs. Thus, HI is not involved in the reaction process. A direct oxidation pathway is proposed for the reaction (Scheme 12).

Scheme 12. Direct Oxidation Pathway for the Iodination with $\text{H}_5\text{V}_2\text{PMo}_{10}$, I_2 , and O_2 ³⁷¹



Molecular iodine is directly oxidized to two I^+ -type species by $\text{H}_5\text{V}_2\text{PMo}_{10}$, which react with arene substrates to give the products. After iodination, the reduced catalyst is reoxidized by O_2 .

Mizuno's group disclosed the effectiveness of the di-V-substituted phosphotungstate $\text{TBA}_3(\gamma\text{-V}_2\text{PW}_{10})$ for oxidative bromination of a range of alkenes, alkynes, and aromatics with H_2O_2 as the terminal oxidant and NaBr as the nontoxic bromine source.³⁷² The results are shown in Table 11. Exemplarily, the bromination of 1-octene with 0.05 mol % $\text{TBA}_3(\gamma\text{-V}_2\text{PW}_{10})$, 1 equiv of H_2O_2 , and 2 equiv of NaBr with respect to 1-octene gives 1,2-dibromoocane with 90% yield in 10 min under mild conditions. In this case, the efficiencies of H_2O_2 and NaBr utilization are higher than 90%, and the TOF is up to $10\,880\text{ h}^{-1}$. Under similar conditions, the TOF for methoxybenzene is 3840 h^{-1} , much higher than those with $\text{NH}_4\text{VO}_3/\text{HBr}/\text{KBr}$ (0.4 h^{-1}),³⁷³ $\text{V}_2\text{O}_5/\text{HBr}/\text{KBr}$ ($5.1\text{--}41\text{ h}^{-1}$),³⁷⁴ and $(\text{NH}_4)_6\text{Mo}_7\text{O}_{24}/\text{KBr}$ (222 h^{-1}).³⁷⁵ In the reactions, the catalyst reacts with H_2O_2 in the presence of H^+ to form active electrophilic intermediates reversibly, i.e., $\{\text{V}_2(\mu$

Table 11. $\text{TBA}_3(\gamma\text{-V}_2\text{PW}_{10})$ -Catalyzed Oxidative Bromination of Various Alkenes, Alkynes, and Aromatics³⁷²

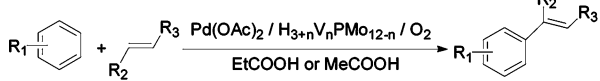
| alkenes | $\text{H}_2\text{O}_2 / \text{TBA}_3(\gamma\text{-V}_2\text{PW}_{10}) / \text{NaBr}$ | brominated products | Time (min) | Yield (%) |
|-----------|--|---------------------|------------|-----------|
| alkynes | $\text{CH}_3\text{COOH}-\text{ClCH}_2\text{CH}_2\text{Cl}, 293\text{ K, Ar}$ | | | |
| substrate | product | | | |
| | | | 10 | 90 |
| | | | 10 | 87 |
| | | | 10 | 76 |
| | | | 10 | 82 |
| | | | 60 | 92 |
| | | | 30 | 96 |
| | | | 30 | 94 |
| | | | 30 | 96 |
| | | | 30 | 95 |

$\text{OH})(\mu\text{-OOH})\}$ and $\{\text{V}_2(\mu\text{-}\eta^2\text{-}\eta^2\text{-O}_2)\}$ (Scheme 4), which oxidize Br^- to bromonium-like species Br^+ or Br_2 .^{372,376} Excitingly, the system is even effective for oxidative chlorination using LiCl as the chlorine source.

Some chemists also pay attention to heterogeneous systems for oxidative halogenation of unsaturated compounds. In 2003, Firouzabadi et al. achieved regioselective bromination of phenols and some other aromatic compounds with the cesium salt of H_3PW_{12} as a solid catalyst,³⁷⁷ although H_3PW_{12} was proved to be unserviceable for the iodination of arenes using O_2 in Neumann's system.³⁷¹ In combination with cetyltrimethylammonium bromide (CTAB), the salt actively catalyzes the reaction using molecular bromine as the bromine source. It is known that the bromination of phenol with Br_2 usually gives multibrominated products, such as 2,4,6-tribromophenol. It is difficult to obtain monobrominated products, especially a single monobrominated product. However, the heterogeneous $\text{Cs}_{2.5}\text{H}_{0.5}\text{PW}_{12}$ absolutely gives 4-bromophenol with 94% isolated yield. In the binary catalytic system, CTAB contributes to the excellent regioselectivity for the *para*-brominated product, while $\text{Cs}_{2.5}\text{H}_{0.5}\text{PW}_{12}$ should be responsible for the elevation of the reaction rate. In addition, HPA-impregnated titanium phosphate³⁷⁸ and HPA supported on zirconia^{379,380} are also used for oxidative halogenation of unsaturated compounds.

2.12. Oxidative Coupling Reactions

Pd-containing compounds are traditional catalysts for C–C coupling reactions. In recent years, the combinations of Pd compounds and POMs/HPAs have received much attention. POMs/HPAs not only act as cocatalysts to account for the regeneration of Pd^{II} , but also solve many other problems

Table 12. Oxidative Coupling Reaction of Arenes with Alkenes in $\text{Pd}(\text{OAc})_2/\text{H}_{3+n}\text{V}_n\text{PMo}_{12-n}/\text{O}_2$ Systems


| n | Arene | Alkene | Product | Yield d (%) | Ref. | n | Arene | Alkene | Product | Yield d (%) | Ref. |
|---|-------|--------|---------------------|-------------|------|---|-------|--------|--------------------|-------------|------|
| 1 | | | o:m:p=13:44:43 | 59 | 384 | 1 | | | o:m:p=15:41:44 | 70 | 383 |
| 1 | | | o:m:p=0:56:44 | 54 | 384 | 1 | | | o:m:p=17:7:76 | 73 | 383 |
| 1 | | | o:m:p=17:10:73 | 45 | 384 | 1 | | | | 67 | 383 |
| 1 | | | | 47 | 384 | 1 | | | | 65 | 383 |
| 1 | | | 2,3:3,4 = 45:55 | 45 | 384 | 1 | | | | 86 | 383 |
| 1 | | | | 68 | 383 | 1 | | | | 47 | 383 |
| 1 | | | | 74 | 383 | 4 | | | | 65 | 382 |
| 1 | | | | 73 | 383 | 4 | | | | 72 | 382 |
| 1 | | | | 93 | 383 | 4 | | | | 75 | 382 |
| 1 | | | | 31 | 383 | 4 | | | | 84 | 382 |
| 1 | | | | 70 | 383 | 4 | | | | 70 | 382 |
| 1 | | | | 88 | 383 | 4 | | | | 32 | 382 |
| 1 | | | | 76 | 383 | 4 | | | o:m:p=14:42:44 | 69 | 382 |
| 1 | | | | 9 | 383 | 4 | | | | 62 | 382 |

existing in conventional Pd-catalyzed systems. For example, Heck–Mizoroki arylation of alkenes with aryl halides or triflates is a good candidate for C–C bond formation in the presence of Pd catalyst and stoichiometric base. However, massive salts are

formed as the undesired waste in the process and cause boring post-treatment. The use of arenes without halides such as benzene instead of halobenzenes and triflates will avoid the production of waste salts. However, such reactions usually

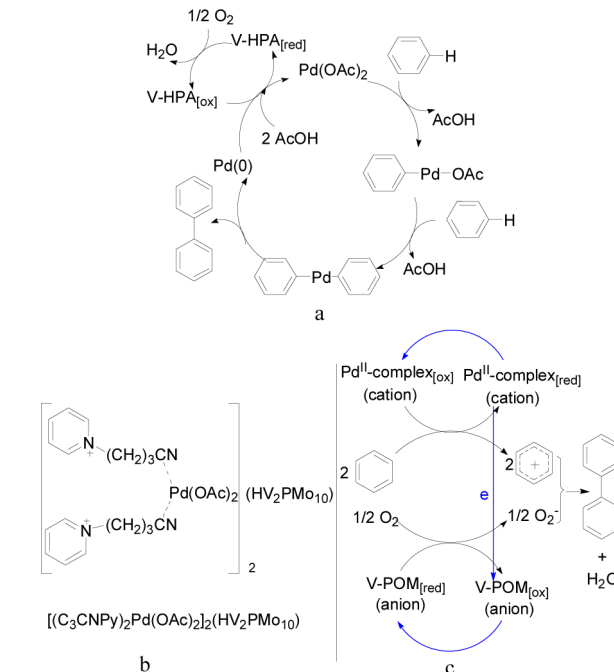
proceed via direct activation of the C–H bond, which calls for severe reaction conditions, e.g., elevated reaction temperature and high pressurized O₂ and CO.³⁸¹ The combinations of POMs/HPAs with Pd-containing compounds allow the reactions to proceed under mild conditions. The homogeneous systems Pd(OAc)₂/H_{3+n}V_nPMo_{12-n}/O₂ provide rich evidence for the scheme.^{382–384}

The system Pd(OAc)₂/H₇V₄PMo₈/O₂ promotes the oxidative coupling of unhalogenated arenes with various acrylates at a temperature below 373 K, with 1 atm of O₂ as the oxidant (Table 12).³⁸² The analogical combination of Pd(OAc)₂/H₄VPMo₁₁/O₂ enlarged the scope of alkenes to α,β -unsaturated aldehydes,³⁸⁴ ketones, nitrile, and other electron-deficient alkenes.³⁸³ For electron-deficient alkenes, moderate to good results are obtained (Table 12). The oxidative arylation of simple alkenes without electron-withdrawing groups, such as ethylene, is much more difficult. Envisaging the attractive but challenging reaction of nonsubstituted benzene with simple alkenes without electron-withdrawing groups, the system Pd(OAc)₂/H₄VPMo₁₁/O₂ is used for the coupling reaction of benzene with ethylene, and exhibits delightful catalytic performance.³⁸⁵ The total TON of Pd toward the formation of styrene and stilbene is up to 167.

Apart from the arylation of alkenes, Pd(OAc)₂/H_{3+n}V_nPMo_{12-n}/O₂ systems are applicable for homocoupling of benzene to afford biphenyl.³⁸⁶ Kozhevnikov³⁸⁷ and Yamaji³⁸⁸ reported the systems Pd(OAc)₂/H₅V₂PMo₁₀/O₂/AcOH–H₂O and Pd(OAc)₂/H₃PMo₁₂/O₂/AcOH–H₂O, respectively, for the reaction. In the system Pd(OAc)₂/H₃PMo₁₂/O₂/AcOH–H₂O, biphenyl is obtained with 100% selectivity and 19% yield under the conditions of 403 K, 10 atm of O₂, and 4 h.³⁸⁸ Although the control catalyst PdHPMo₁₂ also serves the reaction, a lower yield is given. Ishii's group combined Pd(OAc)₂ with a mixture of H₄VPMo₁₁ and H₃PMo₁₂ with a ratio of 1:1.³⁸⁶ The system produces biphenyl in 14.3% yield under 1 atm of O₂ at 363 K after 15 h. The TON reaches up to 109. In the above systems, H_{3+n}V_nPMo_{12-n} and Pd(OAc)₂ individually act as the cocatalyst and major catalyst. In catalytic cycles, HPAs account for the regeneration of Pd^{II}, and the reduced HPAs are reoxidized by O₂ in the following step (Scheme 13a).

Most recently, Wang's group developed a new heterogeneous catalyst for the oxidative homocoupling of benzene to biphenyl, via pairing POM anions with Pd^{II}-coordinated nitrile-tethered cations by electrostatic interaction (Scheme 13b).³⁸⁹ The catalyst is formulated as [(C₃CNPy)₂Pd(OAc)₂]₂(HV₂PMo₁₀). With AcOH as the solvent, the liquid–solid biphasic system with [(C₃CNPy)₂Pd(OAc)₂]₂(HV₂PMo₁₀) produces biphenyl with 18.3% yield and 88.0% selectivity under the conditions of 3 atm of O₂, 373 K, and 7 h. The intramolecular charge transfer from the ionically linked Pd^{II}-coordinated cations to the POM anions significantly increases the redox capability of the POM anions, and should be responsible for the high activity of the catalyst for the overall reaction. In contrast, the imidazolium-based analogue [(C₃CNMim)₂Pd(OAc)₂]₂(HV₂PMo₁₀) shows much lower activity, mostly because of the hindering of the intramolecular electron transfer by the strong interaction between the highly active C-2 protons of the imidazole rings and nitrile groups. Compared with the homogeneous Pd(OAc)₂/H_{3+n}V_nPMo_{12-n}/O₂/AcOH–H₂O systems, the hybrid catalyst takes advantage of easier recovery. Notice that the reaction mechanism with [(C₃CNPy)₂Pd(OAc)₂]₂(HV₂PMo₁₀) (Scheme 13c)³⁸⁹ is essentially different from

Scheme 13. (a) Classical Mechanism for the Oxidative Coupling of Benzene with Individual Pd(OAc)₂ and V–HPAs, (b) Structure of [(C₃CNPy)₂Pd(OAc)₂]₂(HV₂PMo₁₀), and (c) Proposed Mechanism for the Oxidative Coupling of Benzene with [(C₃CNPy)₂Pd(OAc)₂]₂(HV₂PMo₁₀)^{388,389}

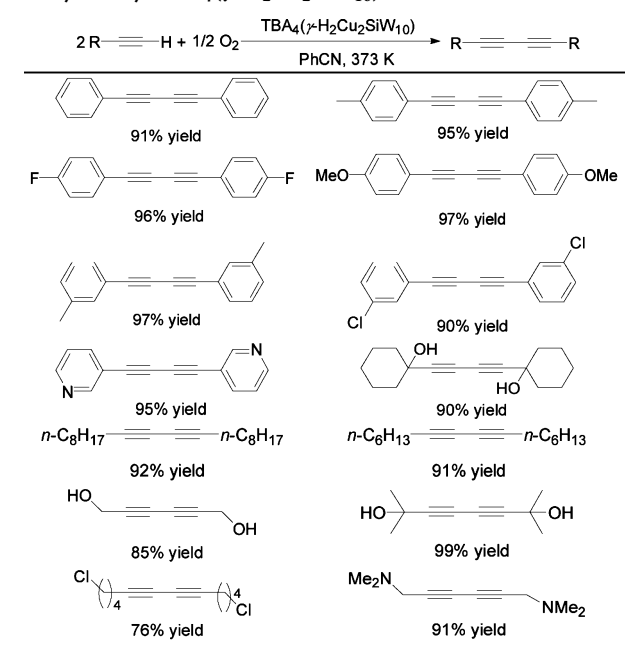


that with individual Pd(OAc)₂ and V–HPAs (Scheme 13a).^{386,390} The Pd^{II} complex_[ox] activates neutral benzene to phenyl cation, accompanied by the production of Pd^{II} complex_[red]. Simultaneously, V–POM_[red] activates O₂ to O₂[–], accompanied by the production of V–POM_[ox]. Subsequently, the active phenyl cation readily reacts with active O₂[–] to form biphenyl, and Pd^{II} complex_[red] transfers an electron to V–POM_[ox] to ensure the regeneration of Pd^{II} complex_[ox] and V–POM_[red].

The oxidative homocoupling of terminal alkynes to 1,3-diyne derivatives is typically catalyzed by copper salts. Many conventional systems suffer from low TON, significant formation of byproducts, severe catalyst deactivation, narrow applicability to a limited number of alkynes, and/or the need for additives. The monomeric di-Cu-substituted silicotungstate TBA₄[γ -H₂Cu₂(μ -1,1-N₃)₂SiW₁₀O₃₆] (TBA₄(γ -H₂Cu₂SiW₁₀)), wherein two copper atoms are bridged by two azido groups, successfully overcomes these shortcomings.³⁹¹ Without any additives, the di-Cu-substituted silicotungstate promotes the oxidative homocoupling of structurally diverse alkynes to 1,3-diyne in the presence of 1 atm of O₂ (Scheme 14). After 2–18 h, the yields of 1,3-diyne are higher than 90% for most cases.

The selectivities for all cases are higher than 99%. Susceptible hydroxyl and amido groups are substantial under turnover conditions. The POM catalyst shows much higher activity than conventional copper salts. When phenylacetylene is selected as a model substrate, TBA₄(γ -H₂Cu₂SiW₁₀) gives a yield of 91%, while Cu(OAc)₂, CuCl₂, CuCl, CuI, copper(I) phenylacetylides, TBA₄[α -H₂CuSiW₁₁O₃₉], and the mixture of TBA₄(γ -H₂SiW₁₀) and CuCl₂ give yields of 10%, 4%, 7%, 2%, <1%, 2%, and 5%, respectively, under totally identical conditions. The TON of TBA₄(γ -H₂Cu₂SiW₁₀) is as high as 468 for a 20 mmol scale

Scheme 14. Oxidative Homocoupling of Various Alkynes Catalyzed by $\text{TBA}_4(\gamma\text{-H}_2\text{Cu}_2\text{SiW}_{10})^{391}$



reaction of phenylacetylene, a high value for copper-catalyzed oxidative alkyne homocoupling reactions. Furthermore, the POM catalyst takes advantages of easy recovery and reuse with retention of its high catalytic performance, which are absent for conventional copper salts. In consonance with the generally accepted mechanism for copper-catalyzed oxidative homocoupling of alkynes, a catalytically active alkynylcopper(II) intermediate, $\{\text{Cu}_2(\mu\text{-C}\equiv\text{CR})_2\}$, is formed by ligand exchange between the azido groups and alkynyl groups. The process is responsible for the observed induction period. After the pretreatment of $\text{TBA}_4(\gamma\text{-H}_2\text{Cu}_2\text{SiW}_{10})$ with alkyne, the induction period disappears. Upon the formation of 1,3-diyne over the catalyst, Cu^{II} species are simultaneously reduced to Cu^{I} species, which are subsequently reoxidized by O_2 .³⁹²

3. REDUCTION

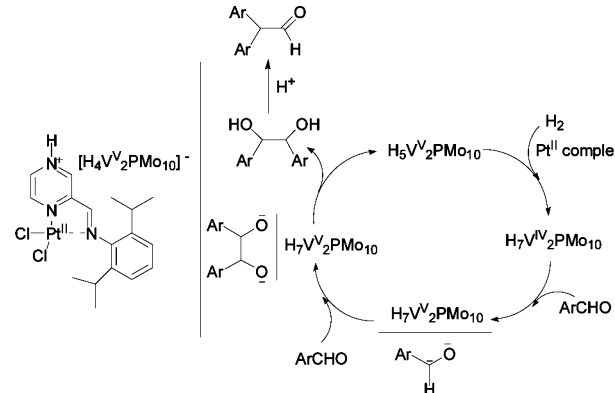
3.1. Reduction of Organic Compounds

The use of POM catalysts in oxidative transformations is universal. In contrast, reductive transformations with POM catalysts have been less explored, although there are a few reductive examples catalyzed by noble metals (Pt, Pd, Rh, and Ir) in the presence of POMs.^{393–395} In 2011, Fehrmann found some POMs were good protectors in the selective reduction of NO with ammonia.^{396,397} They protected active TM catalysts, such as CuO/TiO_2 , $\text{Fe}_2\text{O}_3/\text{TiO}_2$, and $\text{V}_2\text{O}_5/\text{TiO}_2$, from alkaline metal poisons by bonding of the alkaline metals to the Brønsted acid centers to enhance their acidity and activity. This feature makes these POMs promising for flue gas cleaning in both coal- and biomass-fired power plant installations. POMs are also used to modify other organometallic catalysts for hydrogenation reactions. In most of the cases, the reactions are mainly catalyzed by the organometallic moieties, rather than POMs themselves. However, the nature of the POM moieties significantly influences the activities and selectivities of the organometallic moieties.³⁹⁸ For example, after covalent attachment to Keggin-type $[\text{SiW}_{11}\text{O}_{39}]^{8-}$ through two alkylene bridging groups, the activity of the Wilkinson-type catalyst

$\text{Rh}^{\text{I}}\text{Cl}(\text{Ph})_3$ is enhanced by approximately 50% in the hydrogenation of 1-octene.³⁹⁹ The improvement probably results from the stabilization of the intermediate Rh^{III} species that is derived from the oxidative addition of hydrogen to Rh^{I} by the POM-functionalized alkyl chains in the phosphine ligands.

In fact, POM moieties can be the true active components for some binary catalysts. The reductive coupling of aryl aldehyde with a binary catalyst, Pt^{II} complex– $\text{H}_5\text{V}_2\text{PMo}_{10}$, provides evidence (Scheme 15).⁴⁰⁰ In the reaction, the platinum center

Scheme 15. Structure of Pt^{II} Complex– $\text{H}_5\text{V}_2\text{PMo}_{10}$ and the Proposed Reaction Pathway for Pinacol Coupling⁴⁰⁰



in a typical square planar coordination mode first activates molecular hydrogen. Next, the activated molecular hydrogen reduces $\text{H}_5\text{V}_2\text{PMo}_{10}$ to $\text{H}_7\text{V}_2\text{PMo}_{10}$. Afterward, the reduced POM reacts with an aryl aldehyde by a two-electron transfer (perhaps stepwise) to the aryl aldehyde to form an anionic intermediate that subsequently couples with another aryl aldehyde substrate to yield the vicinal diol as the initial diol product. Due to the existence of acidic protons in the catalyst, the initial product undergoes pinacol rearrangement to give diarylacetaldehyde. The combination of the Pt^{II} complex and $\text{H}_5\text{V}_2\text{PMo}_{10}$ makes it possible to use molecular hydrogen as the terminal reductant instead of reductive metals, typically Mg and Zn. Apparently, the protocol constricts the cost of the reaction and leaves out the production of waste metal ions.

Sometimes, POMs can be used as reductive catalysts alone in H_2 -mediated systems, but relatively severe reaction conditions are needed. In 1999, Neumann reported the reduction of carbonyl compounds with $\text{V}_2\text{PMo}_{10}$, which can be reduced by H_2 at 523–573 K.⁴⁰¹ The reduced form can strip oxygen atoms from ketones or aldehydes, resulting in the deoxygenation of these carbonyl compounds. With $\text{K}_5\text{V}_2\text{PMo}_{10}$ supported on Al_2O_3 , the conversion of benzophenone to diphenylmethane was quantitative under the conditions of 23 atm of H_2 and 573 K. The control experiments reveal that $\text{V}_2\text{PMo}_{10}$ is more active than SiW_{12} , PW_{12} , and PMo_{12} . The activity sequence is $\text{SiW}_{12} < \text{PW}_{12} < \text{PMo}_{12} < \text{V}_2\text{PMo}_{10}$, in line with that of the reducibility with H_2 and the oxidation potential of these POMs. Mo-based POMs are generally more active than W-based POM anions. The product distribution of the reductive reactions strongly depends on the used POM. The use of $\text{V}_2\text{PMo}_{10}$ prefers the formation of more highly reduced saturated compounds, whereas less highly reduced alkenes are often led by SiW_{12} . In the case of simple benzylic ketones such as benzophenone, fluorenone, and acetophenone, the sole products for both $\text{V}_2\text{PMo}_{10}$ and SiW_{12} are the simple methylene derivatives that

are formally formed by the deoxygenation and the addition of hydrogen. However, for other substrates, especially aliphatic ketones and aldehydes, the two catalysts provide very different selectivities. For cycloheptanone and 2-octanone, V_2PMo_{10} mostly gives saturated compounds, cycloheptane/ethylcyclopentane and octane, respectively, while SiW_{12} only gives alkenes. For 9,10-anthraquinone, V_2PMo_{10} gives more highly reduced species, tetra- and octahydroanthracene mostly, along with dihydroanthracene and anthracene but no anthrone, while SiW_{12} mainly gives dihydroanthracene, along with anthracene, anthrone, and tetrahydroanthracene.

Interesting selectivities are also observed for the hydrogenation of ketones with $K_5(PdPW_{11}O_{39})$ ($K_5(PdPW_{11})$) supported on γ -alumina or active carbon.⁴⁰² As shown in Table 13 (values in parentheses are the yields with commercial 10% Pd/C catalyst), this feature is exemplified by the following:

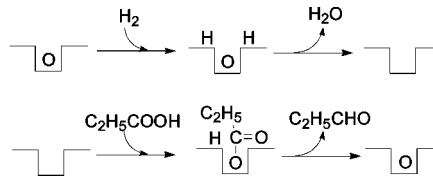
Table 13. Hydrogenation of Aromatic Ketones Catalyzed by 10 wt % $K_5(PdPW_{11})/C$ ⁴⁰²

| Entry | Substrate | $H_2/K_5(PdPW_{11})/C$ | Products and yields (%) | |
|-------|-----------|------------------------|-------------------------|-------------|
| | | | 473 K | products |
| 1 | | | 100 (0) | 0 (100) |
| 2 | | | 100 (0) | 0 (10) |
| 3 | | | 100 (0) | 0 (65) |
| 4 | | | 100 | 0 (35) |
| 5 | | | 100 (0) | 0 (83) |
| 6 | | | 100 | 0 (17) |
| 7 | | | 68 | 32 |
| 8 | | | 100 | 100 |
| 9 | | | 90 | 10 |

(i) the hydrogenation of aromatic distal ketone occurs on the aromatic rings and leaves the distal ketone groups unchanged (Table 13, entries 3–6); (ii) the aromatic compounds with vicinal ketone moieties are completely hydrogenated to saturated hydrocarbons (Table 13, entries 1, 2, and 8); (iii) catalytic McMurry coupling is observed for aliphatic aldehydes (Table 13, entry 9). The selectivity difference between commercial Pd/C catalyst and $K_5(PdPW_{11})/C$ is apparent. With commercial Pd/C, ketone moieties are always reduced to alcohols, while, with $K_5(PdPW_{11})/C$, distal or aliphatic ketones are inert and aromatic ketones are reduced or deoxygenated to methylene moieties.

$H_{3+n}V_nPMo_{12-n}$ ($n = 0–2$) and their Cs salts serve the vapor-phase hydrogenation of propanoic acid under the conditions of 1 bar of H_2 pressure and 623 K.⁴⁰³ Partial substitution of Mo^{VI} by V^V in the anions has a small effect on the catalytic results. The Cs content more significantly influences the reduction properties of the catalysts. As the Cs content increases, the selectivity for propanal passes a maximum (74–76%), that for propane sharply decreases, and that for 3-pentanone monotonously increases. 3-Pentanone is likely to form via a cesium propanoate intermediate. The formation of propanal is supported to proceed via a two-step Mars–Van Krevelen mechanism (Scheme 16) that has a pronounced resemblance to

Scheme 16. A Mars–Van Krevelen Mechanism for Carboxylic Acid Hydrogenation⁴⁰³



selective oxidation with O_2 over these POMs, e.g., the oxidation of methacrolein to methacrylic acid and the oxidative dehydrogenation of isobutyric acid to methacrylic acid.^{404,405} In the first step, the adsorbed hydrogen strips the lattice oxygen of the catalyst to generate an oxygen vacancy by desorption of a water molecule. In the second step, the vacancy is refilled by an oxygen atom from propanoic acid, resulting in the formation of propanal and the regeneration of the catalyst in its oxidized form. According to the postulated mechanism, the metal–oxygen bond of the suitable POM catalysts for the reaction should be of a moderate strength, neither too strong nor too weak. If the metal–oxygen bond is too strong, the first step will proceed slowly; if it is too weak, the ability of the vacancy to abstract oxygen from propanoic acid will be weak. Thus, a too strong or too weak metal–oxygen bond of the catalysts will limit the reaction rate.

3.2. Photoreduction of CO_2

CO_2 is a renewable C_1 feedstock for the production of chemicals, materials, and fuels. Photochemical reduction is a sustainable way to utilize CO_2 that employs solar energy as the only energy input. As excellent photocatalysts, POM complexes are of interest in this field. Superficially, the interactions between CO_2 and the negatively polarized oxo shell of the POM anion are electrostatically nonfavored.⁷⁴ In 1998, Kozik et al. suggested that special binding sites (e.g., Co, Ni, Mn) with weakly bound ligands (e.g., H_2O) could be introduced into the POM catalysts via substitution.⁴⁰⁶ Under apolar anhydrous conditions, the weak ligands are expected to exchange for CO_2 ,

resulting in the binding of CO₂ to POM anions. In 2008, Xu et al. found that the CO₂-ligated anions of (C₃H₅N₂)₃(C₃H₄N₂)-[Co(CO₂)PMo₁₁O₃₈]·4H₂O and (C₃H₅N₂)₄[Co(CO₂)-SiMo₁₁O₃₈]·4H₂O are stable in organic solvent.⁴⁰⁷ In the presence of a sacrificial electron donor, the bound CO₂ can be reductively activated by the irradiation of light. In 2010, Neumann et al. developed a homogeneous system for the binding and subsequent photochemical reduction of CO₂ by C=O bond activation.⁵⁸ With the mono-Ru-substituted Keggin anion of RuSiW₁₁ as the catalyst and triethylamine as the sacrificial electron donor, CO₂ was effectively reduced to the sole product of CO in a toluene solution under the irradiation of UV light. The computational study of the proposed reaction intermediates showed that triethylamine not only acts as a sacrificial electron donor but also acts as a supramolecular stabilizer in the POM-based CO₂ activation. The DFT (density functional theory) calculations suggest that the CO₂ molecule binds to the Ru center in an end-on fashion. Triethylamine associates with the Ru-CO₂ group to form attractive Et₃N···CO₂ interactions (Figure 18a). Additionally, a

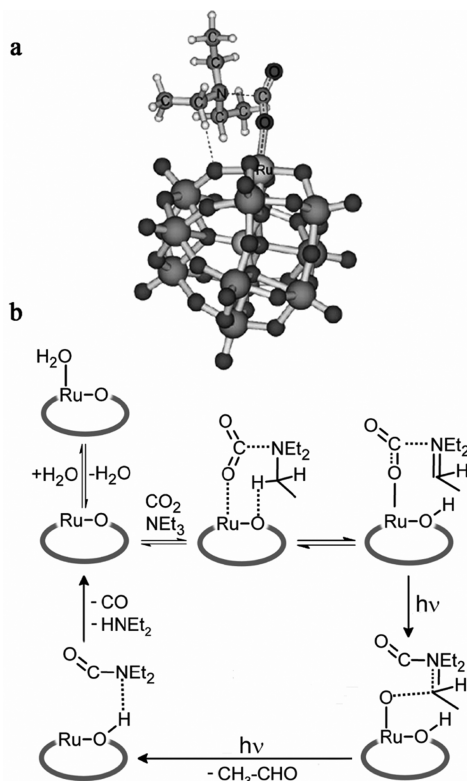


Figure 18. (a) Optimized geometry of amine-assisted CO₂ coordination with RuSiW₁₁. (b) Proposed mechanism for the photoreduction of CO₂ catalyzed by RuSiW₁₁.

C–H group of triethylamine interacts with the bridging oxo ligand located in proximity of the Ru center to form attractive N–C–H···O interactions. On the basis of experimental and computational results, a reaction mechanism was proposed for the POM-catalyzed photoreduction of CO₂ to CO (Figure 18b). Initially, the water ligand on the Ru center is replaced by CO₂ with the assistance of triethylamine, resulting in the formation of the intermediate {Ru(CO₂···NEt₃)SiW₁₁O₃₉}. Subsequently, a proton transfers from triethylamine to the POM anion. The cleavage of the C–O bond of CO₂ is achieved

photochemically in two consecutive steps, resulting in the formation of carbon monoxide, acetaldehyde, and diethylamine.

To use molecular hydrogen instead of triethylamine as the sacrificial electron donor, Neumann et al. reported an advanced approach in 2011.⁵⁹ They coupled a photoactive rhenium complex, [Re^I(L)(CO)₃(MeCN)]⁺, with a Keggin anion, [MHPW₁₂]⁻, via a crown ether-functionalized phenanthroline ligand L (L = 5,6-(15-crown-5)-1,10-phenanthroline; M = Na⁺, H₃O⁺) to form a supramolecular catalyst (Figure 19a). The

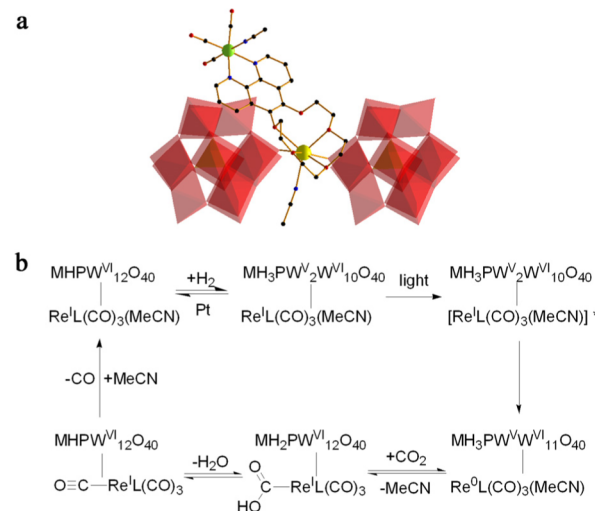


Figure 19. (a) Structure of the supramolecular catalyst [Re^I(L)(CO)₃(MeCN)][MHPW₁₂] used for the light-induced reduction of CO₂ to CO using H₂ as the reducing agent. (b) A possible pathway for the photoreduction of CO₂ to CO with H₂ and [Re^I(L)(CO)₃(MeCN)][MHPW₁₂] catalyst (M = Na⁺, H₃O⁺).

catalyst can promote CO₂ reduction in a synergistic manner. The rhenium complex represents the photoactive site, whereas the Keggin anion acts as the redox shuttle, which provides two electrons for the reduction of CO₂ to CO (Figure 19b). In the initial step, the POM anion undergoes a two-electron reduction by H₂ in the presence of colloidal Pt. Irradiation of the reduced supramolecular catalyst by visible light results in an intramolecular one-electron transfer from the POM anion to the Re^I center, resulting in the formation of a one-electron-reduced POM anion and a Re⁰ species. In the following step, CO₂ undergoes an oxidative addition to the Re⁰ center with simultaneous electron transfer of the remaining POM-based electron, resulting in the formation of a [Re^I(L)(CO)₃(CO₂H)] species. The subsequent cleavage of the C–O bond leads to the release of CO.

3.3. Photoreduction of Metal Cations

The reduction of metal cations is a good alternative for metal recovery or synthesis of metal nanoparticles. In recent years, Ruhlmann et al. have devoted their effort to photoreduction of precious metal cations using POM catalysts. Generally, porphyrins are introduced into the catalysts as the photosensitizer. In 2009, hybrid POM–porphyrin copolymeric films were obtained by the electrooxidation of zinc octaethylporphyrin (ZnOEP) and zinc 5,15-dipyridinium octaethylporphyrin (5,15-ZnOEP(py)₂⁺) in the presence of the POM {MnMo₆O₁₈[(OCH₂)₃CNHCO(4-C₅H₄N)]₂}³⁻.⁴⁰⁸ These films allow the photocatalytic reduction of silver ions under visible irradiation in air in the presence of propan-2-ol at the 2D

interface between water and the copolymeric films, resulting in the formation of silver nanowires and triangular nanosheets. After that, the group prepared nanocomposite films on the basis of electrostatic interactions between tetracationic zinc porphyrin $\text{ZnOEP}(\text{py})_4^{4+}$ or ZnTMePyP^{4+} and the tetra-Co-sandwiched Dawson-type polyanions $\alpha\beta\beta\alpha\text{-}[\text{Co}_4(\text{H}_2\text{O})_2\text{-}(\text{P}_2\text{W}_{15}\text{O}_{56})_2]^{16-}$.^{409,410} Upon the irradiation of visible light, the films catalyze the reduction of silver and gold ions in the presence of propan-2-ol (sacrificial electron donor), leading to the formation of silver nanowires and gold nanosheets. In fact, the photoreduction of silver ions still occurs when the tetra-Co core is replaced by other TMs (Zn, Ni, Fe).⁴¹¹ The catalytic activity depends on the nature of the tetra-M core in the polyanions. The catalyst $[\text{ZnTMePyP}^{4+}]_3\text{-}[\text{Fe}_4(\text{P}_2\text{W}_{15}\text{O}_{56})_2]^{12-}$ is even photoactive in aqueous solution under air and presents no degradation after its utilization. This result is very promising and can lead to its utilization in green chemistry. Similarly, the film containing tetracationic porphyrins $[\text{H}_2\text{TPhN}(\text{Me})_3\text{P}]^{4+}$ and Dawson-type polyanions $\alpha_2\text{-}[\text{Fe}(\text{P}_2\text{W}_{17}\text{O}_{61})]^{7-}$ catalyzes the photoreduction of silver ions to giant silver dendrites.⁴¹² It is notable that the photoreduction of silver ions also happens in the absence of photosensitizer, but light with more energy is required. The investigation indicated that the catalytic material, which is prepared via covalently linking an organotin-substituted Dawson-type phosphotungstate to a trithiocarbonate group, shows good performance in the presence of UV light.⁴¹³ Compared with the parent Dawson-type polyanion $[\text{P}_2\text{W}_{18}\text{O}_{62}]^{6-}$, the linked catalyst gives smaller, more homogeneous, and colloidally more stable silver nanoparticles.

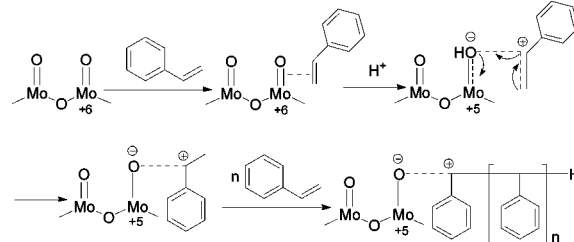
4. ALKENE POLYMERIZATION

In the early years, acid-catalyzed gas-phase propene oligomerization with HPA catalysts was communicated.⁴¹⁴ It is found that coke formation causes rapid deactivation of the catalyst. In 2001, Kozhevnikov et al. minutely studied the formation of coke and the regeneration of HPA catalysts using the reaction over silica-supported H_3PW_{12} and its palladium-doped form (1.6–2.5 wt % Pd) as a model.⁴¹⁵ During the reaction, coke is formed and causes rapid deactivation of both undoped and Pd-doped $\text{H}_3\text{PW}_{12}/\text{SiO}_2$, although the Keggin structures of the catalysts are unaffected by coke deposition. Palladium doping of $\text{H}_3\text{PW}_{12}/\text{SiO}_2$ inhibits the formation of polyaromatic coke; only aliphatic coke, which appears easier to burn, is detected. In contrast, a mixture of aliphatic and aromatic coke is found over the undoped catalysts. Addition of water, methanol, or acetic acid to the propene flow causes the formation of oxygenated products at the expense of propene oligomers. These additives are found to inhibit the coking, water being the most effective inhibitor. The removal of coke from the catalysts is attempted by using solvent extraction, ozone treatment, and aerobic oxidation. The extraction with CH_2Cl_2 allows removal of soft coke but is unable to remove hard coke. Ozone treatment can remove both soft and hard coke at 423 K. The aerobic burning of coke on the undoped $\text{H}_3\text{PW}_{12}/\text{SiO}_2$ proceeds to completion in the temperature range centered at 773–833 K, exceeding the temperature of H_3PW_{12} decomposition. Doping the catalyst with Pd significantly decreases this temperature to allow catalyst regeneration at temperatures as low as 623 K without loss of catalytic activity.

In recent years, Chen et al. reported the POM/HPA-catalyzed liquid-phase polymerization of a series of vinyl monomers, including styrene, methyl methacrylate, butyl

methacrylate, and vinyl acetate.^{416–419} The most attractive feature of POM/HPA-catalyzed polymerization of vinyl monomers is that no extra initiator is needed. Thus, these catalysts open up savings and green methods for the polymerization of vinyl monomer. In the presence of $\text{H}_3\text{PMo}_{12}$, styrene polymerizes rapidly via a cationic pattern.⁴¹⁶ The catalyst acts as the oxidizing agent, the polymerization initiator, and the operating anion of the growing cationic center. A monomer conversion of 84% and a polymer yield of 74.66% are achieved in less than 20 min. Although the molecular weight of the polymer products is not large, the polydispersity is narrow, revealing that the function of the catalyst is to stabilize the active center. After reaction, part of the Mo^{6+} ions are reduced to Mo^{5+} ions via accepting electrons from the styrene monomer. The reaction mechanism is put forward as electron coordination–cationic polymerization (Scheme 17). The electron deviates from C and leans toward O, and the weak force of the cationic active center is formed between the atoms of C and O.

Scheme 17. Mechanism of Cationic Polymerization of Styrene with $\text{H}_3\text{PMo}_{12}$ ⁴¹⁶



Notice that the function of $\text{H}_3\text{PMo}_{12}$ in polymerization of styrene is dual, depending on the construction of the system. In an AIBN (azodiisobutyronitrile)-initiated system, $\text{H}_3\text{PMo}_{12}$ inhibits the free radical polymerization of styrene.⁴¹⁷ The inhibition function occurs through redox reaction between $\text{H}_3\text{PMo}_{12}$ and the initiator AIBN. After redox reaction, if AIBN is the residual reagent, styrene is polymerized following a free radical mechanism; if the residual reagent is $\text{H}_3\text{PMo}_{12}$, styrene polymerization still happens, but follows a cationic mechanism.

The polymerization reaction with $\text{H}_3\text{PMo}_{12}$ proceeds so rapidly that its plant application and the use of many other vinyl monomers are limited.⁴¹⁸ The 4,4'-dipyridine phosphotungstic salt ($\text{Dipy})_{1,5}\text{PW}_{12}$) addresses the problem. It more gently catalyzes the cationic photopolymerization of vinyl monomers. In the presence of $(\text{Dipy})_{1,5}\text{PW}_{12}$, the polymerization of styrene proceeds readily under a 359 nm light irradiation and gives 92% conversion after 60 min at 293 K. The process is controllable. More importantly, the system is propitious to other industrially important vinyl monomers, such as vinyl isobutyl ether, methyl methacrylate, and butyl acrylate. The activity of the dipyridine salt is higher than that of H_3PW_{12} . An imidazolium salt, $[(\text{Bmim})_2\text{Dmim}]\text{PW}_{12}$ ($\text{Dmim} = 3,3'\text{-dimethyl-1,1'-diimidazolium}$), is also effective for photopolymerization of vinyl monomers, but the reaction follows a radical mechanism.⁴¹⁹ In the reaction, PW_{12} acts as the photoactive radical generating component, and the imidazolyl provides a radical that directly reacts with the double bond of the vinyl monomers. The dangling butyl chains on Bmim generate hydrophobic channels and thus exert a stabilizing effect on emerging oligomeric chains. Upon the irradiation of UV light, PW_{12} changes into its

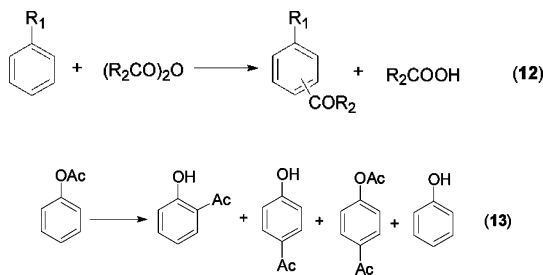
excited state (marked as POM*). Subsequently, POM* extracts a hydrogen free radical, H[•], from the imidazolium cation to generate reduced POM and an imidazolium radical cation. In the following step, the reduced anion is reoxidized by O₂ and the imidazolium radical cation reacts with the vinyl monomer.

5. ACID CATALYSIS

POM/HPA catalysts can bear one or two types of acidic sites, acidic protons, or/and metals with Lewis acidity. Both types of acidic sites can work as active sites in acid catalysis. Thus, these compounds provoke a huge interest for acid catalysis in the scientific community.

5.1. Reactions Involving C–C Bond Formation

Friedel–Crafts aromatic acylation (eq 12) and the related Fries rearrangement of aryl esters (eq 13) over strong acids are the



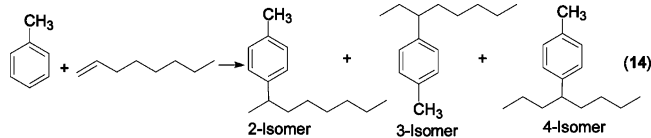
most important routes for the synthesis of aromatic ketones that are important intermediates in manufacturing fine and special chemicals as well as pharmaceuticals.^{420,421} Despite the fact that numerous solid acid catalysts such as zeolites, clays, and Nafion-H have been developed for the reactions, only a few of them have been hitherto proven efficient for the acylation of nonactivated arenes.⁹⁷ Upon consideration of the stronger acidity than that of conventional solid acids such as mixed oxides and zeolites, solid POM/HPA catalysts are attractive for this type of reaction. Using a small quantity of POMs/HPAs instead of a stoichiometric amount of soluble Lewis acids (e.g., AlCl₃) or strong mineral acids (e.g., HF, H₂SO₄) as the catalysts in an industrial Friedel–Crafts acylation process is a promising protocol. The protocol allows the use of carboxylic acids as the acylating agents instead of acyl chlorides or acid anhydrides that are used in the present industrial processes. It has been confirmed that the activity of silica-supported H₃PW₁₂ is 100 times higher than that of H-β zeolite, in agreement with the higher acid strength of silica-supported H₃PW₁₂.⁴²² In the presence of insoluble Cs_{2.5}H_{0.5}PW₁₂, Friedel–Crafts acylation of more inert benzene with benzoic anhydride quantitatively proceeds at 423 K, producing benzophenone without a byproduct.⁴²³

With Wells–Dawson-type phosphotungstic compound H₆P₂W₁₈ as a model catalyst and acetic anhydride as the acylating reagent, Collins et al. studied the formation of acylium ion intermediate CH₃CO⁺, the accepted reactive intermediate.⁴²⁴ Both gaseous and liquid acetic anhydrides adsorb and decompose on the Brønsted acid sites of the catalyst and generate the key intermediate acyl species of CH₃CO⁺, along with acetate species and acetic acid, which remain strongly adsorbed. The acetate species observed in the gas-phase adsorption cannot be removed even at 473 K, and the molecular acetic acid adsorbed on the catalyst in the liquid medium cannot be removed after recycling of the cosolvent. We should always keep in mind that the activities of solid

catalysts in Friedel–Crafts chemistry are often deteriorated by coking and the adsorption of acylating reagent and products on the catalysts. The regeneration of the catalysts usually needs a high temperature, which may lead to a decrease of their catalytic activities resulting from the loss of acid sites.⁴²⁵ Hence, an appropriate calcining temperature is necessary in the regeneration process. In view of the relatively low thermal stability and difficult regeneration (decoking) of POM/HPA catalysts, measures should be taken to restrain the deactivation. According to Kozhevnikov's research, several approaches are instrumental.⁴²⁶ These approaches include developing new POM/HPA catalysts possessing high thermal stability, modifying POM/HPA catalysts to enhance coke combustion, inhibiting coke formation on POM/HPA catalysts during the reactions, and conducting reactions in supercritical fluids and cascade reactions using multifunctional POM/HPA catalysts.

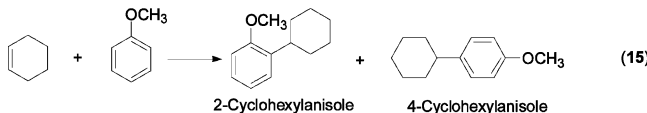
As for Fries rearrangement, Kozhevnikov's group afforded rich evidence for the available activities of various POM/HPA catalysts, such as H₃PW₁₂, Cs_{2.5}H_{0.5}PW₁₂, Ce_{0.87}H_{0.4}PW₁₂, silica-supported H₃PW₁₂, and sol–gel silica-included H₃PW₁₂.^{427–429} Being a much stronger acid, H₃PW₁₂ is almost 200 times more active than H₂SO₄ in homogeneous reactions, and more selective for acetophenones. Bulk and silica-supported H₃PW₁₂ samples act as homogeneous catalysts without solvent or in polar solvents, such as nitrobenzene and *o*-dichlorobenzene, and act as heterogeneous catalysts in nonpolar solvents such as dodecane. The Cs⁺ and Ce³⁺ salts and sol–gel silica-included H₃PW₁₂ catalysts heterogeneously perform in all these reaction media. The sol–gel silica-included H₃PW₁₂ is much less active than silica-supported H₃PW₁₂, because it has a relatively high amount of water and a weaker acid strength due to the strong interaction of the protons on H₃PW₁₂ with the silica matrix. In the presence of the sol–gel silica-included H₃PW₁₂, Fries reactions of phenyl acetate mainly give phenol with 92–100% selectivities. The best results are achieved by the homogeneous system with H₃PW₁₂ and the heterogeneous system with silica-supported H₃PW₁₂ or bulk acidic Cs_{2.5}H_{0.5}PW₁₂, but H₃PW₁₂ leaches from the silica support even in nonpolar solvents, whereas Cs_{2.5}H_{0.5}PW₁₂ is perfectly stable. As observed in Friedel–Crafts acylation, the reactions are inhibited by products adsorbed on catalysts in both homogeneous and heterogeneous systems. After reaction, 6–13 wt % coke forms for the high-porosity silica-supported H₃PW₁₂, whereas only about 2 wt % carbon forms for the low-porosity Cs_{2.5}H_{0.5}PW₁₂. In comprehensive consideration, Cs_{2.5}H_{0.5}PW₁₂ is superior to silica-supported H₃PW₁₂. The reusability of Cs_{2.5}H_{0.5}PW₁₂ can be further improved if the workup includes air calcination at 623 K, followed by steaming at 473 K. Doping Cs_{2.5}H_{0.5}PW₁₂ with Pd (ca. 2%) allows full regeneration of the catalyst activity and selectivity by air calcination and steaming.

Highly dispersed POM/HPA catalysts have larger surface areas that are beneficial to their activity. In liquid-phase Friedel–Crafts alkylation of toluene with 1-octene (eq 14),

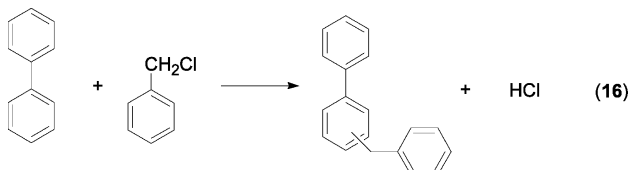


H₄SiW₁₂/MCM-41 and H₃PW₁₂/MCM-41 show much higher activities than their bulk forms.⁴³⁰ The conversion of 1-octene is nearly 100%, and the selectivity to monoalkylation products

is 99.9% after 2 h at 393 K over $\text{H}_4\text{SiW}_{12}/\text{MCM}-41$. The 2-isomer is the major product. The nanosized $\text{Cs}_{2.5}\text{H}_{0.5}\text{PW}_{12}/\text{K}-10$ particles are effective for the alkylation of anisole with cyclohexene in the liquid phase, leading to the formation of useful 2-cyclohexylanisole and 4-cyclohexylanisole (eq 15).⁴³¹



Conversion of cyclohexene is 96% after 3 h at 378 K, and no cyclohexene oligomerization is produced under the optimized reaction conditions. The selectivity for C-monoalkylation of anisole is influenced by the temperature and the amount of feedstock. The monoalkylation of biphenyl using benzyl chloride is achieved by $\text{Cs}_{2.5}\text{H}_{0.5}\text{PW}_{12}$ supported on hexagonal mesoporous silica, with 100% selectivity toward the mono-alkylated product (eq 16).⁴³² As is the case for Friedel–Crafts

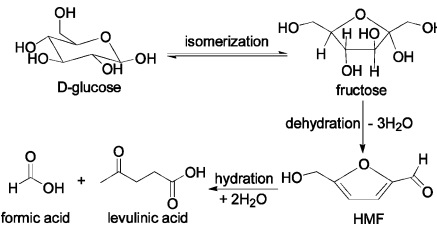


acylation and related Fries rearrangement, deactivation of catalysts often occurs in Friedel–Crafts alkylation reactions. Thus, the addition of a noble metal to POM/HPA catalysts is carried out to enhance their activities. The activity of Pt-decorated H_3PW_{12} is 8 times higher than that of H_3PW_{12} .⁴³³ The dramatically enhanced activities may be caused by the prevention of heavy aromatic coking on the catalyst surface in the presence of noble metals. Besides, Pd- or Pt-doped POM catalysts also decrease the temperature of decoking and facilitate the regeneration of the catalyst.^{415,429,434}

HPAs and their salts are attractive for intramolecular dehydration of alcohols to alkenes. Bare H_3PW_{12} and $\text{Cs}_{2.5}\text{H}_{0.5}\text{PW}_{12}$ are more active than their oxide-matrix-supported counterparts in the reaction.⁴³⁵ H_3PW_{12} and $\text{Cs}_{2.5}\text{H}_{0.5}\text{PW}_{12}$ only possess strong Brønsted acid sites, while the samples supported on TiO_2 , ZrO_2 , and Nb_2O_5 have both Brønsted and Lewis acid sites. At the superficial level, the supported samples should be more active. However, the strength of the Brønsted acid sites in supported catalysts is weaker than that in the parent H_3PW_{12} and $\text{Cs}_{2.5}\text{H}_{0.5}\text{PW}_{12}$. Thus, the activities for gas-phase 2-propanol dehydration follow the sequence $\text{H}_3\text{PW}_{12} > \text{Cs}_{2.5}\text{H}_{0.5}\text{PW}_{12} > 15\% \text{H}_3\text{PW}_{12}/\text{SiO}_2 > 15\% \text{H}_3\text{PW}_{12}/\text{TiO}_2 > 15\% \text{H}_3\text{PW}_{12}/\text{Nb}_2\text{O}_5 > 15\% \text{H}_3\text{PW}_{12}/\text{ZrO}_2$, in line with the acid strength sequence determined by NH_3 adsorption calorimetry. The interactions between supports and H_3PW_{12} increase in the sequence $\text{SiO}_2 < \text{TiO}_2 < \text{Nb}_2\text{O}_5 < \text{ZrO}_2$. The sequences indicate that the catalyst acidity decreases with an increase of the interaction between the supports and H_3PW_{12} .

The production of 5-(hydroxymethyl)furfural (HMF), the most important platform molecule in the utilization of biomass, from biomass has raised great research interest. The process involves the intramolecular dehydration of alcohols. The effectiveness of $\text{Cs}_{2.5}\text{H}_{0.5}\text{PW}_{12}$,⁴³⁶ $\text{Ag}_3\text{PW}_{12}$,⁴³⁷ and $(\text{MIMPS})_3\text{PW}_{12}$ ($\text{MIMPS} = 1\text{-[3-(sulfonic acid)propyl]-3-methylimidazolium}$)⁴³⁸ for the intramolecular dehydration of fructose or glucose to HMF has been proven. Scheme 18

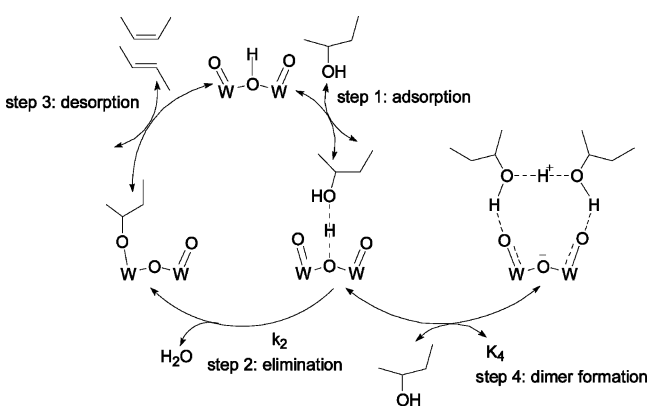
Scheme 18. Production of HMF from Glucose⁴³⁹



depicts the route of HMF production from glucose.⁴³⁹ As is seen, the whole process is catalyzed by acid, and the yield of HMF depends on the promotion of isomerization and dehydration steps and the suppression of the following hydration step. It is believed that Lewis acid sites favor the isomerization step and Brønsted acid sites favor the dehydration step. A catalyst possessing two kinds of acid sites may be effective for the process. The water-tolerant catalyst $[\text{C}_{16}\text{H}_{33}\text{N}(\text{CH}_3)_3]\text{H}_3\text{CrPW}_{11}\text{O}_{39}$ possesses both Brønsted and Lewis acid sites and hydrophobic surroundings.⁴³⁹ The dual acid sites guarantee the isomerization and dehydration of glucose into HMF. Thus, the catalyst shows activity comparable to that of H_3PW_{12} and gives a high yield of HMF in water. Notice that the hydrophobic surroundings may inhibit the hydration of HMF in the presence of water, and thus contribute to the high yield of HMF. To some extent, $[\text{C}_{16}\text{H}_{33}\text{N}(\text{CH}_3)_3]\text{H}_3\text{CrPW}_{11}\text{O}_{39}$ can be regarded as a multifunctional catalyst. On the basis of the above analysis, the aforementioned oxide-matrix-supported HPAs and their salts⁴³⁵ may also be suitable for the production of HMF from glucose or cellulose, because they have relatively strong Lewis acid sites and relatively weak Brønsted acid sites compared to their parent HPAs or salts and the strength of the acids can be tuned by varying the oxide matrixes. They can improve the yield and selectivity of HMF due to the improvement of the glucose isomerization into fructose by Lewis acid sites, the enhancement of fructose dehydration by Brønsted acid sites, and the inhibition of HMF decomposition by weaker Brønsted acid sites.

For W-based Keggin-type HPAs, $\text{H}_{8-n}\text{X}^{n+}\text{W}_{12}\text{O}_{40}$ ($\text{H}_{8-n}\text{X}^{n+}\text{W}_{12}$; X = P, Si, Al, Co), the activity of protons for alcohol dehydration is affected by the X atom. This fact is revealed by calculated deprotonation enthalpies on the basis of a rigorous analysis of elementary rate constants, using 2-butanol dehydration as a probe reaction.¹⁸ The overall reaction rates depend on the rate constant k_2 for C–O cleavage and the equilibrium constant K_4 for dimer formation (Scheme 19). Both constants increase with increasing valence of the central atom and decreasing deprotonation enthalpy. The C–O bond breaking in chemisorbed butanol monomers is the kinetically relevant step, while butanol dimers that form by solvation of adsorbed butanol with another butanol molecule are unreactive spectators. At 2-butanol pressures below 0.1 kPa, dehydration rates decrease in the sequence $\text{H}_3\text{PW}_{12} > \text{H}_4\text{SiW}_{12} > \text{H}_5\text{AlW}_{12} > \text{H}_6\text{CoW}_{12}$, whereas the trends are essentially reversed at higher pressures ($\text{H}_5\text{AlW}_{12} > \text{H}_4\text{SiW}_{12} > \text{H}_6\text{CoW}_{12} > \text{H}_3\text{PW}_{12}$). These sequences indicate that reaction rates reflect k_2 and K_4 values in a manner that leads to compensating effects and to rates that benefit from stronger acids at low butanol pressures but from weaker acids at higher pressures. The dehydration reaction proceeds through an E1 mechanism where the C–O bond is heterolytically cleaved, resulting in the formation of an ion pair consisting of a carbonium ion closely associated with an HPA anion (Scheme 19).⁴⁴⁰ At low pressures, these HPAs

Scheme 19. Proposed Pathway for 2-Butanol Dehydration over Tungsten-Based Catalysts¹⁸



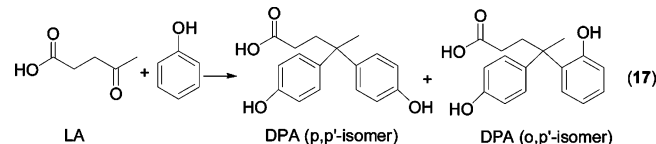
catalyze 2-butanol dehydration without detectable deactivation or structural changes. However, reaction rates sharply decrease with increasing 2-butanol pressure over all the HPA catalysts. One reason for the observation is the formation of the stable and less reactive butanol dimers.

POM/HPA catalysts also work for the isomerization of alkanes.^{441–444} The skeletal isomerization of *n*-decane has been achieved by H₃PW₁₂/SBA-15 via the formation of carbocations, accompanied by cracking.⁴⁴⁵ The HPA catalyst shows a broader optimum reaction temperature window and higher dibraning selectivity, compared to ultrastable Y zeolites. In 1999, Misono et al. reported the skeletal isomerization of *n*-pentane over Pt-promoted Cs_{2.5}H_{0.5}PW₁₂.⁴⁴⁶ The reaction proceeds in the presence of hydrogen at 453–573 K. Unpromoted Cs_{2.5}H_{0.5}PW₁₂ shows a high initial activity but rapidly deactivates. Addition of Pt greatly suppresses the deactivation and increases the selectivity for isopentane. High stationary conversion of 34.8% and selectivity of 96.9% are obtained by using Pt–Cs_{2.5}H_{0.5}PW₁₂ at a relatively low temperature of 453 K and a low hydrogen pressure of 0.05 atm. These values are significantly higher than those of Pt-promoted H-ZSM-5 or SO₄²⁻/ZrO₂. It is deduced that the remarkable effect of Pt in suppressing the catalyst deactivation is brought about by activated hydrogen, which is formed on Pt, transferred to Cs_{2.5}H_{0.5}PW₁₂, and utilized to remove carbonaceous deposits or their precursors. In 2004, Ivanov et al. reported another Pt-doped catalyst, Pt/H₃PW₁₂/ZrO₂, for alkane isomerization. It dramatically promotes *n*-hexane isomerization at 463 K, yielding isohexanes with ca. 80% yield and 96–98% selectivities.⁴⁴⁷ After being supported on ZrO₂, the grafted Keggin ions become sufficiently stable and undergo partial distortion, which should be responsible for the high reactivity. The anions in Pt/H₆P₂W₁₈/ZrO₂, Pt/H₆P₂W₂₁O₇₁/ZrO₂, and Pt/H₅ZrPW₁₁O₄₀/ZrO₂ cannot bear the distortion because of insufficient stability of parent acids in contact with a support. Therefore, they show lower catalytic activities than Pt/H₃PW₁₂/ZrO₂ at low temperature. However, these less reactive catalysts take advantage of higher selectivity due to the lower density of active sites and the inhibition of bimolecular alkylation–cracking side reactions.

Besides alkanes, α -pinene oxide,⁴⁴⁸ α -pinene,^{449,450} and longifolene⁴⁴⁹ are also isomerized to more valuable isomers in the presence of HPA catalysts. H₃PW₁₂/SiO₂ catalyzes the isomerization of α -pinene oxide into campholenic aldehyde and *trans*-carveol.⁴⁴⁸ The total selectivity for the main products (campholenic aldehyde and *trans*-carveol) reaches up to 98% at

complete conversion of α -pinene oxide, with 70% selectivity for campholenic aldehyde. The isomerizations of α -pinene and longifolene with H₃PW₁₂/SiO₂ produce camphene and isolongifolene, respectively.⁴⁴⁹ Under solvent-free conditions, the TON reaches up to 6000 per proton in the temperature range of 353–373 K, with 0.15–5 wt % catalyst loadings. In gas-phase isomerization of α -pinene, bulk H₃PW₁₂ and Cs_{2.5}H_{0.5}PW₁₂ exhibit high initial activities, but suffer from deactivation, finally resulting in low camphene yields.⁴⁵⁰ The composites of H₃PW₁₂/Nb₂O₅, H₃PW₁₂/ZrO₂, and H₃PW₁₂/TiO₂ with both Brønsted and Lewis acid sites with moderate strength show more stable performance in the reaction. The TiO₂-supported sample gives a 51% yield of camphene and a 58% total yield of camphene and limonene in a fixed-bed continuous flow reactor at 473 K and ambient pressure after 15 h.

Guo et al. have published several papers on the POM/HPA-catalyzed conversion of levulinic acid (LA), one of the top biomass platform molecules, into diphenolic acid (DPA), a valuable polymer intermediate (eq 17).^{451–454} The samples



resulting from the combination of H₃PW₁₂ with a mesoporous silica support give satisfying results.^{451,453,454} As for the Cs salts of Cs_xH_{6-x}P₂W₁₈ ($x = 1.5–6.0$), the sample with $x = 1.5$ exhibits the highest activity.⁴⁵² The activity sequence is H₆P₂W₁₈ > Cs_{1.5}H_{4.5}P₂W₁₈ > Cs_{2.0}H_{4.0}P₂W₁₈ > Cs_{2.5}H_{3.5}P₂W₁₈ > Cs_{3.5}H_{2.5}P₂W₁₈ > Cs_{4.5}H_{1.5}P₂W₁₈ > Cs_{6.0}P₂W₁₈. Obviously, the activities of Cs salts are consistent with the number of left protons. However, the case is totally different for Cs_xH_{3-x}PW₁₂, for which the activity sequence is H₃PW₁₂ > Cs_{2.5}H_{0.5}PW₁₂ > Cs_{2.0}H_{1.0}PW₁₂ > Cs_{1.5}H_{1.5}PW₁₂ > Cs_{1.0}H_{2.0}PW₁₂ > Cs_{3.0}PW₁₂. Furthermore, both the selectivity and activity of Cs_{1.5}H_{4.5}P₂W₁₈ are higher than those of Cs_{2.5}H_{0.5}PW₁₂. The authors rationalized the sequences using different mechanisms. For Cs_xH_{6-x}P₂W₁₈, pseudoliquid behavior should be considered as the governing factor of high catalytic activity and selectivity. In the case of Cs_xH_{3-x}PW₁₂ samples, a surface-type reaction is followed, in which the activity is determined by the relative number of available surface acid sites.

The protonation of chiral amines (CAs) by the protons from HPAs results in hybrids involving HPAs and chiral centers (Figure 20).⁴⁵⁵ The hybrids with a 1:1 stoichiometry of amines/polyanions, originated from the combination of **1a–1e** and **2a–2e**, are explored as recyclable and reusable enamine-

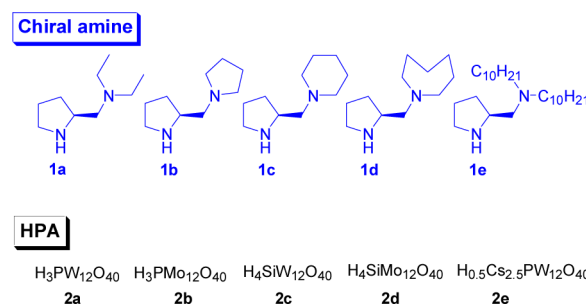
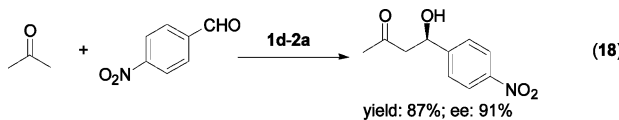
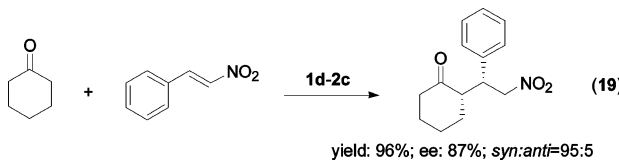


Figure 20. Components for CA–POM chiral catalysts.

type catalysts for asymmetric reactions. They perform with high activities and excellent stereoselectivities under either neat or aqueous conditions. In the asymmetric aldol reaction, H_3PW_{12} -based catalysts provide the best results in terms of both activities and enantioselectivities because of the strongest acidity. In the presence of 0.33 mol % **1d–2a**, the reaction of acetone with *p*-nitrobenzaldehyde gives an 87% yield of aldol products and 91% ee after 24 h (eq 18). When cyclohexanone

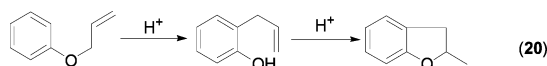


is selected as a donor, **1d–2a** gives the aldol products with 98% yield, a 97% ee value, and a 9:1 ratio of *anti*-isomer to *syn*-isomer in a shorter time. These results are better than those with the corresponding 3:1 catalyst.⁴⁵⁶ In the Michael addition reaction, **1d–2c** is the optimal catalyst. In the presence of 5 mol % **1d–2c**, the reaction between nitrostyrene and cyclohexanone in aqueous media gives products with 96% yield, an 87% ee value, and a 95:5 ratio of *syn*-isomer to *anti*-isomer (eq 19). In brief, the strategy of protonating chiral

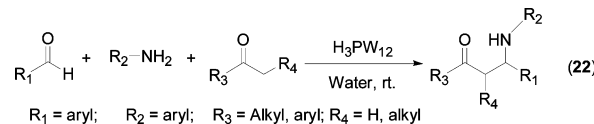


amine with HPA affords an attractive application of POM catalysts to asymmetric catalysis because of the remarkable effectiveness and easy preparation of the chiral catalysts. The immobilization of these chiral catalysts on magnetic nanoparticles protected by silica layers endows them with improved recyclability.⁴⁵⁷ The used catalyst is quickly concentrated on the side wall of the reaction vial once the magnet is placed nearby. Thus, the products can be separated by simple decantation with the assistance of a small magnet after each run.

Vinu's group found that the nanocomposite H_3PW_{12} /SBA-15/TiO₂, prepared by embedding H_3PW_{12} into the meso-channels of TiO₂-supported mesoporous SBA-15, efficiently worked in Claisen rearrangement.⁴⁵⁸ The Claisen rearrangement of allyl phenyl ether with H_3PW_{12} /SBA-15/TiO₂ provides a bicyclic compound with quantitative conversion of allyl phenyl ether and high selectivity for 2,3-dihydro-2-methylbenzofuran (eq 20).⁴⁵⁸ Similar aza-Cope rearrangement of a



nitrogen analogue is achieved by H_3PMo_{12} (eq 21).⁴⁵⁹ In the presence of pure H_3PW_{12} , the one-pot, three-component Mannich reaction of ketones with aromatic aldehydes and different amines (eq 22) efficiently proceeds in water.⁴⁶⁰ The corresponding β -aminocarbonyl compounds are given in good



to excellent yields and with moderate diastereoselectivity. Unusually, the unmodified ketones are reactive in the present protocol. H_3PW_{12} /SBA-15/TiO₂ also serves the three-component Mannich reaction.⁴⁵⁸ In the presence of H_3PW_{12} /SBA-15/TiO₂, an iminium salt is formed under slightly acidic conditions, and electrophilically attacks the enol form of the active methylene compound in the following step. The reaction of 3-chlorobenzaldehyde with aniline and acetophenone gives the target product in a yield of 98.7%, whereas with 4-bromoaniline a yield of 75% is obtained after 12 h. Benzaldehyde exhibits a lower activity than halogenated benzaldehydes. The reactions with 2,4-xylidene and *o*-hydroxyacetophenone hardly proceed due to their steric hindrance.

The simple salts $Ln(OTf)_3$ ($Ln = La, Sm, Eu, Yb$) can catalyze both Mannich-type reactions of silyl enol ethers with imines and Mukaiyama aldol reactions of silyl enol ethers with aldehydes at room temperature (Scheme 20).³⁰ When imine

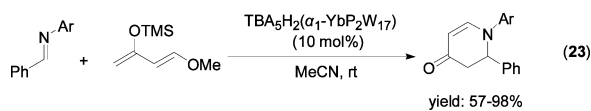
Scheme 20. Competitive Mannich Reactions and Mukaiyama Aldol Reactions in Three-Component Systems with $TBA_5H_2(\alpha_1-LnP_2W_{17})$ or $Ln(OTf)_3$ ($Ln = La, Sm, Eu, Yb$)³⁰

| | | | | | |
|--|----------------------------------|----------------|--------------|-------------|---------|
| | $TBA_5H_2(\alpha_1-YbP_2W_{17})$ | 97% , 100:0 | a : b | $Yb(OTf)_3$ | $77:23$ |
| | | | | | |
| | $TBA_5H_2(\alpha_1-SmP_2W_{17})$ | 97% , 100:0 | a : b | $Sm(OTf)_3$ | $40:60$ |
| | | | | | |
| | $TBA_5H_2(\alpha_1-LaP_2W_{17})$ | 82% , 100:0 | a : b | $La(OTf)_3$ | $95:5$ |
| | | | | | |
| | $TBA_5H_2(\alpha_1-EuP_2W_{17})$ | 96% , 100:0 | a : b | $Eu(OTf)_3$ | $36:64$ |
| | | | | | |

and aldehyde are presented in one system, the chemoselectivity for any product (a or b) is low. The combination of lanthanide ions and monovacant Dawson POM ligand $[\alpha_1-P_2W_{17}O_{61}]^{10-}$ ($\alpha_1-P_2W_{17}$) leads to a dramatically decreased Lewis acidity of active lanthanide ions. Consequently, the catalysts $TBA_5H_2[\alpha_1-Ln(H_2O)_4P_2W_{17}O_{61}]$ ($TBA_5H_2(\alpha_1-LnP_2W_{17})$) with lower Lewis acidity than $Ln(OTf)_3$ catalyze the Mannich-type reaction chemoselectively in the three-component system (Scheme 20). The reaction is supported to proceed via a Lewis acidic pathway. The Hf⁴⁺ ion with a smaller radius and more charge than the Yb³⁺ ion shows a higher Lewis acidity. Using the Hf⁴⁺ ion instead of Ln ions in $\alpha_1-LnP_2W_{17}$ yields a stronger Lewis acidic POM, $TBA_5K[\alpha_1-Hf(H_2O)_4P_2W_{17}O_{61}]$ ($TBA_5K(\alpha_1-HfP_2W_{17})$), which also effectively works in the Mannich-type reaction.⁴⁶¹ However, the mechanistic case for the Mannich reaction with $TBA_5K(\alpha_1-HfP_2W_{17})$ may be quite different. As is reported, Mannich-type reactions can be catalyzed by both a Lewis acid and a Brønsted acid. The Hf center of POMs can activate a water molecule, leading to the formation of a proton.^{462,463} Thus, the Mannich-type reaction with $TBA_5K(\alpha_1-HfP_2W_{17})$ may proceed via two different pathways, a direct Lewis acidic pathway and an indirect Brønsted acidic pathway.

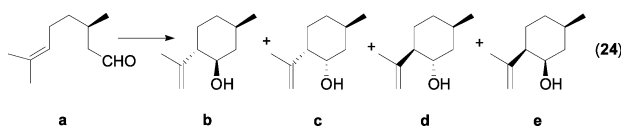
Note that the Mukaiyama aldol reaction is totally suppressed in the three-component system with $\text{TBA}_5\text{H}_2(\alpha_1\text{-LnP}_2\text{W}_{17})$ (Scheme 20).³⁰ However, the reaction readily proceeds in the presence of $\text{TBA}_5\text{K}(\alpha_1\text{-HfP}_2\text{W}_{17})$.⁴⁶¹ Superficially, the reaction may undergo a direct Lewis acidic pathway and an indirect Brønsted acidic pathway. However, it has been shown that the Yb center in $\text{TBA}_5\text{H}_2(\alpha_1\text{-YbP}_2\text{W}_{17})$ cannot activate a water molecule.⁴⁶³ The total inertia of $\text{TBA}_5\text{H}_2(\alpha_1\text{-YbP}_2\text{W}_{17})$ excludes the direct Lewis acidic pathway. In other words, the Mukaiyama aldol reaction with $\text{TBA}_5\text{K}(\alpha_1\text{-HfP}_2\text{W}_{17})$ undergoes an indirect Brønsted acidic pathway.

On the basis of the activation of imines by $\text{TBA}_5\text{H}_2(\alpha_1\text{-YbP}_2\text{W}_{17})$ in the Mannich-type reaction, $\text{TBA}_5\text{H}_2(\alpha_1\text{-YbP}_2\text{W}_{17})$ may be active for imino-Diels–Alder reaction of imines. This point is confirmed by Malacria.³⁰ With the Danishefsky diene as the nucleophile, the cyclic adducts are provided in yields of 57–98% (eq 23). Valuably, when imines and cyclic enol ethers are



used as azadienes and dienophiles, respectively, numerous multicyclic products are afforded with higher diastereoselectivity than that with $\text{Yb}(\text{OTf})_3$ (Table 14; the values in parentheses refer to the same reaction using $\text{Yb}(\text{OTf})_3$), despite the slightly lower yields compared to those with $\text{Yb}(\text{OTf})_3$.

Intramolecular cyclization of (+)-citronellal (eq 24, compound a) to (−)-isopulegol (eq 24, compound b) is another



attractive acid-catalyzed reaction, because the produced (−)-isopulegol can be readily hydrogenated to industrially important (+)-menthol. Generally speaking, the cyclization can be catalyzed by both a Brønsted acid and a Lewis acid. In the reaction, $\text{H}_3\text{PW}_{12}/\text{SiO}_2$ performs as a solid Brønsted acid,⁴⁶⁴ and Pd-doped $\text{H}_3\text{PW}_{12}/\text{SiO}_2$ acts as a bifunctional catalyst, with which (+)-citronellal is converted into menthol in one pot.⁴⁶⁵ In the latter case, the reaction proceeds via acid-catalyzed cyclization and the following Pd-catalyzed hydrogenation. With 5 wt % Pd-doped 20 wt % $\text{H}_3\text{PW}_{12}/\text{SiO}_2$, a 92% yield of menthol at 100% citronellal conversion and 85% stereoselectivity toward the desired (−)-menthol are achieved.

Compared to Brønsted acids, Lewis acids are more desirable in intramolecular cyclization of (+)-citronellal, because etherification and dehydration are often observed as side reactions in the presence of Brønsted acids.³² Zr, Hf, Al, and rare-earth ions are useful Lewis acid centers. The complexes $\text{Cs}_8\{\text{M}_4(\text{H}_2\text{O})_4(\mu_4\text{-O})(\mu\text{-OH})_6\}(\gamma\text{-SiW}_{10}\text{O}_{36})_2\}$ ($\text{Cs}_8[\text{M}_4(\gamma\text{-SiW}_{10})_2]$; M = Zr, Hf), consisting of two $\gamma\text{-SiW}_{10}$ units sandwiching distorted adamantanoid clusters $[\text{M}_4(\mu_4\text{-O})(\mu\text{-OH})_6]^{8+}$ (Figure 21a), show high catalytic activities in the reaction. With them, the cyclization of (+)-citronellal gives the corresponding isopulegol isomers in high yields. Etherification and dehydration reactions are not observed in the present cases. As shown in eq 24, the selectivity pattern of the cyclization of (+)-citronellal is very complicated because several diastereoisomers are produced in the process. However, the reactions

Table 14. $\text{TBA}_5\text{H}_2(\alpha_1\text{-YbP}_2\text{W}_{17})$ -Catalyzed Imino-Diels–Alder Reaction Using Imines as the Azadienes³⁰

| Imine | n | Product | Yield (%) | d.r. |
|-------|---|---------|-----------|---------------|
| | 1 | | 67 (80) | 60:40 (50:50) |
| | 2 | | 79 (89) | 80:20 (50:50) |
| | 1 | | 63 (74) | 90:10 (55:45) |
| | 2 | | 39 (64) | 80:20 (50:50) |
| | 1 | | 39 | 50:50 |
| | 2 | | <40 | 50:50 |
| | 1 | | 67 (48) | 50:50 (50:50) |
| | 2 | | 62 (<20) | 50:50 (50:50) |

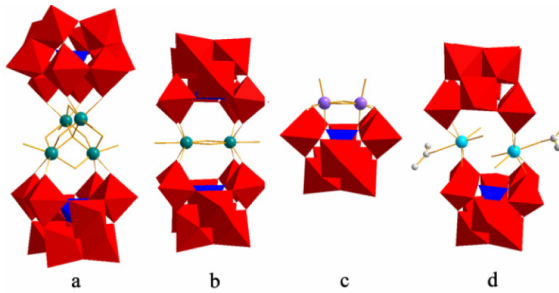


Figure 21. Structures of (a) $\text{M}_4(\gamma\text{-SiW}_{10})_2$ ($\text{M} = \text{Zr}, \text{Hf}$), (b) $\text{Cs}_{10}[\text{M}_2(\gamma\text{-SiW}_{10})_2]$ ($\text{M} = \text{Zr}, \text{Hf}$), (c) $\gamma\text{-HAl}_2\text{SiW}_{10}$, and (d) $\text{Y}_2(\text{SiW}_{10})_2$.

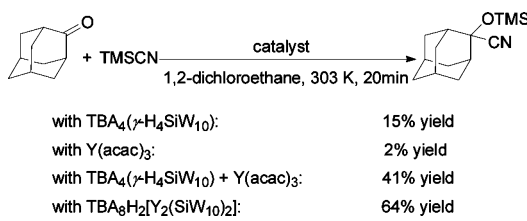
with $\text{Cs}_8[\text{M}_4(\gamma\text{-SiW}_{10})_2]$ feature high diastereoselectivity (>70%) toward (−)-isopulegol. Although there are Lewis acid sites and Brønsted acid sites in $\text{Cs}_8[\text{M}_4(\gamma\text{-SiW}_{10})_2]$, the activity is mostly contributed by Lewis acid sites, consistent with the higher diastereoselectivities with $\text{Cs}_8[\text{M}_4(\gamma\text{-SiW}_{10})_2]$ than those with Brønsted acids. The cyclization reaction hardly occurs under the same conditions with dinuclear complexes $\text{Cs}_{10}\{\text{M}_2(\text{H}_2\text{O})_2(\mu\text{-OH})_2\}(\gamma\text{-SiW}_{10}\text{O}_{36})_2\}$ ($\text{Cs}_{10}[\text{M}_2(\gamma\text{-SiW}_{10})_2]$; M = Zr, Hf), which consist of two $\gamma\text{-SiW}_{10}$ units sandwiching the bis- μ -hydroxodimetal core $[\text{M}_2(\mu\text{-OH})_2]^{6+}$ with a distorted diamond shape (Figure 21b). The ineffectiveness of $\text{Cs}_{10}[\text{M}_2(\gamma\text{-SiW}_{10})_2]$ can be explained by the inaccessibility of (+)-citronellal to the active metal centers in $\text{Cs}_{10}[\text{M}_2(\gamma$

$\text{SiW}_{10})_2$], which is caused by the steric repulsion from the $\gamma\text{-SiW}_{10}$ skeleton.

The di-Al-substituted silicotungstate $\text{TBA}_3\{\gamma\text{-H}[\text{Al}_2(\text{OH}_2)_2(\mu\text{-OH})_2]\text{SiW}_{10}\text{O}_{36}\}\cdot 4\text{H}_2\text{O}$ ($\text{TBA}_3(\gamma\text{-HAl}_2\text{SiW}_{10})$) with a $[\text{Al}_2(\mu\text{-OH})_2]^{4+}$ diamond core (Figure 21c) is even more reactive and selective than $\text{Cs}_8[\text{M}_4(\gamma\text{-SiW}_{10})_2]$ for the intramolecular diastereoselective cyclization of citronellal derivatives, even though there are less acid sites in $\text{TBA}_3(\gamma\text{-HAl}_2\text{SiW}_{10})$.³¹ Although all the three acid sites in $\text{TBA}_3(\gamma\text{-HAl}_2\text{SiW}_{10})$ (one Brønsted acid site and two Lewis acid sites) are acidic enough to readily react with pyridine to yield $\text{TBA}_3[(\text{C}_5\text{H}_5\text{N})\text{H}]\{\gamma\text{-}[\text{Al}_2(\text{C}_5\text{H}_5\text{N})_2(\mu\text{-OH})_2]\text{SiW}_{10}\text{O}_{36}\}\cdot 2\text{H}_2\text{O}$, where two of the three pyridine molecules coordinate to the axial positions of the aluminum centers and one of them exists as a pyridinium cation, the cyclization is still mainly promoted by the Lewis acid sites, just like that with $\text{Cs}_8[\text{M}_4(\gamma\text{-SiW}_{10})_2]$. For the cyclization of (+)-citronellal, the yield of the corresponding isopulegol isomers **b–e** reaches up to 93% and the diastereoselectivity toward (−)-isopulegol is 87%, compared to a 17% yield and an 80% diastereoselectivity with $\text{Cs}_8[\text{Hf}_4(\gamma\text{-SiW}_{10})_2]$ under identical conditions. DFT calculation discloses that the formation of the transition state to produce (−)-isopulegol is sterically and electronically more favorable than that of the other three transition states.

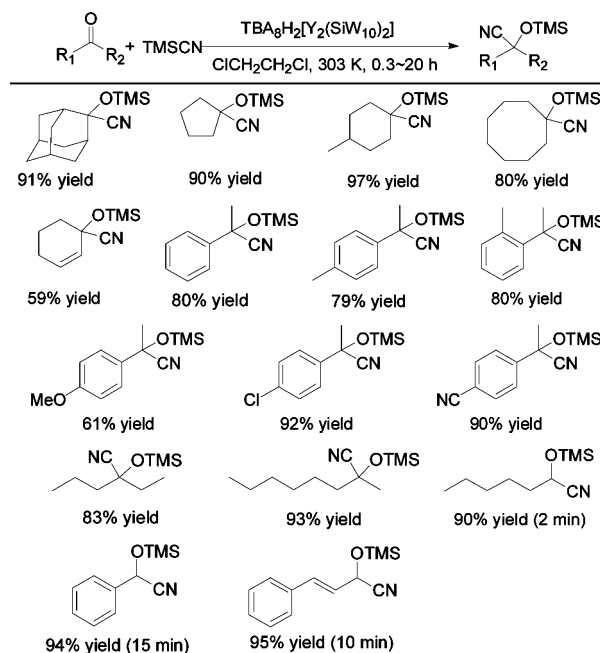
Cyanosilylation of carbonyl compounds yields cyanohydrin ether, an important intermediate to cyanohydrins.^{466,467} The reaction is typically catalyzed by acids or bases. Lewis acid catalysts can act as electrophilic sites to activate carbonyl compounds. POMs with large negative charges are expected to nucleophilically activate trimethylsilyl cyanide ((TMS)CN), one of the most useful and safe cyanating reagents. Logically, Lewis acid containing POMs serve the cyanosilylations of carbonyl compounds with (TMS)CN due to the simultaneous activation of carbonyl compounds and (TMS)CN. The yttrium-pillared silicotungstate dimer $\text{TBA}_8\text{H}_2[\text{Y}_2(\text{SiW}_{10}\text{O}_{36})_2]$ ($\text{TBA}_8\text{H}_2[\text{Y}_2(\text{SiW}_{10})_2]$) (Figure 21d) performs more actively than the sole precursors of $\text{TBA}_4(\gamma\text{-H}_4\text{SiW}_{10})$ and $\text{Y}(\text{acac})_3$ (Scheme 21).⁴⁶⁸ It readily catalyzes the cyanosilylation

Scheme 21. Activity Comparison of $\text{TBA}_8\text{H}_2[\text{Y}_2(\text{SiW}_{10})_2]$ and Its Precursors⁴⁶⁸



of aliphatic ketone, cycloalkanone, aromatic ketone, and aldehyde (Scheme 22). In all cases, ketones convert into the corresponding cyanohydrin trimethylsilyl ethers, and no desilylated products (cyanohydrins) form. The reactions show good chemoselectivity. Double C=C bonds are solid under turnover conditions. Structurally parallel aldehyde is much more reactive than ketone, because it is sterically less hindered. A TON of 18 000 and a TOF of 540 000 h^{-1} are obtained for *n*-hexanal. For cinnamaldehyde, no 1,4-addition product is observed in the cyanosilylation process. In the cyanosilylation process, the nucleophilic oxygens on the negatively charged POM surfaces work as Lewis bases to activate (TMS)CN and the incorporated Y^{3+} ions work as Lewis acids to activate the

Scheme 22. $\text{TBA}_8\text{H}_2[\text{Y}_2(\text{SiW}_{10})_2]$ -Catalyzed Cyanosilylation of Carbonyl Compounds⁴⁶⁸



carbonyl compounds. The simultaneous activation results in promoted cyanosilylation. To improve the catalytic performance of Lewis acidic metal containing POMs, rare-element cations with large ionic radii (Y^{3+} , Nd^{3+} , Eu^{3+} , Gd^{3+} , Tb^{3+} , or Dy^{3+}) are introduced into the bilacunary POM precursor $\gamma\text{-SiW}_{10}$ with large negative charges.⁴⁶⁹ The structures of all resultant POM catalysts are intrinsically identical to that of $\text{Y}_2(\text{SiW}_{10})_2$ according to Figure 21d. The activities of these catalysts increase with increasing ionic radii of the rare-element cations due to the corresponding decrease of steric hindrance. Among them, $\text{Nd}_2(\text{SiW}_{10})_2$ shows the highest activity in the cyanosilylation of various ketones and aldehydes. In particular, a TOF of 714 000 h^{-1} and a TON of 23 800 are obtained for the cyanosilylation of *n*-hexanal with $\text{Nd}_2(\text{SiW}_{10})_2$. These values are higher than that with $\text{Y}_2(\text{SiW}_{10})_2$. The enhanced performance of $\text{Nd}_2(\text{SiW}_{10})_2$ is explained by the higher Lewis acidity and less steric hindrance of Lewis acid sites.

5.2. Reactions Involving C–X Bond Formation (X = N, S)

The formation of C–X bonds (X = N, S) is relevant to the synthesis of biologically and pharmacologically active compounds. Some examples with HPA catalysts are listed in Table 15. Aminolysis of epoxides with deactivated aromatic amines in the presence of $\text{H}_3\text{PMo}_{12}$ or H_3PW_{12} affords the corresponding β -amino alcohols in moderate to excellent yields (Table 15, entry 1).⁴⁷⁰ These water-soluble strong acids allow the use of water as a green reaction medium. Aminolysis occurs at the interface of organic reactants with water. The addition of surfactants such as sodium dodecyl sulfate improves the yield of target products. In the hydroamination of ethyl acrylate with aniline, the composites $\text{H}_3\text{PW}_{12}/\text{SBA-15}/\text{TiO}_2$ show good performance (Table 15, entry 2).⁴⁵⁸ The anti-Markovnikov monoaddition product $N\text{-}[2\text{-}(ethoxycarbonyl)\text{ethyl}]$ aniline is given in a yield of almost 90% at 383 K. Neither the Markovnikov adduct $N\text{-}[1\text{-}(ethoxycarbonyl)\text{ethyl}]$ aniline nor the double-addition product $N,N\text{-bis}[2\text{-}(ethoxycarbonyl)\text{ethyl}]$ aniline is produced. $\text{H}_4\text{SiW}_{12}$ is effective for the reaction of *o*-phenylenediamines with aryl aldehydes, giving 1-methyl-2-

Table 15. Examples Involving the Formation of C–N and C–S Bonds Catalyzed by HPAs

| Entry | Materials/product | HPA |
|---------------------------|-------------------|---|
| 1 ⁴⁷⁰ | | H ₃ PW ₁₂ H ₃ PMo ₁₂ |
| 2 ⁴⁵⁸ | | H ₃ PW ₁₂ |
| 3 ⁴⁷¹ | | H ₄ SiW ₁₂ |
| 4 ⁴⁷¹ | | H ₄ SiW ₁₂ |
| 5 ⁴⁷² | | H ₃ PMo ₁₂ |
| 6 ^{473,474} 4 | | H ₃ PW ₁₂ H ₃ PMo ₁₂ H ₄ SiW ₁₂ |
| 7 ⁴⁷⁵ | | H ₃ PW ₁₂ H ₃ PMo ₁₂ H ₄ SiW ₁₂ |
| 8 ⁴⁷⁶ | | H ₃ PW ₁₂ |
| 9 ⁴⁷⁷ | | H ₃ PW ₁₂ |

(hetero)arylbenzimidazoles in yields of 52–99% in 5–60 min (Table 15, entries 3 and 4).⁴⁷¹ The expeditious processes save much time and produce various polycyclic compounds. In the presence of H₃PMo₁₂, diverse *trans*-4,5-disubstituted cyclopentenones are synthesized from furan-2-ylphenylmethanol and arylamines via aza-Piancatelli rearrangement (Table 15, entry 5).⁴⁷² For all cases, high yields (>80%) are achieved in 1 h. The three-component Dakin–West reactions with HPAs produce β -acetamido ketones (Table 15, entry 6),^{473,474} and the condensation of 1,3-dicarbonyl compound, aldehyde, and urea or thiourea gives dihydropyrimidinones (Table 15, entry 7).⁴⁷⁵ These multicomponent one-pot reactions with HPAs are attractive because of the time, energy, and raw material savings due to the absent isolation of intermediates. The formation of C–S bonds happens in the synthesis of symmetrical diaryl sulfoxides from arenes and thionyl chloride (Table 15, entry 8)⁴⁷⁶ and the synthesis of sulfides from aryl halides and thiols (Table 15, entry 9) in the presence of H₃PW₁₂.⁴⁷⁷ Both catalytic protocols are highlighted by short reaction times, high yields, ambient conditions, and simple workup.

5.3. Esterification, Hydration, and Related Reactions

5.3.1. Esterification, Transesterification, and Reversible Hydrolysis. The most common acid-catalyzed reactions with POMs/HPAs include esterification, transesterification, the related hydrolysis reactions, and hydration/dehydration reactions. Pristine HPA catalysts usually lead to homogeneous systems because of their excellent solubilities in reaction

media.⁴⁷⁸ In this case, the leaching of active components often occurs. Solid POM/HPA catalysts not only overcome the shortcomings of homogeneous HPAs, but evidently suppress the disadvantages of conventional strong mineral acids, including severe corrosivity, tedious workup, low activity, and side reactions. Therefore, recent studies on POM/HPA-catalyzed esterification mainly focus on the design of solid catalysts. Silica,^{479,480} montmorillonite clay,⁴⁸¹ MCM-41,^{482,483} Nb₂O₅,⁴⁸⁴ TiO₂,⁴⁸⁴ ZrO₂,^{484,485} and WO₃–Nb₂O₅⁴⁸⁶ are often used as staple carriers for active POMs/HPAs. The resulting solid catalysts are environmentally benign, highly effective, and easily recoverable. Parida's group intercalated molybdophosphoric acid and tungstophosphoric acid of different concentrations (5–20 wt %) in Zn–Al hydrotalcite-like compounds by indirect intercalation via the terephthalate route.⁴⁸⁷ The intercalation leads to a great increase of the basal spacing, surface area, and acid sites. The solid samples robustly catalyze the liquid-phase esterification of acetic acid using 1-butanol under autogenous conditions, which assumes commercial significance in view of the vital application of *n*-butyl acetate in the manufacture of artificial perfume, leather, photographic films, lacquer, plastic, and safety glass. Molybdophosphoric acid intercalated samples show better catalytic activity than their tungstophosphoric acid counterparts. With the highest surface area and maximum number of Brønsted acid sites, the 15 wt % molybdophosphoric acid intercalated sample exhibits the highest catalytic activity. It gives 84.15% conversion of 1-butanol and 100% selectivity for *n*-butyl acetate with a rate constant of $12.6 \times 10^{-5} \text{ s}^{-1}$.

In this energy-short age, biodiesel production from vegetable oil, animal fat, and even recycled oil from the food industry is a desirable route to develop new energy sources, because the physical properties of biodiesel are similar to those of petrodiesel and, more importantly, biodiesel is renewable, biodegradable, and nontoxic and produces low emissions. Standard biodiesel production involves the catalytic transesterification of long- or branched-chain triglycerides with short-chain alcohols.⁴⁸⁸ The traditional catalysts for this reaction are strong bases such as alkali-metal hydroxides and alkoxides.^{489–492} However, these alkaline catalysts are usually sensitive to moisture and free fatty acid, and often lead to saponification, which consumes catalysts and causes the formation of emulsions, resulting in the tedious recovery and purification of biodiesel.⁴⁹³ As a strong acid, solid HPA catalysts can efficiently catalyze the reaction and leave out the problems with alkaline catalysts. The mesoporous composite catalyst H₃PW₁₂/Ta₂O₅ works for the esterification of lauric acid and myristic acid, the transesterification of tripalmitin, and the direct use of soybean oil for biodiesel production under mild conditions.^{494,495} Its activity is higher than that of H₃PW₁₂ or Ta₂O₅ alone. The improved activity of the as-prepared composite catalyst is mainly attributed to the strong interaction of Keggin units and surface hydroxyl groups of Ta₂O₅. The same activity improvement is also observed for hydrous zirconia-supported 12-tungstophosphoric acid.⁴⁹⁶ In addition, the larger three-dimensionally interconnected pores, larger Brunauer–Emmett–Teller (BET) surface area, high porosity, and uniform pore diameter of the composite H₃PW₁₂/Ta₂O₅ as well as homogeneous dispersion of H₃PW₁₂ on the composite also play important roles in enhancing catalytic activity.⁴⁹⁴ For such a composite catalyst, the supports are pivotal for improving activity. The comparison among four different supports, including hydrous ZrO₂, SiO₂, Al₂O₃, and activated

carbon, reveals that hydrous ZrO_2 is the most appropriate support for H_3PW_{12} owing to the strong interaction of Keggin units and surface hydroxyl groups on hydrous ZrO_2 .⁴⁹⁶ In the biodiesel production from low-quality canola oil containing about 20 wt % free fatty acids, H_3PW_{12} /hydrous ZrO_2 gives the maximum ester yield of 90 wt % with a 1:9 oil to alcohol molar ratio and 3 wt % catalyst loading at 473 K.

Although $\text{H}_3\text{PW}_{12}/\text{Ta}_2\text{O}_5$ improves the activity of biodiesel production, the high affinity of $\text{H}_3\text{PW}_{12}/\text{Ta}_2\text{O}_5$ for hydrophilic species (water or glycerol) results in the strong adsorption of these species on the catalyst surface, which prevents hydrophobic reactants from accessing the acidic sites and thereby inhibiting the reactions.⁴⁹⁷ Simultaneously, deactivation occurs during the process of recycling of the catalyst. An improvement is achieved by tuning the hydrophilic–hydrophobic properties of the catalyst via the incorporation of hydrophobic alkyl groups terminally bonded on the Ta_2O_5 framework via $\text{Ta}=\text{O}-\text{Si}-\text{C}$ bonds.^{497–499} The resulting hybrid catalyst exhibits much higher catalytic reactivity for the esterification and transesterification reactions compared with $\text{H}_3\text{PW}_{12}/\text{Ta}_2\text{O}_5$. Importantly, the catalyst can be reused four times without obvious deactivation.^{498,499} Subsequently, the idea is successfully applied to $\text{H}_3\text{PW}_{12}/\text{ZrO}_2$.^{500–502}

The exchange of protons with large monovalent ions such as Cs^+ , NH_4^+ , and Ag^+ can enhance the porosity and surface area as well as the insolubility of HPA catalysts.¹ The resulting salts are expected to have higher activities and good recyclabilities, but the degree of the exchange should be moderate because protons are pivotal in acid-catalyzed reactions. For example, the partially exchanged $(\text{NH}_4)_x\text{H}_{3-x}\text{PW}_{12}$ are more active than the fully exchanged analogues.⁵⁰³ The investigation on insoluble cesium salts of $\text{Cs}_x\text{H}_{3-x}\text{PW}_{12}$ shows that those with Cs^+ content in the range $x = 2.0–2.7$ have surface areas of $\sim 100 \text{ m}^2 \text{ g}^{-1}$ and Brønsted acid strengths similar to those of the parent HPA.⁵⁰⁴ The total acid site density decreases with the Cs^+ ion exchange. Samples with Cs^+ loadings of $x = 2.0–2.3$ have the most accessible surface acid sites and show optimum performance in palmitic acid esterification and tributyrin transesterification to methyl butyrate. All samples with $x > 1$ are resistant to leaching of active components and can be recycled without obvious loss of activities. $\text{Cs}_{2.3}\text{H}_{0.7}\text{PW}_{12}$ can be used in simultaneous esterification and transesterification reactions without loss of activity or selectivity. Additionally, the effectiveness of $\text{Cs}_{2.5}\text{H}_{0.5}\text{PW}_{12}$ mitigates the harsh reaction conditions for transesterification of used vegetable oils in supercritical methanol.⁵⁰⁵

Wang's group created a clean, facile, and ecologically benign method for the biodiesel production with methanol by using insoluble $\text{Cs}_{2.5}\text{H}_{0.5}\text{PW}_{12}$.⁵⁰⁶ Environmentally compatible high-quality biodiesel fuel is produced in 99% yield from low-cost *Eruca Sativa* Gars oil (ESG oil) by using a low catalyst concentration ($(1.85 \times 10^{-3}):1$ weight ratio of catalyst to oil), a low methanol to oil ratio (5.3:1), and some cosolvent in a relatively short reaction time (45 min) at a low temperature (328 K). In the reaction, the heterogeneous catalyst $\text{Cs}_{2.5}\text{H}_{0.5}\text{PW}_{12}$ shows almost the same activity as a conventional homogeneous catalyst such as sodium hydroxide or sulfuric acid. Significant facts are that the activity of $\text{Cs}_{2.5}\text{H}_{0.5}\text{PW}_{12}$ is not considerably affected by the fatty acid content and moisture in the ESG oil, and that the catalyst is easily separated from the production mixture and can be reused six times at least. The viscosity of the resulting biodiesel is near that of diesel. The flash point is 400 K, higher than that of diesel, and the cetane

value is near that of standard biodiesel. These properties meet the ASTM (American Society for Testing and Materials) standard well. In addition, the resulting biodiesel can be stored for about 7 months without any significant change. These facts suggest that the biodiesel from unrefined ESG oil is quite suitable as a substitute for diesel.

The research on the related hydrolysis reactions mainly involves the cleavage of ester, phosphoester, and amide. Liu's group constructed a series of MOF–POM catalysts for ester hydrolysis by embodying POMs into a copper-linked MOF, which has two types of cages, A and B (Figure 22).⁵⁰⁷ These

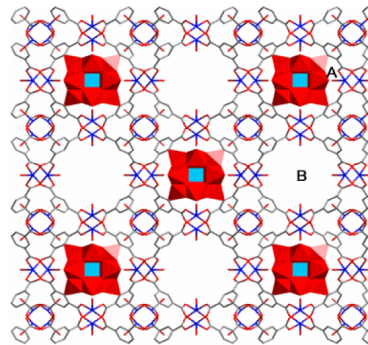


Figure 22. View of the 001 sheet with two kinds of pores, A and B, in $[\text{Cu}_2(\text{BTC})_{4/3}(\text{H}_2\text{O})_2]_6[\text{H}_n\text{XM}_{12}\text{O}_{40}] \cdot (\text{C}_4\text{H}_{12}\text{N})_2$.

crystalline compounds are denoted as $[\text{Cu}_2(\text{BTC})_{4/3}(\text{H}_2\text{O})_2]_6 \cdot (\text{H}_n\text{XM}_{12}\text{O}_{40}) \cdot (\text{C}_4\text{H}_{12}\text{N})_2$ (X = Si, Ge, P, As; M = W, Mo; BTC = benzenetricarboxylate). The catalytically active POM anions are alternately arrayed as noncoordinating guests in the cuboctahedral cages A of the Cu–BTC-based MOF host matrix. The unique contributions of the POM and well-dispersed level of POMs prohibit the conglomeration and deactivation of POMs. These MOF–POM compounds are extremely water-resistant, and have high stability and toleration of thermal and acid–base conditions. They are effective catalysts for the hydrolysis of esters in excess water, and can be used repeatedly without POM leaching or skeleton decomposition. Thus, they are regarded as true heterogeneous acid catalysts. Notably, these catalysts have a visible shape-selective effect on the substrates depending on the molecular size of the substrates and substrate accessibility to the pore surface.

Inumaru's group made another water-tolerant, highly active solid acid catalyst for the hydrolysis of ester, denoted as $\text{PW}_{12}/\text{C}_8\text{-AP-SBA}$ (Figure 23), by immobilizing H_3PW_{12} in hydro-

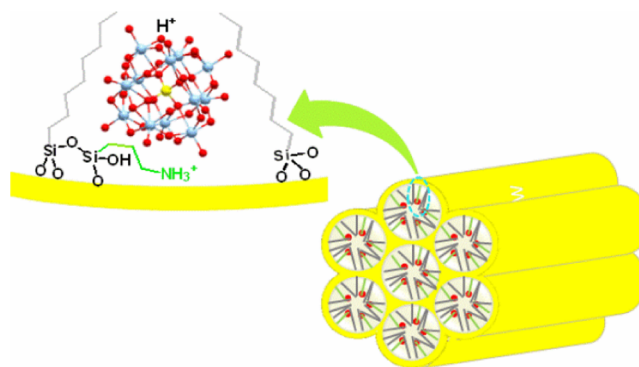
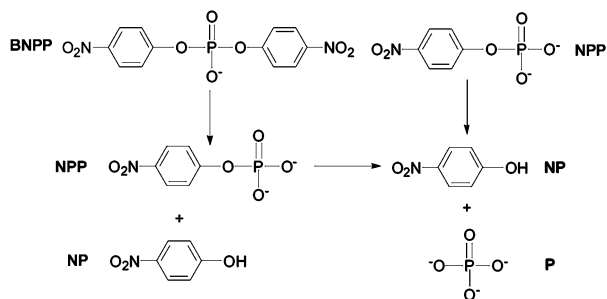


Figure 23. An illustration of $\text{PW}_{12}/\text{C}_8\text{-AP-SBA}$.

phobic nanospaces of organomodified mesoporous silica.⁵⁰⁸ They first grafted *n*-octyl and 3-aminopropyl in succession onto the pore walls of mesoporous SBA-15, then successively neutralized the amino groups with hydrochloric acid, and finally immersed the resulting material into aqueous solutions of H₃PW₁₂ to load H₃PW₁₂ into the nanospaces. As a result, the polyanions of PW₁₂ are immobilized on the pore walls by 3-ammoniopropyl groups, -(CH₂)₃NH₃⁺, leaving some portion of acidic protons on the anions, and the octyl groups create hydrophobic regions around the polyanions. In the hydrolysis reaction, water and reactant molecules penetrate into the nanospaces through the remaining spaces at the center of the SBA-15 pores. The acidic protons in the hydrophobic environment of organomodified mesoporous silica show extremely high catalytic activity for ester hydrolysis in water. The catalyst gives an activity of 275 mmol mol_{acid}⁻¹ min⁻¹ in the case of ethyl acetate hydrolysis, higher than those with hydrophobic H-ZSM-5, Cs_{2.5}H_{0.5}PW₁₂, and many other inorganic acids, and much higher than those with H₃PW₁₂ and H₂SO₄. In detail, the activity of PW₁₂/C₈-AP-SBA is 6 times higher than that of H₂SO₄ in term of per acidic proton.

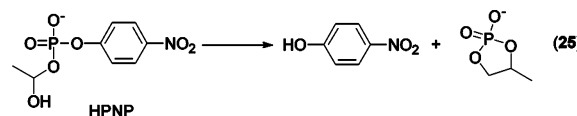
5.3.2. Hydrolysis of Phosphoester. In 2008, Parac-Vogt's group found the highly negatively charged heptamolybdate anion, [Mo₇O₂₄]⁶⁻, could efficiently catalyze the cleavage of the phosphodiester bond in bis(4-nitrophenyl) phosphate (BNPP), a commonly used DNA model substrate (Scheme 23).^{509,510}

Scheme 23. Hydrolysis of BNPP and NPP^{509,510}



The reaction rate over [Mo₇O₂₄]⁶⁻ is accelerated by nearly 4 orders of magnitude compared to the rate of uncatalyzed cleavage at pH 5.5. The cleavage of the first phosphoester bond in BNPP is much slower than that of the phosphoester bond in the initial product, 4-nitrophenyl phosphate (NPP). Concretely, the cleavage rate of the phosphoester bond in NPP is nearly 40 times faster than that of the first phosphodiester bond in BNPP under identical conditions. The pH of the reaction medium has a great effect on the hydrolysis reaction. At pH 8, where [MoO₄]²⁻ is the only derived Mo^{VI} species in solution, BNPP hydrolysis hardly occurs. Similarly, slow hydrolysis at lower pH values implies low catalytic activity of [Mo₈O₂₆]⁴⁻, which is the most abundant derived polyanion in the pH range from 2 to 4. Generally, it is believed that metal catalysts for phosphate ester hydrolysis have to meet some criteria, such as an overall positive charge, a free coordination site for the binding of phosphoryl oxygen, the presence of coordinated water or hydroxide, and the presence of functional groups for acid–base catalysis.^{511–513} From this point of view, the heptamolybdate anion [Mo₇O₂₄]⁶⁻ seems to be an unlikely catalyst for phosphate ester hydrolysis considering its high negative charge, coordination saturation, and lack of coordinated water or hydroxide, but this assumption is incompatible

with the experimental results. The most reasonable explanation is that the ester hydrolysis with [Mo₇O₂₄]⁶⁻ occurs following a mechanism different from that with other hydrolytically active metal complexes. It is proposed that the hydrolytic activity of [Mo₇O₂₄]⁶⁻ arises from its high internal lability and an intramolecular exchange that results in partial detachment of one MoO₄ tetrahedron. This detachment may allow the attachment of the structurally related phosphodiester tetrahedron into the POM structure. The incorporation of the phosphodiester group into the polyoxomolybdate skeleton and the sharing of oxygen atoms with the Mo^{VI} center may lead to bond strain and polarization of the P–O ester bond and its activation toward external attack by water. Encouraged by the excellent hydrolytic activity of [Mo₇O₂₄]⁶⁻ toward BNPP and NPP, the group investigated its hydrolytic activity toward 2-hydroxypropyl 4-nitrophenyl phosphate (HPNP), an RNA model phosphodiester.⁵¹⁴ At 323 K and pD 5.9 (pD = pH + 0.41), the cleavage of the phosphodiester bond in HPNP proceeds with a rate constant of 6.62 × 10⁻⁶ s⁻¹, giving a cyclic phosphate ester and 4-nitrophenol as the only products of hydrolysis (eq 25).



In 2010, Parac-Vogt's group reported the same reaction with polyoxovanadates, [HV₁₀O₂₈]⁵⁻, resulting from 40 mM VO₄³⁻ at pH 5.0.⁵¹⁵ Just like [Mo₇O₂₄]⁶⁻, [HV₁₀O₂₈]⁵⁻ does not possess free coordination sites, an overall positive charge, and coordinated water or hydroxide, which may act as an effective nucleophile. However, in the presence of the catalyst, the hydrolysis of the phosphoester bond in NPP at 323 K and pH 5.0 proceeds with a rate constant of 1.74 × 10⁻⁵ s⁻¹. The cleavage of the phosphoester bond in BNPP at 343 K and pH 5.0 proceeds with a rate constant of 3.32 × 10⁻⁶ s⁻¹, representing an acceleration of 4 orders of magnitude compared to the rate of the uncatalyzed cleavage. The origin of the hydrolytic activity of [HV₁₀O₂₈]⁵⁻ toward NPP and BNPP is most likely due to its high lability and its dissociation into smaller fragments, allowing the attachment of NPP and BNPP into the polyoxovanadate skeleton. Notice that the solution chemistry of vanadates highly depends on the pH and the concentration. Thus, the hydrolytic activity of [HV₁₀O₂₈]⁵⁻ is significantly affected by these parameters. In fact, the group has previously reported the hydrolytic activity of [V₄O₁₂]⁴⁻ toward HPNP.⁵¹⁶ The vanadate [V₄O₁₂]⁴⁻ is derived from VO₄³⁻ at pH 7.0. It gives a hydrolysis rate constant of (1.9 ± 0.1) × 10⁻⁶ s⁻¹ at pH 7.0 and 310 K, representing a 60-fold acceleration compared to the rate of the uncatalyzed cleavage. Here, [V₄O₁₂]⁴⁻ is the hydrolytically active species. However, the case is different for the hydrolysis of carboxyesters in a similar catalyst solution.⁵¹⁷ Although polyoxo forms of vanadate, [H₂V₂O₇]²⁻, [V₄O₁₂]⁴⁻, and [V₅O₁₅]⁵⁻, exist in the solution, the monomeric vanadate is identified as the hydrolytically active species. The origin of the hydrolytic activity of the monomeric vanadate is deduced to relate to its nucleophilic nature and the chelation by the reaction intermediate, which can lead to the stabilization of the transition state.

In 2012, the same group reported the performance of Dawson-type [M^{IV}(α_2 -P₂W₁₇O₆₁)₂]¹⁶⁻ (M(α_2 -P₂W₁₇)₂; M =

Zr, Hf) (Figure 24) for phosphoester hydrolysis.⁵¹⁸ In water, an equilibrium is formed among the 1:2 precursor $\text{Zr}(\alpha_2\text{-P}_2\text{W}_{17})_2$,

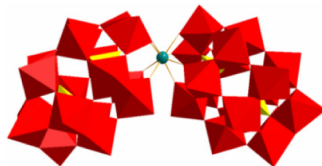
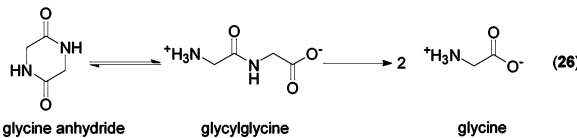


Figure 24. Structure of $\text{M}(\alpha_2\text{-P}_2\text{W}_{17})_2$ ($\text{M} = \text{Zr}, \text{Hf}$).

the monosubstituted 1:1 $\text{Zr}(\text{H}_2\text{O})_3(\alpha_2\text{-P}_2\text{W}_{17})$, species and the 2:2 $[\text{Zr}(\mu\text{-OH})(\text{H}_2\text{O})_2(\alpha_2\text{-P}_2\text{W}_{17})]_2$ dimer. The equilibrium depends on the pD, temperature, and concentration.^{519–521} Among these Zr-containing POMs, the 1:1 monomer is the hydrolytically active compound, while the 1:2 precursor $\text{Zr}(\alpha_2\text{-P}_2\text{W}_{17})_2$ is catalytically inert due to the lack of a labile water ligand. Thus, the reaction rate is proportional to the amount of the 1:1 monosubstituted Zr^{IV} -POM in the solution and faster in acidic conditions. An NPP hydrolysis rate constant of $7.71 \times 10^{-4} \text{ min}^{-1}$ ($t_{1/2} = 15 \text{ h}$) is obtained at pD 7.2 and 323 K, representing a rate enhancement of nearly 2 orders of magnitude in comparison with the rate of the spontaneous hydrolysis of NPP. In addition, the hydrolysis of more inert phenyl phosphate (PP) and BNPP readily proceeds over $\text{Zr}(\alpha_2\text{-P}_2\text{W}_{17})_2$. The catalyst $\text{Hf}(\alpha_2\text{-P}_2\text{W}_{17})_2$ with similar coordination chemistry even exhibits higher activity than $\text{Zr}(\alpha_2\text{-P}_2\text{W}_{17})_2$.

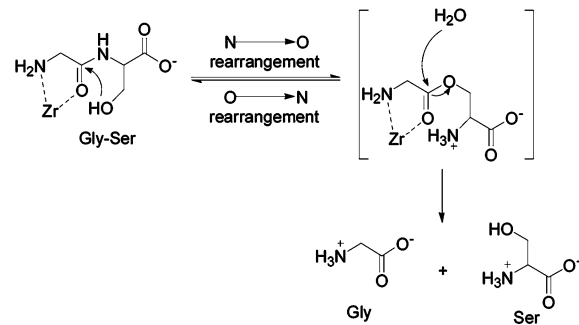
5.3.3. Hydrolysis of Peptides. Apart from the hydrolysis of the phosphoester, the 1:2 precursors $\text{M}(\alpha_2\text{-P}_2\text{W}_{17})_2$ ($\text{M} = \text{Zr}, \text{Hf}$) also serve peptide hydrolysis, which is important in biotechnology and modern proteomics.⁵²² It has been reported that the effective metal catalysts for peptide hydrolysis have to hold at least two free coordination sites on the metal center: one for the attachment of the peptide and the other for the internal delivery of a water molecule that acts as a nucleophile.⁵²³ The first-row TMs ($\text{Mn}^{\text{III}}, \text{Fe}^{\text{III}}, \text{Co}^{\text{II}}, \text{Ni}^{\text{II}}, \text{Cu}^{\text{II}}$) in monosubstituted Wells–Dawson POMs are in a 6-fold octahedral coordination environment where the basic POM unit acts as a pentadentate ligand and the sixth coordination site is occupied by water. Thus, these $\text{Mn}^{\text{III}}\text{-}, \text{Fe}^{\text{III}}\text{-}, \text{Co}^{\text{II}}\text{-}, \text{Ni}^{\text{II}}\text{-}, \text{Cu}^{\text{II}}$ -substituted Wells–Dawson POM catalysts lack reactivity. Although rare-earth ions $\text{Y}^{\text{III}}, \text{La}^{\text{III}}, \text{Eu}^{\text{III}}$, and Yb^{III} in Wells–Dawson POMs have more free coordination sites around the metal ions, the POM catalysts also show low activity toward peptide hydrolysis due to the decreased Lewis acidity of the rare-earth ions resulting from incorporation into the POM structure³⁰ or the formation of dimeric POM species in solution.⁵²⁴ However, the analogous Zr^{IV} - and Hf^{IV} -substituted Wells–Dawson POMs $\text{Zr}(\alpha_2\text{-P}_2\text{W}_{17})_2$ and $\text{Hf}(\alpha_2\text{-P}_2\text{W}_{17})_2$ show excellent performance in the hydrolysis of the highly inert peptide bond in glycylglycine (eq 26), yielding glycine as the



final product. In fact, the use of $\text{Zr}(\alpha_2\text{-P}_2\text{W}_{17})_2$ has been extended to many other dipeptides.⁵²⁵ The results elucidated that the hydrolysis rate is significantly influenced by the size and the nature of the amino acid side chain. Summarily, the hydrophobic aliphatic side chains and the carbonyl groups on

the side chains hinder the hydrolysis process, and the hydroxyl groups on the side chains accelerate the process. Rich free coordination sites on the derived 1:1 catalytic species $\text{Zr}(\text{H}_2\text{O})_3(\alpha_2\text{-P}_2\text{W}_{17})$ provide the substrates with an ample chance of interacting with the catalyst.⁴⁶² The reaction happens through the coordination of peptide to the Zr^{IV} center in $\text{Zr}(\alpha_2\text{-P}_2\text{W}_{17})_2$ via its N-terminal amine group and amide carbonyl oxygen (Scheme 24).⁵²² The coordination of the amide

Scheme 24. Hydrolysis of Glycylserine with the Aid of a Hydroxyl Group in the Presence of a Zr-Containing POM Catalyst⁵²⁶



carbonyl leads to Lewis acid activation of the amide bond and makes it more susceptible toward nucleophilic attack by water. The coordination of the N-terminal amine group also appears very essential for the effective attachment of the peptide. These findings are confirmed by the inactivity of $\text{Zr}(\alpha_2\text{-P}_2\text{W}_{17})_2$ toward the N-blocked analogue acetamidoglycylglycine and the inhibitory effect of oxalic, malic, and citric acid. The hydroxyl groups on the side chains may promote a $\text{N} \rightarrow \text{O}$ acyl rearrangement (Scheme 24), and accordingly accelerate the reaction, while the carboxylate groups on the side chains competitively coordinate to Zr^{IV} , thus preventing the coordination of peptide carbonyl groups and encumbering the hydrolysis reaction.⁵²⁵

The dimeric Keggin-type POM $(\text{Et}_2\text{NH}_2)_8\{[\alpha\text{-Zr}(\mu\text{-OH})(\text{H}_2\text{O})\text{PW}_{11}\text{O}_{39}]_2\}$ also significantly accelerates the hydrolysis of peptides.⁵²⁶ The hydrolysis rate constants for glycylserine and glycylglycine at pD 5.4 and 333 K are 63.3×10^{-7} and $4.44 \times 10^{-7} \text{ s}^{-1}$, respectively. These values are affected by the temperature, pH, inhibitors, and ionic strength. The polarization of the amide oxygen caused by its binding to the Zr^{IV} center and the intramolecular attack of the hydroxyl group on the amide carbonyl carbon are responsible for the rapid hydrolysis of glycylserine. The highest activity of the catalyst appears at pD 5.5–6.0, where no catalyst dissociation occurs. The species distribution of the catalyst is more controllable, and thereby allows a more profound mechanistic study when compared to that for $\text{Zr}(\alpha_2\text{-P}_2\text{W}_{17})_2$, which is typically characterized by multiple equilibria at pD 5.5–6.0. At higher pD values, the catalyst develops into $[\text{Zr}(\alpha\text{-PW}_{11}\text{O}_{39})_2]^{10-}$, which is sluggish for the hydrolysis reaction due to the saturated coordination of the Zr^{IV} center. However, if the Zr^{IV} center in $[\text{Zr}(\alpha\text{-PW}_{11}\text{O}_{39})_2]^{10-}$ is substituted by Ce^{IV} with more coordination sites, the resulting POM $[\text{Ce}(\alpha\text{-PW}_{11}\text{O}_{39})_2]^{10-}$ works smoothly for the hydrolysis reaction.⁵²⁷

Although Zr-containing POMs $\text{Zr}(\alpha_2\text{-P}_2\text{W}_{17})_2$ and $[\{\alpha\text{-Zr}(\mu\text{-OH})(\text{H}_2\text{O})\text{PW}_{11}\text{O}_{39}\}_2]^{8-}$ show good performance under acidic conditions, they are sluggish at higher pD values. At neutral pD values, the two catalysts develop into inactive 1:2 species, and

hence, their application to peptide bond hydrolysis under physiological conditions is limited. Another Zr-containing POM, Lindqvist-type (Me_4N)₂[Zr(H₂O)₃W₅O₁₈], can promote the hydrolysis of a series of unactivated dipeptides at physiological pH.⁵²⁸ For histidylserine, a hydrolysis rate constant of $(95.3 \pm 0.1) \times 10^{-7} \text{ s}^{-1}$ is obtained at pH 7.4 and 333 K. The free coordination sites and labile water ligands on the Zr^{IV} center allow the cooperative chelation of histidylserine with Zr^{IV} via its imidazole nitrogen, amine nitrogen, and amide carbonyl oxygen. Standing on the excellent performance of [Zr(H₂O)₃W₅O₁₈]²⁻ at physiological conditions, it is expected to represent a class of novel artificial metalloproteases.

According to available reports, the activation of a water molecule by Zr/Hf may occur during the hydrolysis processes of a phosphoester and peptide with Zr/Hf-POMs.^{462,463} Although Zr/Hf is assigned as the active site in these reactions, the effect of protons cannot be excluded under acidic or neutral conditions.

5.3.4. Other Hydrolysis and Reversible Dehydration Reactions.

The popular project of biomass conversion also involves hydrolysis reaction. HPAs H₃PW₁₂ and H₄SiW₁₂ and their polyvalent metal salts have been used for the hydrolysis of cellobiose and cellulose.⁵²⁹ H₃PW₁₂ and H₄SiW₁₂ show good performance due to their strong Brønsted acidity. The polyvalent metal salts M_{3/n}PW₁₂ hold potential Lewis acidity and Brønsted acidity, originating from the capacity of M to accept one or more electrons and the dissociation of coordinated water under the polarizing effect of the cation, respectively.^{530,531} The identity of M has a great influence on the activity and selectivity of the hydrolysis reaction due to the special acidities of the metals. Among 11 metal ions, Ag⁺, Ca²⁺, Co²⁺, Y³⁺, Sn⁴⁺, Sc³⁺, Ru³⁺, Fe³⁺, Hf⁴⁺, Ga³⁺, and Al³⁺, Sn⁴⁺ and Ru³⁺ with moderate Lewis acidity give the highest hydrolysis rates.

Hydration of unsaturated compounds^{20,532} and intermolecular dehydration of alcohols⁵³³ are classical acid-catalyzed reactions and can be conducted over POM/HPA catalysts. In the case of the hydration of unsaturated bonds to alcohols, an industrially important reaction, the technique with HPA catalysts is full-fledged, particularly for the hydration of C₃–C₄ alkenes. In 2012, Mizuno et al. applied a monomeric di-Pd-substituted γ -Keggin POM catalyst, TBA₄[γ -H₂Pd₂(OAc)₂SiW₁₀O₃₆]²⁻ (TBA₄(γ -H₂Pd₂SiW₁₀)), to the hydration of nitriles, the main route to manufacture amides.⁵³⁴ Two Pd atoms of the catalyst are incorporated into the lacunary sites of γ -H₂Pd₂SiW₁₀ and bridged by two bidentate acetate ligands (Figure 25). In the presence of TBA₄(γ -H₂Pd₂SiW₁₀), the hydration of structurally diverse nitriles, including aromatic, aliphatic, heteroaromatic, and double-bond-containing ones, proceeds smoothly. After 5–48 h, excellent yields are obtained for all the tested substrates (Scheme 25). The high activity of TBA₄(γ -H₂Pd₂SiW₁₀) is caused by the cooperative activation of nitriles and water by the dipalladium sites on the rigid POM skeleton. Notably, the hydrations of heteroaromatic nitriles readily yield the corresponding amides in the present system, while the reaction rates were lower than those of common nitriles due to the strong coordination of heteroatoms on the ring to the metal centers.

After that, the reversible dehydration of primary amides to nitriles was also realized by the same group, with monovacant TBA₄(α -H₄SiW₁₁O₃₉) as the catalyst.⁵³⁵ The system is characterized by the absence of water scavengers and the

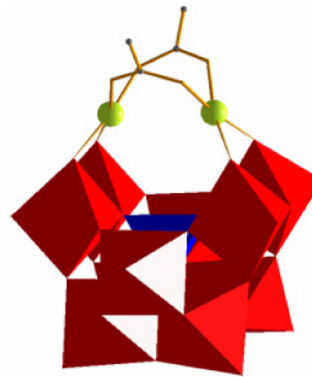
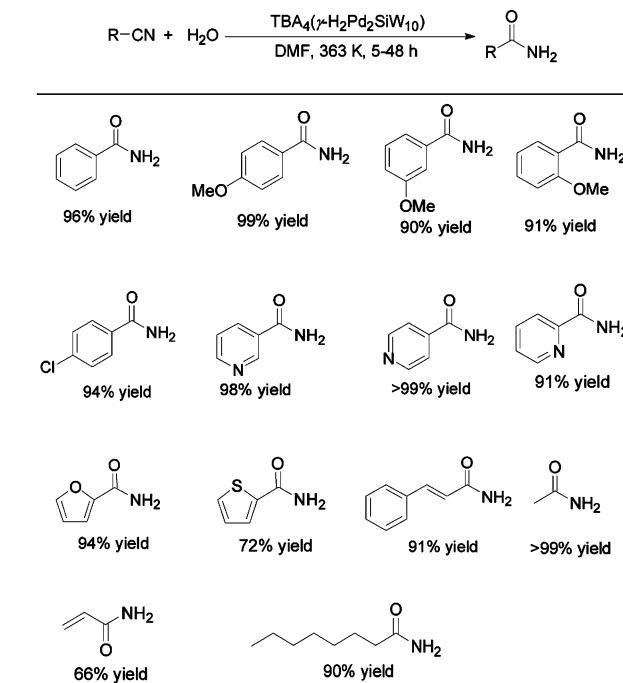


Figure 25. Structure of γ -H₂Pd₂SiW₁₀.

Scheme 25. Hydration of Various Nitriles with TBA₄(γ -H₂Pd₂SiW₁₀)⁵³⁴

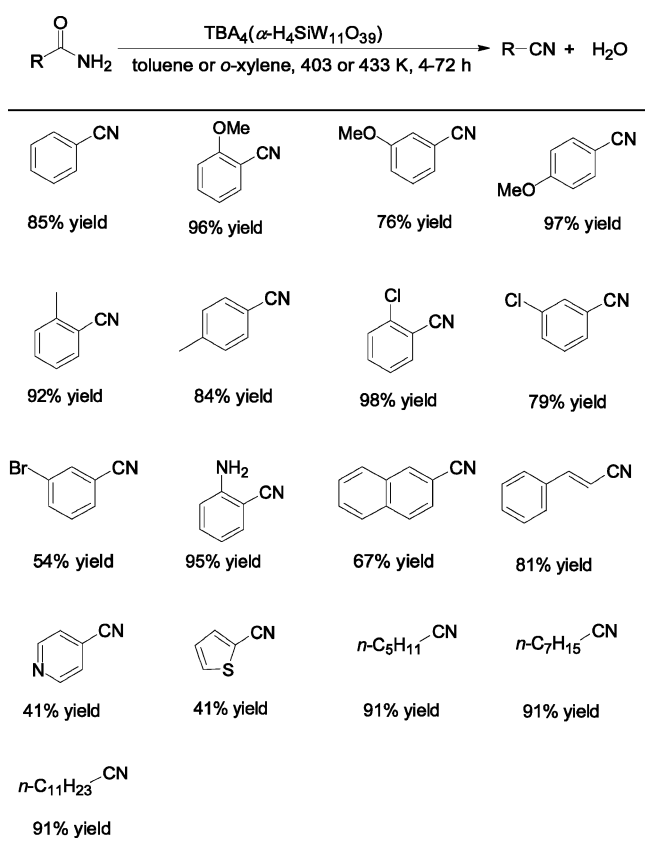


high atom efficiency. Several nitriles are obtained with moderate to high yields (Scheme 26). The dehydration of *o*-methylbenzamide efficiently proceeds with 0.5 mol % TBA₄(α -H₄SiW₁₁O₃₉) at 433 K (bath temperature) in *o*-xylene, giving a 92% yield of the corresponding nitrile. In this case, the TOF is 46 h⁻¹ and the TON is 184, the highest levels among the previously reported catalysts for dehydration without non-renewable water scavengers. Additionally, the double bond of cinnamamide is unaffected. No isomerization and hydration happen on it.

6. BASE CATALYSIS

In the past few years, researchers have paid much attention to the redox activity and acidity of POM/HPA compounds in catalysis. The basicity of these compounds has been less explored for catalysis. In fact, some HPAs/POMs are efficient basic catalysts if they are stripped of protons and put in an organic solvent. Recently, the applications of POM catalysts to base-catalyzed reactions have been reported. Lacunary POMs receive more attention in this subfield. Highly charged POM

Scheme 26. Dehydration of Primary Amides to Nitriles with $\text{TBA}_4(\alpha\text{-H}_4\text{SiW}_{11}\text{O}_{39})^{535}$



anions have electron-rich oxygen atoms on their surfaces. These oxygen atoms can act as basic active sites to attack the electrophiles. As mentioned before, lacunary POMs, especially $\gamma\text{-SiW}_{10}$, have been utilized to construct metal-substituted clusters. In fact, the oxo ligands at the vacant sites are basic enough to react with not only metal cations but also active H^+ . Moreover, the negative charge of the lacunary POM can be increased by introducing more lacunary sites. The higher negative charge makes the oxygen atoms at lacunary sites more basic. Thus, these lacunary POMs can be used as basic catalysts, and their basicity can be adjusted.

The divacant POM $\gamma\text{-H}_4\text{SiW}_{10}$ undergoes dehydrative condensation, forming two structurally different dimers in different pH surroundings, the S-shaped dimer ($\gamma\text{-H}_4\text{SiW}_{10})_2(\mu\text{-O})_2$ (formed in H^+ -equipped solution) and the closed dimer ($\gamma\text{-SiW}_{10})_2(\mu\text{-O})_4$ (formed in neutral solution) (Figure 14). As previously mentioned, the S-shaped cluster with more aquo ligands can catalyze the Baeyer–Villiger oxidation of cycloalkanones to lactones, while the monomer $\gamma\text{-H}_4\text{SiW}_{10}$ and the closed dimer are almost inactive, although all three compounds share a common $[\gamma\text{-SiW}_{10}\text{O}_{32}]$ unit.³⁰² The same trend is also observed for the Mukaiyama aldol reaction, the intramolecular cyclization of (*R*)-(+)-citronellal, and the Diels–Alder reaction.⁵³⁶ However, a reversed trend is observed for Knoevenagel condensation (typically catalyzed by a weak base) and the cyanosilylation reaction (typically catalyzed by an acid or a base). Monomeric $\gamma\text{-H}_4\text{SiW}_{10}$ and the closed dimeric ($\gamma\text{-SiW}_{10})_2(\mu\text{-O})_4$ promote the two reactions as basic catalysts, whereas the S-shaped dimer is almost inactive for Knoevenagel condensation and decomposed in the cyanosilylation reaction (Table 16). The different trends for the above reactions can be

Table 16. Activities of $\gamma\text{-H}_4\text{SiW}_{10}$ and Its Two Dimers for Knoevenagel Condensation and the Cyanosilylation Reaction⁵³⁶

| catalyst (concn, mol %) | reaction | yield (%) | (a) |
|---|----------|-----------|-----|
| | | | (b) |
| $\gamma\text{-H}_4\text{SiW}_{10}$ (0.5) | a | 90 | |
| $(\gamma\text{-H}_4\text{SiW}_{10})_2(\mu\text{-O})_2$ (0.25) | a | trace | |
| $(\gamma\text{-SiW}_{10})_2(\mu\text{-O})_4$ (0.25) | a | 96 | |
| $\gamma\text{-H}_4\text{SiW}_{10}$ (1) | b | 30 | |
| $(\gamma\text{-SiW}_{10})_2(\mu\text{-O})_4$ (0.5) | b | 24 | |

explained as follows: the S-shaped dimer has more aquo ligands and more protons, which increase the acidity of the catalysts, facilitating oxidation reactions and acid-catalyzed reactions, while monomeric $\gamma\text{-H}_4\text{SiW}_{10}$ and closed $(\gamma\text{-SiW}_{10})_2(\mu\text{-O})_4$ with less protons exhibit rather basic properties. In Knoevenagel condensation, the latter can abstract protons from the activated methylene moiety and resultantly promote the reaction. In the cyanosilylation reaction, they can activate (TMS)CN. However, $\gamma\text{-H}_4\text{SiW}_{10}$ and $(\gamma\text{-SiW}_{10})_2(\mu\text{-O})_4$ are much less active for the cyanosilylation reaction than for the Knoevenagel reaction. This may be related to the basicity and the bulky environment of the basic sites on $\gamma\text{-H}_4\text{SiW}_{10}$ and $(\gamma\text{-SiW}_{10})_2(\mu\text{-O})_4$.

Compared with $\gamma\text{-H}_4\text{SiW}_{10}$, the more highly negatively charged POM $[\gamma\text{-H}_2\text{GeW}_{10}\text{O}_{36}]^{6-}$ ($\gamma\text{-H}_2\text{GeW}_{10}$) exhibits better catalytic performance for Knoevenagel reactions of a wide range of substrates, including unreactive phenylacetonitrile and ketones (Table 17).⁵³⁷ The nonprotonated lacunary oxygen atoms in $\gamma\text{-H}_2\text{GeW}_{10}$ are regarded as active sites that abstract protons from donating substrates. For most cases, the reactions readily proceed at 305 K in the presence of $\text{TBA}_6(\gamma\text{-H}_2\text{GeW}_{10})$. As for unreactive phenylacetonitrile with a higher pK_a value of 21.9, it is transferred into α -phenylcinnamonnitrile in 96% yield at 353 K, while large amounts of strong bases such as NaOH (≥ 10 mol %) or higher reaction temperatures (383–453 K) are usually required to attain high yields. A substituted 4H-chromene derivative is produced in 82% yield by the reaction of malononitrile with salicylaldehyde. As a basic catalyst, $\text{TBA}_6(\gamma\text{-H}_2\text{GeW}_{10})$ is also active for the cyanosilylation of carbonyl compounds using (TMS)CN. The reaction of hexanal gives the corresponding cyanohydrin trimethylsilyl ether in 95% yield under the conditions of 1 min, 0.01 mol % $\text{TBA}_6(\gamma\text{-H}_2\text{GeW}_{10})$ loading, and 298 K. In this case, the TOF is 572 000 h^{-1} and the TON is 9530. Even the unreactive acetophenone can be quantitatively converted into the target product in the presence of $\text{TBA}_6(\gamma\text{-H}_2\text{GeW}_{10})$. These results indicate that the activity of basic $\text{TBA}_6(\gamma\text{-H}_2\text{GeW}_{10})$ is much higher than that of bifunctional $\text{TBA}_8\text{H}_2[\text{Y}_2(\text{SiW}_{10})_2]$ for the cyanosilylation of carbonyl compounds, although the latter simultaneously activates carbonyl compounds and cyanating reagents.⁴⁶⁸

7. OTHER REACTIONS

The diversity of TMs that can be introduced into POMs means that POMs can promote other reactions besides the aforementioned examples. In fact, some attempts have been made by scientists, and encouraging results are achieved. These

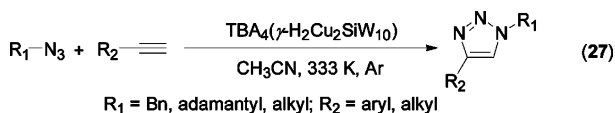
Table 17. $TBA_6(\gamma\text{-H}_2\text{GeW}_{10})$ -Catalyzed Knoevenagel Condensation⁵³⁷

| Donor | Acceptor | Product | Yield (%) |
|--------------------------------------|----------|---------|-----------|
| $\text{NC}-\text{CH}_2-\text{COOEt}$ | | | 98 |
| $\text{NC}-\text{CH}_2-\text{CN}$ | | | 99 |
| $\text{NC}-\text{CH}_2-\text{Ph}$ | | | 96 |
| $\text{NC}-\text{CH}_2-\text{COOEt}$ | | | 92 |
| | | | 97 |
| | | | 82 |
| | | | 60 |
| | | | 99 |
| | | | 72 |
| | | | 86 |
| $\text{NC}-\text{CH}_2-\text{CN}$ | | | 82 |

results will impel scientists to develop more reactions catalyzed by POMs. There is a large fallow domain to be developed.

7.1. Cycloaddition of Organic Azides

The monomeric di-Cu-substituted POM $TBA_4(\gamma\text{-H}_2\text{Cu}_2\text{SiW}_{10})$ is a charming catalyst candidate for Cu-catalyzed reactions due to the lability of the bridging azido groups. Apart from the aforementioned oxidative homocoupling of alkynes (section 2.12), it is also competent for other reactions. In 2008, its robustness for regioselective 1,3-dipolar cycloaddition of organic azides to alkynes (eq 27) was reported by Mizuno's



group.³⁴ Several 1,2,3-triazole derivatives are synthesized in excellent yields (80–98%) through the reaction. No additives such as reducing agents and nitrogen bases are needed. A 100 mmol scale reaction of benzyl azide with phenylacetylene under solvent-free conditions produces 21.5 g of the analytically pure corresponding triazole. In this case, the TOF and the TON reach up to $14\ 800 \text{ h}^{-1}$ and 91 500, respectively, and these values are remarkable in copper-mediated systems. In the previous reports, nearly all the copper catalysts for 1,3-dipolar cycloaddition were mononuclear. $TBA_4(\gamma\text{-H}_2\text{Cu}_2\text{SiW}_{10})$ is the first dinuclear copper catalyst for this reaction. Its activity is

much higher than that of many mononuclear copper catalysts. Besides, $TBA_4(\gamma\text{-H}_2\text{Cu}_2\text{SiW}_{10})$ has the advantage of reuse over traditional copper salts. Notably, the one-pot synthesis of triazole from a halide, sodium azide, and an alkyne can be realized in the presence of $TBA_4(\gamma\text{-H}_2\text{Cu}_2\text{SiW}_{10})$. 1-Benzyl-4-phenyl-1*H*-1,2,3-triazole is isolated in 72% yield from the reaction of benzyl chloride with sodium azide and phenylacetylene.

7.2. Cyclopropanation of Alkenes

The high oxidation state metal–oxo function can be electronically stabilized by adjusting the fine balance of the π -donor oxo ligands and the π -acceptor metallic backbone. Accordingly, oxygen transfer by TM-substituted POMs has been extensively illustrated. Similarly, other groups such as carbene or nitrene should also be transferred by POM catalysts. In 2010, Gallo et al. reported the transfer of carbene from ethyl diazoacetate to alkenes in the presence of Keggin-type $TBA_4(\gamma\text{-H}_2\text{Cu}_2\text{SiW}_{10})$ or Krebs-type $\text{Na}_{10}[\text{Co}_2(\text{H}_2\text{O})_6\text{Bi}_2\text{W}_{20}\text{O}_{70}]$, affording cyclopropanes, important building blocks in organic synthesis due to the high reactivity of the three-membered ring.³⁵ The results are listed in Scheme 27. In general, the product yields with

Scheme 27. Cyclopropanation Reactions of Alkenes Catalyzed by (a) $\text{Na}_{10}[\text{Co}_2(\text{H}_2\text{O})_6\text{Bi}_2\text{W}_{20}\text{O}_{70}]$ or (b) $TBA_4(\gamma\text{-H}_2\text{Cu}_2\text{SiW}_{10})$ ³⁵

| | | |
|-----------------------------------|-----------------------------------|--|
| $\text{R}_1=\text{R}_2=\text{Ph}$ | $\text{R}_1=\text{R}_2=\text{Cl}$ | $\text{R}_1=\text{R}_2=\text{C}_6\text{H}_4-\text{NH}_2$ |
| | | |
| yield a: 58% b: 90% | yield a: 74% b: 94% | yield a: 72% b: 95% |
| $cis/trans$ 28 : 72 49 : 51 | $cis/trans$ 32 : 68 49 : 51 | |
| | | |
| yield a: 40% b: 80% | yield a: 70% b: 98% | yield a: 67% b: 98% |
| $cis/trans$ 26 : 74 34 : 66 | $cis/trans$ 38 : 62 38 : 62 | $cis/trans$ 38 : 62 31 : 69 |
| | | |
| yield a: 25% b: 33% | yield a: 37% b: 63% | yield a: 35 : 65 b: 44 : 56 |
| $cis/trans$ 35 : 65 44 : 56 | | |

$TBA_4(\gamma\text{-H}_2\text{Cu}_2\text{SiW}_{10})$ are higher than those with $\text{Na}_{10}[\text{Co}_2(\text{H}_2\text{O})_6\text{Bi}_2\text{W}_{20}\text{O}_{70}]$. In the presence of $TBA_4(\gamma\text{-H}_2\text{Cu}_2\text{SiW}_{10})$, the reaction of α -methylstyrene with ethyl diazoacetate even provides a TON as high as 100 000. However, $\text{Na}_{10}[\text{Co}_2(\text{H}_2\text{O})_6\text{Bi}_2\text{W}_{20}\text{O}_{70}]$ provides slightly better diastereoselectivities. The steric hindrance around the double bond of the alkene does not significantly affect the yield. The cyclopropanations of dienes give the desired products in relatively low yields, but the reaction of 2,5-dimethyl-2,4-hexadiene provides an important precursor to the synthesis of chrysanthemic acid, a pyrethroid compound employed as a household insecticide. Other POM catalysts, such as $[\text{M}(\text{OH}_2)\text{PW}_{11}\text{O}_{39}]^{5-}$ ($\text{M} = \text{Co}^{2+}, \text{Cu}^{2+}$), also work for the reaction, but with lower activities.

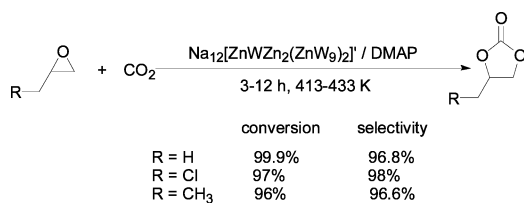
7.3. Cycloaddition of CO₂ to Epoxides

As described in section 3, CO₂ can be captured by substituting TMs in POM anions and subsequently reduced under the irradiation of light. Another promising technology for the further utilization of CO₂ is its reactions with epoxides to produce cyclic carbonates.

The reaction of CO₂ with propylene oxide or ethylene oxide is investigated in PEG, in the presence of $(n\text{-Bu}_4\text{N})_6[\alpha_2\text{-}(\text{Co-Br})\text{P}_2\text{W}_{17}\text{O}_{61}]$ and $n\text{-Bu}_4\text{NBr}$.⁵³⁸ In the present system, propylene carbonate or ethylene carbonate is produced with over 98% yield and 100% selectivity within 1 h at 393 K. The deduced mechanism indicates that the POM anion activates CO₂ while the Br⁻ dissociated from $n\text{-Bu}_4\text{NBr}$ nucleophilically attacks the carbon atom of an epoxide, resulting in the formation of an oxyanion species that eventually gives the target product. The synergistic effect is also observed for $[(n\text{-C}_7\text{H}_{15})_4\text{N}]_8[\text{CrSiW}_{11}\text{O}_{39}]$ and Br⁻.⁵³⁹

Sandwich-type Na₁₂[ZnWZn₂(ZnW₉)₂]['] is effective for the reaction of CO₂ with epichlorohydrin, propylene oxide, and butylene oxide, in conjunction with a Lewis base, (dimethylamino)pyridine (DMAP).⁵⁴⁰ With 0.4 MPa of CO₂ pressure, the selected substrates are almost quantitatively converted into the corresponding cyclic carbonates (Scheme 28) in the temperature range of 413–433 K. Excellent results

Scheme 28. Cycloaddition of CO₂ to Epoxides Catalyzed by Na₁₂[ZnWZn₂(ZnW₉)₂][']⁵⁴⁰



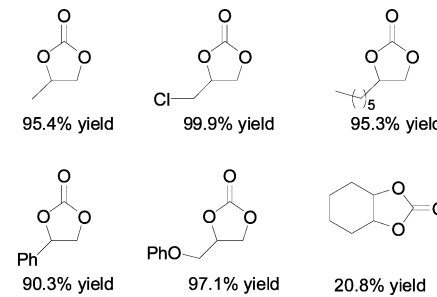
can be obtained even at a low catalyst loading (0.002 mol %). With dichloromethane as the solvent, the reaction system is heterogeneous, easy to separate after completion of the reactions, and reusable for many runs. Notice that DMAP plays an important role in the reaction. Without it, the selectivity for cyclic carbonate is unsatisfactory.

In 2005, Sakakura et al. used the TM-substituted POMs $[(n\text{-C}_7\text{H}_{15})_4\text{N}]_x[\alpha\text{-M}(\text{H}_2\text{O})\text{SiW}_{11}\text{O}_{39}]$ ($\text{M} = \text{Co}^{2+}, \text{Mn}^{2+}, \text{Ni}^{2+}, \text{Fe}^{3+}, \text{Cu}^{2+}; x = 5, 6$) for the reaction of CO₂ with 1,2-epoxypropane.⁵⁴¹ They found that Co- and Mn-substituted catalysts show the highest activities under base- and halogen-free conditions. The Co-substituted catalyst gives propylene carbonate with 83% yield and 99% selectivity after 2 h at 423 K and 3.5 MPa of total pressure, with DMF as the solvent. The catalyst loading is only 0.1 mol %. Under identical conditions, the Mn-substituted catalyst gives propylene carbonate with 73% yield and 99% selectivity. Ni- and Fe-substituted catalysts show moderate activities, whereas the Cu-substituted catalyst is ineffective. The difference in activity may be caused by the different abilities of the substituting metals to coordinate CO₂.

Under neat conditions, Co- and Mn-substituted catalysts even show higher activities. Propylene oxide almost quantitatively converts into propylene carbonate. The performances of TM-substituted Keggin type germanotungstates $[(n\text{-C}_7\text{H}_{15})_4\text{N}]_x[\text{M}(\text{H}_2\text{O})\text{GeW}_{11}\text{O}_{39}]$ ($\text{M} = \text{Mn}^{2+}, \text{Fe}^{3+}, \text{Co}^{2+}, \text{Ni}^{2+}, \text{Cu}^{2+}, \text{Zn}^{2+}; n = 5, 6$) are also evaluated in a similar way. However, the scope of substrates is enlarged. In the presence of $[(n\text{-C}_7\text{H}_{15})_4\text{N}]_6[\text{Mn}(\text{H}_2\text{O})\text{GeW}_{11}\text{O}_{39}]$, six cyclic carbonates are obtained with high yields and selectivities (Scheme 29).⁵⁴²

$\text{C}_7\text{H}_{15})_4\text{N}]_6[\text{Mn}(\text{H}_2\text{O})\text{GeW}_{11}\text{O}_{39}]$, six cyclic carbonates are obtained with high yields and selectivities (Scheme 29).⁵⁴²

Scheme 29. Six Cyclic Carbonates Obtained from a $[(n\text{-C}_7\text{H}_{15})_4\text{N}]_6[\text{Mn}(\text{H}_2\text{O})\text{GeW}_{11}\text{O}_{39}]$ -Mediated System⁵⁴²



The postulated reaction mechanism suggests that CO₂ is activated by POM anion initially via coordination to the exposed substituting TM.^{541,542} Simultaneously, epoxide is activated by the quaternary ammonium salt anion. Then the O atom of CO₂ attacks the C atom of the activated epoxide ring, followed by a ring-opening reaction step. Finally, the corresponding cyclic carbonates are achieved through the intramolecular cyclization step. Reasonably, the bonding mode between POMs and CO₂ involves the interaction of M···O, rather than M···C.⁵⁴² However, the mechanism is challenged by the DFT calculations with $[(n\text{-C}_4\text{H}_9)_4\text{N}]_4\text{H}[\text{Co}(\text{H}_2\text{O})\text{PW}_{11}\text{O}_{39}]$.⁵⁴³ DFT calculations support that the doublet Co^{II} catalyst activates the C–O bond of the epoxide via a single-electron transfer, resulting in a doublet Co^{III}–carbon radical intermediate. Subsequent CO₂ addition forms the cyclic carbonate product. The existence of radical intermediates is supported by free radical termination experiments.

7.4. Coupling Reactions

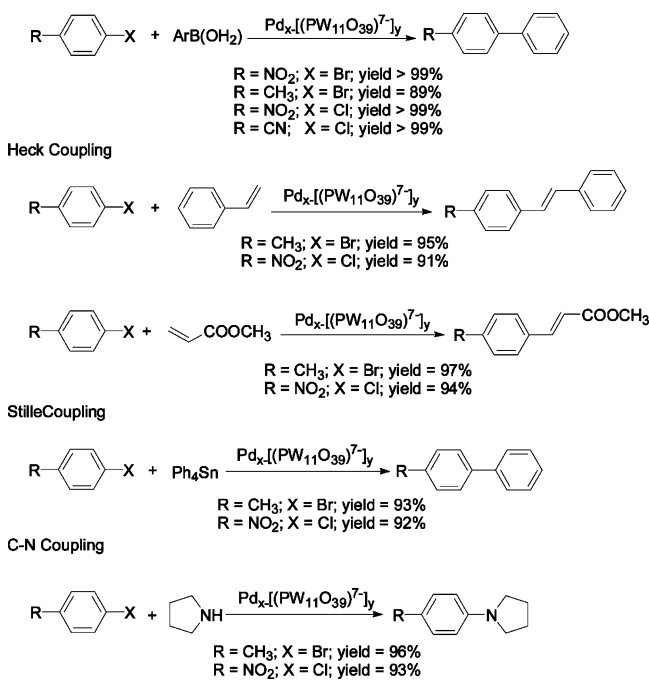
It is reported that POMs can act as supports of organometallic catalysts by covalently attaching the catalysts to the POM skeletons.⁵⁴⁴ Bonchio et al. reported a POM-based N-heterocyclic carbene (NHC) complex for palladium-mediated Suzuki coupling.⁵⁴⁵ In the hybrid structure, Pd–NHC is covalently attached to $\gamma\text{-SiW}_{10}$. Although the active Pd center is located at the organic moiety of the hybrid structure, the inorganic POM moiety stabilizes the organic Pd–NHC owing to its bulk/charge, resulting in improved TONs. Neumann et al. used a mono-Pd-substituted POM, K₅[PdPW₁₁O₃₉], as a pure inorganic catalyst precursor for Suzuki-, Heck-, and Stille-type C–C coupling and C–N coupling reactions.¹⁸⁴ The reduction of K₅[PdPW₁₁O₃₉] by H₂ results in 15–20 nm palladium particles of $\text{Pd}_x[(\text{PW}_{11}\text{O}_{39})^{7-}]_x$. In aqueous media, the reactions of bromoarenes proceed smoothly (Scheme 30). Chloroarenes are also reactive without solvent. Promisingly, Patel et al. reported the cesium salt of mono-Ni^{II}-substituted phosphomolybdate for Suzuki-type reactions.³³ Notice that no extra organic ligands are needed by the above systems, because the Keggin skeletons can act as ligands to stabilize the active metal centers.

8. POM-BASED BIFUNCTIONAL CATALYSTS

Bifunctional POM-based catalysts are generally divided into two categories.

In the first category, POM itself is bifunctional. The multiple catalytic properties of POMs endow their bifunctionalities,

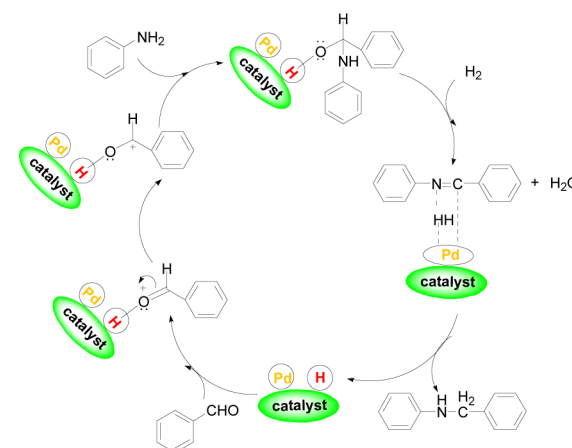
Scheme 30. Suzuki-, Heck-, and Stille-Type C–C Coupling and C–N Coupling Reactions with $\text{Pd}_x[(\text{PW}_{11}\text{O}_{39})^{7-}]_y$ Nanoparticles¹⁸⁴



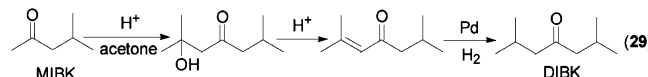
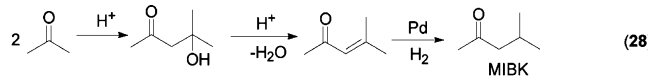
which may come from the anion alone, from the anion and cation, respectively, or from different cations. The bifunctionality of rare-element-containing POM anions, such as $\text{TBA}_8\text{H}_2[\text{Y}_2\text{-}(\text{SiW}_{10})_2]$, originates from the POM anions.^{468,469} In the cyanosilylation of carbonyl compounds with $(\text{TMS})\text{CN}$, nucleophilic oxygens on the surfaces of negatively charged POMs work as Lewis bases to activate $(\text{TMS})\text{CN}$ and the incorporated rare-earth-metal cations work as Lewis acids to activate carbonyl compounds. The synergy of rare elements and basic oxygens on the surface makes the reaction proceed efficiently. The bifunctionality of $[\text{C}_{16}\text{H}_{33}\text{N}(\text{CH}_3)_3]\text{-H}_3\text{CrPW}_{11}\text{O}_{39}$ is illustrated by the production of HMF from glucose.⁴³⁹ The Lewis acid site (Cr^{3+}) and Brønsted acid site (H^+) of the catalyst promote the process cooperatively. As for the Pd-containing catalyst $\text{Pd}_{2.8}\text{H}_{0.2}\text{PMo}_{12}/\text{SiO}_2$ for reductive amination of carbonyl compounds, the bifunctionality comes from Pd^{2+} and H^+ , respectively.⁵⁴⁶ The two cations work in a synergic manner to boost the production of a variety of secondary and tertiary amines in excellent yields. The plausible mechanism consists of two steps (Scheme 31). The first step is the formation of the imine intermediate via the condensation reaction of the carbonyl compound with amine on the catalyst surface, utilizing the acidic sites on the catalyst surface. In the second step, the imine is coordinated with the hydrogen atoms activated by the Pd sites of the catalyst and undergoes subsequent reduction to yield an amine derivative.

The second category of bifunctional POM-based catalysts are those composed of two individuals, POM and another individual, which is usually a supported functional metal. For example, the catalyst resulting from the impregnation of Pt on $\text{Cs}_{2.5}\text{H}_{0.5}\text{PW}_{12}$ is qualified for the hydroisomerization of *n*-butane in a fixed-bed gas-flow reactor;⁵⁴⁷ the combination of Pd with $\text{Cs}_{2.5}\text{H}_{0.5}\text{PW}_{12}$ in a manner of supporting the Pd metal on $\text{Cs}_{2.5}\text{H}_{0.5}\text{PW}_{12}$ is efficient for the one-step synthesis of MIBK (methyl isobutyl ketone) from acetone in both the gas and

Scheme 31. Proposed Mechanism for Reductive Amination of Carbonyl Compounds with Bifunctional $\text{Pd}_{2.8}\text{H}_{0.2}\text{PMo}_{12}/\text{SiO}_2$ ⁵⁴⁶



liquid phases (eqs 28 and 29).⁵⁴⁸ For the latter case, $\text{Cs}_{2.5}\text{H}_{0.5}\text{PW}_{12}$ accounts for the condensation and dehydration



in the initial steps and the Pd component is responsible for the hydrogenation of the formed double bonds. The continuous gas-phase process and the batch liquid-phase process yield MIBK together with DIBK (diisobutyl ketone) with total selectivities of 91% and 98%, respectively. The selectivity can be dramatically changed by replacing Pd with other metals. These findings may provoke the study of new combinations for other cascade reactions, especially those involving acid catalysis and oxidation (or reduction). One important application of this kind of catalyst is in the conversion of biomass, which usually involves hydrolysis and oxidation (or reduction) reactions. In hydrolysis–hydrogenation systems, the combinations of Ru and POMs receive the most attention. POMs are mainly responsible for the initial hydrolysis, and Ru is responsible for the hydrogenation functions. Even the proton-lacking Ru/ $\text{Cs}_3\text{PW}_{12}$ can catalyze the conversions of cellobiose and cellulose into sorbitol under mild conditions.⁵⁴⁹ In hydrolysis–oxidation combinations, several Au/ $\text{Cs}_{x}\text{H}_{3-x}\text{PW}_{12}$ systems have been developed. This work has been minutely summarized by Wang.⁵⁵⁰ More detailed information can be seen in his review.⁵⁵⁰ In an objective way, these combinations are promising because they can efficiently realize the cascade reactions in one pot. In the future, they will probably contribute to the exploitation of new energy sources and the industrial utilization of waste biomass.

9. OXYGEN EVOLUTION

As the most abundant renewable resource on the earth, water has been expected to be utilized intellectually and practically to provide pollution-free fuels for a long time, especially in conjunction with the conversion of solar energy into chemical energy.^{551–553} Water oxidation to oxygen is ubiquitous in nature and closely related to the life of living creatures. Evoked

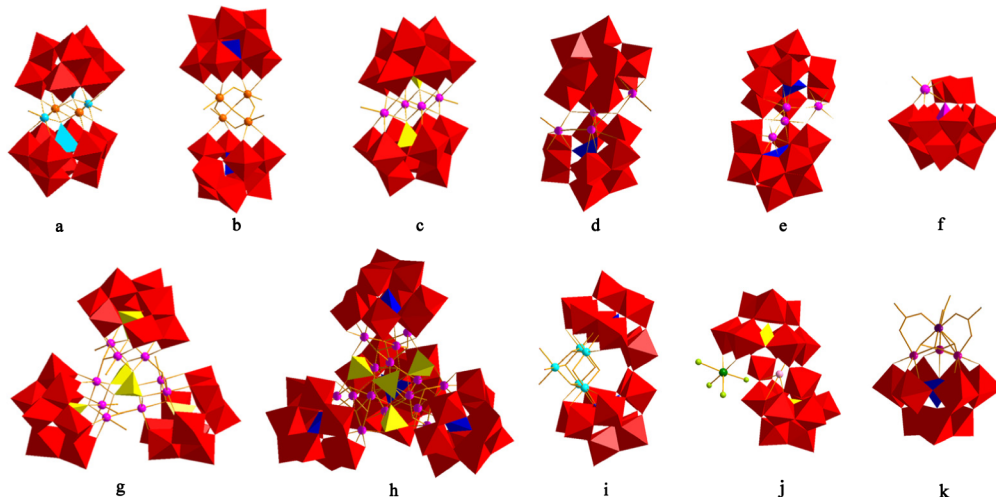


Figure 26. Structures of (a) $\text{Ru}_2\text{Zn}_2(\text{ZnW}_9)_2$, (b) $\text{Ru}_4(\gamma\text{-SiW}_{10})_2$, (c) $\text{Co}_4(\alpha\text{-PW}_9)_2$, (d, e) two isomers of $\{[\text{Co}_4(\mu\text{-OH})(\text{H}_2\text{O})_3](\text{Si}_2\text{W}_{19}\text{O}_{70})\}^{11-}$, (f) $[\text{Co}^{\text{III}}\text{Co}^{\text{II}}(\text{H}_2\text{O})\text{W}_{11}\text{O}_{39}]^{7-}$, (g) $\text{Co}_9(\text{PW}_9)_3$, (h) $\text{Co}_{16}(\text{XW}_9)_4$ ($\text{X} = \text{Si, Ge, P, As}$), (i) $\text{Ni}_5(\text{SiW}_9)_2$, (j) $[(\text{IrCl}_4)\text{KP}_2\text{W}_{20}\text{O}_{72}]^{14-}$, and (k) $\text{Mn}_4(\text{SiW}_9)$.

by the efficient processes in nature, people have put much effort into designing well-defined molecular catalysts for oxygen evolution from water, where the core challenge is to develop sufficiently stable and fast catalysts.^{554,555} To date, significant progress has been made for this prospective project.⁵⁵⁶ Many catalysts containing TMs, such as Ru,^{556–560} Fe,^{561,562} Mn,^{553,563} Co,^{564,565} Ir,^{566,567} and Cu,⁵⁶⁸ have been developed. As presented before, POM catalysts are remarkable in catalysis owing to their unique activities and stabilities. Those containing appropriate TMs may exhibit sufficient activity and stability required by excellent catalysts for oxygen evolution. From this point of view, POMs are promising alternatives for the reaction.⁴⁸ The most popular POMs in this field are those containing Ru or Co. They are active in chemical, photochemical, and electrochemical oxygen evolution from water, and address the solar fuel challenge and the urgent call for a sustainable-energy future to some extent.

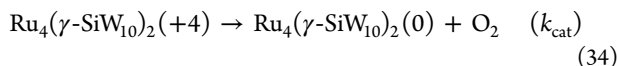
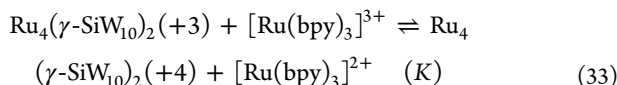
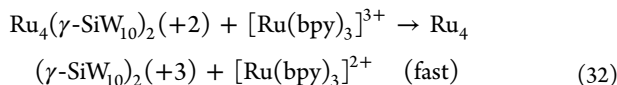
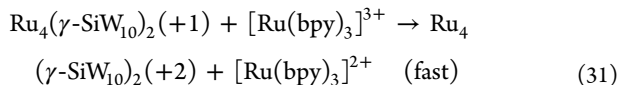
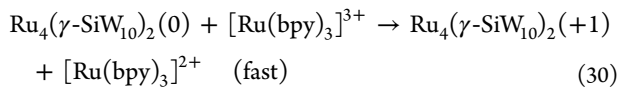
Shannon and co-workers themselves thought that $\text{Na}^{14-}[\text{Ru}^{\text{III}}_2\text{Zn}_2(\text{H}_2\text{O})_2(\text{ZnW}_9\text{O}_{34})_2]$ ($\text{Ru}_2\text{Zn}_2(\text{ZnW}_9)_2$) with a Ru–Ru distance of 0.318 nm (Figure 26a) is active for the electrochemical evolution of O_2 using pulsed voltammetry in 0.1 M sodium phosphate buffer (pH 8.0) solution.⁵⁶⁹ The proximity of the two Ru atoms is supported as a key factor in the ability of the electrocatalyst in O_2 evolution. The calculated $E_{1/2}$ for electrocatalytic oxygen evolution is approximately +0.750 V, consistent with the results by cyclic voltammetry (+0.760 V for the Ru^{IV/V} couple) and the thermodynamics of oxygen evolution ($E^\circ = +0.760$ V vs NHE at pH 8). The oxygen evolution takes place only when the working electrode potential is stepped positively from the rest potential of +0.2 V and disappears when the potential is stepped back to +0.2 V. As a control experiment, the monoruthenium–POM $[\text{Ru}^{\text{III}}(\text{H}_2\text{O})\text{PW}_{11}\text{O}_{39}]^{4-}$ is proven to be inactive for water oxidation under the same conditions.

The molecular tetra-Ru–POM catalyst $[\text{Ru}^{\text{IV}}_4(\mu\text{-O})_4(\mu\text{-OH})_2(\text{H}_2\text{O})_4(\gamma\text{-SiW}_{10}\text{O}_{36})_2]^{10-}$ ($\text{Ru}_4(\gamma\text{-SiW}_{10})_2$) (Figure 26b) makes a great breakthrough in water oxidation toward oxygen. Several groups have made great effort on the promising structure. Hill's and Bonchio's groups first reported the structure for water oxidation at almost the same time.^{570,571} Hill's group synthesized $\text{Rb}_8\text{K}_2[\text{Ru}_4(\gamma\text{-SiW}_{10})_2]$ by the reaction

of $\gamma\text{-SiW}_{10}$ with RuCl_3 in acidic aqueous solutions (pH 1.6),⁵⁷⁰ while Bonchio's group made $\text{Cs}_{10}[\text{Ru}_4(\gamma\text{-SiW}_{10})_2]$ by using a different Ru source, $\mu\text{-oxobis(pentachlororuthenate(IV))}$ ($\text{Ru}_2\text{OCl}_{10}^{4-}$), in pH 1.8 solution.⁵⁷¹ The water-soluble $\text{Ru}_4(\gamma\text{-SiW}_{10})_2$ is featured with especially oxidative and hydrolytic stability. With the pyridine-ligated complex $[\text{Ru}(\text{bpy})_3]^{3+}$ as the oxidant, the catalyst $\text{Rb}_8\text{K}_2[\text{Ru}_4(\gamma\text{-SiW}_{10})_2]$ dramatically accelerates water oxidation.⁵⁷⁰ In the presence of 1.5 μM $\text{Rb}_8\text{K}_2[\text{Ru}_4(\gamma\text{-SiW}_{10})_2]$, the oxidation is complete within 30–40 s in aqueous solution at pH 7, whereas in the absence of the catalyst, the typical reaction time is more than 30 min under the same conditions. A 10 mL aqueous solution of 12 μmol of $[\text{Ru}(\text{bpy})_3]^{3+}$ and 0.1 μmol of $\text{Rb}_8\text{K}_2[\text{Ru}_4(\gamma\text{-SiW}_{10})_2]$ gives 10.7 μmol of $[\text{Ru}(\text{bpy})_3]^{2+}$ (ca. 90% based on the initial $[\text{Ru}(\text{bpy})_3]^{3+}$) and 1.78 μmol of O_2 (ca. 66% based on the initial $[\text{Ru}(\text{bpy})_3]^{3+}$). The catalytic activity of $\text{Rb}_8\text{K}_2[\text{Ru}_4(\gamma\text{-SiW}_{10})_2]$ is 100 times higher than that of RuCl_3 . The addition of $\gamma\text{-SiW}_{10}$ to the reaction with RuCl_3 does not result in a high water oxidation rate because $\text{Ru}_4(\gamma\text{-SiW}_{10})_2$ forms more slowly in the highly buffered solution (pH 7). The dependence of the O_2 yield on the catalyst concentration obeys a hyperbolic function, $Y (\%) = [X]/([X] + 0.021 \mu\text{M})$, where $Y = 4[\text{O}_2]/[[\text{Ru}(\text{bpy})_3]^{3+}] \times 100$ and $[X]$ is the catalyst concentration (μM).⁵⁷² The stoichiometries, TON values, and isotopically labeled experiments make it clear that the oxygen atoms in O_2 are from water rather than other sources. With Ce^{IV} as a sacrificial oxidant, $\text{Cs}_{10}[\text{Ru}_4(\gamma\text{-SiW}_{10})_2]$ dramatically promotes water oxidation toward O_2 in acidic aqueous solution (pH 0.6) at 293 K.⁵⁷¹ When 4.3 μmol of $\text{Cs}_{10}[\text{Ru}_4(\gamma\text{-SiW}_{10})_2]$ and 1720 μmol of Ce^{IV} are used in 10 mL of water, 385 μmol of O_2 is generated in 2 h, with an overall 90% yield based on the added oxidant. The maximum TOF is up to 450 h^{-1} . From the stability standpoint, $\text{Ru}_4(\gamma\text{-SiW}_{10})_2$ excels over the extensively studied Ru-blue dimer, $[(\text{bpy})_2(\text{O})\text{Ru}^{\text{V}}(\mu\text{-O})\text{Ru}^{\text{V}}(\text{O})(\text{bpy})_2]^{4+}$, which is unstable due to the oxidation of the ligand.⁵⁷³ $\text{Ru}_4(\gamma\text{-SiW}_{10})_2$ keeps its structural integrity after the treatment with $[\text{Ru}(\text{bpy})_3]^{3+}$ or Ce^{IV} in water,^{571,573} and is stable under neutral or mildly acidic conditions, although it is prepared in acidic aqueous solutions (pH 1.6 or 1.8).^{570,572} However, it decomposes slowly in strongly acidic solution (pH < 1.5).⁵⁷²

In the $\text{Ru}_4(\gamma\text{-SiW}_{10})_2/\text{[Ru(bpy)}_3]^{3+}$ system, self-decomposition of $[\text{Ru(bpy)}_3]^{3+}$ occurs on account of oxidative decomposition of the bpy ligand and competes with water oxidation.⁵⁷² An increase of the initial $[\text{Ru(bpy)}_3]^{3+}$ concentration causes more rapid self-decomposition and results in an almost linear decrease of the O_2 yield. However, the addition of $[\text{Ru(bpy)}_3]^{2+}$ to the catalytic system slightly decreases the O_2 yield, and the addition of free bpy brings a negligible increase of the O_2 yield. These findings seem to be intricate because the oxygen evolution is influenced by more than one factor. Ion pairing in the reaction solution is one of them. The addition of NaCl and KCl, especially KCl, into the reactor results in a considerable drop of the O_2 yield due to the reinforced ion pairing. Nevertheless, the replacement of K^+ by Li^+ in phosphate buffer leads to a slight increase of the O_2 yield. The results are consistent with the documented relative ion pairing association constants for these alkali-metal cations and POMs ($\text{K}^+ > \text{Na}^+ > \text{Li}^+$).^{574–576}

The mechanism for $\text{Ru}_4(\gamma\text{-SiW}_{10})_2$ -mediated water oxidation with $[\text{Ru(bpy)}_3]^{3+}$ is proposed as eqs 30–34 by Hill's group ($\text{Ru}_4(\gamma\text{-SiW}_{10})_2(0) = [\text{Ru}_4(\mu\text{-O})_4(\mu\text{-OH})_2(\text{H}_2\text{O})_4(\gamma\text{-SiW}_{10}\text{O}_{36})_2]^{10-}$, and $\text{Ru}_4(\gamma\text{-SiW}_{10})_2(+n) = n$ -electron-oxidized $\text{Ru}_4(\gamma\text{-SiW}_{10})_2(0)$).⁵⁷²

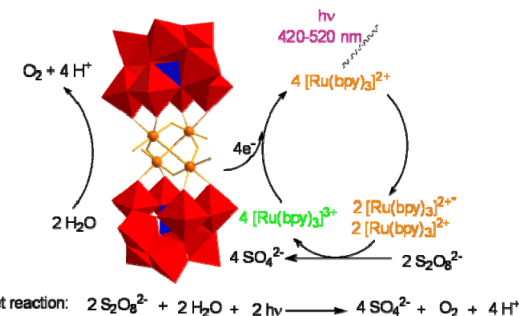


Four one-electron-transfer steps are involved in the mechanism. The four-electron-oxidized form of the catalyst, $\text{Ru}^{\text{V}}_4(\gamma\text{-SiW}_{10})_2$, is responsible for the direct water oxidation. Equations 30–32 are thermodynamically favorable and therefore proceed rapidly. Equilibrium 33 is a reversible electron transfer between $\text{Ru}_4(\gamma\text{-SiW}_{10})_2(+3)$ and $\text{Ru}_4(\gamma\text{-SiW}_{10})_2(+4)$ with an equilibrium constant K and is estimated to be thermoneutral. Equation 34, presented in a very simplified manner, is assumed to be the rate-limiting step and may have a complex detailed mechanism involving the catalyst and water molecules. The $\{\text{Ru}_4\}$ – $\{\text{SiW}_{10}\}$ distance shortens with a decrease of the total negative charge of $\text{Ru}_4(\gamma\text{-SiW}_{10})_2(0)$ – $\text{Ru}_4(\gamma\text{-SiW}_{10})_2(+4)$, whereas the geometry parameters within the $\{\text{Ru}_4\}$ core or the $\{\gamma\text{-SiW}_{10}\}$ polyanion are insusceptible.⁵⁷³ The results based on DFT calculations support that the consecutive electron transfers are coupled with proton transfer.⁵⁷⁷ Four $\text{Ru}^{\text{IV}}\text{-OH}_2$ units are successively oxidized to four $\text{Ru}^{\text{V}}\text{-OH}$ centers, the supported active form. The computational result is consistent with the viewpoint proposed by Hill's and Bonchio's groups,^{571,572,578} but contradicts the computational basicity study of the oxygen centers in the $\{\text{Ru}_4\}$ core and oxygens located in the vicinity of this core, which gives the basicity sequence $\mu\text{-O}_{\text{Ru}-\text{O}-\text{Ru}} < \mu-$

$\text{OH}_{\text{Ru}-\text{OH}-\text{Ru}} < \mu\text{-O}_{\text{W}-\text{O}-\text{Ru}} < \text{O}_{\text{Ru}-\text{H}_2\text{O}}$.⁵⁷³ According to the sequence, $\text{Ru}_4(\gamma\text{-SiW}_{10})_2$ initially releases protons on $\mu\text{-OH}$ in the $\{\text{Ru}_4\}$ core at higher pH values, but the deprotonation of ligated H_2O is universally accepted at present. Acid–base titration and spectrophotometric titration of $\text{Cs}_{10}[\text{Ru}_4(\gamma\text{-SiW}_{10})_2]$ reveal a reversible monoprotonation equilibrium in water with a $\text{p}K_a$ of 3.62, and the equilibrium is concentration-independent, ruling out POM dissociation or aggregation.⁵⁷¹ Multiple redox states associative with the $\{\text{Ru}_4\}$ core and reversible protonation equilibria are critical components for efficient oxygen-evolving catalysis, whereby deprotonation of ligated H_2O triggers the formation of OH^-/O_2^- reactive sites.

Driven by the renewable pollution-free solar fuels, the highly active $\text{Ru}_4(\gamma\text{-SiW}_{10})_2$ is used for the direct, sustained oxygen evolution from water in a totally homogeneous visible-light-driven artificial photosynthesis system at physiologically neutral pH.⁵⁷⁹ In such a light-driven system, the dosage of expensive $[\text{Ru(bpy)}_3]^{3+}$ sharply decreases. The small amount of pyridine-ligated complex plays the role of photosensitizer and direct oxidant for $\text{Ru}_4(\gamma\text{-SiW}_{10})_2$. The oxidized $\text{Ru}_4(\gamma\text{-SiW}_{10})_2$ is responsible for the direct water oxidation. Budget $\text{S}_2\text{O}_8^{2-}$ is introduced into the system as a sacrificial electron acceptor to regenerate $[\text{Ru(bpy)}_3]^{3+}$ from its reduced state. The overall process and the net reaction are presented in Scheme 32. The

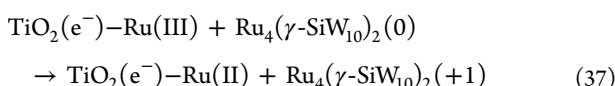
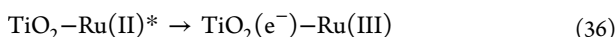
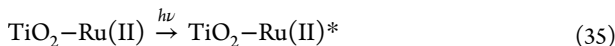
Scheme 32. Process of Photodriven Water Oxidation with $\text{Ru}_4(\gamma\text{-SiW}_{10})_2$ ⁵⁷⁹



regeneration process of $[\text{Ru(bpy)}_3]^{3+}$ involves quenching of the excited state of $[\text{Ru(bpy)}_3]^{2+*}$ by $\text{S}_2\text{O}_8^{2-}$ to produce $[\text{Ru(bpy)}_3]^{3+}$ and SO_4^{2-} , and the sequential reaction of sulfate radical anion with $[\text{Ru(bpy)}_3]^{2+}$ to give a second molecule of $[\text{Ru(bpy)}_3]^{3+}$. When a reactor stocked with 1.0 mM $[\text{Ru(bpy)}_3]^{2+}$, 5.0 mM $\text{Na}_2\text{S}_2\text{O}_8$, 5.0 μM $\text{Ru}_4(\gamma\text{-SiW}_{10})_2$, and 20 mM sodium phosphate buffer is exposed to 420–520 nm visible light illumination, O_2 is quickly evolved with the consumption of persulfate and a decrease of pH (from 7.2 to 6.3), although a small portion of $[\text{Ru(bpy)}_3]^{2+}$ gradually decomposes. The final O_2 yield is $\sim 38\%$, and the TON is $\sim 1.8 \times 10^2$ with an initial TOF of $\sim 8 \times 10^{-2} \text{ s}^{-1}$. The quantum efficiency for oxygen evolution (defined as the number of molecules of O_2 formed per two absorbed photons) is up to $\sim 9\%$, a delightful value in photocatalytic water oxidation using molecular catalysts. All the parameters, including light intensity, photosensitizer concentration, persulfate concentration, and catalyst concentration, have a significant impact on the O_2 production. With a lower ratio of photosensitizer ($[\text{Ru(bpy)}_3]^{3+}$) to $\text{Ru}_4(\gamma\text{-SiW}_{10})_2$ (compared to that in chemical catalysis with $[\text{Ru(bpy)}_3]^{3+}$ as the terminal oxidant), the self-decomposition of photosensitizer is significantly restrained by $\text{Ru}_4(\gamma\text{-SiW}_{10})_2$ during photocatalytic turnover. However, the

electrostatic interaction between $[\text{Ru}(\text{bpy})_3]^{2+}$ and $\text{Ru}_4(\gamma\text{-SiW}_{10})_2$ leads to efficient static quenching of the $[\text{Ru}(\text{bpy})_3]^{2+}$ excited state when the stoichiometry of $\text{Ru}_4(\gamma\text{-SiW}_{10})_2$ and $[\text{Ru}(\text{bpy})_3]^{2+}$ is up to 1:4.⁵⁸⁰ The quenching occurs via rapid electron transfer to $\text{Ru}_4(\gamma\text{-SiW}_{10})_2$, followed by rapid charge recombination. Apparently, this is an energy-wasting process and is detrimental to photocatalytic activity, because it competes with the reaction between the excited photosensitizer and the sacrificial oxidant. In this context, keeping the catalyst concentration as low as possible can prevent quenching of excited $[\text{Ru}(\text{bpy})_3]^{2+}$, however, at the cost of slowing the hole-transfer process. In chemical water oxidation, the hole-transfer rate is not a major issue, because the main processes potentially competing with the hole transfer are prevented by the irreversible reduction of the sacrificial oxidant. Nevertheless, a fast hole-scavenging rate is still beneficial to the chemical water oxidation, because it minimizes the occurrence of self-decomposition of $[\text{Ru}(\text{bpy})_3]^{3+}$. However, the hole-transfer rate becomes very crucial in a regenerative system, which is involved in most practical schemes of oxygen evolution. In such a system, the hole-transfer rate must be faster than the rate of the recombination process.

The quantum efficiencies for regenerating Ru^{III} photosensitizer and its reaction with the catalyst to form O_2 are major limiting factors in the above light-driven system.⁵⁷⁹ The overall quantum efficiency can be improved by the introduction of nanocrystalline TiO_2 , a method closely related to the design of practical devices for photochemical water splitting.⁵⁸¹ In the improved system using $[\text{Ru}(\text{bpy})_2(\text{dpy})]^{2+}$ ($\text{dpy} = 4,4'$ -diphosphonic-2,2'-bipyridine acid) as the photosensitizer, the fast regeneration of Ru^{III} species is triggered by nanosecond laser flash via charge injection from the excited state of the Ru^{II} species into the conduction band of nanocrystalline TiO_2 (eqs 35–37).⁵⁸²



In the presence of $\text{Ru}_4(\gamma\text{-SiW}_{10})_2$, the main quenching way of the excited photosensitizer is the electron transfer from the photosensitizer to TiO_2 .⁵⁸³ The accelerated recovery of $[\text{Ru}(\text{bpy})_2(\text{dpy})]^{2+}$ in its ground state results from ultrafast (nanosecond) electron transfer from $\text{Ru}_4(\gamma\text{-SiW}_{10})_2$ to $[\text{Ru}(\text{bpy})_2(\text{dpy})]^{3+}$. The oxidized catalyst is long-lived. Thus, it energetically reacts with H_2O to produce O_2 . Similar photosensitizer ground-state regeneration by TiO_2 occurs in another $\text{Ru}_4(\gamma\text{-SiW}_{10})_2$ -based system with Ru470 (tris(2,2'-bipyridyl-4,4'-dicarboxylic acid)ruthenium(II) dichloride) as the photosensitizer.⁵⁸⁴ SnO_2 plays a role equal to that of TiO_2 . Thus, these metal oxides afford better schemes for the fast regeneration of Ru^{III} species, in which a sacrificial electron acceptor is not essentially necessary.

Most POM anions show no or very little light absorption in the visible region.⁵⁸⁵ Some measures have been taken to extend the absorbed light to the visible region. Combining POM anions with highly conjugated cationic chromophores is one of them.⁵⁸⁶ The catalyst consisting of $\text{Ru}_4(\gamma\text{-SiW}_{10})_2$ and a tetrานuclear Ru^{II} dendrimeric photosensitizer, $\{\text{Ru}[(\mu\text{-dpp})\text{Ru}(\text{bpy})_2]_3\}^{8+}$ (Figure 27a), poses an outstanding quantum yield

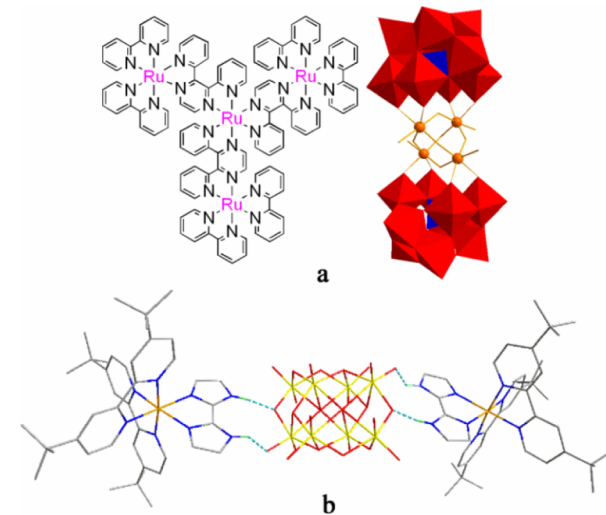


Figure 27. (a) Catalyst consisting of $\text{Ru}_4(\gamma\text{-SiW}_{10})_2$ and $[\text{Ru}\{(\mu\text{-dpp})\text{Ru}(\text{bpy})_2\}_3\}^{8+}$. (b) Hydrogen-bonding model between $[\beta\text{-Mo}_8\text{O}_{26}]^{4-}$ and $[\text{Ru}(\text{tbbpy})_2(\text{biH}_2)]^{2+}$.

of 30% for photodriven water oxidation, producing O_2 at an excitation wavelength of 550 nm.⁵⁸⁷ Another useful method to improve light absorption of the POM catalyst is to create strong interactions between cations and POM anions via designing the structure of the cationic moieties. The strong hydrogen bonds between $[\text{Ru}(\text{tbbpy})_2(\text{biH}_2)]^{2+}$ and $[\beta\text{-Mo}_8\text{O}_{26}]^{4-}$ (Figure 27b) cause the maximum absorption wavelength of single $[\text{Ru}(\text{tbbpy})_2(\text{biH}_2)]^{2+}$ (484 nm) and $[\beta\text{-Mo}_8\text{O}_{26}]^{4-}$ (<400 nm) to red shift to 522 nm.⁵⁸⁸ The intermolecular processes govern the energy and electron transfer between the cationic photosensitizer and anionic POM. In such a scheme, the challenging task is designing a cationic Ru photosensitizer with hydrogen-bonding components, because there are rich oxygen atoms on the POM surface. According to the above two examples, the connection of POM anions to a highly conjugated cationic photosensitizer with hydrogen-bonding components will make more visible light useful for light-driven water oxidation.

The electrochemical performance of $\text{Ru}_4(\gamma\text{-SiW}_{10})_2$ for oxygen evolution is first investigated using the assemblies of $\text{Ru}_4(\gamma\text{-SiW}_{10})_2$ with a conducting bed of carbon nanotubes (CNTs).^{589–591} The redox-active center of $\text{Ru}_4(\gamma\text{-SiW}_{10})_2$ is immobilized on the electrode surface using multiwalled carbon nanotubes (MWCNTs) decorated with poly(amidoamine) ammonium dendrimers. MWCNTs serve as conductive nanowire scaffolds to provide heterogeneous support of the redox-active center, to control the material morphology, to increase the surface area, to funnel the sequential electron transfer to the electrode, and thus to favor energy dispersion and relieve catalytic fatigue.⁵⁸⁹ The assemblies $\text{Ru}_4(\gamma\text{-SiW}_{10})_2@\text{MWCNT}$ have the advantages of high surface area and domains of nanometric dimensions with enhanced hydrophilic character due to the coexistence of tungsten and ruthenium sites and the charged nitrogen and oxygen residues, prone to assist water diffusion and stabilization through coordination and hydrogen-bonding interactions. A nanostructured, oxygen-evolving anode is fabricated by coating $\text{Ru}_4(\gamma\text{-SiW}_{10})_2@\text{MWCNT}$ on an indium tin oxide (ITO) electrode. Using Ag/AgCl as the reference electrode and platinum wire as the counter electrode, the catalyst-modified ITO electrode creates a TOF of 36–306 h^{-1} for oxygen evolution at pH 7, depending on the used

overpotential. The TOF is 36 h⁻¹ initially at $\eta = 0.35$ V and reaches a peak performance of 306 h⁻¹ at $\eta = 0.60$ V, exceeding the previous values for Co- and Mn-based systems.^{592–594} The excellent performance of the Ru₄(γ -SiW₁₀)₂-modified electrode is attributed to a synergistic interplay of factors coupling the redox features of Ru₄(γ -SiW₁₀)₂ with the MWCNT-enabled nanoscale structure and electrical wiring of the hybrid material. Apart from extreme robustness, the hybrid nanomaterial shows excellent structural stability and retention of electrocatalytic properties upon multicycle activity. Notice that in electrochemical water oxidation with Ru₄(γ -SiW₁₀)₂ both the four-electron-oxidized form Ru₄(γ -SiW₁₀)₂(+4) and the three-electron-oxidized form Ru₄(γ -SiW₁₀)₂(+3) are capable of oxidizing water directly under appropriate conditions, and proton transfer is not necessarily coupled with all electron-transfer steps.⁵⁹⁵

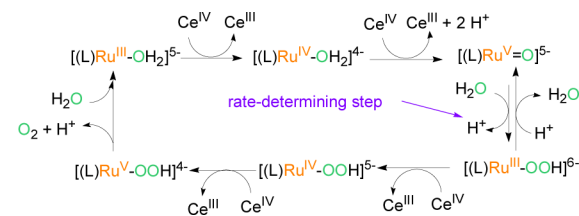
In contrast to carbon nanotubes, graphene seems to be more attractive. It can minimize the applied overpotential, create a high turnover frequency, and endorse long-term robustness. A definite upgrade of the electrocatalytic performance of Ru₄(γ -SiW₁₀)₂ is confirmed by using nanographene instead of carbon nanotubes with similar surface modification.⁵⁹⁶ The hybrid material catalyzes oxygen evolution at an overpotential as low as 300 mV at neutral pH with negligible loss of performance after 4 h of testing. The nanographene platform outperforms by 1 order of magnitude the catalytic efficiency of the isolated Ru₄(γ -SiW₁₀)₂, with a 2-fold enhancement compared to the efficiency of the CNT analogues. The noninvasive and high-scale surface modification of the graphene nanoplatelets enables electron transport and accumulation across the extended π -bond network. Notice that graphene without a modified surface can adsorb Ru₄(γ -SiW₁₀)₂ strongly. On the basis of this point, another Ru₄(γ -SiW₁₀)₂-modified electrode is fabricated by confining Ru₄(γ -SiW₁₀)₂ within the highly porous wet graphene film.⁵⁹⁷ The catalytic activity of the Ru₄(γ -SiW₁₀)₂-graphene electrode is nearly 2 orders of magnitude higher than that of the Ru₄(γ -SiW₁₀)₂@MWCNT-modified electrode at $\eta = 0.35$ V, and comparable to that of IrO₂, one of the most active and best known water oxidation catalysts. Additionally, the graphene-supported Ru₄(γ -SiW₁₀)₂ electrode exhibits high stability toward water oxidation under neutral pH conditions, particularly with 1.0 M Ca(NO₃)₂ as the electrolyte. To obtain excellent activity, a higher concentration of supporting electrolyte is needed under neutral pH conditions to overcome the electrical double layer effect associated with the highly negatively charged Ru₄(γ -SiW₁₀)₂. A well-defined voltammogram is obtained only when double layer effects are suppressed in buffered media.

A detailed investigation on the electrochemical properties over wide pH (2–12) and ionic strength ranges reveals that the reversible potential associated with the Ru₄(γ -SiW₁₀)₂(0)/Ru₄(γ -SiW₁₀)₂(+1) process is pH-dependent.⁵⁹⁵ K⁺ and H⁺ competitively interact with Ru₄(γ -SiW₁₀)₂(0) and Ru₄(γ -SiW₁₀)₂(+1), and the interaction of K⁺ with Ru₄(γ -SiW₁₀)₂(+1) is much stronger than that of Li⁺, Na⁺, Mg²⁺, or Ca²⁺. Thus, the presence of K⁺ can significantly change the pH dependence of the Ru₄(γ -SiW₁₀)₂(0)/Ru₄(γ -SiW₁₀)₂(+1) reversible potential. In acidic media, the electrochemistry of the catalyst is significantly affected by the presence of H⁺ and K⁺ in both the thermodynamic and kinetic senses.⁵⁹⁸ The protonation of the Ru core changes the reaction thermodynamics, while K⁺ creates a faster and dominant electron-transfer pathway.

The congenic POM catalyst [Ru^{IV}₄(μ -O)₅(μ -OH)(H₂O)₄(γ -PW₁₀O₃₆)₂]⁹⁻ (Ru₄(γ -PW₁₀)₂) is synthesized by the reaction of poorly stable Cs₇(γ -PW₁₀O₃₆) with RuCl₃ in water at pH 0.6.⁵⁹⁹ The anion structure is almost the same as that of Ru₄(γ -SiW₁₀)₂, except the lack of one proton on the bridging oxygen between two Ru atoms. With pH in the range of 0.6–3.1, the proton on the only –OH is lost to form [Ru₄(μ -O)₆(H₂O)₄(γ -PW₁₀O₃₆)₂]¹⁰⁻; when the pH is higher than 3.1, another two protons on the ligand H₂O are lost to form [Ru₄(μ -O)₆(OH)₂(H₂O)₂(γ -PW₁₀O₃₆)₂]¹²⁻, and the latter process is reversible at around pH 3. The activity of Cs₉[Ru₄(γ -PW₁₀)₂] for water oxidation is restrained by its low solubility in the presence of excess [Ru(bpy)₃]³⁺ or [Ru(bpy)₃]²⁺. The satisfying thing is that just a small amount of [Ru(bpy)₃]³⁺ is required in photochemical water oxidation with S₂O₈²⁻ as the sacrificial electron acceptor because of its regeneration by S₂O₈²⁻ with the aid of light. However, unlike the case with Ru₄(γ -SiW₁₀)₂ at pH 7, the irreversible eq 34 is ~0.07 V thermodynamically unfavorable for Ru₄(γ -PW₁₀)₂ at pH 5.8 ($E_{\text{O}_2/\text{H}_2\text{O}} = 0.89$ V vs NHE at pH 5.8; $E_{\text{Ru}^{\text{V}}/\text{Ru}^{\text{IV}}} = 0.82$ V vs NHE). Thus, the overall catalytic activity of Ru₄(γ -PW₁₀)₂ is lower than that of Ru₄(γ -SiW₁₀)₂.

[Ru^{III}(H₂O)XW₁₁O₃₉]ⁿ⁻ (RuXW₁₁; X = P, Si, Ge; n = 4, 5) are single-site Ru-containing POMs for water oxidation.^{600,601} They can promote oxygen evolution with the one-electron oxidant Ce^{IV}, but they are less robust than Ru₄(γ -SiW₁₀)₂, despite the exposed and more accessible metal center. In contrast to RuSiW₁₁, RuGeW₁₁ performs much better due to the stronger electronegativity of Ge atoms, which makes the Ru center more acidic.⁶⁰⁰ The mechanism for the single-site Ru-containing POMs involves a Ru^V–oxo complex ([L]Ru^V=O)⁵⁻; L = XW₁₁), as presented in Scheme 33. The two-

Scheme 33. Mechanism for Water Oxidation with Ru^{III}(H₂O)XW₁₁ (X = Si, Ge)⁶⁰⁰



electron-oxidized species ([L]Ru^V=O)⁵⁻ is assignable to an active intermediate in the rate-determining step of the whole catalytic cycle to give (L)Ru^{III}OOH via the O–O bond formation step, where the reverse O–O bond cleavage process is in competition with the follow-up two-electron oxidation process to generate oxygen. The DFT characterization of the mechanism suggests that, in the formation process of (L)Ru^{III}OOH, the bridging O atom of the polytungstate ligand is the most favorable proton acceptor, rather than the O atom of Ru^V=O.⁶⁰²

In terms of application, the abundant metal Co is more acceptable than the noble-metal Ru. The tetra-Co-sandwiched POM Na₁₀[Co₄(H₂O)₂(α -PW₉O₃₄)₂] (Na₁₀[Co₄(α -PW₉)₂]; Figure 26c) makes the second breakthrough in POM-catalyzed water oxidation.⁶⁰³ It shows higher activity than Ru₄(γ -SiW₁₀)₂ in chemical, photochemical, and electrochemical water oxidation. With [Ru(bpy)₃]³⁺ as the oxidant, the TOF of Na₁₀[Co₄(α -PW₉)₂] for dark chemical water oxidation is higher than 5 s⁻¹ at pH 8, much higher than that of Rb₈K₂[Ru₄(γ -

$\text{SiW}_{10})_2$] ($0.45\text{--}0.60 \text{ s}^{-1}$). The rate of water oxidation with $\text{Na}_{10}[\text{Co}_4(\alpha\text{-PW}_9)_2]$ highly depends on the pH. It increases with an increase of the initial pH in the range of 7.5–8.0, and the reaction time is shortened from 270 to 90 s. However, high pH will speed up the decomposition of $[\text{Ru}(\text{bpy})_3]^{3+}$. In the $[\text{Ru}(\text{bpy})_3]^{2+}/\text{S}_2\text{O}_8^{2-}$ photoinduced system, $\text{Na}_{10}[\text{Co}_4(\alpha\text{-PW}_9)_2]$ affords an O_2 evolution quantum yield of 30% and a TON higher than 220 at pH 8.⁶⁰⁴ Due to the sensitivity of the reaction to the pH, 80 mM sodium borate is used to maintain the pH around 8. Only a pH decrease of 0.1–0.3 pH unit is observed by the end of the reaction. As $\text{Ru}_4(\gamma\text{-SiW}_{10})_2$, $\text{Co}_4(\alpha\text{-PW}_9)_2$ can protect the photosensitizer from decomposition. $\text{Co}_4(\alpha\text{-PW}_9)_2$ enwrapped into ordered mesoporous carbon nitride exhibits noticeable electrocatalytic activity in water oxidation.⁶⁰⁵ At 1.4 V vs Ag/AgCl, the TOF reaches up to 0.3 s^{-1} at pH 7, which is nearly 6 times higher than that with $\text{Ru}_4(\gamma\text{-SiW}_{10})_2@\text{MWCNT}$ (0.055 s^{-1} at 1.4 V).⁵⁸⁹ Hill's group showed that $\text{Co}_4(\alpha\text{-PW}_9)_2$ was a stable homogeneous molecular catalyst for water oxidation,⁶⁰³ but this viewpoint is challenged.⁶⁰⁶ Finke's group suggested that, in the electrocatalytic water oxidation beginning with $500 \mu\text{M} \text{ Co}_4(\alpha\text{-PW}_9)_2$ at 1.1 V vs Ag/AgCl and pH 8.0, the true catalyst is dominantly heterogeneous CoO_x , resulting from partial decomposition of $\text{Co}_4(\alpha\text{-PW}_9)_2$ under oxidizing conditions, rather than homogeneous $\text{Co}_4(\alpha\text{-PW}_9)_2$. However, the system with a lower catalyst concentration ($2.5 \mu\text{M}$) and a higher potential ($\geq 1.3 \text{ V}$) argues against this conclusion.⁶⁰⁷ Scandola et al. pointed out that $\text{Co}_4(\alpha\text{-PW}_9)_2$ developed into catalytically active species by laser flash photolysis in the $[\text{Ru}(\text{bpy})_3]^{2+}/\text{S}_2\text{O}_8^{2-}$ system.⁶⁰⁸ Most recently, Hill's group provided strong evidence for the conclusion that $\text{Co}_4(\alpha\text{-PW}_9)_2$ was a genuine molecular catalyst under the used conditions described in his paper.^{603,609} X-ray absorption spectroscopy by Limberg and co-workers also reveals that the integrity of $\text{Co}_4(\alpha\text{-PW}_9)_2$ is uncompromised by oxidant-driven water oxidation.⁶¹⁰ The conflicting conclusions reached by different research groups originate from their different operating conditions. The stability of $\text{Co}_4(\alpha\text{-PW}_9)_2$ is closely condition-dependent. Thus, the difference in the reaction mechanism with $\text{Co}_4(\alpha\text{-PW}_9)_2$ is understandable.

Although $\text{Co}_4(\alpha\text{-PW}_9)_2$ is stable in the catalytically most relevant pH region of 6–10 where water oxidation is thermodynamically favorable due to the decreasing redox potentials at higher pH values,⁶¹¹ it is not a perfect complex because it is unstable in the presence of an electrode with a high positive bias and at high catalyst concentrations due to the hydrolysis of the Co ion.⁶⁰⁶ The instability of the tetra-Co-sandwiched POM is also observed for $\{[\text{Co}_4(\mu\text{-OH})(\text{H}_2\text{O})_3](\text{Si}_2\text{W}_{19}\text{O}_{70})\}^{11-}$, which has two isomers (Figure 26d,e).⁶¹² The catalyst undergoes slow hydrolysis to more inactive $[\{\text{Co}(\text{H}_2\text{O})\}(\mu\text{-H}_2\text{O})_2\text{K}\{\text{Co}(\text{H}_2\text{O})_4\}(\text{Si}_2\text{W}_{18}\text{O}_{66})]^{11-}$ and $[\text{Co}(\text{H}_2\text{O})\text{SiW}_{11}\text{O}_{39}]^{6-}$ during water oxidation. In terms of the stability, the performance of the mixed-valence monomeric $[\text{Co}^{\text{III}}\text{Co}^{\text{II}}(\text{H}_2\text{O})\text{W}_{11}\text{O}_{39}]^{7-}$ (Figure 26f) having an acitivity comparable to that of $\text{Co}_4(\alpha\text{-PW}_9)_2$ should garner further attention.⁶¹³ In the $[\text{Ru}(\text{bpy})_3]^{2+}/\text{S}_2\text{O}_8^{2-}$ light-driven system, the integrity of the structure keeps well; neither free Co^{2+} ions nor $\text{CoO}_x/\text{Co}(\text{OH})_x$ is produced. The peripheral $\text{Co}^{\text{II}}\text{O}_6$ cluster is proposed as the active site for water oxidation. The central $\text{Co}^{\text{III}}\text{O}_4$ cluster strongly affects the activity of peripheral $\text{Co}^{\text{II}}\text{O}_6$. Additionally, the mixed-valence POM catalyst is electrochemically stable. The remarkable stability of the catalyst is mainly contributed by the central $\text{Co}^{\text{III}}\text{O}_4$.

Most recently, Hill et al. reported an exceptionally fast homogeneous water oxidation catalyst, $[\text{Co}_4(\text{H}_2\text{O})_2(\text{VW}_9\text{O}_{34})_2]^{10-} (\text{Co}_4(\text{VW}_9)_2)$.⁶¹⁴ Although $\text{Co}_4(\text{VW}_9)_2$ and $\text{Co}_4(\text{PW}_9)_2$ have the same charge and very similar geometrical structures, they exhibit different electronic structures and catalytic activities. $\text{Co}_4(\text{VW}_9)_2$ shows a much higher activity than $\text{Co}_4(\text{PW}_9)_2$ under both dark and visible-light-driven conditions. A $1 \mu\text{M}$ concentration of $\text{Co}_4(\text{VW}_9)_2$ gives $\sim 50\%$ conversion of $[\text{Ru}(\text{bpy})_3]^{3+}$ in 0.08 s at pH 9.0 under dark conditions, which is about 20 times faster than that given by $1 \mu\text{M} \text{ Co}_4(\text{PW}_9)_2$ and more than 2 orders of magnitude faster than the self-decomposition rate of $[\text{Ru}(\text{bpy})_3]^{3+}$. On the basis of the initial rate of $[\text{Ru}(\text{bpy})_3]^{3+}$ consumption and the O_2 yields, an initial TOF as high as $1 \times 10^3 \text{ s}^{-1}$ is achieved. In the $[\text{Ru}(\text{bpy})_3]^{2+}/\text{S}_2\text{O}_8^{2-}$ photoinduced system, the final O_2 yield by $\text{Co}_4(\text{VW}_9)_2$ is twice as high as that of using $\text{Co}_4(\text{PW}_9)_2$, and the quantum efficiency of O_2 formation at $6.0 \mu\text{M} \text{ Co}_4(\text{VW}_9)_2$ reaches $\sim 68\%$. To the best of our knowledge, $\text{Co}_4(\text{VW}_9)_2$ is by far the fastest POM water oxidation catalyst. Thus, Hill et al. have made great progress in improving the activity of POM catalysts for water oxidation. In addition, multiple experimental results confirm that $\text{Co}_4(\text{VW}_9)_2$ is a molecular catalyst. The polyanion unit itself, rather than free Co^{2+} ions or CoO_x , is the dominant active catalyst.

The catalytic properties of a nona-Co-containing POM, $[\text{Co}_9(\text{H}_2\text{O})_6(\text{OH})_3(\text{HPO}_4)_2(\text{PW}_9\text{O}_{34})_3]^{16-} (\text{Co}_9(\text{PW}_9)_3)$,⁶¹⁵ was investigated by Galán-Mascarós's group. In chemical water oxidation with NaClO as the oxidant, the catalyst is amazingly stable and robust. When the ratio of catalyst to NaClO is 1:100, the reaction rate with $\text{Co}_9(\text{PW}_9)_3$ is at least 8 times faster than that with $\text{Co}_4(\alpha\text{-PW}_9)_2$ at pH 8. In a pH range of 7–9, the catalytic process can be maintained for several days without fatigue or decomposition of $\text{Co}_9(\text{PW}_9)_3$. The $\text{Co}_9(\text{PW}_9)_3$ -equipped solution that is aged for weeks presents activity identical to that of the freshly prepared one. The electrocatalytic performance of $\text{Co}_9(\text{PW}_9)_3$ is evaluated with fluorine-doped tin oxide coated glass electrodes at reasonable low overpotentials and rates. $\text{Na}_8\text{K}_8[\text{Co}_9(\text{PW}_9)_3]$ is directly put into a sodium phosphate buffer solution. It dissolves into the buffer solution homogeneously. To prevent the deposit of cobalt oxide on the electrode, excess 2,2'-bipyridyl is added to chelate the free Co^{II} ions derived from the decomposition of $\text{Co}_9(\text{PW}_9)_3$. In the reaction process, no heterogeneous species is generated in situ and no residue is left on the electrode. After the reaction cycles, the catalyst can be recovered from the solution by recrystallization with additional alkali-metal cations or by slow evaporation of the reaction medium. The Cs^+ salt of $\text{Co}_9(\text{PW}_9)_3$ is insoluble in water and routine organic solvent. It can be blended into a carbon paste electrode to yield a robust catalytic process.⁶¹⁶ The modified electrode robustly performs for water oxidation toward oxygen in a wide pH range of 1–8. At pH 7, its activity is sustained for at least 8 h, maintaining constant rates without catalytic fatigue or decomposition. In addition, $\text{Co}_9(\text{PW}_9)_3$ is much more active than Co_3O_4 and $\text{Co}(\text{NO}_3)_2$ under the same conditions. The highlight of the catalyst is its remarkable stability at a low pH value (<1.5), where cobalt oxide is unstable. The higher activity compared to those of Co^{2+} and Co_3O_4 at pH 1 suggests that the real active species exclude Co^{2+} and Co_3O_4 . Thus, the catalyst is proposed as a molecular catalyst in the present condition.

Recently, four isostructural catalysts with higher cobalt nuclearity, $\{[\text{Co}_4(\text{OH})_3(\text{PO}_4)]_4(\text{XW}_9\text{O}_{34})_4\}^{n-}$ ($\text{X} = \text{Si}, \text{Ge}, \text{P}, \text{As}; n = 32, 28$) ($\text{Co}_{16}(\text{XW}_9)_4$; Figure 26h), were synthesized

and used as molecular photocatalysts for water oxidation.⁶¹⁷ The activity comparison in the $[\text{Ru}(\text{bpy})_3]^{2+}/\text{S}_2\text{O}_8^{2-}/\text{Co}_{16}(\text{XW}_9)_4$ photoinduced system gives the activity sequence $\text{Co}_{16}(\text{GeW}_9)_4 > \text{Co}_{16}(\text{AsW}_9)_4 > \text{Co}_{16}(\text{SiW}_9)_4 \geq \text{Co}_{16}(\text{PW}_9)_4$. In the presence of these catalysts, O_2 is rapidly formed after 5 min of visible light irradiation at pH 9, and the O_2 evolution rate decreases over time. A maximum value of O_2 yield and O_2 evolution amount are achieved after 90 min of irradiation. The values for $\text{Co}_{16}(\text{GeW}_9)_4$ are 31.0% and 15.5 μmol , respectively. In this case, the TON is 38.75. The initial TOF of $\text{Co}_{16}(\text{GeW}_9)_4$ in the first 300 s is 0.105 s^{-1} . Valuably, the used catalysts ($\text{Co}_{16}(\text{GeW}_9)_4$, $\text{Co}_{16}(\text{SiW}_9)_4$, and $\text{Co}_{16}(\text{PW}_9)_4$) can be readily recrystallized from the photocatalytic systems. X-ray crystallography shows that the polyoxoanion structures are unchanged. Notice that the high cobalt nuclearity is not essential for high activity, although POMs with high cobalt nuclearity show good to excellent performance for water oxidation. Anderson-type $(\text{NH}_4)_3[\text{CoMo}_6\text{O}_{24}\text{H}_6]\cdot 7\text{H}_2\text{O}$ and Evans–Showell-type $(\text{NH}_4)_6[\text{Co}_2\text{Mo}_{10}\text{O}_{38}\text{H}_4]\cdot 7\text{H}_2\text{O}$ even show higher activities than $\text{Co}_4(\alpha\text{-PW}_9)_2$ and $\text{Co}_{16}(\text{GeW}_9)_4$ in the light-driven $[\text{Ru}(\text{bpy})_3]^{2+}/\text{S}_2\text{O}_8^{2-}$ system at pH 8.0.⁶¹⁸

The analogue of $\text{Co}_4(\alpha\text{-PW}_9)_2$ with a different heteroatom, $[\text{Co}_4(\text{H}_2\text{O})_2(\text{SiW}_9\text{O}_{34})_2]^{12-}$, gives an initial TOF of 0.4 s^{-1} with 470 nm visible light illumination in the $[\text{Ru}(\text{bpy})_3]^{2+}/\text{S}_2\text{O}_8^{2-}$ system at pH 5.8.⁶¹⁹ However, the isostructural catalyst $[\text{Ni}_4(\text{H}_2\text{O})_2(\text{SiW}_9\text{O}_{34})_2]^{12-}$ is totally inactive under the same conditions, but we cannot generally say that Ni is an ineffective metal for water oxidation. The penta-Ni-containing POM $[\text{Ni}_5(\text{OH})_6(\text{OH}_2)_3(\text{SiW}_9\text{O}_{33})_2]^{12-}$ ($\text{Ni}_5(\text{SiW}_9)_2$; Figure 26i) efficiently catalyzes both dark water oxidation using $[\text{Ru}(\text{bpy})_3]^{3+}$ as the oxidant and light-driven water oxidation in the $[\text{Ru}(\text{bpy})_3]^{2+}/\text{S}_2\text{O}_8^{2-}$ system.⁶²⁰ During the water oxidation process, $\text{Ni}_5(\text{SiW}_9)_2$ associates with $[\text{Ru}(\text{bpy})_3]^{n+}$ to form the $[\text{Ru}(\text{bpy})_3]^{n+}-\text{Ni}_5(\text{SiW}_9)_2$ complex, which has a very low solubility in the buffer solution and thus exists in the form of nanoparticles. Virtually, the pairing phenomenon is also observed for the small “open” Ru-containing POM catalyst $[\{\text{Ru}_3\text{O}_3(\text{H}_2\text{O})\text{Cl}_2\}(\text{SiW}_9\text{O}_{34})]^{7-}$.⁶¹⁹ The pairing effect may make the POM–photosensitizer assemblies stable and recyclable, prevent POM decomposition into colloidal oxide, and resultantly lead to enhanced catalytic activity.

The activity of the Ir-substituted POM for water oxidation is represented by $[(\text{IrCl}_4)\text{KP}_2\text{W}_{20}\text{O}_{72}]^{14-}$ (Figure 26j). Its catalytic performance is evaluated at pH 7.2 using $[\text{Ru}(\text{bpy})_3]^{3+}$ as the stoichiometric oxidant.⁶²¹ The activity is almost the same as that of IrCl_3 . In the presence of small amounts of catalyst, the reaction time for $[\text{Ru}(\text{bpy})_3]^{3+}$ reduction is shortened from 30 min to less than 3 min, and an oxygen yield of $\sim 30\%$ is reached. However, the catalyst is hydrolytically unstable. It slowly dissociates into $[\text{IrCl}_4(\text{H}_2\text{O})_2]^-$ and $[\text{KP}_2\text{W}_{20}\text{O}_{72}]^{13-}$ in aqueous solution, and the process is completed in 24 h. Fortunately, the rate of the hydrolytic decomposition is ca. 2 orders of magnitude slower than that of water oxidation with $[(\text{IrCl}_4)\text{KP}_2\text{W}_{20}\text{O}_{72}]^{14-}$. Notice that $[(\text{IrCl}_4)\text{KP}_2\text{W}_{20}\text{O}_{72}]^{14-}$ catalyzes water oxidation far faster than authentic IrO_2 nanoparticles under identical conditions. In addition, $[(\text{IrCl}_4)\text{KP}_2\text{W}_{20}\text{O}_{72}]^{14-}$ is a tractable molecular model of iridium supported on redox-active metal oxides, which will serve further research on Ir-catalyzed water oxidation.

Most recently, a tetra-Mn-substituted POM, $[\text{Mn}^{\text{III}}_3\text{Mn}^{\text{IV}}\text{O}_3\text{(CH}_3\text{COO)}_3(\text{A-}\alpha\text{-SiW}_9\text{O}_{34})]^{6-}$ ($\text{Mn}_4(\text{SiW}_9)$), was reported by Bonchio and co-workers.⁶²² The compound contains a mixed-valent $\{\text{Mn}_4\}$ core, which is stabilized by a hybrid set of ligands,

including an inorganic tungstosilicate and three acetate bridges (Figure 26k). It offers an unprecedented mimicry of the natural complex $\text{Mn}_4\text{O}_5\text{Ca}$, which is harbored within photosystem II. Upon the irradiation of visible light, $\text{Mn}_4(\text{SiW}_9)$ undergoes fast and multiple electron transfers, leading to water photooxidation and oxygen evolution. In the $[\text{Ru}(\text{bpy})_3]^{2+}/\text{S}_2\text{O}_8^{2-}$ photo-induced system, oxygen evolution is achieved at pH 5 with a quantum efficiency of 1.7%. To the best of our knowledge, $\text{Mn}_4(\text{SiW}_9)$ is the first Mn-substituted POM that is catalytically active toward photoinduced water oxidation. The hybrid set of ligands provides a coordination environment with both stability and flexibility to assist stepwise one-electron oxidation of the $\{\text{Mn}_4\}$ core and to access high-valent Mn states that are responsible for water oxidation. Tuning the composite ligand set may lower the overpotential and increase the quantum efficiency, resulting in more effective tetra-Mn-substituted POM catalysts for water oxidation.

10. HYDROGEN EVOLUTION

The reduction of H^+ to H_2 provides clean renewable energy. Hence, the reaction has launched great research interest in the scientific community. The process needs two elemental conditions, a H^+ donor and an electron donor. H^+ can be theoretically generated by any compounds with active H^+ , such as alcohols, H_2O_2 , and water, but these compounds can also serve as electron donors. Therefore, the H^+ donor and the electron donor in a H_2 evolution system can be one compound or two different compounds. In all H_2 evolution reactions, those starting with water are the most desirable. However, the reduction process cannot be easily initiated without catalyst. To date, many catalysts have been developed for H_2 evolution. Metal oxide semiconductors are dominant among these catalysts. The catalysts TiO_2 , titanates, Ta_2O_5 , tantalates, In_2O_3 , and indate are well-known in this field.^{623,624} As clusters of metal oxides, POMs have similar electronic and light-absorption characteristics.⁶²⁵ Thus, they pave a new way to develop H_2 evolution catalysts.

POM-catalyzed H_2 evolution is usually driven by light or electricity. In the early years, the performances of $[\text{XW}_{12}\text{O}_{40}]^{n-}$ ($\text{X} = \text{B}, \text{Si}, \text{P}, \text{Ge}, \text{Fe}, \text{Co}$, or H_2),^{626–630} $[\text{W}_6\text{O}_{20}(\text{OH})]^{5-}$,^{631,632} $[\text{W}_{10}\text{O}_{32}]^{4-}$,⁶³³ and $[(\text{Ti}_3\text{GeW}_9\text{O}_{37})_2\text{O}_3]^{14-}$,⁶³⁴ have been evaluated. However, the activation of these catalysts usually needs UV irradiation. From the practical point of view, visible-light-activated POM catalysts are in demand. Considering the high flat band potential required by H^+ reduction, polyoxotungstates, polyoxomolybdates, polyoxoniobates, and polyoxotantalates are potentially useful for H_2 evolution reactions. To date, several POM catalysts containing W, Mo, Nb, and Ta have been exploited for light-driven H_2 evolution, but most of these POM catalysts cannot catalyze the process alone; cocatalysts are usually needed to lower the overpotential for H_2 evolution.⁶³⁵ Pt, NiO, and Co complexes are the most used cocatalysts.

Visible-light-induced H_2 evolution with POM catalysts can be achieved by introducing a photosensitizer into the catalytic system.^{636–639} With eosin Y as the photosensitizer, $[\alpha\text{-AlSiW}_{11}(\text{H}_2\text{O})\text{O}_{39}]^{5-}$ ($\alpha\text{-AlSiW}_{11}$) effectively catalyzes H_2 evolution in aqueous solution in the presence of triethanolamine as the sacrificial electron donor and Pt as the cocatalyst.⁶³⁶ The highest quantum efficiency of 28.0% is achieved under the irradiation of 520 nm monochromatic light. The coordination of eosin Y with $\alpha\text{-AlSiW}_{11}$ during the reaction is beneficial to the charge transfer from eosin Y to $\alpha\text{-AlSiW}_{11}$. In

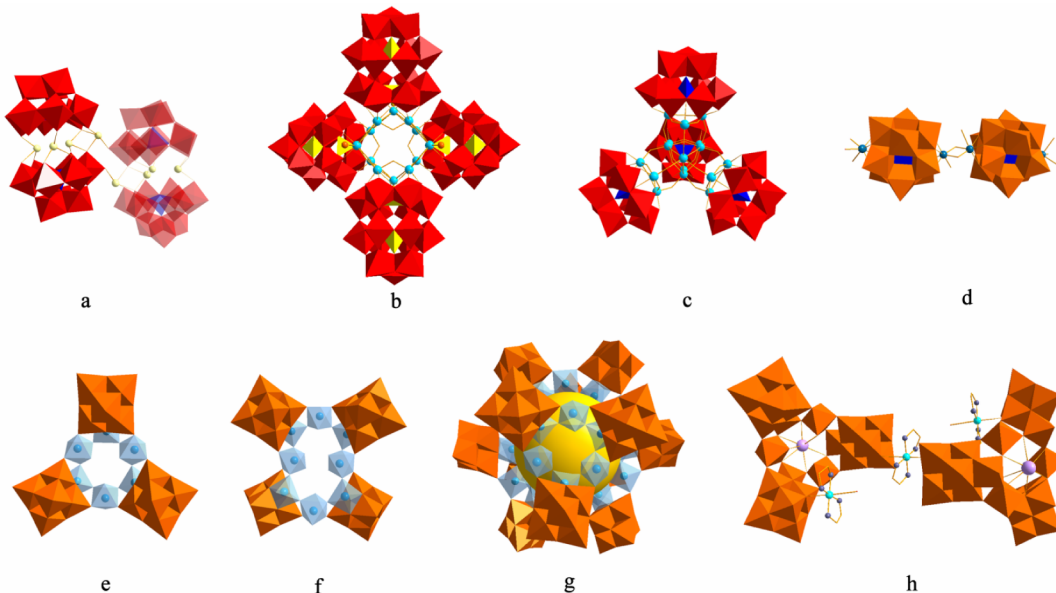


Figure 28. Structures of (a) a dimer of $\text{Sn}_4(\text{SiW}_9)_2$, (b) $\text{Ta}_{12}(\text{P}_2\text{W}_{15})_4$, (c) $\text{Ta}_{16}(\text{SiW}_9)_4$, (d) $[\text{Nb}_2(\text{SiNb}_{12})]$, (e) Nb_{24} , (f) Nb_{32} , (g) Nb_{96} , and (h) $\text{Cu}(\text{en})_2\text{Nb}_{24}$.

2013, Izzet et al. attached an Ir-containing photosensitizer covalently to $[\text{P}_2\text{W}_{17}\text{O}_{61}]^{10-}$.⁶³⁷ The resulting catalyst catalyzes H_2 evolution with a TON of 41 after 7 days of irradiation of visible light in the presence of trimethylamine and acetic acid in DMF. It is notable that no cocatalyst is needed in the system. After that, Hill's group reported a tetra-Mn-sandwiched POM, $\text{Na}_{10}[\text{Mn}_4(\text{H}_2\text{O})_2(\text{VW}_9\text{O}_{34})_2]$ ($\text{Na}_{10}[\text{Mn}_4(\text{VW}_9)_2]$) for H_2 evolution from water with $[\text{Ru}(\text{bpy})_3]^{2+}$ and triethanolamine as the photosensitizer and the sacrificial electron donor, respectively.⁶³⁸ The structure of $\text{Na}_{10}[\text{Mn}_4(\text{VW}_9)_2]$ is similar to that of $\text{Na}_{10}[\text{Co}_4(\alpha\text{-PW}_9)_2]$ (Figure 26c). Without a cocatalyst, $\text{Na}_{10}[\text{Mn}_4(\text{VW}_9)_2]$ provides a TON of 42 after 5.5 h of visible light irradiation. The efficiency of the $\text{Na}_{10}[\text{Mn}_4(\text{VW}_9)_2]$ system is much higher than that of the Ir complex sensitized $[\text{P}_2\text{W}_{17}\text{O}_{61}]^{10-}$. Recently, the same group revealed that the analogue of $\text{Na}_{10}[\text{Mn}_4(\text{VW}_9)_2]$, $\text{Na}_6\text{K}_4[\text{Ni}_4(\text{H}_2\text{O})_2(\text{PW}_9\text{O}_{34})_2]\cdot 32\text{H}_2\text{O}$ ($\text{Na}_6\text{K}_4[\text{Ni}_4(\text{PW}_9)_2]$), works as a more viable and more efficient molecular catalyst for H_2 evolution under visible light irradiation.⁶³⁹ A three-component homogeneous system composed of $[\text{Ir}(\text{ppy})_2(\text{dtbbpy})]^+$ (photosensitizer), triethanolamine (electron donor), and $\text{Na}_6\text{K}_4[\text{Ni}_4(\text{PW}_9)_2]$ (catalyst) affords a TON of ~ 290 after 2.5 h of irradiation, more than 20 times higher than that of $\text{Na}_{10}[\text{Mn}_4(\text{VW}_9)_2]$. The activity comparison between $\text{Na}_6\text{K}_4[\text{Ni}_4(\text{PW}_9)_2]$ and NiCl_2 reveals that $\text{Na}_6\text{K}_4[\text{Ni}_4(\text{PW}_9)_2]$ is much more active than NiCl_2 , which leads to the heterogeneity of the system. Additionally, the catalyst is featured with long-term robustness. In a scale-up experiment, $\text{Na}_6\text{K}_4[\text{Ni}_4(\text{PW}_9)_2]$ works over 1 week nearly without catalytic fatigue or decomposition, reaching a TON of 6500, a remarkable value. However, H_2 evolution is influenced by the concentrations of $\text{Na}_6\text{K}_4[\text{Ni}_4(\text{PW}_9)_2]$, $[\text{Ir}(\text{ppy})_2(\text{dtbbpy})]^+$, and triethanolamine. In the homogeneous system, although the excited state of $[\text{Ir}(\text{ppy})_2(\text{dtbbpy})]^+$ can be both oxidatively and reductively quenched by $\text{Na}_6\text{K}_4[\text{Ni}_4(\text{PW}_9)_2]$ and triethanolamine, respectively, under visible light irradiation, the reductive process is still dominant given the much higher concentration of triethanolamine relative to $\text{Na}_6\text{K}_4[\text{Ni}_4(\text{PW}_9)_2]$.

An inherent problem in developing visible-light-active metal oxide photocatalysts is the low valence band positions of metal oxides due to O 2p (-2.97 eV). Once their conductive bands are high enough for H_2 evolution, the band gaps of oxides will be close to or larger than 3.0 eV, and thus, they are only UV active.⁶⁴⁰ Increasing the valence band position is the only way to achieve visible light H_2 evolution activity of the photocatalysts. Doping TM cations (e.g., Ni^{2+} , Cr^{3+}) or introducing main-group cations (e.g., Sn^{2+} , Pb^{2+} , Bi^{3+}) into the metal oxide photocatalyst can effectively increase the valence band position by hybridization of O 2p with d or s orbitals of metal cations. Owing to the suitable band position of Sn 5s, Sn^{2+} seems to be very useful in the band gap engineering of POM photocatalysts. The catalyst $\text{K}_{11}\text{H}[\text{Sn}_4(\text{SiW}_9\text{O}_{34})_2]$ ($\text{K}_{11}\text{H}[\text{Sn}_4(\text{SiW}_9)_2]$; Figure 28a) is a successful example.⁶⁴¹ In the structure, four Sn^{2+} ions sandwiched by two SiW_9 groups with a 30° rotation angle have different coordination environments. Three Sn^{2+} ions are three-coordinated without the formation of a $\text{Sn}-\text{O}-\text{Sn}$ bond among them, while the fourth one is four-coordinated. It interacts with one terminal O^{2-} of the other catalyst unit to make a dimer. The unique structure and the $\text{Sn}-\text{O}$ dimer endow the photocatalyst with extraordinary stability and a narrower band gap. When 270 mL of solution containing 100 mg of $\text{K}_{11}\text{H}[\text{Sn}_4(\text{SiW}_9)_2]$, 0.5 g of H_2PtCl_6 , and 20% methanol is irradiated by 400 nm visible light, the H_2 evolution rates in five runs are 4.2, 4.9, 4.1, 4.8, and $5.1 \text{ mmol h}^{-1} \text{ g}^{-1}$, respectively. The quantum efficiency at 420 nm reaches up to 0.025%, and the TOF reaches up to 0.025 h^{-1} . The total evolved H_2 is 24 mmol over 56 h, exceeding the amount of the photocatalyst. In a word, the performance of $\text{K}_{11}\text{H}[\text{Sn}_4(\text{SiW}_9)_2]$ presages the promising application of main-group cation-sandwiched POMs in visible light photocatalysis.

Recently, the tetra-Ce-sandwiched POM $\text{TBA}_6\{[\text{Ce}(\text{H}_2\text{O})]_2\cdot [\text{Ce}(\text{CH}_3\text{CN})]_2(\mu_4\text{O})(\gamma\text{-SiW}_{10}\text{O}_{36})_2\}$ ($\text{TBA}_6[\text{Ce}_4(\gamma\text{-SiW}_{10})]$) was proven to be visible-light-responsive.⁶⁴² In the absence of photosensitizer, it effectively catalyzes H_2 evolution under visible light irradiation, using alcohols as the electron donor.⁶⁴³ The system stocked with $\text{TBA}_6[\text{Ce}_4(\gamma\text{-SiW}_{10})]$, H_2PtCl_6 , 4-methoxybenzyl alcohol, and dimethylacetamide gives a TON of

249. The catalyst is highly durable. When the reaction time is prolonged to 80 h, the TON reaches up to 1960. In contrast, no H₂ is evolved in the absence of TBA₆[Ce₄(γ -SiW₁₀)] or using Ce(acac)₃ as a substitute. The activity of TBA₆[Ce₄(γ -SiW₁₀)] is much higher than that of K₁₁H[Sn₄(SiW₉)₂].

Liu's group developed two effective polytantalotungstates, K₈Na₈H₄[P₈W₆₀O₂₃₆Ta₁₂(H₂O)₄(OH)₈]·42H₂O (K₈Na₈H₄·[Ta₁₂(P₂W₁₅)₄]; Figure 28b) and Cs_{10.5}K₄H_{5.5}[Ta₄O₆-(SiW₉Ta₃O₄₀)₄]·30H₂O (Cs_{10.5}K₄H_{5.5}·[Ta₁₆(SiW₉)₄]; Figure 28c), for H₂ evolution.⁶⁴⁴ In the system stocked with methanol and Pt, the H₂ evolution rates of K₈Na₈H₄[Ta₁₂(P₂W₁₅)₄] and Cs_{10.5}K₄H_{5.5}·[Ta₁₆(SiW₉)₄] are 1250 and 803 $\mu\text{mol h}^{-1} \text{g}^{-1}$, respectively, under 250 W high-pressure Hg lamp irradiation. The values are much higher than that of the control catalyst K₆P₂W₁₈ (297 $\mu\text{mol h}^{-1} \text{g}^{-1}$). The higher activities of K₈Na₈H₄[Ta₁₂(P₂W₁₅)₄] and Cs_{10.5}K₄H_{5.5}·[Ta₁₆(SiW₉)₄] than that of K₆P₂W₁₈ indicate that the incorporation of Ta into the W-based cluster has a positive effect on the photocatalytic activity. This may be caused by the modulation of the electronic structure by the method of mixing the W 5d and Ta 5d orbitals and specifically raising the LUMO level of the polytantalotungstates with respect to Ta-free polyoxotungstate. The activity difference between K₈Na₈H₄[Ta₁₂(P₂W₁₅)₄] and Cs_{10.5}K₄H_{5.5}·[Ta₁₆(SiW₉)₄] is rationalized by their different structures. Among all known polyoxotungstates, K₈Na₈H₄[Ta₁₂(P₂W₁₅)₄] exhibits the highest catalytic activity for H₂ evolution. In the presence of 0.3 g of K₈Na₈H₄[Ta₁₂(P₂W₁₅)₄], a 270 mL solution containing 50 mL of methanol evolves 4.5 mmol of H₂ over 12 h, and the TON is 247. The high activity remains for at least 36 h without an obvious decline. Most importantly, K₈Na₈H₄[Ta₁₂(P₂W₁₅)₄] can be regenerated and recovered by exposing it to air or oxygen.

Feng's group reported a polyoxoniobate, K₁₀[Nb₂O₂(H₂O)₂][SiNb₁₂O₄₀]·12H₂O (K₁₀[Nb₂(SiNb₁₂)]; Figure 28d), for light-driven H₂ evolution.⁶⁴⁵ In the POM structure, the bridging Nb⁵⁺ site is seven-coordinated with four O²⁻ anions from the Keggin cluster, two bridging O²⁻ sites shared with another Nb⁵⁺, and one water molecule. The seven-coordination trains a distorted TbO₇. Using Pt as the cocatalyst, the rate of H₂ evolution reaches up to about 2100 $\mu\text{mol h}^{-1} \text{g}^{-1}$ with a 300 W Xe lamp in 20% methanol solution. The system stocked with 100 mg of 0.5% Pt-loaded K₁₀[Nb₂(SiNb₁₂)] and 270 mL of a 20% methanol mixed aqueous solution evolves 1616 μmol of H₂ over 7.5 h, with a TON of 44. However, the analogous polyoxoniobate Na₁₀[Nb₂O₂][SiNb₁₂O₄₀]·12H₂O (Na₁₀[Nb₂(SiNb₁₂)']) having a band gap and BET surface area comparable to those of K₁₀[Nb₂(SiNb₁₂)] gives a H₂ evolution rate of 1205 $\mu\text{mol h}^{-1} \text{g}^{-1}$ under the totally identical conditions. Ruling out the effect of the band gap and BET surface area, the great activity difference between the two compounds should be attributed to the fine distinction in their structures. The H₂O molecules directly bonded to Nb and the distortion of NbO₇ in K₁₀[Nb₂(SiNb₁₂)], which are absent in Na₁₀[Nb₂(SiNb₁₂)'], are regarded as the main reasons for the higher activity of K₁₀[Nb₂(SiNb₁₂)]. The distorted configuration of NbO₇ can create a large dipole moment in the materials that facilitates the electron–hole charge separation.^{646–649} Therefore, the electron–hole separation and the coordination of water to Nb sites are easier for K₁₀[Nb₂(SiNb₁₂)], and consequently, more long-lived charge trapping states exist in K₁₀[Nb₂(SiNb₁₂)]. In combination with the photosensitizer [Ru(bpy)₃]²⁺, K₁₀[Nb₂(SiNb₁₂)]-catalyzed H₂ evolution can be conducted under visible light. Additionally, with K₁₀[Nb₂(SiNb₁₂)] as the

catalyst and NiO as the cocatalyst, both H₂ and O₂ evolve at rates of 222 and 97 $\mu\text{mol h}^{-1} \text{g}^{-1}$, respectively, in pure water without additional sacrificial electron donor under UV irradiation. The total H₂ evolved over 3.5 h is 35 μmol , about twice the amount of the used photocatalyst, confirming the photocatalytic nature of K₁₀[Nb₂(SiNb₁₂)]. In this pure water system, water acts as both a H⁺ donor and an electron donor. Thus, H₂ and O₂ are obtained simultaneously in a ratio of 2.3:1.

Wang's group developed three polyoxoniobates for homogeneous photocatalytic H₂ evolution, which were formulated as KNa₂[Nb₂₄O₇₂H₂₁]·38H₂O (KNa₂Nb₂₄; Figure 28e), K₂Na₂·[Nb₃₂O₉₆H₂₈]·80H₂O (K₂Na₂Nb₃₂; Figure 28f), and K₁₂·[Nb₂₄O₇₂H₂₁]₄·107H₂O (K₁₂Nb₉₆) (Figure 28g), respectively.⁶⁵⁰ With 100 mg of KNa₂Nb₂₄ as the catalyst, 0.25 mmol of Co^{III}(dmgh)₂pyCl as the cocatalyst, and 10% triethylamine as the sacrificial agent (in a 100 mL aqueous solution), the H₂ evolution rates in three runs are 5161.4, 5233.5, and 5186.7 $\mu\text{mol h}^{-1} \text{g}^{-1}$, respectively, under UV irradiation by a 500 W Hg lamp, and the total evolved H₂ over 12 h is 6232.7 μmol . For K₂Na₂Nb₃₂, the H₂ evolution rates in three runs are 5312.5, 5032.5, and 4824.3 $\mu\text{mol h}^{-1} \text{g}^{-1}$, and the total H₂ evolved over 12 h is 6069.6 μmol . For K₁₂Nb₉₆, the H₂ evolution rates in three runs are 4804.1, 4802.3, and 4537.7 $\mu\text{mol h}^{-1} \text{g}^{-1}$, respectively, and the total evolved H₂ over 12 h is 5657.6 μmol . In these systems, triethylamine cannot donate H⁺. It only acts as an electron donor. Indubitably, the H atoms in H₂ come from water. The control experiments indicate that H₂ evolution cannot proceed in the absence of the catalyst. The cocatalyst Co^{III}(dmgh)₂pyCl alone cannot catalyze the reaction. The catalysts K₂Na₂Nb₃₂ and K₁₂Nb₉₆ also work well in the combination with Pt in place of Co^{III}(dmgh)₂pyCl. Although the activities of these oxoniobium clusters are inferior to that of the related heterogeneous catalyst KTaO₃, there is much room for improvement. Significantly, these catalysts afford new opportunities for developing polyoxoniobate chemistry and highly efficient photocatalysts.

With the expectation of extending the absorbed light by oxoniobium clusters to the visible region, a copper(II)–ethylenediamine (Cu(en)₂) complex having a strong absorption in the visible light region is introduced into polyoxoniobates.⁶⁵¹ The resulting dimer [Cu(en)₂]₁₁K₄·Na₂[KNb₂₄O₇₂H₉]₂·120H₂O (Cu(en)₂Nb₂₄; Figure 28h) presents strong absorption in a wide wavelength range from the UV to visible light region. However, the precursor of K₈[Nb₆O₁₉]·16H₂O only presents absorption in the UV region. When the system stocked with 100 mg of Cu(en)₂Nb₂₄, 0.25 mmol of Co^{III}(dmgh)₂pyCl, and 100 mL of 10% triethylamine aqueous solution is exposed to visible light irradiation of a 500 W Xe lamp with a 400 nm cutoff filter, the H₂ evolution rates in five runs are 14.0, 14.8, 13.6, 13.9, and 13.2 $\mu\text{mol h}^{-1} \text{g}^{-1}$, respectively. The total evolved H₂ over 50 h is 79.5 μmol . The results under UV irradiation are much better than those obtained under visible light due to the synergistic effect of Cu(en)₂ and the oxoniobium clusters, which occurs during the process of photoexcitation.⁵⁰ With Pt as the cocatalyst, the activity of Cu(en)₂Nb₂₄ is as high as that of K₁₀[Nb₂(SiNb₁₂)] under UV light irradiation, and much higher than that of dye-sensitized K₁₀[Nb₂(SiNb₁₂)] under visible light irradiation. The results with Cu(en)₂Nb₂₄ are also obviously better than those with the Cu-connected polyoxomolybdate Cu₈BBTZ₆[$(\alpha$ -Mo₈O₂₆) $(\beta$ -Mo₈O₂₆)], Cu₃BBTZ₅[β -Mo₈O₂₆], and Cu₄BBTZ₄[$[\text{Mo}_7\text{CuO}_{24}(\text{H}_2\text{O})_2]\cdot6\text{H}_2\text{O}$ (BBTZ = 1,4-bis(1,2,4-triazol-1-

ylmethyl)benzene).⁶⁵² Thus, organic ligand modified polyoxoniobates have potential in visible-light-driven catalysis.

Electricity-driven H₂ evolution abandons the consumption of an organic sacrificial agent. Besides the aforementioned Ru₄(γ -SiW₁₀)₂@MWCNT,⁵⁸⁹ the polyoxomolybdate of TBA₃⁺[PMo₈Mo^{VI}₄O₃₆(OH)₄Zn₄]²⁻[C₆H₅(COO)₃]_{4/3}·6H₂O (ϵ -(trim)_{4/3}) also serves the process.⁶⁵³ The working electrode ϵ -(trim)_{4/3}/CPE made by entrapping ϵ -(trim)_{4/3} in a carbon paste electrode (CPE) shows a notable catalytic performance for electrocatalytic H₂ evolution in Li⁺ supporting electrolyte. On the basis of the consumed charge, a yield higher than 95% is achieved. Electrolysis conducted at $\eta = 200$ mV consumes 728.4 C, and gives a TON of 1.2×10^5 after 5 h (TOF = 6.7 s⁻¹), comparing well with those of biomimetic nickel complexes covalently attached⁶⁵⁴ or physisorbed⁶⁵⁵ on carbon nanotubes. The ϵ -(trim)_{4/3}/CPE electrode is stable, and its activity keeps well during the electrolysis process. Moreover, the composite electrode ϵ -(trim)_{4/3}/CPE is more active than the Pt electrode because of the introduction of proton-accepting basic sites into the structure and the presence of channels in which cations are confined. The activity of ϵ -(trim)_{4/3}/CPE is significantly affected by the cations in the electrolyte. When Li⁺ is replaced by Na⁺ or K⁺, the activity of ϵ -(trim)_{4/3} is 2.8 and 2.5 times less active, respectively; when it is replaced by Cs⁺, ϵ -(trim)_{4/3} is inactive. These results are in line with the sizes of the hydrated alkali-metal ions: Li⁺ (340 pm) > Na⁺ (276 pm) > K⁺ (232 pm) > Cs⁺ (226 pm). Considering the radius of the unhydrated TBA⁺ cation (494 pm), hydrated lithium appears as the cation most likely to ensure the cohesion of the ϵ -(trim)_{4/3} network. Besides, the cations with larger radii carry water molecules into the ϵ -(trim)_{4/3} framework, a favorable microenvironment for H₂ evolution reaction, more easily.

The electrochemical H₂ evolution usually involves a two-electron-transfer mechanism. In the first step, a proton accepts an electron to form a catalyst-bound hydrogen intermediate H* (H⁺ + e⁻ → H*). In the second step, either two H* atoms recombine or a H* reacts with a proton and an electron to form H₂ (H⁺ + H* + e⁻ → H₂).⁶⁵⁶ A good catalyst should bind the intermediate H* moderately, neither too strongly nor too weakly. The performances of Cu₃(Mo₈O₂₆)(H₂O)₂(OH)₂(L₁)₄ (L₁ = 4H-4-amino-1,2,4-triazole) and Ag₄(Mo₈O₂₆)(L₂)_{2.5}·(H₂O) (L₂ = 3,5-dimethyl-4-amino-4H-1,2,4-triazole) for H₂ evolution were reported in 2013.⁶⁵⁷ With the Cu complex, a 98% faradic efficiency and a TON of 2.6×10^3 are obtained under the conditions of 0.5 M H₂SO₄, a sweep rate of 50 mV·s⁻¹, $\eta = -0.56$ V, and a current density of 0.1 μ A/cm². The values for the Ag complex are 97% and 3.0×10^2 , respectively. For both catalysts, the electrocatalytic current grows larger with increasing acid concentrations. The catalysts can lower the overpotential of H₂ evolution owing to the binding of H* by the Cu or Ag site. Due to the different unsaturated coordinations, the binding abilities of Cu and Ag are different. The reduction overpotential of H⁺ at the Cu complex modified carbon glassy electrode (-0.43 V) is more positive than that at the Ag complex modified carbon glassy electrode (-0.49 V), indicating the Cu complex is more effective than the Ag complex. The result is evidenced by different TON values. The free ligands L₁ and L₂ cannot catalyze the H₂ evolution reaction. The main catalytic function is contributed by the [Mo₈O₂₆]⁴⁻ moiety with superior redox properties, and the MOF moiety is responsible for the binding of H*. Thus, the two catalysts can be regarded as binary catalysts.

11. CONCLUSION AND PERSPECTIVES

This review describes various reactions catalyzed by POMs, including oxidation reactions, reduction reactions, acid-catalyzed reactions, base-catalyzed reactions, water splitting to O₂ and/or H₂, etc. In these reactions, POM catalysts elegantly exhibit their efficiency and stability, especially in moisture- and oxygen-rich environments. The reviewed examples fully illustrate that the catalytic properties of POMs can be tuned finely upon the consideration of satisfying the requirements of different reactions and bifunctional catalysts can be easily constructed due to the multiple catalytic functionalities and easy modification of POMs. Especially, these bifunctional POM catalysts make some cascade reactions proceed smoothly in one pot, and thus afford simple schemes for organic synthesis. Thus, they are of great importance in enhancing the productivity and simplifying the procedures of the overall reactions. In brief, POM catalysts are inherently stable, effective, and designable. These advantages make POM catalysts outstanding candidates for industrial catalysts.

Considering the diversity of the metals introduced into POM catalysts, the reactions with POM catalysts can be extended to a wider scope. Apart from the aforementioned reactions, other reactions belonging to oxidation, reduction, and acid/base-catalyzed reactions can be tried with expectations. Creatively, reactions excluded by these types should be in consideration because POM catalysts can be regarded as metal complexes with multidentate oxo ligands. Theoretically, those catalyzed by organometallic complexes can probably be promoted by POM catalysts with appropriate TMs and inorganic oxygen ligands. The bulky inorganic ligands are likely to yield interesting results. Thus, POM catalysts deserve more endeavors.

AUTHOR INFORMATION

Corresponding Author

*E-mail: ygy@fjirsm.ac.cn; ygy@bit.edu.cn. Fax: (+)86-591-8371-0051. Phone: (+)86-10-6891-8572.

Notes

The authors declare no competing financial interest.

Biographies



Sa-Sa Wang was born in Henan Province, China, in 1986. She received her B.S. degree in chemistry from Henan University in 2007 and then her Ph.D. degree in physical chemistry from East China Normal University in 2012. Since the summer of 2012, she has worked as a research associate at the Fujian Institute of Research on the Structure of Matter, Chinese Academy of Sciences. Her research topics focus on the synthesis and catalytic applications of oxometal clusters.



Guo-Yu Yang received his M.S. and Ph.D. degrees from Jilin University in 1991 and 1998, respectively. In 1991, he joined the faculty at Jilin University. From 1998 to 2001, he worked as a postdoctoral researcher at the University of Notre Dame and Stockholm University successively. He moved to the Fujian Institute of Research on the Structure of Matter, Chinese Academy of Sciences, in 2001 as a professor of chemistry. He was awarded the Cheung Kong Professorship in 2009. His research interest is focused on (1) oxo cluster chemistry, including transition-metal, main-group, and rare-element clusters, and (2) functionality of oxo clusters, including nonlinear optical properties, magnetic properties, and catalytic properties.

ACKNOWLEDGMENTS

We gratefully acknowledge financial support from the National Natural Science Foundation of China (NSFC) for Distinguished Young Scholars (Grant 20725101), the NSFC (Grants 91122028, 21221001, 50872133, and 21403236), and the 973 Program (Grants 2014CB932101 and 2011CB932504).

REFERENCES

- (1) Pope, M. T. *Heteropoly and Isopoly Oxometalates*, 8th ed.; Springer Verlag: New York, 1983.
- (2) Bassil, B. S.; Ibrahim, M.; Al-Oweini, R.; Asano, M.; Wang, Z.; van Tol, J.; Dalal, N. S.; Choi, K. Y.; Ngo Biboum, R.; Keita, B.; Nadjo, L.; Kortz, U. *Angew. Chem., Int. Ed.* **2011**, *50*, 5961.
- (3) Lydon, C.; Busche, C.; Miras, H. N.; Delf, A.; Long, D. L.; Yellowlees, L.; Cronin, L. *Angew. Chem., Int. Ed.* **2012**, *51*, 2115.
- (4) Mitchell, S. G.; Molina, P. I.; Khanra, S.; Miras, H. N.; Prescimone, A.; Cooper, G. J.; Winter, R. S.; Brechin, E. K.; Long, D. L.; Cogdell, R. J.; Cronin, L. *Angew. Chem., Int. Ed.* **2011**, *50*, 9154.
- (5) Botar, B.; Ellern, A.; Hermann, R.; Kogerler, P. *Angew. Chem., Int. Ed.* **2009**, *48*, 9080.
- (6) Yan, J.; Long, D. L.; Miras, H. N.; Cronin, L. *Inorg. Chem.* **2010**, *49*, 1819.
- (7) Pradeep, C. P.; Long, D. L.; Cronin, L. *Dalton Trans.* **2010**, *39*, 9443.
- (8) Hill, C. L.; White, G. C. *Chem. Rev.* **1998**, *98*, 1.
- (9) Kozhevnikov, I. V. *Chem. Rev.* **1998**, *98*, 171.
- (10) Mizuno, N.; Misono, M. *Chem. Rev.* **1998**, *98*, 199.
- (11) Sadakane, M.; Steckhan, E. *Chem. Rev.* **1998**, *98*, 219.
- (12) Kozhevnikov, I. V. *Catalysts for Fine Chemical Synthesis: Catalysis by Polyoxometalates*; Wiley: Chichester, U.K., 2002.
- (13) Mizuno, N.; Kamata, K.; Uchida, S.; Yamaguchi, K. In *Modern Heterogeneous Oxidation Catalysis*; Mizuno, N., Ed.; Wiley-VCH: Weinheim, Germany, 2009.
- (14) Muller, A.; Peters, F.; Pope, M. T.; Gatteschi, D. *Chem. Rev.* **1998**, *98*, 239.
- (15) Yamase, T. *Chem. Rev.* **1998**, *98*, 307.
- (16) Coronado, E.; Gomez-Garcia, C. J. *Chem. Rev.* **1998**, *98*, 273.
- (17) Rhule, J. T.; Hill, C. L.; Judd, D. A. *Chem. Rev.* **1998**, *98*, 327.
- (18) Macht, J.; Janik, M. J.; Neurock, M.; Iglesia, E. *Angew. Chem., Int. Ed.* **2007**, *46*, 7864.
- (19) Weissermel, K.; Arpe, H. J. *Industrial Organic Chemistry*, 3rd ed.; VCH: Weinheim, Germany, 1997.
- (20) Misono, M.; Nojiri, N. *Appl. Catal.* **1990**, *64*, 1.
- (21) Izumi, Y. *Catal. Today* **1997**, *33*, 371.
- (22) Izumi, Y.; Urabe, K.; Onaka, M. *Zaolite, Clay and Heteropoly Acid in Organic Reactions*; Kodansha/VCH: Tokyo, 1992.
- (23) Aoshima, A.; Tonomura, S.; Yamamatsu, S. *Polym. Adv. Technol.* **1990**, *2*, 127.
- (24) Armor, J. N. *Appl. Catal., A: Gen.* **2001**, *222*, 407.
- (25) Sano, K.; Uchida, H.; Wakabayashi, S. *Catal. Surv. Asia* **1999**, *3*, 55.
- (26) Howard, M. J.; Sunley, G. J.; Poole, A. D.; Watt, R. J.; Sharma, B. K. *Stud. Surf. Sci. Catal.* **1999**, *121*, 61.
- (27) Nakagawa, Y.; Mizuno, N. *Inorg. Chem.* **2007**, *46*, 1727.
- (28) Balula, M. S. S.; Santos, I. C. M. S.; Simões, M. M. Q.; Neves, M. G. P. M. S.; Cavaleiro, J. A. S.; Cavaleiro, A. M. V. *J. Mol. Catal. A: Chem.* **2004**, *222*, 159.
- (29) Khenkin, A. M.; Shimon, L. J. W.; Neumann, R. *Inorg. Chem.* **2003**, *42*, 3331.
- (30) Boglio, C.; Lemiere, G.; Hasenkopf, B.; Thorimbert, S.; Lacote, E.; Malacria, M. *Angew. Chem., Int. Ed.* **2006**, *45*, 3324.
- (31) Kikukawa, Y.; Yamaguchi, S.; Nakagawa, Y.; Uehara, K.; Uchida, S.; Yamaguchi, K.; Mizuno, N. *J. Am. Chem. Soc.* **2008**, *130*, 15872.
- (32) Kikukawa, Y.; Yamaguchi, S.; Tsuchida, K.; Nakagawa, Y.; Uehara, K.; Yamaguchi, K.; Mizuno, N. *J. Am. Chem. Soc.* **2008**, *130*, 5472.
- (33) Pathan, S.; Patel, A. *Dalton Trans.* **2013**, *42*, 11600.
- (34) Kamata, K.; Nakagawa, Y.; Yamaguchi, K.; Mizuno, N. *J. Am. Chem. Soc.* **2008**, *130*, 15304.
- (35) Boldini, I.; Guillemot, G.; Caselli, A.; Proust, A.; Gallo, E. *Adv. Synth. Catal.* **2010**, *352*, 2365.
- (36) Kozhevnikov, I. V. *J. Mol. Catal. A: Chem.* **2007**, *262*, 86.
- (37) Shinachi, S.; Matsushita, M.; Yamaguchi, K.; Mizuno, N. *J. Catal.* **2005**, *233*, 81.
- (38) Molinari, J. E.; Nakka, L.; Kim, T.; Wachs, I. E. *ACS Catal.* **2011**, *1*, 1536.
- (39) Knapp, C.; Ui, T.; Nagai, K.; Mizuno, N. *Catal. Today* **2001**, *71*, 111.
- (40) Kamata, K.; Yamaguchi, K.; Hikichi, S.; Mizuno, N. *Adv. Synth. Catal.* **2003**, *345*, 1193.
- (41) Sloboda-Rozner, D.; Witte, P.; Alsters, P. L.; Neumann, R. *Adv. Synth. Catal.* **2004**, *346*, 339.
- (42) Botar, B.; Geletii, Y. V.; Kögerler, P.; Musaev, D. G.; Morokuma, K.; Weinstock, I. A.; Hill, C. L. *J. Am. Chem. Soc.* **2006**, *128*, 11268.
- (43) Haimov, A.; Neumann, R. *J. Am. Chem. Soc.* **2006**, *128*, 15697.
- (44) Rezaeifard, A.; Haddad, R.; Jafarpour, M.; Hakimi, M. *J. Am. Chem. Soc.* **2013**, *135*, 10036.
- (45) Carraro, M.; Nsouli, N.; Oelrich, H.; Sartorel, A.; Soraru, A.; Mal, S. S.; Scorrano, G.; Walder, L.; Kortz, U.; Bonchio, M. *Chem.—Eur. J.* **2011**, *17*, 8371.
- (46) Mal, S. S.; Nsouli, N. H.; Carraro, M.; Sartorel, A.; Scorrano, G.; Oelrich, H.; Walder, L.; Bonchio, M.; Kortz, U. *Inorg. Chem.* **2010**, *49*, 7.
- (47) Ding, Y.; Zhao, W.; Song, W.; Zhang, Z.; Ma, B. *Green Chem.* **2011**, *13*, 1486.
- (48) Lv, H. J.; Geletii, Y. V.; Zhao, C. C.; Vickers, J. W.; Zhu, G. B.; Luo, Z.; Song, J.; Lian, T. Q.; Musaev, D. G.; Hill, C. L. *Chem. Soc. Rev.* **2012**, *41*, 7572.
- (49) Mizuno, N.; Kamata, K. *Coord. Chem. Rev.* **2011**, *255*, 2358.
- (50) Guo, Y. H.; Hu, C. W. *J. Mol. Catal. A: Chem.* **2007**, *262*, 136.
- (51) Papaconstantinou, E. *Chem. Soc. Rev.* **1989**, *18*, 1.
- (52) Bonchio, M.; Carraro, M.; Scorrano, G.; Fontananova, E.; Drioli, E. *Adv. Synth. Catal.* **2003**, *345*, 1119.
- (53) Farhadi, S.; Afshari, M.; Maleki, M.; Babazadeh, Z. *Tetrahedron Lett.* **2005**, *46*, 8483.
- (54) Troupis, A.; Hiskia, A.; Papaconstantinou, E. *Angew. Chem., Int. Ed.* **2002**, *41*, 1911.

- (55) Schulz, M.; Paulik, C.; Knor, G. *J. Mol. Catal. A: Chem.* **2011**, *347*, 60.
- (56) Bonchio, M.; Carraro, M.; Scorrano, G.; Bagno, A. *Adv. Synth. Catal.* **2004**, *346*, 648.
- (57) Molinari, A.; Varani, G.; Polo, E.; Vaccari, S.; Maldotti, A. *J. Mol. Catal. A: Chem.* **2007**, *262*, 156.
- (58) Khenkin, A. M.; Efremenko, I.; Weiner, L.; Martin, J. M. L.; Neumann, R. *Chem.—Eur. J.* **2010**, *16*, 1356.
- (59) Ettedgui, J.; Diskin-Posner, Y.; Weiner, L.; Neumann, R. *J. Am. Chem. Soc.* **2011**, *133*, 188.
- (60) Ozer, R. R.; Ferry, J. L. *J. Phys. Chem. B* **2002**, *106*, 4336.
- (61) Gao, S. Y.; Cao, R.; Lu, J.; Li, G. L.; Li, Y. F.; Yang, H. X. *J. Mater. Chem.* **2009**, *19*, 4157.
- (62) Fu, Z. Y.; Zeng, Y.; Liu, X. L.; Song, D. S.; Liao, S. J.; Dai, J. C. *Chem. Commun.* **2012**, *48*, 6154.
- (63) Guo, Y. H.; Wang, Y. H.; Hu, C. W.; Wang, Y. H.; Wang, E. B.; Zhou, Y. C.; Feng, S. H. *Chem. Mater.* **2000**, *12*, 3501.
- (64) Yang, H. X.; Liu, T. F.; Cao, M. N.; Li, H. F.; Gao, S. Y.; Cao, R. *Chem. Commun.* **2010**, *46*, 2429.
- (65) Biboum, R. N.; Doungmene, F.; Keita, B.; de Oliveira, P.; Nadjo, L.; Lepoittevin, B.; Roger, P.; Brisset, F.; Mialane, P.; Dolbecq, A.; Mbomekalle, I. M.; Pichon, C.; Yin, P. C.; Liu, T. B.; Contant, R. *J. Mater. Chem.* **2012**, *22*, 319.
- (66) Lei, P. X.; Chen, C. C.; Yang, J.; Ma, W. H.; Zhao, J. C.; Zang, L. *Environ. Sci. Technol.* **2005**, *39*, 8466.
- (67) Yue, B.; Zhou, Y.; Xu, J. Y.; Wu, Z. Z.; Zhang, X. A.; Zou, Y. F.; Jin, S. L. *Environ. Sci. Technol.* **2002**, *36*, 1325.
- (68) Dolbecq, A.; Mialane, P.; Keita, B.; Nadjo, L. *J. Mater. Chem.* **2012**, *22*, 24509.
- (69) Tucher, J.; Wu, Y. L.; Nye, L. C.; Ivanovic-Burmazovic, I.; Khusniyarov, M. M.; Streb, C. *Dalton Trans.* **2012**, *41*, 9938.
- (70) Rengifo-Herrera, J. A.; Blanco, M. N.; Pizzio, L. R. *Appl. Catal., B: Environ.* **2011**, *110*, 126.
- (71) Troupis, A.; Hiskia, A.; Papaconstantinou, E. *Environ. Sci. Technol.* **2002**, *36*, 5355.
- (72) Marci, G.; Garcia-Lopez, E. I.; Palmisano, L. *Appl. Catal., A: Gen.* **2012**, *421*, 70.
- (73) Marci, G.; Garcia-Lopez, E.; Bellardita, M.; Parisi, F.; Colbeau-Justin, C.; Sorgues, S.; Liotta, L. F.; Palmisano, L. *Phys. Chem. Chem. Phys.* **2013**, *15*, 13329.
- (74) Streb, C. *Dalton Trans.* **2012**, *41*, 1651.
- (75) Li, K. X.; Yang, X.; Guo, Y. N.; Ma, F. Y.; Li, H. C.; Chen, L.; Guo, Y. H. *Appl. Catal., B: Environ.* **2010**, *99*, 364.
- (76) Li, D. F.; Guo, Y. H.; Hu, C. W.; Jiang, C. J.; Wang, E. B. *J. Mol. Catal. A: Chem.* **2004**, *207*, 183.
- (77) Yang, Y.; Wu, Q. Y.; Guo, Y. H.; Hu, C. W.; Wang, E. J. *Mol. Catal. A: Chem.* **2005**, *225*, 203.
- (78) Zhang, S. Q.; Chen, L.; Liu, H. B.; Guo, W.; Yang, Y. X.; Guo, Y. H.; Huo, M. X. *Chem. Eng. J.* **2012**, *200*, 300.
- (79) Li, L.; Wu, Q. Y.; Guo, Y. H.; Hu, C. W. *Microporous Mesoporous Mater.* **2005**, *87*, 1.
- (80) Li, D. F.; Guo, Y. H.; Hu, C. W.; Mao, L.; Wang, E. *Appl. Catal., A: Gen.* **2002**, *235*, 11.
- (81) Guo, Y. H.; Hu, C. W.; Jiang, S. C.; Guo, C. X.; Yang, Y.; Wang, E. *Appl. Catal., B: Environ.* **2002**, *36*, 9.
- (82) Guo, Y. H.; Hu, C. W.; Wang, X. L.; Wang, Y. H.; Wang, E. B.; Zou, Y. C.; Ding, H.; Feng, S. H. *Chem. Mater.* **2001**, *13*, 4058.
- (83) Guo, Y. H.; Hu, C. W.; Jiang, C. J.; Yang, Y.; Jiang, S. C.; Li, X. L.; Wang, E. B. *J. Catal.* **2003**, *217*, 141.
- (84) Guo, Y. H.; Yang, Y.; Hu, C. W.; Guo, C. X.; Wang, E. B.; Zou, Y. C.; Feng, S. H. *J. Mater. Chem.* **2002**, *12*, 3046.
- (85) Farhadi, S.; Zaidi, M. *Appl. Catal., A: Gen.* **2009**, *354*, 119.
- (86) Qu, X. S.; Guo, Y. H.; Hu, C. W. *J. Mol. Catal. A: Chem.* **2007**, *262*, 128.
- (87) Yang, Y.; Guo, Y. H.; Hu, C. W.; Wang, E. *Appl. Catal., A: Gen.* **2003**, *252*, 305.
- (88) Yang, Y.; Guo, Y. H.; Hu, C. W.; Jiang, C. J.; Wang, E. B. *J. Mater. Chem.* **2003**, *13*, 1686.
- (89) Friesen, D. A.; Gibson, D. B.; Langford, C. H. *Chem. Commun.* **1998**, *543*.
- (90) Marci, G.; Garcia-Lopez, E. I.; Palmisano, L. *Eur. J. Inorg. Chem.* **2014**, *2014*, 21.
- (91) Sivakumar, R.; Thomas, J.; Yoon, M. *J. Photochem. Photobiol. C* **2012**, *13*, 277.
- (92) Keita, B.; Nadjo, L. *J. Mol. Catal. A: Chem.* **2007**, *262*, 190.
- (93) Li, G.; Ding, Y.; Wang, J.; Wang, X.; Suo, J. *J. Mol. Catal. A: Chem.* **2007**, *262*, 67.
- (94) Bielański, A.; Lubańska, A.; Micek-Ilnicka, A.; Poźniczek, J. *Coord. Chem. Rev.* **2005**, *249*, 2222.
- (95) Sumliner, J. M.; Lv, H.; Fielden, J.; Geletii, Y. V.; Hill, C. L. *Eur. J. Inorg. Chem.* **2014**, *2014*, 635.
- (96) Sun, M.; Zhang, J.; Putaj, P.; Caps, V.; Lefebvre, F.; Pelletier, J.; Bassett, J.-M. *Chem. Rev.* **2013**, *114*, 981.
- (97) Kozhevnikov, I. V. *Appl. Catal., A: Gen.* **2003**, *256*, 3.
- (98) Miras, H. N.; Yan, J.; Long, D. L.; Cronin, L. *Chem. Soc. Rev.* **2012**, *41*, 7403.
- (99) Song, Y. F.; Tsunashima, R. *Chem. Soc. Rev.* **2012**, *41*, 7384.
- (100) Muller, A.; Gouzerh, P. *Chem. Soc. Rev.* **2012**, *41*, 7431.
- (101) Banerjee, A.; Bassil, B. S.; Rosenthaler, G. V.; Kortz, U. *Chem. Soc. Rev.* **2012**, *41*, 7590.
- (102) Long, D. L.; Tsunashima, R.; Cronin, L. *Angew. Chem., Int. Ed.* **2010**, *49*, 1736.
- (103) Clemente-Juan, J. M.; Coronado, E.; Gaita-Arino, A. *Chem. Soc. Rev.* **2012**, *41*, 7464.
- (104) Wang, Y.; Weinstock, I. A. *Chem. Soc. Rev.* **2012**, *41*, 7479.
- (105) Zheng, S. T.; Yang, G. Y. *Chem. Soc. Rev.* **2012**, *41*, 7623.
- (106) Venturello, C.; D'Aloisio, R.; Bart, J. C. J.; Ricci, M. *J. Mol. Catal.* **1985**, *32*, 107.
- (107) Venturello, C.; Alneri, E.; Ricci, M. *J. Org. Chem.* **1983**, *48*, 3831.
- (108) Venturello, C.; Gambaro, M. *Synthesis* **1989**, 295.
- (109) Lambert, A.; Plucinski, P.; Kozhevnikov, I. V. *Chem. Commun.* **2003**, *0*, 714.
- (110) Plault, L.; Hauseler, A.; Nlate, S.; Astruc, D.; Ruiz, J.; Gatard, S.; Neumann, R. *Angew. Chem., Int. Ed.* **2004**, *43*, 2924.
- (111) Nlate, S.; Astruc, D.; Neumann, R. *Adv. Synth. Catal.* **2004**, *346*, 1445.
- (112) Jahier, C.; Mal, S. S.; Al-Oweini, R.; Kortz, U.; Nlate, S. *Polyhedron* **2013**, *57*, 57.
- (113) Liu, L.; Chen, C.; Hu, X.; Mohamood, T.; Ma, W.; Lin, J.; Zhao, J. *New J. Chem.* **2008**, *32*, 283.
- (114) Leng, Y.; Wang, J.; Zhu, D.; Zhang, M.; Zhao, P.; Long, Z.; Huang, J. *Green Chem.* **2011**, *13*, 1636.
- (115) Sakamoto, T.; Pac, C. *Tetrahedron Lett.* **2000**, *41*, 10009.
- (116) Xi, Z.; Zhou, N.; Sun, Y.; Li, K. *Science* **2001**, *292*, 1139.
- (117) Gao, J.; Chen, Y.; Han, B.; Feng, Z.; Li, C.; Zhou, N.; Gao, S.; Xi, Z. *J. Mol. Catal. A: Chem.* **2004**, *210*, 197.
- (118) Yamaguchi, K.; Yoshida, C.; Uchida, S.; Mizuno, N. *J. Am. Chem. Soc.* **2005**, *127*, 530.
- (119) Kamata, K.; Yamaguchi, K.; Mizuno, N. *Chem.—Eur. J.* **2004**, *10*, 4728.
- (120) Ishimoto, R.; Kamata, K.; Mizuno, N. *Angew. Chem., Int. Ed.* **2012**, *51*, 4662.
- (121) Thiel, W. R.; Eppinger, J. *Chem.—Eur. J.* **1997**, *3*, 696.
- (122) Arends, I. W. C. E.; Sheldon, R. A. *Top. Catal.* **2002**, *19*, 133.
- (123) Oyama, S. T. In *Mechanisms in Homogeneous and Heterogeneous Epoxidation Catalysis*; Oyama, S. T., Ed.; Elsevier: Amsterdam, 2008.
- (124) Qiao, Y.; Hou, Z.; Li, H.; Hu, Y.; Feng, B.; Wang, X.; Hua, L.; Huang, Q. *Green Chem.* **2009**, *11*, 1955.
- (125) Kamata, K.; Kuzuya, S.; Uehara, K.; Yamaguchi, S.; Mizuno, N. *Inorg. Chem.* **2007**, *46*, 3768.
- (126) Qiao, Y.; Li, H.; Hua, L.; Orzechowski, L.; Yan, K.; Feng, B.; Pan, Z.; Theyssen, N.; Leitner, W.; Hou, Z. *ChemPlusChem* **2012**, *77*, 1128.
- (127) Brégeault, J.-M.; Vennat, M.; Laurent, S.; Piquemal, J.-Y.; Mahha, Y.; Briot, E.; Bakala, P. C.; Atlamsansi, A.; Thouvenot, R. *J. Mol. Catal. A: Chem.* **2006**, *250*, 177.

- (128) Kamata, K.; Hirano, T.; Kuzuya, S.; Mizuno, N. *J. Am. Chem. Soc.* **2009**, *131*, 6997.
- (129) Kamata, K.; Ishimoto, R.; Hirano, T.; Kuzuya, S.; Uehara, K.; Mizuno, N. *Inorg. Chem.* **2010**, *49*, 2471.
- (130) Kamata, K.; Yonehara, K.; Sumida, Y.; Yamaguchi, K.; Hikichi, S.; Mizuno, N. *Science* **2003**, *300*, 964.
- (131) Kamata, K.; Kotani, M.; Yamaguchi, K.; Hikichi, S.; Mizuno, N. *Chem.—Eur. J.* **2007**, *13*, 639.
- (132) Kamata, K.; Nakagawa, Y.; Yamaguchi, K.; Mizuno, N. *J. Catal.* **2004**, *224*, 224.
- (133) Sartorel, A.; Carraro, M.; Bagno, A.; Scorrano, G.; Bonchio, M. *Angew. Chem., Int. Ed.* **2007**, *46*, 3255.
- (134) Sugahara, K.; Kuzuya, S.; Hirano, T.; Kamata, K.; Mizuno, N. *Inorg. Chem.* **2012**, *51*, 7932.
- (135) Musaev, D. G.; Morokuma, K.; Geletii, Y. V.; Hill, C. L. *Inorg. Chem.* **2004**, *43*, 7702.
- (136) Prabhakar, R.; Morokuma, K.; Hill, C. L.; Musaev, D. G. *Inorg. Chem.* **2006**, *45*, 5703.
- (137) Mizuno, N.; Uchida, S.; Kamata, K.; Ishimoto, R.; Nojima, S.; Yonehara, K.; Sumida, Y. *Angew. Chem., Int. Ed.* **2010**, *49*, 9972.
- (138) Uchida, S.; Kamata, K.; Ogasawara, Y.; Fujita, M.; Mizuno, N. *Dalton Trans.* **2012**, *41*, 9979.
- (139) Hua, L.; Qiao, Y.; Yu, Y.; Zhu, W.; Cao, T.; Shi, Y.; Li, H.; Feng, B.; Hou, Z. *New J. Chem.* **2011**, *35*, 1836.
- (140) Carraro, M.; Sandei, L.; Sartorel, A.; Scorrano, G.; Bonchio, M. *Org. Lett.* **2006**, *8*, 3671.
- (141) Berardi, S.; Bonchio, M.; Carraro, M.; Conte, V.; Sartorel, A.; Scorrano, G. *J. Org. Chem.* **2007**, *72*, 8954.
- (142) Johnson, B. J. S.; Stein, A. *Inorg. Chem.* **2001**, *40*, 801.
- (143) Kholdeeva, O. *Top. Catal.* **2006**, *40*, 229.
- (144) Kholdeeva, O.; Grigoriev, V.; Maksimov, G.; Zamaraev, K. *Top. Catal.* **1996**, *3*, 313.
- (145) Kholdeeva, O. A.; Grigoriev, V. A.; Maksimov, G. M.; Fedotov, M. A.; Golovin, A. V.; Zamaraev, K. I. *J. Mol. Catal. A: Chem.* **1996**, *114*, 123.
- (146) Villanneau, R.; Carabineiro, H.; Carrier, X.; Thouvenot, R.; Herson, P.; Lemos, F.; Ramôa Ribeiro, F.; Che, M. *J. Phys. Chem. B* **2004**, *108*, 12465.
- (147) Maksimchuk, N.; Melgunov, M.; Chesarov, Y.; Mrowiecbialon, J.; Jarzebski, A.; Kholdeeva, O. *J. Catal.* **2007**, *246*, 241.
- (148) Maksimchuk, N.; Timofeeva, M.; Melgunov, M.; Shmakov, A.; Chesarov, Y.; Dybtsev, D.; Fedin, V.; Kholdeeva, O. *J. Catal.* **2008**, *257*, 315.
- (149) Kato, C. N.; Negishi, S.; Yoshida, K.; Hayashi, K.; Nomiya, K. *Appl. Catal., A: Gen.* **2005**, *292*, 97.
- (150) Kholdeeva, O. A.; Trubitsina, T. A.; Timofeeva, M. N.; Maksimov, G. M.; Maksimovskaya, R. I.; Rogov, V. A. *J. Mol. Catal. A: Chem.* **2005**, *232*, 173.
- (151) Kholdeeva, O. A.; Maksimovskaya, R. I. *J. Mol. Catal. A: Chem.* **2007**, *262*, 7.
- (152) Jimenez-Lozano, P.; Ivanchikova, I. D.; Kholdeeva, O. A.; Poblet, J. M.; Carbo, J. *J. Chem. Commun.* **2012**, *48*, 9266.
- (153) Kholdeeva, O. A.; Maksimov, G. M.; Maksimovskaya, R. I.; Vanina, M. P.; Trubitsina, T. A.; Naumov, D. Y.; Kolesov, B. A.; Antonova, N. S.; Carbó, J. J.; Poblet, J. M. *Inorg. Chem.* **2006**, *45*, 7224.
- (154) Mizuno, N.; Nozaki, C.; Kiyoto, I.; Misono, M. *J. Catal.* **1999**, *182*, 285.
- (155) Bonchio, M.; Carraro, M.; Farinazzo, A.; Sartorel, A.; Scorrano, G.; Kortz, U. *J. Mol. Catal. A: Chem.* **2007**, *262*, 36.
- (156) Nishiyama, Y.; Nakagawa, Y.; Mizuno, N. *Angew. Chem., Int. Ed.* **2001**, *40*, 3639.
- (157) Nakagawa, Y.; Kamata, K.; Kotani, M.; Yamaguchi, K.; Mizuno, N. *Angew. Chem., Int. Ed.* **2005**, *44*, 5136.
- (158) Kasai, J.; Nakagawa, Y.; Uchida, S.; Yamaguchi, K.; Mizuno, N. *Chem.—Eur. J.* **2006**, *12*, 4176.
- (159) Kamata, K.; Sugahara, K.; Yonehara, K.; Ishimoto, R.; Mizuno, N. *Chem.—Eur. J.* **2011**, *17*, 7549.
- (160) Neumann, R.; Gara, M. *J. Am. Chem. Soc.* **1995**, *117*, 5066.
- (161) Neumann, R.; Khenkin, A. M.; Dahan, M. *Angew. Chem., Int. Ed. Engl.* **1995**, *34*, 1587.
- (162) Neumann, R.; Gara, M. *J. Am. Chem. Soc.* **1994**, *116*, 5509.
- (163) Neumann, R.; Khenkin, A. M. *Chem. Commun.* **1998**, 1967.
- (164) Neumann, R.; Khenkin, A. M. *J. Mol. Catal. A: Chem.* **1996**, *114*, 169.
- (165) Neumann, R.; Khenkin, A. M.; Juwiler, D.; Miller, H.; Gara, M. *J. Mol. Catal. A: Chem.* **1997**, *117*, 169.
- (166) Neumann, R.; Juwiler, D. *Tetrahedron* **1996**, *52*, 8781.
- (167) Neumann, R.; Khenkin, A. M. *Inorg. Chem.* **1995**, *34*, 5753.
- (168) Adam, W.; Alsters, P. L.; Neumann, R.; Saha-Möller, C. R.; Sloboda-Rozner, D.; Zhang, R. *Synlett* **2002**, 2011.
- (169) Adam, W.; Alsters, P. L.; Neumann, R.; Saha-Möller, C. R.; Sloboda-Rozner, D.; Zhang, R. *J. Org. Chem.* **2003**, *68*, 1721.
- (170) Adam, W.; Alsters, P. L.; Neumann, R.; Saha-Möller, C. R.; Seebach, D.; Beck, A. K.; Zhang, R. *J. Org. Chem.* **2003**, *68*, 8222.
- (171) Adam, W.; Alsters, P. L.; Neumann, R.; Saha-Möller, C. R.; Seebach, D.; Zhang, R. *Org. Lett.* **2003**, *5*, 725.
- (172) Witte, P. T.; Alsters, P. L.; Jary, W.; Müllner, R.; Pöchlauer, P.; Sloboda-Rozner, D.; Neumann, R. *Org. Process Res. Dev.* **2004**, *8*, 524.
- (173) Sloboda-Rozner, D.; Alsters, P. L.; Neumann, R. *J. Am. Chem. Soc.* **2003**, *125*, 5280.
- (174) Witte, P. T.; Chowdhury, S. R.; ten Elshof, J. E.; Sloboda-Rozner, D.; Neumann, R.; Alsters, P. L. *Chem. Commun.* **2005**, 1206.
- (175) Han, Q. X.; He, C.; Zhao, M.; Qi, B.; Niu, J. Y.; Duan, C. Y. *J. Am. Chem. Soc.* **2013**, *135*, 10186.
- (176) Linguito, S. L.; Zhang, X.; Padmanabhan, M.; Biradar, A. V.; Xu, T.; Emge, T. J.; Asefa, T.; Li, J. *New J. Chem.* **2013**, *37*, 2894.
- (177) Shringarpure, P.; Patel, K.; Patel, A. *J. Cluster Sci.* **2011**, *22*, 587.
- (178) Pathan, S.; Patel, A. *Ind. Eng. Chem. Res.* **2013**, *52*, 11913.
- (179) Balula, S. S.; Cunha-Silva, L.; Santos, I. C. M. S.; Estrada, A. C.; Fernandes, A. C.; Cavaleiro, J. A. S.; Pires, J.; Freire, C.; Cavaleiro, A. M. V. *New J. Chem.* **2013**, *37*, 2341.
- (180) Hu, J. L.; Li, K. X.; Li, W.; Ma, F. Y.; Guo, Y. H. *Appl. Catal., A: Gen.* **2009**, *364*, 211.
- (181) Tang, J.; Yang, X. L.; Zhang, X. W.; Wang, M.; Wu, C. D. *Dalton Trans.* **2010**, *39*, 3396.
- (182) Ozkar, S.; Finke, R. G. *J. Am. Chem. Soc.* **2002**, *124*, 5796.
- (183) Troupis, A.; Hiskia, A.; Papaconstantinou, E. *Angew. Chem., Int. Ed.* **2002**, *41*, 1911.
- (184) Kogan, V.; Aizenshtat, Z.; Popovitz-Biro, R.; Neumann, R. *Org. Lett.* **2002**, *4*, 3529.
- (185) Maayan, G.; Neumann, R. *Chem. Commun.* **2005**, 4595.
- (186) Santos, I. C. M. S.; Rebelo, S. L. H.; Balula, M. S. S.; Martins, R. R. L.; Pereira, M. M. M. S.; Simões, M. M. Q.; Neves, M. G. P. M. S.; Cavaleiro, J. A. S.; Cavaleiro, A. M. V. *J. Mol. Catal. A: Chem.* **2005**, *231*, 35.
- (187) Wang, S.-S.; Zhang, J.; Zhou, C.-L.; Vo-Thanh, G.; Liu, Y. *Catal. Commun.* **2012**, *28*, 152.
- (188) Araghi, M.; Mirkhani, V.; Moghadam, M.; Tangestaninejad, S.; Mohammndoar-Baltork, I. *Dalton Trans.* **2012**, *41*, 3087.
- (189) Zhizhina, E. G.; Simonova, M. V.; Odyakov, V. F.; Matveev, K. I. *Appl. Catal., A: Gen.* **2007**, *319*, 91.
- (190) Ettedgui, J.; Neumann, R. *J. Am. Chem. Soc.* **2009**, *131*, 4.
- (191) Korhevnikov, I. V.; Matveev, K. I. *Russ. Chem. Rev.* **1982**, *51*, 1075.
- (192) Kozhevnikov, I. V.; Matveev, K. I. *Appl. Catal.* **1983**, *5*, 135.
- (193) Grate, J. H. *J. Mol. Catal. A: Chem.* **1996**, *114*, 93.
- (194) Pettersson, L.; Andersson, I.; Selling, A.; Grate, J. H. *Inorg. Chem.* **1994**, *33*, 982.
- (195) Saxton, R. J.; Hamm, D. R.; Klingman, K. A.; Downey, S. J.; Grate, J. H. U.S. Patent US5557014-A, 1995.
- (196) Grate, J. H.; Hamm, D. R.; Saxton, R. J.; Muraoka, M. T. European Patent EP518948-A1, 1991.
- (197) Grate, J. H.; Mahajan, S.; Hamm, D. R.; Klingman, K. A.; Downey, S. L. European Patent EP518990-A1, 1991.
- (198) Cavani, F.; Ballarini, N.; Cericola, A. *Catal. Today* **2007**, *127*, 113.

- (199) Lin, M.; Sen, A. *Nature* **1994**, *368*, 613.
- (200) Periana, R. A.; Mironov, O.; Taube, D.; Bhalla, G.; Jones, C. J. *Science* **2003**, *301*, 814.
- (201) Santos, I. C. M. S.; Paz, F. A. A.; Simões, M. M. Q.; Neves, M. G. P. M. S.; Cavaleiro, J. A. S.; Klinowski, J.; Cavaleiro, A. M. V. *Appl. Catal., A: Gen.* **2008**, *351*, 166.
- (202) Simões, M. M. Q.; Conceição, C. M. M.; Gamelas, J. A. F.; Domingues, P. M. D. N.; Cavaleiro, A. M. V.; Cavaleiro, J. A. S.; Ferrer-Correia, A. J. V.; Johnstone, R. A. W. *J. Mol. Catal. A: Chem.* **1999**, *144*, 461.
- (203) Yamaguchi, K.; Mizuno, N. *New J. Chem.* **2002**, *26*, 972.
- (204) Mizuno, N.; Nozaki, C.; Kiyoto, I.; Misono, M. *J. Am. Chem. Soc.* **1998**, *120*, 9267.
- (205) Clerici, M. G. *Appl. Catal.* **1991**, *68*, 249.
- (206) Mizuno, N.; Hirose, T.; Tateishi, M.; Iwamoto, M. *J. Mol. Catal.* **1994**, *88*, L125.
- (207) Menage, S.; Vincent, J. M.; Lambeaux, C.; Fontecave, M. *J. Chem. Soc., Dalton Trans.* **1994**, 2081.
- (208) Barton, D. H. R.; Hu, B.; Taylor, D. K.; Wahl, R. U. R. *Tetrahedron Lett.* **1996**, *37*, 1133.
- (209) Nam, W.; Valentine, J. S. *New J. Chem.* **1989**, *13*, 677.
- (210) Mizuno, N.; Kiyoto, I.; Nozaki, C.; Misono, M. *J. Catal.* **1999**, *181*, 171.
- (211) Bonchio, M.; Carraro, M.; Scorrano, G.; Kortz, U. *Adv. Synth. Catal.* **2005**, *347*, 1909.
- (212) Hayashi, T.; Kishida, A.; Mizuno, N. *Chem. Commun.* **2000**, *381*.
- (213) Seki, Y.; Mizuno, N.; Misono, M. *Appl. Catal., A: Gen.* **1997**, *158*, L47.
- (214) Seki, Y.; Mizuno, N.; Misono, M. *Appl. Catal., A: Gen.* **2000**, *194–195*, 13.
- (215) Min, J.-S.; Ishige, H.; Misono, M.; Mizuno, N. *J. Catal.* **2001**, *198*, 116.
- (216) Bar-Nahum, I.; Khenkin, A. M.; Neumann, R. *J. Am. Chem. Soc.* **2004**, *126*, 10236.
- (217) Shilov, A. E.; Shul'pin, G. B. *Russ. Chem. Rev.* **1987**, *56*, 442.
- (218) Kamata, K.; Yonehara, K.; Nakagawa, Y.; Uehara, K.; Mizuno, N. *Nat. Chem.* **2010**, *2*, 478.
- (219) Neumann, R.; Dahan, M. *J. Am. Chem. Soc.* **1998**, *120*, 11969.
- (220) Yin, C. X.; Finke, R. G. *Inorg. Chem.* **2005**, *44*, 4175.
- (221) Santos, I. C. M. S.; Gamelas, J. A. F.; Balula, M. S. S.; Simões, M. M. Q.; Neves, M. G. P. M. S.; Cavaleiro, J. A. S.; Cavaleiro, A. M. V. *J. Mol. Catal. A: Chem.* **2007**, *262*, 41.
- (222) Chen, L. F.; Zhu, K.; Bi, L. H.; Suchopar, A.; Reicke, M.; Mathys, G.; Jaensch, H.; Kortz, U.; Richards, R. M. *Inorg. Chem.* **2007**, *46*, 8457.
- (223) Bi, L. H.; Al-Kadamany, G.; Chubarova, E. V.; Dickman, M. H.; Chen, L.; Gopala, D. S.; Richards, R. M.; Keita, B.; Nadio, L.; Jaensch, H.; Mathys, G.; Kortz, U. *Inorg. Chem.* **2009**, *48*, 10068.
- (224) Meng, R.-Q.; Suo, L.; Hou, G.-F.; Liang, J.; Bi, L.-H.; Li, H.-L.; Wu, L.-X. *CrystEngComm* **2013**, *15*, 5867.
- (225) Chen, L.; Hu, J.; Mal, S. S.; Kortz, U.; Jaensch, H.; Mathys, G.; Richards, R. M. *Chem.—Eur. J.* **2009**, *15*, 7490.
- (226) Carraro, M.; Gardan, M.; Scorrano, G.; Drioli, E.; Fontananova, E.; Bonchio, M. *Chem. Commun.* **2006**, 4533.
- (227) Khenkin, A. H.; Neumann, R. *J. Am. Chem. Soc.* **2001**, *123*, 6437.
- (228) Mizuno, N.; Suh, D.-J. *Appl. Catal., A: Gen.* **1996**, *146*, L249.
- (229) Dimitratos, N.; Védrine, J. C. *Appl. Catal., A: Gen.* **2003**, *256*, 251.
- (230) Sun, M.; Zhang, J.; Cao, C.; Zhang, Q.; Wang, Y.; Wan, H. *Appl. Catal., A: Gen.* **2008**, *349*, 212.
- (231) Dimitratos, N.; Védrine, J. C. *Catal. Commun.* **2006**, *7*, 811.
- (232) Zhang, M.; Liu, J.; Liu, C.; Lan, R.; Ji, L.; Chen, X. *J. Chem. Soc., Chem. Commun.* **1993**, *0*, 1480.
- (233) Schuurman, Y.; Ducarme, V.; Chen, T.; Li, W.; Mirodatos, C.; Martin, G. A. *Appl. Catal., A: Gen.* **1997**, *163*, 227.
- (234) Zhang, X.; Liu, J.; Jing, Y.; Xie, Y. *Appl. Catal., A: Gen.* **2003**, *240*, 143.
- (235) Zhang, Q. H.; Cao, C. J.; Xu, T.; Sun, M.; Zhang, J. H.; Wang, Y.; Wan, H. L. *Chem. Commun.* **2009**, 2376.
- (236) Khenkin, A. M.; Neumann, R. *Angew. Chem., Int. Ed.* **2000**, *39*, 4088.
- (237) Khenkin, A. M.; Weiner, L.; Wang, Y.; Neumann, R. *J. Am. Chem. Soc.* **2001**, *123*, 8531.
- (238) Bordoloi, A.; Lefebvre, F.; Halligudi, S. *J. Catal.* **2007**, *247*, 166.
- (239) Kuznetsova, L. I.; Detusheva, L. G.; Fedotov, M. A.; Likholobov, V. A. *J. Mol. Catal. A: Chem.* **1996**, *111*, 81.
- (240) Nomiya, K.; Yanagibayashi, H.; Nozaki, C.; Kondoh, K.; Hiramatsu, E.; Shimizu, Y. *J. Mol. Catal. A: Chem.* **1996**, *114*, 181.
- (241) Passoni, L. C.; Cruz, A. T.; Buffon, R.; Schuchardt, U. *J. Mol. Catal. A: Chem.* **1997**, *120*, 117.
- (242) Nomiya, K.; Nemoto, Y.; Hasegawa, T.; Matsuoka, S. *J. Mol. Catal. A: Chem.* **2000**, *152*, 55.
- (243) Tani, M.; Sakamoto, T.; Mita, S.; Sakaguchi, S.; Ishii, Y. *Angew. Chem., Int. Ed.* **2005**, *44*, 2586.
- (244) Sumimoto, S.; Tanaka, C.; Yamaguchi, S.-t.; Ichihashi, Y.; Nishiyama, S.; Tsuruya, S. *Ind. Eng. Chem. Res.* **2006**, *45*, 7444.
- (245) Yang, H.; Wu, Q.; Li, J.; Dai, W.; Zhang, H.; Lu, D.; Gao, S.; You, W. *Appl. Catal., A: Gen.* **2013**, *457*, 21.
- (246) Panov, G. I.; Uriarte, A. K.; Rodkin, M. A.; Sobolev, V. I. *Catal. Today* **1998**, *41*, 365.
- (247) Khenkin, A. M.; Weiner, L.; Neumann, R. *J. Am. Chem. Soc.* **2005**, *127*, 9988.
- (248) Gao, F.; Hua, R. *Appl. Catal., A: Gen.* **2004**, *270*, 223.
- (249) Sheldon, R. A.; Arends, I. W. C. E.; Hanefeld, U. *Green Chemistry and Catalysis*; Wiley-VCH: Weinheim, Germany, 2007.
- (250) Blanksby, S. J.; Ellison, G. B. *Acc. Chem. Res.* **2003**, *36*, 255.
- (251) Warren, J. J.; Tronic, T. A.; Mayer, J. M. *Chem. Rev.* **2010**, *110*, 6961.
- (252) Kamata, K.; Yamaura, T.; Mizuno, N. *Angew. Chem., Int. Ed.* **2012**, *51*, 7275.
- (253) Nomiya, K.; Hashino, K.; Nemoto, Y.; Watanabe, M. *J. Mol. Catal. A: Chem.* **2001**, *176*, 79.
- (254) Chandrasekhar, V.; Boomishankar, R.; Nagendran, S. *Chem. Rev.* **2004**, *104*, 5847.
- (255) Murugavel, R.; Walawalkar, M. G.; Dan, M.; Roesky, H. W.; Rao, C. N. R. *Acc. Chem. Res.* **2004**, *37*, 763.
- (256) Ishimoto, R.; Kamata, K.; Mizuno, N. *Angew. Chem., Int. Ed.* **2009**, *48*, 8900.
- (257) Kikukawa, Y.; Kuroda, Y.; Yamaguchi, K.; Mizuno, N. *Angew. Chem., Int. Ed.* **2012**, *51*, 2434.
- (258) Kikukawa, Y.; Kuroda, Y.; Suzuki, K.; Hibino, M.; Yamaguchi, K.; Mizuno, N. *Chem. Commun.* **2013**, *49*, 376.
- (259) Wang, S. S.; Popovic, Z.; Wu, H. H.; Liu, Y. *ChemCatChem* **2011**, *3*, 1208.
- (260) Hamamoto, H.; Suzuki, Y.; Yamada, Y. M. A.; Tabata, H.; Takahashi, H.; Ikegami, S. *Angew. Chem., Int. Ed.* **2005**, *44*, 4536.
- (261) Yamada, Y. M. A.; Jin, C. K.; Uozumi, Y. *Org. Lett.* **2010**, *12*, 4540.
- (262) Lang, X. J.; Li, Z.; Xia, C. G. *Synth. Commun.* **2008**, *38*, 1610.
- (263) ten Brink, G. J.; Arends, I. W. C. E.; Sheldon, R. A. *Science* **2000**, *287*, 1636.
- (264) Yamaguchi, K.; Mizuno, N. *Angew. Chem., Int. Ed.* **2002**, *41*, 4538.
- (265) Pathan, S.; Patel, A. *Appl. Catal., A: Gen.* **2013**, *459*, 59.
- (266) Jing, L.; Shi, J.; Zhang, F.; Zhong, Y.; Zhu, W. *Ind. Eng. Chem. Res.* **2013**, *52*, 10095.
- (267) Khenkin, A. M.; Neumann, R. *J. Org. Chem.* **2002**, *67*, 7075.
- (268) Haimov, A.; Neumann, R. *Chem. Commun.* **2002**, 876.
- (269) Maayan, G.; Ganegui, B.; Leitner, W.; Neumann, R. *Chem. Commun.* **2006**, 2230.
- (270) Bordoloi, A.; Sahoo, S.; Lefebvre, F.; Halligudi, S. B. *J. Catal.* **2008**, *259*, 232.
- (271) Ben-Daniel, R.; Alsters, P.; Neumann, R. *J. Org. Chem.* **2001**, *66*, 8650.
- (272) Neumann, R.; Khenkin, A. M.; Vigdergauz, I. *Chem.—Eur. J.* **2000**, *6*, 875.

- (273) Zhu, J.; Wang, P. C.; Lu, M. *RSC Adv.* **2012**, *2*, 8265.
- (274) Huang, X. Q.; Zhang, X. M.; Zhang, D.; Yang, S.; Feng, X.; Li, J. K.; Lin, Z. G.; Cao, J.; Pan, R.; Chi, Y. N.; Wang, B.; Hu, C. W. *Chem.—Eur. J.* **2014**, *20*, 2557.
- (275) Forster, J.; Rosner, B.; Fink, R. H.; Nye, L. C.; Ivanovic-Burmazovic, I.; Kastner, K.; Tucher, J.; Streb, C. *Chem. Sci.* **2013**, *4*, 418.
- (276) Khenkin, A. M.; Leitus, G.; Neumann, R. *J. Am. Chem. Soc.* **2010**, *132*, 11446.
- (277) Jana, S. K.; Kubota, Y.; Tatsumi, T. *J. Catal.* **2008**, *255*, 40.
- (278) Ni, L. B.; Patscheider, J.; Baldridge, K. K.; Patzke, G. R. *Chem.—Eur. J.* **2012**, *18*, 13293.
- (279) Barats, D.; Neumann, R. *Adv. Synth. Catal.* **2010**, *352*, 293.
- (280) Carraro, M.; Bassil, B. S.; Soraru, A.; Berardi, S.; Suchopar, A.; Kortz, U.; Bonchio, M. *Chem. Commun.* **2013**, *49*, 7914.
- (281) Kikukawa, Y.; Yamaguchi, K.; Mizuno, N. *Angew. Chem., Int. Ed.* **2010**, *49*, 6096.
- (282) Kikukawa, Y.; Yamaguchi, K.; Mizuno, N. *Inorg. Chem.* **2010**, *49*, 8194.
- (283) Dermeche, L.; Salhi, N.; Hocine, S.; Thouvenot, R.; Rabia, C. J. *Mol. Catal. A: Chem.* **2012**, *356*, 29.
- (284) Chubarova, E. V.; Dickman, M. H.; Keita, B.; Nadjo, L.; Misserque, F.; Mifsud, M.; Arends, I. W. C. E.; Kortz, U. *Angew. Chem., Int. Ed.* **2008**, *47*, 9542.
- (285) Chen, B. K.; Huang, X. Q.; Wang, B.; Lin, Z. G.; Hu, J. F.; Chi, Y. N.; Hu, C. W. *Chem.—Eur. J.* **2013**, *19*, 4408.
- (286) Galli, C.; Gentili, P.; Pontes, A. S. N.; Gamelas, J. A. F.; Evtuguin, D. V. *New J. Chem.* **2007**, *31*, 1461.
- (287) Kholdeeva, O. A.; Trubitsina, T. A.; Maksimovskaya, R. I.; Golovin, A. V.; Neiwert, W. A.; Kolesov, B. A.; Lopez, X.; Poblet, J. M. *Inorg. Chem.* **2004**, *43*, 2284.
- (288) Kholdeeva, O. A.; Trubitsina, T. A.; Maksimov, G. M.; Golovin, A. V.; Maksimovskaya, R. I. *Inorg. Chem.* **2005**, *44*, 1635.
- (289) El Aakel, L.; Launay, F.; Atlamsani, A.; Brégeault, J.-M. *Chem. Commun.* **2001**, 2218.
- (290) Bregeault, J. M. *Dalton Trans.* **2003**, 3289.
- (291) Khenkin, A. M.; Neumann, R. *J. Am. Chem. Soc.* **2008**, *130*, 14474.
- (292) Rozhko, E.; Raabova, K.; Macchia, F.; Malmusi, A.; Righi, P.; Accorinti, P.; Alini, S.; Babini, P.; Cerrato, G.; Manzoli, M.; Cavani, F. *ChemCatChem* **2013**, *5*, 1998.
- (293) Bregeault, J.-M.; Launay, F.; Atlamsani, A. *C. R. Acad. Sci., Ser. IIC: Chim.* **2001**, *4*, 11.
- (294) Albert, J.; Lüders, D.; Bösmann, A.; Guldi, D. M.; Wasserscheid, P. *Green Chem.* **2014**, *16*, 226.
- (295) Wolfel, R.; Taccardi, N.; Bosmann, A.; Wasserscheid, P. *Green Chem.* **2011**, *13*, 2759.
- (296) Sarma, B. B.; Neumann, R. *Nat. Commun.* **2014**, *5*, 4621.
- (297) Khenkin, A. M.; Efremenko, I.; Martin, J. M.; Neumann, R. *J. Am. Chem. Soc.* **2013**, *135*, 19304.
- (298) Kholdeeva, O. A.; Vanina, M. P.; Timofeeva, M. N.; Maksimovskaya, R. I.; Trubitsina, T. A.; Melgunov, M. S.; Burgina, E. B.; Mrowiec-Bialon, J.; Jarzebski, A. B.; Hill, C. L. *J. Catal.* **2004**, *226*, 363.
- (299) Kholdeeva, O. A.; Timofeeva, M. N.; Maksimov, G. M.; Maksimovskaya, R. I.; Neiwert, W. A.; Hill, C. L. *Inorg. Chem.* **2005**, *44*, 666.
- (300) Guo, W.; Luo, Z.; Lv, H.; Hill, C. L. *ACS Catal.* **2014**, *4*, 1154.
- (301) ten Brink, G. J.; Arends, I. W. C. E.; Sheldon, R. A. *Chem. Rev.* **2004**, *104*, 4105.
- (302) Yoshida, A.; Yoshimura, M.; Uehara, K.; Hikichi, S.; Mizuno, N. *Angew. Chem., Int. Ed.* **2006**, *45*, 1956.
- (303) Sloboda-Rozner, D.; Neumann, R. *Green Chem.* **2006**, *8*, 679.
- (304) Zhao, S.; Xu, J. H.; Wei, M.; Song, Y. F. *Green Chem.* **2011**, *13*, 384.
- (305) Zhao, S.; Liu, L.; Song, Y. F. *Dalton Trans.* **2012**, *41*, 9855.
- (306) Liu, P.; Wang, H.; Feng, Z.; Ying, P.; Li, C. *J. Catal.* **2008**, *256*, 345.
- (307) Liu, P.; Wang, C.; Li, C. *J. Catal.* **2009**, *262*, 159.
- (308) Carreno, M. C. *Chem. Rev.* **1995**, *95*, 1717.
- (309) Prilezhaeva, E. N. *Russ. Chem. Rev.* **2001**, *70*, 897.
- (310) Fernandez, I.; Khiar, N. *Chem. Rev.* **2003**, *103*, 3651.
- (311) Kukushkin, V. Y. *Coord. Chem. Rev.* **1995**, *139*, 375.
- (312) Song, J.; Luo, Z.; Britt, D. K.; Furukawa, H.; Yaghi, O. M.; Hardcastle, K. I.; Hill, C. L. *J. Am. Chem. Soc.* **2011**, *133*, 16839.
- (313) Zhao, S.; Jia, Y.; Song, Y.-F. *Appl. Catal., A: Gen.* **2013**, *453*, 188.
- (314) Yamaura, T.; Kamata, K.; Yamaguchi, K.; Mizuno, N. *Catal. Today* **2013**, *203*, 76.
- (315) Hou, Y. Q.; Hill, C. L. *J. Am. Chem. Soc.* **1993**, *115*, 11823.
- (316) Zeng, H. D.; Newkome, G. R.; Hill, C. L. *Angew. Chem., Int. Ed.* **2000**, *39*, 1772.
- (317) Miao, W.-K.; Yan, Y.-K.; Wang, X.-L.; Xiao, Y.; Ren, L.-J.; Zheng, P.; Wang, C.-H.; Ren, L.-X.; Wang, W. *ACS Macro Lett.* **2014**, *3*, 211.
- (318) Oble, J.; Riflaide, B.; Noel, A.; Malacria, M.; Thorimbert, S.; Hasenknopf, B.; Lacote, E. *Org. Lett.* **2011**, *13*, 5990.
- (319) Riflaide, B.; Lachkar, D.; Oble, J.; Li, J.; Thorimbert, S.; Hasenknopf, B.; Lacote, E. *Org. Lett.* **2014**, *16*, 3860.
- (320) Tundo, P.; Romanelli, G. P.; Vázquez, P. G.; Aricò, F. *Catal. Commun.* **2010**, *11*, 1181.
- (321) Romanelli, G. P.; Villabrille, P. I.; Cáceres, C. V.; Vázquez, P. G.; Tundo, P. *Catal. Commun.* **2011**, *12*, 726.
- (322) Romanelli, G. P.; Vaquez, P. G.; Tundo, P. *Synlett* **2005**, 75.
- (323) Craven, M.; Yahya, R.; Kozhevnikova, E.; Boomishankar, R.; Robertson, C. M.; Steiner, A.; Kozhevnikov, I. *Chem. Commun.* **2013**, *49*, 349.
- (324) Zhao, P. P.; Zhang, M. J.; Wu, Y. J.; Wang, J. *Ind. Eng. Chem. Res.* **2012**, *51*, 6641.
- (325) Yang, Y.; Zhang, B.; Wang, Y.; Yue, L.; Li, W.; Wu, L. *J. Am. Chem. Soc.* **2013**, *135*, 14500.
- (326) Carraro, M.; Modugno, G.; Sartorel, A.; Scorrano, G.; Bonchio, M. *Eur. J. Inorg. Chem.* **2009**, *5164*.
- (327) Zeng, H. D.; Newkome, G. R.; Hill, C. L. *Angew. Chem., Int. Ed.* **2000**, *39*, 1772.
- (328) Jahier, C.; Mal, S. S.; Kortz, U.; Nlate, S. *Eur. J. Inorg. Chem.* **2010**, *2010*, 1559.
- (329) Jahier, C.; Cantuel, M.; McClenaghan, N. D.; Buffeteau, T.; Cavagnat, D.; Agbossou, F.; Carraro, M.; Bonchio, M.; Nlate, S. *Chem.—Eur. J.* **2009**, *15*, 8703.
- (330) Jahier, C.; Coustou, M. F.; Cantuel, M.; McClenaghan, N. D.; Buffeteau, T.; Cavagnat, D.; Carraro, M.; Nlate, S. *Eur. J. Inorg. Chem.* **2011**, *727*.
- (331) Wang, Y. Z.; Li, H. L.; Qi, W.; Yang, Y.; Yan, Y.; Li, B.; Wu, L. *X. J. Mater. Chem.* **2012**, *22*, 9181.
- (332) Wang, Y. Z.; Li, H. L.; Wu, C.; Yang, Y.; Shi, L.; Wu, L. X. *Angew. Chem., Int. Ed.* **2013**, *52*, 4577.
- (333) Kholdeeva, O. A.; Maksimov, G. M.; Maksimovskaya, R. I.; Kovaleva, L. A.; Fedotov, M. A.; Grigoriev, V. A.; Hill, C. L. *Inorg. Chem.* **2000**, *39*, 3828.
- (334) Yang, C. B.; Jin, Q. P.; Zhang, H.; Liao, J.; Zhu, J.; Yu, B.; Deng, J. G. *Green Chem.* **2009**, *11*, 1401.
- (335) Kamata, K.; Hirano, T.; Mizuno, N. *Chem. Commun.* **2009**, 3958.
- (336) Kamata, K.; Hirano, T.; Ishimoto, R.; Mizuno, N. *Dalton Trans.* **2010**, *39*, 5509.
- (337) Al-Kadamany, G.; Mal, S. S.; Milev, B.; Donoeva, B. G.; Maksimovskaya, R. I.; Kholdeeva, O. A.; Kortz, U. *Chem.—Eur. J.* **2010**, *16*, 11797.
- (338) Huang, L.; Wang, S. S.; Zhao, J. W.; Cheng, L.; Yang, G. Y. *J. Am. Chem. Soc.* **2014**, *136*, 7637.
- (339) Okun, N. M.; Tarr, J. C.; Hillesheim, D. A.; Zhang, L.; Hardcastle, K. I.; Hill, C. L. *J. Mol. Catal. A: Chem.* **2006**, *246*, 11.
- (340) Okun, N. M.; Anderson, T. M.; Hill, C. L. *J. Am. Chem. Soc.* **2003**, *125*, 3194.
- (341) Shi, X.-Y.; Wei, J.-F. *J. Mol. Catal. A: Chem.* **2008**, *280*, 142.
- (342) Sasaki, Y.; Ushimaru, K.; Iteya, K.; Nakayama, H.; Yamaguchi, S.; Ichihara, J. *Tetrahedron Lett.* **2004**, *45*, 9513.

- (343) Yan, X.-M.; Mei, P.; Lei, J.; Mi, Y.; Xiong, L.; Guo, L. *J. Mol. Catal. A: Chem.* **2009**, *304*, 52.
- (344) Rhule, J. T.; Neiwert, W. A.; Hardcastle, K. I.; Do, B. T.; Hill, C. L. *J. Am. Chem. Soc.* **2001**, *123*, 12101.
- (345) Okun, N. M.; Anderson, T. M.; Hardcastle, K. I.; Hill, C. L. *Inorg. Chem.* **2003**, *42*, 6610.
- (346) Han, J. W.; Hardcastle, K. I.; Hill, C. L. *Eur. J. Inorg. Chem.* **2006**, 2598.
- (347) Han, J. W.; Hill, C. L. *J. Am. Chem. Soc.* **2007**, *129*, 15094.
- (348) Huang, W. L.; Zhu, W. S.; Li, H. M.; Shi, H.; Zhu, G. P.; Liu, H.; Chen, G. Y. *Ind. Eng. Chem. Res.* **2010**, *49*, 8998.
- (349) Li, H. M.; He, L. N.; Lu, J. D.; Zhu, W. S.; Jiang, X.; Wang, Y.; Yan, Y. S. *Energy Fuels* **2009**, *23*, 1354.
- (350) Li, H. M.; Jiang, X.; Zhu, W. H.; Lu, J. D.; Shu, H. M.; Yan, Y. S. *Ind. Eng. Chem. Res.* **2009**, *48*, 9034.
- (351) Ding, Y. X.; Zhu, W. S.; Li, H. M.; Jiang, W.; Zhang, M.; Duan, Y. Q.; Chang, Y. H. *Green Chem.* **2011**, *13*, 1210.
- (352) Ribeiro, S.; Granadeiro, C. M.; Silva, P.; Almeida Paz, F. A.; de Biani, F. F.; Cunha-Silva, L.; Balula, S. S. *Catal. Sci. Technol.* **2013**, *3*, 2404.
- (353) Xu, J.; Zhao, S.; Chen, W.; Wang, M.; Song, Y. F. *Chem.—Eur. J.* **2012**, *18*, 4775.
- (354) Qi, W.; Wang, Y. Z.; Li, W.; Wu, L. X. *Chem.—Eur. J.* **2010**, *16*, 1068.
- (355) Salles, L.; Aubry, C.; Thouvenot, R.; Robert, F.; Doremieuxmorin, C.; Chottard, G.; Ledon, H.; Jeannin, Y.; Bregeault, J. M. *Inorg. Chem.* **1994**, *33*, 871.
- (356) Huang, D.; Wang, Y. J.; Yang, L. M.; Luo, G. S. *Ind. Eng. Chem. Res.* **2006**, *45*, 1880.
- (357) Nisar, A.; Zhuang, J.; Wang, X. *Adv. Mater.* **2011**, *23*, 1130.
- (358) Nisar, A.; Wang, X. *Dalton Trans.* **2012**, *41*, 9832.
- (359) Nisar, A.; Lu, Y.; Zhuang, J.; Wang, X. *Angew. Chem., Int. Ed.* **2011**, *50*, 3187.
- (360) Xu, J.; Zhao, S.; Ji, Y.; Song, Y. F. *Chem.—Eur. J.* **2013**, *19*, 709.
- (361) Li, C.; Gao, J.; Jiang, Z.; Wang, S.; Lu, H.; Yang, Y.; Jing, F. *Top. Catal.* **2005**, *35*, 169.
- (362) Li, C.; Jiang, Z. X.; Gao, J. B.; Yang, Y. X.; Wang, S. J.; Tian, F. P.; Sun, F. X.; Sun, X. P.; Ying, P. L.; Han, C. R. *Chem.—Eur. J.* **2004**, *10*, 2277.
- (363) Lu, H. Y.; Gao, J. B.; Jiang, Z. X.; Yang, Y. X.; Song, B.; Li, C. *Chem. Commun.* **2007**, 150.
- (364) Lu, H.; Gao, J.; Jiang, Z.; Jing, F.; Yang, Y.; Wang, G.; Li, C. *J. Catal.* **2006**, *239*, 369.
- (365) Yin, P. C.; Wang, J.; Xiao, Z. C.; Wu, P. F.; Wei, Y. G.; Liu, T. B. *Chem.—Eur. J.* **2012**, *18*, 9174.
- (366) Zhu, W. S.; Huang, W. L.; Li, H. M.; Zhang, M.; Jiang, W.; Chen, G. Y.; Han, C. R. *Fuel Process. Technol.* **2011**, *92*, 1842.
- (367) Bamoharram, F. F.; Heravi, M. M.; Roshani, M.; Tavakoli, N. J. *Mol. Catal. A: Chem.* **2006**, *252*, 219.
- (368) Ding, Y.; Zhao, W. *J. Mol. Catal. A: Chem.* **2011**, *337*, 45.
- (369) Zhao, W.; Yang, C.; Ding, Y.; Ma, B. *New J. Chem.* **2013**, *37*, 2614.
- (370) Podgoršek, A.; Zupan, M.; Iskra, J. *Angew. Chem., Int. Ed.* **2009**, *48*, 8424.
- (371) Branytska, O. V.; Neumann, R. *J. Org. Chem.* **2003**, *68*, 9510.
- (372) Yonehara, K.; Kamata, K.; Yamaguchi, K.; Mizuno, N. *Chem. Commun.* **2011**, *47*, 1692.
- (373) Moriuchi, T.; Yamaguchi, M.; Kikushima, K.; Hirao, T. *Tetrahedron Lett.* **2007**, *48*, 2667.
- (374) Rothenberg, G.; Clark, J. H. *Org. Process Res. Dev.* **2000**, *4*, 270.
- (375) Choudary, B. M.; Sudha, Y.; Reddy, P. N. *Synlett* **1994**, *450*.
- (376) Mizuno, N.; Kamata, K.; Yamaguchi, K. *Catal. Today* **2012**, *185*, 157.
- (377) Firouzabadi, H.; Iranpoor, N.; Amani, K. *J. Mol. Catal. A: Chem.* **2003**, *195*, 289.
- (378) Das, D. P.; Parida, K. M. *J. Mol. Catal. A: Chem.* **2006**, *253*, 70.
- (379) Mallik, S.; Parida, K. M.; Dash, S. S. *J. Mol. Catal. A: Chem.* **2007**, *261*, 172.
- (380) Mallick, S.; Parida, K. M. *Catal. Commun.* **2007**, *8*, 889.
- (381) Weissman, H.; Song, X. P.; Milstein, D. *J. Am. Chem. Soc.* **2001**, *123*, 337.
- (382) Yokota, T.; Tani, M.; Sakaguchi, S.; Ishii, Y. *J. Am. Chem. Soc.* **2003**, *125*, 1476.
- (383) Tani, M.; Sakaguchi, S.; Ishii, Y. *J. Org. Chem.* **2004**, *69*, 1221.
- (384) Yamada, T.; Sakaguchi, S.; Ishii, Y. *J. Org. Chem.* **2005**, *70*, 5471.
- (385) Yamada, T.; Sakakura, A.; Sakaguchi, S.; Obora, Y.; Ishii, Y. *New J. Chem.* **2008**, *32*, 738.
- (386) Yokota, T.; Sakaguchi, S.; Ishii, Y. *Adv. Synth. Catal.* **2002**, *344*, 849.
- (387) Burton, H. A.; Kozhevnikov, I. V. *J. Mol. Catal. A: Chem.* **2002**, *185*, 285.
- (388) Okamoto, M.; Watanabe, M.; Yamaji, T. *J. Organomet. Chem.* **2002**, *664*, 59.
- (389) Zhao, P. P.; Leng, Y.; Zhang, M. J.; Wang, J.; Wu, Y. J.; Huang, J. *Chem. Commun.* **2012**, *48*, 5721.
- (390) Lyons, J. E. In *Oxygen Complexes and Oxygen Activation by Transition Metal Complexes*; Martell, A. E., Sawyer, D. T., Eds.; Plenum Press: New York, 1988.
- (391) Kamata, K.; Yamaguchi, S.; Kotani, M.; Yamaguchi, K.; Mizuno, N. *Angew. Chem., Int. Ed.* **2008**, *47*, 2407.
- (392) Yamaguchi, K.; Kamata, K.; Yamaguchi, S.; Kotani, M.; Mizuno, N. *J. Catal.* **2008**, *258*, 121.
- (393) Mizuno, N.; Katamura, K.; Yoneda, Y.; Misono, M. *J. Catal.* **1983**, *83*, 384.
- (394) Misono, M. *Catal. Rev.* **1987**, *29*, 269.
- (395) Izumi, Y.; Satoh, Y.; Kondoh, H.; Urabe, K. *J. Mol. Catal.* **1992**, *72*, 37.
- (396) Putluru, S. S. R.; Mossin, S.; Riisager, A.; Fehrmann, R. *Catal. Today* **2011**, *176*, 292.
- (397) Putluru, S. S. R.; Jensen, A. D.; Riisager, A.; Fehrmann, R. *Catal. Sci. Technol.* **2011**, *1*, 631.
- (398) Augustine, R. L.; Tanielyan, S. K.; Mahata, N.; Gao, Y.; Zsigmond, A.; Yang, H. *Appl. Catal., A: Gen.* **2003**, *256*, 69.
- (399) Bar-Nahum, I.; Neumann, R. *Chem. Commun.* **2003**, 2690.
- (400) Branytska, O.; Shimon, L. J. W.; Neumann, R. *Chem. Commun.* **2007**, 3957.
- (401) Kogan, V.; Aizenshtat, Z.; Neumann, R. *Angew. Chem., Int. Ed.* **1999**, *38*, 3331.
- (402) Kogan, V.; Aizenshtat, Z.; Neumann, R. *New J. Chem.* **2002**, *26*, 272.
- (403) Benaissa, H.; Davey, P. N.; Khimyak, Y. Z.; Kozhevnikov, I. V. *J. Catal.* **2008**, *253*, 244.
- (404) Okuhara, T.; Mizuno, N.; Misono, M. *Adv. Catal.* **1996**, *41*, 113.
- (405) Centi, G.; Cavani, F.; Trifiro, F. *Selective Oxidation by Heterogeneous Catalysis*; Kluwer: New York, 2001.
- (406) Szczepankiewicz, S. H.; Ippolito, C. M.; Santora, B. P.; Van de Ven, T. J.; Ippolito, G. A.; Fronckowiak, L.; Wiatrowski, F.; Power, T.; Kozik, M. *Inorg. Chem.* **1998**, *37*, 4344.
- (407) Gao, G. G.; Li, F. Y.; Xu, L.; Liu, X. Z.; Yang, Y. Y. *J. Am. Chem. Soc.* **2008**, *130*, 10838.
- (408) Schaming, D.; Allain, C.; Farha, R.; Goldmann, M.; Lobstein, S.; Giraudeau, A.; Hasenknopf, B.; Ruhlmann, L. *Langmuir* **2010**, *26*, S101.
- (409) Schaming, D.; Farha, R.; Xu, H.; Goldmann, M.; Ruhlmann, L. *Langmuir* **2011**, *27*, 132.
- (410) Schaming, D.; Costa-Coquelard, C.; Sorgues, S.; Ruhlmann, L.; Lampre, I. *Appl. Catal., A: Gen.* **2010**, *373*, 160.
- (411) Costa-Coquelard, C.; Sorgues, S.; Ruhlmann, L. *J. Phys. Chem. A* **2010**, *114*, 6394.
- (412) Ahmed, I.; Wang, X.; Boualili, N.; Xu, H.; Farha, R.; Goldmann, M.; Ruhlmann, L. *Appl. Catal., A: Gen.* **2012**, *447–448*, 89.
- (413) Lesage de la Haye, J.; Beaunier, P.; Ruhlmann, L.; Hasenknopf, B.; Lacôte, E.; Rieger, J. *ChemPlusChem* **2014**, *79*, 250.
- (414) Vaughan, J. S.; Oconnor, C. T.; Fletcher, J. C. Q. *J. Catal.* **1994**, *147*, 441.

- (415) Kozhevnikov, I. V.; Holmes, S.; Siddiqui, M. R. H. *Appl. Catal., A: Gen.* **2001**, *214*, 47.
- (416) Chen, D.; Xue, Z.; Su, Z. *J. Mol. Catal. A: Chem.* **2003**, *203*, 307.
- (417) Chen, D.; Xue, Z.; Su, Z. *J. Mol. Catal. A: Chem.* **2004**, *208*, 91.
- (418) Chen, D.; Wang, X.; Yang, G.; Li, Q.; Chai, W.; Yuan, R.; Liu, S.; Gao, F.; Jin, H.; Roy, S. *J. Mol. Catal. A: Chem.* **2012**, *363–364*, 195.
- (419) Chen, D.; Sahasrabudhe, A.; Wang, P.; Dasgupta, A.; Yuan, R.; Roy, S. *Dalton Trans.* **2013**, *42*, 10587.
- (420) Olah, G. A. *Friedel-Crafts and Related Reactions*; Wiley/Interscience: New York, 1973.
- (421) Metivier, P. *Fine Chemicals through Heterogeneous Catalysis*; Wiley-VCH: Weinheim, Germany, 2001.
- (422) Kaur, J.; Griffin, K.; Harrison, B.; Kozhevnikov, I. V. *J. Catal.* **2002**, *208*, 448.
- (423) Tagawa, T.; Amemiya, J.; Goto, S. *Appl. Catal., A: Gen.* **2004**, *257*, 19.
- (424) Collins, S. n. E.; Matkovic, S. R.; Bonivardi, A. L.; Briand, L. E. *J. Phys. Chem. C* **2011**, *115*, 700.
- (425) Parida, K. M.; Rana, S.; Mallick, S.; Rath, D. *J. Colloid Interface Sci.* **2010**, *350*, 132.
- (426) Kozhevnikov, I. V. *J. Mol. Catal. A: Chem.* **2009**, *305*, 104.
- (427) Kozhevnikova, E. F.; Derouane, E. G.; Kozhevnikov, I. V. *Chem. Commun.* **2002**, 1178.
- (428) Kozhevnikova, E. F.; Quartararo, J.; Kozhevnikov, I. V. *Appl. Catal., A: Gen.* **2003**, *245*, 69.
- (429) Kozhevnikova, E. F.; Rafiee, E.; Kozhevnikov, I. V. *Appl. Catal., A: Gen.* **2004**, *260*, 25.
- (430) Liu, Y.; Xu, L.; Xu, B.; Li, Z.; Jia, L.; Guo, W. *J. Mol. Catal. A: Chem.* **2009**, *297*, 86.
- (431) Yadav, G. D.; More, S. R. *Appl. Clay Sci.* **2011**, *53*, 254.
- (432) Yadav, G. D.; George, G. *Catal. Today* **2009**, *141*, 130.
- (433) Omata, K. *Appl. Catal., A: Gen.* **2011**, *407*, 112.
- (434) Siddiqui, M. R. H.; Holmes, S.; He, H.; Smith, W.; Coker, E. N.; Atkins, M. P.; Kozhevnikov, I. V. *Catal. Lett.* **2000**, *66*, 53.
- (435) Alsalme, A. M.; Wiper, P. V.; Khimyak, Y. Z.; Kozhevnikova, E. F.; Kozhevnikov, I. V. *J. Catal.* **2010**, *276*, 181.
- (436) Zhao, Q.; Wang, L.; Zhao, S.; Wang, X.; Wang, S. *Fuel* **2011**, *90*, 2289.
- (437) Fan, C.; Guan, H.; Zhang, H.; Wang, J.; Wang, S.; Wang, X. *Biomass Bioenergy* **2011**, *35*, 2659.
- (438) Qu, Y.; Huang, C.; Zhang, J.; Chen, B. *Bioresour. Technol.* **2012**, *106*, 170.
- (439) Zheng, H.; Sun, Z.; Yi, X.; Wang, S.; Li, J.; Wang, X.; Jiang, Z. *RSC Adv.* **2013**, *3*, 23051.
- (440) Janik, M. J.; Macht, J.; Iglesia, E.; Neurock, M. *J. Phys. Chem. C* **2009**, *113*, 1872.
- (441) Suzuki, S.; Kogai, K.; Ono, Y. *Chem. Lett.* **1984**, 699.
- (442) Na, K.; Okuhara, T.; Misono, M. *Chem. Lett.* **1993**, 1141.
- (443) Na, K.; Okuhara, T.; Misono, M. *J. Chem. Soc., Faraday Trans.* **1995**, *91*, 367.
- (444) Na, K. T.; Okuhara, T.; Misono, M. *J. Chem. Soc., Chem. Commun.* **1993**, 1422.
- (445) Gagea, B. C.; Lorgouilloux, Y.; Altintas, Y.; Jacobs, P. A.; Martens, J. A. *J. Catal.* **2009**, *265*, 99.
- (446) Liu, Y. Y.; Na, K.; Misono, M. *J. Mol. Catal. A: Chem.* **1999**, *141*, 145.
- (447) Ivanov, A. V.; Vasina, T. V.; Nissenbaum, V. D.; Kustov, L. M.; Timofeeva, M. N.; Houzvicka, J. I. *Appl. Catal., A: Gen.* **2004**, *259*, 65.
- (448) da Silva Rocha, K. A.; Kozhevnikov, I. V.; Gusevskaya, E. V. *Appl. Catal., A: Gen.* **2005**, *294*, 106.
- (449) Rocha, K. A. d. S.; Robles-Dutenhelfner, P. A.; Kozhevnikov, I. V.; Gusevskaya, E. V. *Appl. Catal., A: Gen.* **2009**, *352*, 188.
- (450) Alsalme, A.; Kozhevnikova, E. F.; Kozhevnikov, I. V. *Appl. Catal., A: Gen.* **2010**, *390*, 219.
- (451) Guo, Y. H.; Li, K. X.; Clark, J. H. *Green Chem.* **2007**, *9*, 839.
- (452) Yu, X. D.; Guo, Y. H.; Li, K. X.; Yang, X.; Xu, L. L.; Guo, Y. N.; Hu, J. L. *J. Mol. Catal. A: Chem.* **2008**, *290*, 44.
- (453) Guo, Y. H.; Li, K. X.; Yu, X. D.; Clark, J. H. *Appl. Catal., B: Environ.* **2008**, *81*, 182.
- (454) Li, K. X.; Hu, J. L.; Li, W.; Ma, F. Y.; Xu, L. L.; Guo, Y. H. *J. Mater. Chem.* **2009**, *19*, 8628.
- (455) Li, J. Y.; Hu, S. S.; Luo, S.; Cheng, J. P. *Eur. J. Org. Chem.* **2009**, *132*.
- (456) Luo, S. H.; Li, J. Y.; Xu, H.; Zhang, L.; Cheng, J. P. *Org. Lett.* **2007**, *9*, 3675.
- (457) Zheng, X. X.; Zhang, L.; Li, J. Y.; Luo, S. Z.; Cheng, J. P. *Chem. Commun.* **2011**, *47*, 12325.
- (458) Sawant, D. P.; Justus, J.; Balasubramanian, V. V.; Ariga, K.; Srinivasu, P.; Velmathi, S.; Halligudi, S. B.; Vinu, A. *Chem.—Eur. J.* **2008**, *14*, 3200.
- (459) Chaskar, A.; Padalkar, V.; Phatangare, K.; Patil, K.; Bodkhe, A.; Langi, B. *Appl. Catal., A: Gen.* **2009**, *359*, 84.
- (460) Azizi, N.; Torkiyan, L.; Saidi, M. R. *Org. Lett.* **2006**, *8*, 2079.
- (461) Boglio, C.; Micoine, K.; Remy, P.; Hasenknopf, B.; Thorimbert, S.; Lacote, E.; Malacria, M.; Afonso, C.; Tabet, J. C. *Chem.—Eur. J.* **2007**, *13*, 5426.
- (462) Dupre, N.; Remy, P.; Micoine, K.; Boglio, C.; Thorimbert, S.; Lacote, E.; Hasenknopf, B.; Malacria, M. *Chem.—Eur. J.* **2010**, *16*, 7256.
- (463) Derat, E.; Lacote, E.; Hasenknopf, B.; Thorimbert, S.; Malacria, M. *J. Phys. Chem. A* **2008**, *112*, 13002.
- (464) da Silva, K. A.; Robles-Dutenhelfner, P. A.; Sousa, E. M. B.; Kozhevnikova, E. F.; Kozhevnikov, I. V.; Gusevskaya, E. V. *Catal. Commun.* **2004**, *5*, 425.
- (465) da Silva Rocha, K. A.; Robles-Dutenhelfner, P. A.; Sousa, E. M. B.; Kozhevnikova, E. F.; Kozhevnikov, I. V.; Gusevskaya, E. V. *Appl. Catal., A: Gen.* **2007**, *317*, 171.
- (466) Gregory, R. J. H. *Chem. Rev.* **1999**, *99*, 3649.
- (467) Brunel, J. M.; Holmes, I. P. *Angew. Chem., Int. Ed.* **2004**, *43*, 2752.
- (468) Kikukawa, Y.; Suzuki, K.; Sugawa, M.; Hirano, T.; Kamata, K.; Yamaguchi, K.; Mizuno, N. *Angew. Chem., Int. Ed.* **2012**, *51*, 3686.
- (469) Suzuki, K.; Sugawa, M.; Kikukawa, Y.; Kamata, K.; Yamaguchi, K.; Mizuno, N. *Inorg. Chem.* **2012**, *51*, 6953.
- (470) Azizi, N.; Saidi, M. R. *Tetrahedron* **2007**, *63*, 888.
- (471) Chakrabarty, M.; Mukherji, A.; Mukherjee, R.; Arima, S.; Harigaya, Y. *Tetrahedron Lett.* **2007**, *48*, 5239.
- (472) Subba Reddy, B. V.; Narasimhulu, G.; Subba Lakshumma, P.; Vikram Reddy, Y.; Yadav, J. S. *Tetrahedron Lett.* **2012**, *53*, 1776.
- (473) Rafiee, E.; Paknezhad, F.; Shahebrahimi, S.; Josaghani, M.; Eavani, S.; Rashidzadeh, S. *J. Mol. Catal. A: Chem.* **2008**, *282*, 92.
- (474) Rafiee, E.; Tork, F.; Josaghani, M. *Bioorg. Med. Chem. Lett.* **2006**, *16*, 1221.
- (475) Rafiee, E.; Jafari, H. *Bioorg. Med. Chem. Lett.* **2006**, *16*, 2463.
- (476) Bhilare, S. V.; Deorukhkar, A. R.; Darvatkar, N. B.; Rasalkar, M. S.; Salunkhe, M. M. *J. Mol. Catal. A: Chem.* **2007**, *270*, 123.
- (477) Kumar, A.; Singh, P.; Kumar, S.; Chandra, R.; Mozumdar, S. J. *Mol. Catal. A: Chem.* **2007**, *276*, 95.
- (478) Morin, P.; Hamad, B.; Sapaly, G.; Carneiro Rocha, M. G.; Pries de Oliveira, P. G.; Gonzalez, W. A.; Andrade Sales, E.; Essayem, N. *Appl. Catal., A: Gen.* **2007**, *330*, 69.
- (479) de Meireles, A. L. P.; da Silva Rocha, K. A.; Kozhevnikov, I. V.; Gusevskaya, E. V. *Appl. Catal., A: Gen.* **2011**, *409–410*, 82.
- (480) Caetano, C. S.; Fonseca, I. M.; Ramos, A. M.; Vital, J.; Castanheiro, J. E. *Catal. Commun.* **2008**, *9*, 1996.
- (481) Bhorodwaj, S. K.; Dutta, D. K. *Appl. Catal., A: Gen.* **2010**, *378*, 221.
- (482) Khder, A. E. R. S.; Hassan, H. M. A.; El-Shall, M. S. *Appl. Catal., A: Gen.* **2012**, *411–412*, 77.
- (483) Li, B.; Ma, W.; Han, C.; Liu, J.; Pang, X.; Gao, X. *Microporous Mesoporous Mater.* **2012**, *156*, 73.
- (484) Alsalme, A.; Kozhevnikova, E. F.; Kozhevnikov, I. V. *Appl. Catal., A: Gen.* **2008**, *349*, 170.
- (485) Sunita, G.; Devassy, B. M.; Vinu, A.; Sawant, D. P.; Balasubramanian, V. V.; Halligudi, S. B. *Catal. Commun.* **2008**, *9*, 696.

- (486) Katada, N.; Hatanaka, T.; Ota, M.; Yamada, K.; Okumura, K.; Niwa, M. *Appl. Catal., A: Gen.* **2009**, *363*, 164.
- (487) Das, J.; Parida, K. M. *J. Mol. Catal. A: Chem.* **2007**, *264*, 248.
- (488) Lotero, E.; Liu, Y. J.; Lopez, D. E.; Suwannakarn, K.; Bruce, D. A.; Goodwin, J. G. *Ind. Eng. Chem. Res.* **2005**, *44*, 5353.
- (489) Kiss, A. A.; Dimian, A. C.; Rothenberg, G. *Adv. Synth. Catal.* **2006**, *348*, 75.
- (490) Bournay, L.; Casanave, D.; Delfort, B.; Hillion, G.; Chodorge, J. A. *Catal. Today* **2005**, *106*, 190.
- (491) Kinney, A. J.; Clemente, T. E. *Fuel Process. Technol.* **2005**, *86*, 1137.
- (492) Granados, M. L.; Poves, M. D. Z.; Alonso, D. M.; Mariscal, R.; Galisteo, F. C.; Moreno-Tost, R.; Santamaría, J.; Fierro, J. L. G. *Appl. Catal., B: Environ.* **2007**, *73*, 317.
- (493) Zafiropoulos, N. A.; Ngo, H. L.; Foglia, T. A.; Samulski, E. T.; Lin, W. B. *Chem. Commun.* **2007**, 3670.
- (494) Xu, L. L.; Wang, Y. H.; Yang, X.; Yu, X. D.; Guo, Y. H.; Clark, J. H. *Green Chem.* **2008**, *10*, 746.
- (495) Xu, L. L.; Yang, X.; Yu, X. D.; Guo, Y. H.; Maynurkader. *Catal. Commun.* **2008**, *9*, 1607.
- (496) Kulkarni, M. G.; Gopinath, R.; Meher, L. C.; Dalai, A. K. *Green Chem.* **2006**, *8*, 1056.
- (497) Xu, L. L.; Li, W.; Hu, J. L.; Li, K. X.; Yang, X.; Ma, F. Y.; Guo, Y. N.; Yu, X. D.; Guo, Y. H. *J. Mater. Chem.* **2009**, *19*, 8571.
- (498) Xu, L. L.; Wang, Y. H.; Yang, X.; Hu, J. L.; Li, W.; Guo, Y. H. *Green Chem.* **2009**, *11*, 314.
- (499) Xu, L. L.; Li, W.; Hu, J. L.; Yang, X.; Guo, Y. H. *Appl. Catal., B: Environ.* **2009**, *90*, 587.
- (500) Su, F.; Ma, L.; Song, D. Y.; Zhang, X. H.; Guo, Y. H. *Green Chem.* **2013**, *15*, 885.
- (501) Su, F.; Wu, Q. Y.; Song, D. Y.; Zhang, X. H.; Wang, M.; Guo, Y. H. *J. Mater. Chem. A* **2013**, *1*, 13209.
- (502) Su, F.; Ma, L.; Guo, Y. H.; Li, W. *Catal. Sci. Technol.* **2012**, *2*, 2367.
- (503) Giri, B. Y.; Rao, K. N.; Devi, B. L. A. P.; Lingaiah, N.; Suryanarayana, I.; Prasad, R. B. N.; Prasad, P. S. S. *Catal. Commun.* **2005**, *6*, 788.
- (504) Narasimharao, K.; Brown, D. R.; Lee, A. F.; Newman, A. D.; Siril, P. F.; Tavener, S. J.; Wilson, K. J. *Catal.* **2007**, *248*, 226.
- (505) Shin, H.-Y.; An, S.-H.; Sheikh, R.; Park, Y. H.; Bae, S.-Y. *Fuel* **2012**, *96*, 572.
- (506) Chai, F.; Cao, F. H.; Zhai, F. Y.; Chen, Y.; Wang, X. H.; Su, Z. M. *Adv. Synth. Catal.* **2007**, *349*, 1057.
- (507) Sun, C.-Y.; Liu, S.-X.; Liang, D.-D.; Shao, K.-Z.; Ren, Y.-H.; Su, Z.-M. *J. Am. Chem. Soc.* **2009**, *131*, 1883.
- (508) Inumaru, K.; Ishihara, T.; Kamiya, Y.; Okuhara, T.; Yamanaka, S. *Angew. Chem., Int. Ed.* **2007**, *46*, 7625.
- (509) Cartuyvels, E.; Absillis, G.; Parac-Vogt, T. N. *Chem. Commun.* **2008**, 85.
- (510) Van Lokeren, L.; Cartuyvels, E.; Absillis, G.; Willem, R.; Parac-Vogt, T. N. *Chem. Commun.* **2008**, 2774.
- (511) Williams, N. H.; Takasaki, B.; Wall, M.; Chin, J. *Acc. Chem. Res.* **1999**, *32*, 485.
- (512) Hegg, E. L.; Burstyn, J. N. *Coord. Chem. Rev.* **1998**, *173*, 133.
- (513) Morrow, J. R.; Iranzo, O. *Curr. Opin. Chem. Biol.* **2004**, *8*, 192.
- (514) Absillis, G.; Cartuyvels, E.; Van Deun, R.; Parac-Vogt, T. N. *J. Am. Chem. Soc.* **2008**, *130*, 17400.
- (515) Steens, N.; Ramadan, A. M.; Absillis, G.; Parac-Vogt, T. N. *Dalton Trans.* **2010**, *39*, 585.
- (516) Steens, N.; Ramadan, A. M.; Parac-Vogt, T. N. *Chem. Commun.* **2009**, 965.
- (517) Ho, P. H.; Breynaert, E.; Kirschhock, C. E. A.; Parac-Vogt, T. N. *Dalton Trans.* **2011**, *40*, 295.
- (518) Vanhaecht, S.; Absillis, G.; Parac-Vogt, T. N. *Dalton Trans.* **2012**, *41*, 10028.
- (519) Saku, Y.; Sakai, Y.; Nomiya, K. *Inorg. Chim. Acta* **2010**, *363*, 967.
- (520) Sokolov, M. N.; Izarova, N. V.; Peresypkina, E. V.; Mainichev, D. A.; Fedin, V. P. *Inorg. Chim. Acta* **2009**, *362*, 3756.
- (521) Sokolov, M. N.; Izarova, N. V.; Peresypkina, E. V.; Virovets, A. V.; Fedin, V. P. *Russ. Chem. Bull.* **2009**, *58*, 507.
- (522) Absillis, G.; Parac-Vogt, T. N. *Inorg. Chem.* **2012**, *51*, 9902.
- (523) Parac, T. N.; Ullmann, G. M.; Kostic, N. M. *J. Am. Chem. Soc.* **1999**, *121*, 3127.
- (524) Zhang, C.; Bensaid, L.; McGregor, D.; Fang, X. F.; Howell, R. C.; Burton-Pye, B.; Luo, Q. H.; Todaro, L.; Francesconi, L. C. *J. Cluster Sci.* **2006**, *17*, 389.
- (525) Vanhaecht, S.; Absillis, G.; Parac-Vogt, T. N. *Dalton Trans.* **2013**, *42*, 15437.
- (526) Ly, H. G.; Absillis, G.; Parac-Vogt, T. N. *Dalton Trans.* **2013**, *42*, 10929.
- (527) Stroobants, K.; Moelants, E.; Ly, H. G.; Proost, P.; Bartik, K.; Parac-Vogt, T. N. *Chem.—Eur. J.* **2013**, *19*, 2848.
- (528) Ly, H. G. T.; Absillis, G.; Bajpe, S. R.; Martens, J. A.; Parac-Vogt, T. N. *Eur. J. Inorg. Chem.* **2013**, *2013*, 4601.
- (529) Shimizu, K.-i.; Furukawa, H.; Kobayashi, N.; Itaya, Y.; Satsuma, A. *Green Chem.* **2009**, *11*, 1627.
- (530) Shimizu, K.-i.; Niimi, K.; Satsuma, A. *Catal. Commun.* **2008**, *9*, 980.
- (531) Shimizu, K.-i.; Niimi, K.; Satsuma, A. *Appl. Catal., A: Gen.* **2008**, *349*, 1.
- (532) Marci, G.; Garcia-Lopez, E.; Bellardita, M.; Parisi, F.; Colbeau-Justin, C.; Sorgues, S.; Liotta, L. F.; Palmisano, L. *Phys. Chem. Chem. Phys.* **2013**, *15*, 13329.
- (533) Ivanova, S.; Nitsch, X.; Romero-Sarria, F.; Louis, B.; Centeno, M. A.; Roger, A. C.; Odriozola, J. A. *Catal. Today* **2011**, *171*, 236.
- (534) Hirano, T.; Uehara, K.; Kamata, K.; Mizuno, N. *J. Am. Chem. Soc.* **2012**, *134*, 6425.
- (535) Itagaki, S.; Kamata, K.; Yamaguchi, K.; Mizuno, N. *ChemCatChem* **2013**, *5*, 1725.
- (536) Yoshida, A.; Hikichi, S.; Mizuno, N. *J. Organomet. Chem.* **2007**, *692*, 455.
- (537) Sugahara, K.; Kimura, T.; Kamata, K.; Yamaguchi, K.; Mizuno, N. *Chem. Commun.* **2012**, *48*, 8422.
- (538) Sun, D. W.; Zhai, H. *J. Catal. Commun.* **2007**, *8*, 1027.
- (539) Langanke, J.; Greiner, L.; Leitner, W. *Green Chem.* **2013**, *15*, 1173.
- (540) Sankar, M.; Tarte, N. H.; Manikandan, P. *Appl. Catal., A: Gen.* **2004**, *276*, 217.
- (541) Yasuda, H.; He, L. N.; Sakakura, T.; Hu, C. W. *J. Catal.* **2005**, *233*, 119.
- (542) Chen, F. W.; Dong, T.; Chi, Y. N.; Xu, Y. Q.; Hu, C. W. *Catal. Lett.* **2010**, *139*, 38.
- (543) Chen, F. W.; Li, X. F.; Wang, B.; Xu, T. G.; Chen, S. L.; Liu, P.; Hu, C. W. *Chem.—Eur. J.* **2012**, *18*, 9870.
- (544) Dupre, N.; Brazel, C.; Fensterbank, L.; Malacria, M.; Thorimbert, S.; Hasenkopf, B.; Lacote, E. *Chem.—Eur. J.* **2012**, *18*, 12962.
- (545) Berardi, S.; Carraro, M.; Iglesias, M.; Sartorel, A.; Scorrano, G.; Albrecht, M.; Bonchio, M. *Chem.—Eur. J.* **2010**, *16*, 10662.
- (546) Srivani, A.; Prasad, P. S. S.; Lingaiah, N. *Catal. Lett.* **2012**, *142*, 389.
- (547) Liu, Y.; Misono, M. *Materials* **2009**, *2*, 2319.
- (548) Hetterley, R. D.; Kozhevnikova, E. F.; Kozhevnikov, I. V. *Chem. Commun.* **2006**, 782.
- (549) Liu, M.; Deng, W. P.; Zhang, Q. H.; Wang, Y. L.; Wang, Y. *Chem. Commun.* **2011**, *47*, 9717.
- (550) Deng, W. P.; Zhang, Q. H.; Wang, Y. *Dalton Trans.* **2012**, *41*, 9817.
- (551) Anbar, M.; Pecht, I. *J. Am. Chem. Soc.* **1967**, *89*, 2553.
- (552) Ruttinger, W.; Dismukes, G. C. *Chem. Rev.* **1997**, *97*, 1.
- (553) Yagi, M.; Kaneko, M. *Chem. Rev.* **2001**, *101*, 21.
- (554) Herrero, C.; Lassalle-Kaiser, B.; Leibl, W.; Rutherford, A. W.; Aukauloo, A. *Coord. Chem. Rev.* **2008**, *252*, 456.
- (555) Hambourger, M.; Moore, G. F.; Kramer, D. M.; Gust, D.; Moore, A. L.; Moore, T. A. *Chem. Soc. Rev.* **2009**, *38*, 25.
- (556) Chen, Z. F.; Concepcion, J. J.; Luo, H. L.; Hull, J. F.; Paul, A.; Meyer, T. J. *J. Am. Chem. Soc.* **2010**, *132*, 17670.

- (557) Duan, L. L.; Bozoglian, F.; Mandal, S.; Stewart, B.; Privalov, T.; Llobet, A.; Sun, L. C. *Nat. Chem.* **2012**, *4*, 418.
- (558) Karkas, M. D.; Akerman, T.; Johnston, E. V.; Karim, S. R.; Laine, T. M.; Lee, B. L.; Akerman, T.; Privalov, T.; Akerman, B. *Angew. Chem., Int. Ed.* **2012**, *51*, 11589.
- (559) Concepcion, J. J.; Jurss, J. W.; Templeton, J. L.; Meyer, T. J. *J. Am. Chem. Soc.* **2008**, *130*, 16462.
- (560) Concepcion, J. J.; Tsai, M. K.; Muckerman, J. T.; Meyer, T. J. *J. Am. Chem. Soc.* **2010**, *132*, 1545.
- (561) Fillol, J. L.; Codola, Z.; Garcia-Bosch, I.; Gomez, L.; Pla, J. J.; Costas, M. *Nat. Chem.* **2011**, *3*, 807.
- (562) Ellis, W. C.; McDaniel, N. D.; Bernhard, S.; Collins, T. *J. Am. Chem. Soc.* **2010**, *132*, 10990.
- (563) Dismukes, G. C.; Brimblecombe, R.; Felton, G. A. N.; Pryadun, R. S.; Sheats, J. E.; Spiccia, L.; Swiegers, G. F. *Acc. Chem. Res.* **2009**, *42*, 1935.
- (564) Wasylewko, D. J.; Ganeshamoorthy, C.; Borau-Garcia, J.; Berlinguet, C. P. *Chem. Commun.* **2011**, *47*, 4249.
- (565) Thusius, D. D.; Taube, H. *J. Am. Chem. Soc.* **1966**, *88*, 850.
- (566) McDaniel, N. D.; Coughlin, F. J.; Tinker, L. L.; Bernhard, S. *J. Am. Chem. Soc.* **2008**, *130*, 210.
- (567) Wang, C.; Wang, J. L.; Lin, W. B. *J. Am. Chem. Soc.* **2012**, *134*, 19895.
- (568) Barnett, S. M.; Goldberg, K. I.; Mayer, J. M. *Nat. Chem.* **2012**, *4*, 498.
- (569) Howells, A. R.; Sankarraj, A.; Shannon, C. *J. Am. Chem. Soc.* **2004**, *126*, 12258.
- (570) Geletii, Y. V.; Botar, B.; Koegerler, P.; Hillesheim, D. A.; Musaev, D. G.; Hill, C. L. *Angew. Chem., Int. Ed.* **2008**, *47*, 3896.
- (571) Sartorel, A.; Carraro, M.; Scorrano, G.; Zorzi, R. D.; Geremia, S.; McDaniel, N. D.; Bernhard, S.; Bonchio, M. *J. Am. Chem. Soc.* **2008**, *130*, 5006.
- (572) Geletii, Y. V.; Besson, C.; Hou, Y.; Yin, Q.; Musaev, D. G.; Quiñonero, D.; Cao, R.; Hardcastle, K. I.; Proust, A.; Kögerler, P.; Hill, C. L. *J. Am. Chem. Soc.* **2009**, *131*, 17360.
- (573) Quiñonero, D.; Kaledin, A. L.; Kuznetsov, A. E.; Geletii, Y. V.; Besson, C.; Hill, C. L.; Musaev, D. G. *J. Phys. Chem. A* **2010**, *114*, 535.
- (574) Grigoriev, V. A.; Hill, C. L.; Weinstock, I. A. *J. Am. Chem. Soc.* **2000**, *122*, 3544.
- (575) Grigoriev, V. A.; Cheng, D.; Hill, C. L.; Weinstock, I. A. *J. Am. Chem. Soc.* **2001**, *123*, 5292.
- (576) Antonio, M. R.; Nyman, M.; Anderson, T. M. *Angew. Chem., Int. Ed.* **2009**, *48*, 6136.
- (577) Piccinin, S.; Fabris, S. *Phys. Chem. Chem. Phys.* **2011**, *13*, 7666.
- (578) Sartorel, A.; Miro, P.; Salvadori, E.; Romain, S.; Carraro, M.; Scorrano, G.; Di Valentin, M.; Llobet, A.; Bo, C.; Bonchio, M. *J. Am. Chem. Soc.* **2009**, *131*, 16051.
- (579) Geletii, Y. V.; Huang, Z.; Hou, Y.; Musaev, D. G.; Lian, T.; Hill, C. L. *J. Am. Chem. Soc.* **2009**, *131*, 7522.
- (580) Natali, M.; Orlandi, M.; Berardi, S.; Campagna, S.; Bonchio, M.; Sartorel, A.; Scandola, F. *Inorg. Chem.* **2012**, *51*, 7324.
- (581) Youngblood, W. J.; Lee, S.-H. A.; Kobayashi, Y.; Hernandez-Pagan, E. A.; Hoertz, P. G.; Moore, T. A.; Moore, A. L.; Gust, D.; Mallouk, T. E. *J. Am. Chem. Soc.* **2009**, *131*, 926.
- (582) Orlandi, M.; Argazzi, R.; Sartorel, A.; Carraro, M.; Scorrano, G.; Bonchio, M.; Scandola, F. *Chem. Commun.* **2010**, *46*, 3152.
- (583) Xiang, X.; Fielden, J.; Rodríguez-Córdoba, W.; Huang, Z.; Zhang, N.; Luo, Z.; Musaev, D. G.; Lian, T.; Hill, C. L. *J. Phys. Chem. C* **2013**, *117*, 918.
- (584) Huang, Z.; Geletii, Y. V.; Wu, D.; Anfuso, C. L.; Musaev, D. G.; Hill, C. L.; Lian, T. *Proc. SPIE* **2011**, *8109*, 810903.
- (585) Gao, J.; Cao, S.; Tay, Q.; Liu, Y.; Yu, L.; Ye, K.; Mun, P. C.; Li, Y.; Rakesh, G.; Loo, S. C.; Chen, Z.; Zhao, Y.; Xue, C.; Zhang, Q. *Sci. Rep.* **2013**, *3*, 1853.
- (586) Huang, Z.; Geletii, Y. V.; Musaev, D. G.; Hill, C. L.; Lian, T. *Ind. Eng. Chem. Res.* **2012**, *51*, 11850.
- (587) Puntoriero, F.; La Ganga, G.; Sartorel, A.; Carraro, M.; Scorrano, G.; Bonchio, M.; Campagna, S. *Chem. Commun.* **2010**, *46*, 4725.
- (588) Heussner, K.; Peuntinger, K.; Rockstroh, N.; Nye, L. C.; Ivanovic-Burmazovic, I.; Rau, S.; Streb, C. *Chem. Commun.* **2011**, *47*, 6852.
- (589) Toma, F. M.; Sartorel, A.; Iurlo, M.; Carraro, M.; Parisse, P.; Maccato, C.; Rapino, S.; Gonzalez, B. R.; Amenitsch, H.; Da Ros, T.; Casalis, L.; Goldoni, A.; Marcaccio, M.; Scorrano, G.; Scoles, G.; Paolucci, F.; Prato, M.; Bonchio, M. *Nat. Chem.* **2010**, *2*, 826.
- (590) Toma, F. M.; Sartorel, A.; Carraro, M.; Bonchio, M.; Prato, M. *Pure Appl. Chem.* **2011**, *83*, 1529.
- (591) Toma, F. M.; Sartorel, A.; Iurlo, M.; Carraro, M.; Rapino, S.; Hoober-Burkhardt, L.; Da Ros, T.; Marcaccio, M.; Scorrano, G.; Paolucci, F.; Bonchio, M.; Prato, M. *ChemSusChem* **2011**, *4*, 1447.
- (592) Kanan, M. W.; Nocera, D. G. *Science* **2008**, *321*, 1072.
- (593) Brimblecombe, R.; Swiegers, G. F.; Dismukes, G. C.; Spiccia, L. *Angew. Chem., Int. Ed.* **2008**, *47*, 7335.
- (594) Brimblecombe, R.; Kolling, D. R. J.; Bond, A. M.; Dismukes, G. C.; Swiegers, G. F.; Spiccia, L. *Inorg. Chem.* **2009**, *48*, 7269.
- (595) Liu, Y.; Guo, S.-X.; Bond, A. M.; Zhang, J.; Geletii, Y. V.; Hill, C. L. *Inorg. Chem.* **2013**, *52*, 11986.
- (596) Quintana, M.; Lopez, A. M.; Rapino, S.; Toma, F. M.; Iurlo, M.; Carraro, M.; Sartorel, A.; Maccato, C.; Ke, X. X.; Bittencourt, C.; Da Ros, T.; Van Tendeloo, G.; Marcaccio, M.; Paolucci, F.; Prato, M.; Bonchio, M. *ACS Nano* **2013**, *7*, 811.
- (597) Guo, S.-X.; Liu, Y.; Lee, C.-Y.; Bond, A. M.; Zhang, J.; Geletii, Y. V.; Hill, C. L. *Energy Environ. Sci.* **2013**, *6*, 2654.
- (598) Lee, C. Y.; Guo, S. X.; Murphy, A. F.; McCormac, T.; Zhang, J.; Bond, A. M.; Zhu, G.; Hill, C. L.; Geletii, Y. V. *Inorg. Chem.* **2012**, *51*, 11521.
- (599) Besson, C.; Huang, Z. Q.; Geletii, Y. V.; Lense, S.; Hardcastle, K. I.; Musaev, D. G.; Lian, T. Q.; Proust, A.; Hill, C. L. *Chem. Commun.* **2010**, *46*, 2784.
- (600) Murakami, M.; Hong, D. C.; Suenobu, T.; Yamaguchi, S.; Ogura, T.; Fukuzumi, S. *J. Am. Chem. Soc.* **2011**, *133*, 11605.
- (601) Ogo, S.; Miyamoto, M.; Ide, Y.; Sano, T.; Sadakane, M. *Dalton Trans.* **2012**, *41*, 9901.
- (602) Lang, Z. L.; Yang, G. C.; Ma, N. N.; Wen, S. Z.; Yan, L. K.; Guan, W.; Su, Z. M. *Dalton Trans.* **2013**, *42*, 10617.
- (603) Yin, Q. S.; Tan, J. M.; Besson, C.; Geletii, Y. V.; Musaev, D. G.; Kuznetsov, A. E.; Luo, Z.; Hardcastle, K. I.; Hill, C. L. *Science* **2010**, *328*, 342.
- (604) Huang, Z. Q.; Luo, Z.; Geletii, Y. V.; Vickers, J. W.; Yin, Q. S.; Wu, D.; Hou, Y.; Ding, Y.; Song, J.; Musaev, D. G.; Hill, C. L.; Lian, T. Q. *J. Am. Chem. Soc.* **2011**, *133*, 2068.
- (605) Wu, J.; Liao, L. W.; Yan, W. S.; Xue, Y.; Sun, Y. F.; Yan, X.; Chen, Y. X.; Xie, Y. *ChemSusChem* **2012**, *5*, 1207.
- (606) Stracke, J. J.; Finke, R. G. *J. Am. Chem. Soc.* **2011**, *133*, 14872.
- (607) Stracke, J. J.; Finke, R. G. *ACS Catal.* **2013**, *3*, 1209.
- (608) Natali, M.; Berardi, S.; Sartorel, A.; Bonchio, M.; Campagna, S.; Scandola, F. *Chem. Commun.* **2012**, *48*, 8808.
- (609) Vickers, J. W.; Lv, H.; Sumliner, J. M.; Zhu, G.; Luo, Z.; Musaev, D. G.; Geletii, Y. V.; Hill, C. L. *J. Am. Chem. Soc.* **2013**, *135*, 14110.
- (610) Schiwon, R.; Klingan, K.; Dau, H.; Limberg, C. *Chem. Commun.* **2014**, *50*, 100.
- (611) Lieb, D.; Zahl, A.; Wilson, E. F.; Streb, C.; Nye, L. C.; Meyer, K.; Ivanovic-Burmazovic, I. *Inorg. Chem.* **2011**, *50*, 9053.
- (612) Zhu, G. B.; Geletii, Y. V.; Kogerler, P.; Schilder, H.; Song, J.; Lense, S.; Zhao, C. C.; Hardcastle, K. I.; Musaev, D. G.; Hill, C. L. *Dalton Trans.* **2012**, *41*, 2084.
- (613) Song, F. Y.; Ding, Y.; Ma, B. C.; Wang, C. M.; Wang, Q.; Du, X. Q.; Fu, S.; Song, J. *Energy Environ. Sci.* **2013**, *6*, 1170.
- (614) Lv, H.; Song, J.; Geletii, Y. V.; Vickers, J. W.; Sumliner, J. M.; Musaev, D. G.; Kogerler, P.; Zhuk, P. F.; Bacsa, J.; Zhu, G.; Hill, C. L. *J. Am. Chem. Soc.* **2014**, *136*, 9268.
- (615) Goberna-Ferron, S.; Vigara, L.; Soriano-Lopez, J.; Galan-Mascaro, J. R. *Inorg. Chem.* **2012**, *51*, 11707.
- (616) Soriano-Lopez, J.; Goberna-Ferron, S.; Vigara, L.; Carbo, J. J.; Poblet, J. M.; Galan-Mascaro, J. R. *Inorg. Chem.* **2013**, *52*, 4753.

- (617) Han, X. B.; Zhang, Z. M.; Zhang, T.; Li, Y. G.; Lin, W. B.; You, W. S.; Su, Z. M.; Wang, E. B. *J. Am. Chem. Soc.* **2014**, *136*, 5359.
- (618) Tanaka, S.; Annaka, M.; Sakai, K. *Chem. Commun.* **2012**, *48*, 1653.
- (619) Car, P. E.; Guttentag, M.; Baldridge, K. K.; Alberto, R.; Patzke, G. R. *Green Chem.* **2012**, *14*, 1680.
- (620) Zhu, G. B.; Glass, E. N.; Zhao, C. C.; Lv, H. J.; Vickers, J. W.; Geletii, Y. V.; Musaev, D. G.; Song, J.; Hill, C. L. *Dalton Trans.* **2012**, *41*, 13043.
- (621) Cao, R.; Ma, H.; Geletii, Y. V.; Hardcastle, K. I.; Hill, C. L. *Inorg. Chem.* **2009**, *48*, 5596.
- (622) Al-Oweini, R.; Sartorel, A.; Bassil, B. S.; Natali, M.; Berardi, S.; Scandola, F.; Kortz, U.; Bonchio, M. *Angew. Chem., Int. Ed.* **2014**, *53*, 11182.
- (623) Osterloh, F. E. *Chem. Mater.* **2008**, *20*, 35.
- (624) Kudo, A.; Miseki, Y. *Chem. Soc. Rev.* **2009**, *38*, 253.
- (625) Hiskia, A.; Mylonas, A.; Papaconstantinou, E. *Chem. Soc. Rev.* **2001**, *30*, 62.
- (626) Yamase, T.; Watanabe, R. *J. Chem. Soc., Dalton Trans.* **1986**, *0*, 1669.
- (627) Akid, R.; Darwent, J. R. *J. Chem. Soc., Dalton Trans.* **1985**, *0*, 395.
- (628) Darwent, J. R. *J. Chem. Soc., Chem. Commun.* **1982**, *0*, 798.
- (629) Hill, C. L.; Bouchard, D. A. *J. Am. Chem. Soc.* **1985**, *107*, 5148.
- (630) Ioannidis, A.; Papaconstantinou, E. *Inorg. Chem.* **1985**, *24*, 439.
- (631) Yamase, T. *Inorg. Chim. Acta* **1982**, *64*, L155.
- (632) Yamase, T. *Inorg. Chim. Acta* **1983**, *76*, L25.
- (633) Yamase, T.; Takabayashi, N.; Kaji, M. *J. Chem. Soc., Dalton Trans.* **1984**, 793.
- (634) Yamase, T.; Cao, X.; Yazaki, S. *J. Mol. Catal. A: Chem.* **2007**, *262*, 119.
- (635) Li, Y.; Ren, C.; Peng, S.; Lu, G.; Li, S. *J. Mol. Catal. A: Chem.* **2006**, *246*, 212.
- (636) Liu, X.; Li, Y.; Peng, S.; Lu, G.; Li, S. *Int. J. Hydrogen Energy* **2012**, *37*, 12150.
- (637) Matt, B.; Fize, J.; Moussa, J.; Amouri, H.; Pereira, A.; Artero, V.; Izzet, G.; Proust, A. *Energy Environ. Sci.* **2013**, *6*, 1504.
- (638) Lv, H.; Song, J.; Zhu, H.; Geletii, Y. V.; Bacsa, J.; Zhao, C.; Lian, T.; Musaev, D. G.; Hill, C. L. *J. Catal.* **2013**, *307*, 48.
- (639) Lv, H.; Guo, W.; Wu, K.; Chen, Z.; Bacsa, J.; Musaev, D. G.; Geletii, Y. V.; Lauinger, S. M.; Lian, T.; Hill, C. L. *J. Am. Chem. Soc.* **2014**, *136*, 14015.
- (640) Scaife, D. E. *Sol. Energy* **1980**, *25*, 41.
- (641) Zhang, Z. Y.; Lin, Q. P.; Zheng, S. T.; Bu, X. H.; Feng, P. Y. *Chem. Commun.* **2011**, *47*, 3918.
- (642) Suzuki, K.; Tang, F.; Kikukawa, Y.; Yamaguchi, K.; Mizuno, N. *Angew. Chem., Int. Ed.* **2014**, *53*, 5356.
- (643) Suzuki, K.; Tang, F.; Kikukawa, Y.; Yamaguchi, K.; Mizuno, N. *Chem. Lett.* **2014**, *43*, 1429.
- (644) Li, S.; Liu, S.; Liu, S.; Liu, Y.; Tang, Q.; Shi, Z.; Ouyang, S.; Ye, J. *J. Am. Chem. Soc.* **2012**, *134*, 19716.
- (645) Zhang, Z.; Lin, Q.; Kurunthu, D.; Wu, T.; Zuo, F.; Zheng, S.-T.; Bardeen, C. J.; Bu, X.; Feng, P. *J. Am. Chem. Soc.* **2011**, *133*, 6934.
- (646) Kudo, A.; Kato, H.; Nakagawa, S. *J. Phys. Chem. B* **1999**, *104*, 571.
- (647) Ogura, S.; Kohno, M.; Sato, K.; Inoue, Y. *Appl. Surf. Sci.* **1997**, *121–122*, S21.
- (648) Kohno, M.; Ogura, S.; Sato, K.; Inoue, Y. *Chem. Phys. Lett.* **1997**, *267*, 72.
- (649) Sato, J.; Kobayashi, H.; Inoue, Y. *J. Phys. Chem. B* **2003**, *107*, 7970.
- (650) Huang, P.; Qin, C.; Su, Z. M.; Xing, Y.; Wang, X. L.; Shao, K. Z.; Lan, Y. Q.; Wang, E. B. *J. Am. Chem. Soc.* **2012**, *134*, 14004.
- (651) Wang, Z. L.; Tan, H. Q.; Chen, W. L.; Li, Y. G.; Wang, E. B. *Dalton Trans.* **2012**, *41*, 9882.
- (652) Fu, H.; Lu, Y.; Wang, Z.; Liang, C.; Zhang, Z.-m.; Wang, E. *Dalton Trans.* **2012**, *41*, 4084.
- (653) Nohra, B.; El Moll, H.; Rodriguez Albelo, L. M.; Mialane, P.; Marrot, J.; Mellot-Draznieks, C.; O'Keeffe, M.; Ngo Biboum, R.; Lemaire, J.; Keita, B.; Nadjo, L.; Dolbecq, A. *J. Am. Chem. Soc.* **2011**, *133*, 13363.
- (654) Le Goff, A.; Artero, V.; Jousselme, B.; Tran, P. D.; Guillet, N.; Metaye, R.; Fihri, A.; Palacin, S.; Fontecave, M. *Science* **2009**, *326*, 1384.
- (655) Tran, P. D.; Le Goff, A.; Heidkamp, J.; Jousselme, B.; Guillet, N.; Palacin, S.; Dau, H.; Fontecave, M.; Artero, V. *Angew. Chem., Int. Ed.* **2011**, *50*, 1371.
- (656) Koper, M. T. M.; Bouwman, E. *Angew. Chem., Int. Ed.* **2010**, *49*, 3723.
- (657) Gong, Y.; Wu, T.; Jiang, P. G.; Lin, J. H.; Yang, Y. X. *Inorg. Chem.* **2013**, *52*, 777.